DISSERTATION

THE ROLE OF CD8 T CELLS DURING PULMONARY INFECTION WITH *MYCOBACTERIUM TUBERCULOSIS*

Submitted by

Scott M. Irwin

Department of Microbiology, Immunology, & Pathology

In partial fulfillment of the requirements

For the Degree of Doctor of Philosophy

Colorado State University

Fort Collins, Colorado

Summer, 2006

COLORADO STATE UNIVERSITY

May 26, 2006

WE HEREBY RECOMMEND THAT THE DISSERATAION PREPARED UNDER OUR SUPERVISION BY SCOTT M. IRWIN ENTITLED THE ROLE OF CD8 T CELLS DURING PULMONARY INFECTION WITH MYCOBACTERIUM TUBERCULOSIS BE ACCEPTED AS FULFILLING IN PART REQUIREMENTS FOR THE DEGREE OF DOCTOR OF PHILOSOPHY.

Committee on Graduate Work

John T. Belisle

Angelo A. Izzo

Randall J. Basaraba

Dennis W. Macy

Ian M. Orme - Adviser

Jeffery Wilusz - Department Head

ABSTRACT OF DISSERTATION

THE ROLE OF CD8 T CELLS DURING PULMONARY INFECTION WITH *MYCOBACTERIUM TUBERCULOSIS*

With over 8 million deaths per year and incidence rates increasing in many countries, tuberculosis is a world-wide pandemic that is responsible for more human suffering, death, and lost productivity than any other infectious disease in the history of mankind. Although a vaccine for tuberculosis exists and is currently in widespread usage, experimental evidence indicates that the bacille Calmette-Guérin live attenuated vaccine provides limited protective efficacy that decreases with age. As the preponderance of cases typically occurs in underdeveloped nations with limited resources to combat the problem, a major multinational effort is currently underway to develop a safer, more effective vaccine. Identification of the immunological correlates of protection is therefore an essential prerequisite for vaccine development. Recent evidence indicates a role for CD8 T cells in protective immunity. We therefore sought to investigate the role that CD8 T cells play during pulmonary infection with *Mycobacterium tuberculosis* to elucidate the protective effector functions and ultimately determine if epitopes targeting CD8 T cells should be included in candidate tuberculosis vaccines.

In order to understand the CD8 T cell response, we began these studies by characterizing the magnitude and the kinetics of CD8 T cell recruitment into the infected lung, in conjunction with phenotypic characterization of the CD8 T cell response to pulmonary infection with *M. tuberculosis*.

Observations by our laboratory of the preferentially peripheral location of CD8 T cells around the murine granuloma led us to examine CD8 T cell expression of integrin adhesion molecules. Although we were ultimately unable to correlate poor migration with deficient integrin molecule expression, we were able to verify the presence of four principal integrin molecules on CD8 T cells and observe their upregulation and maintenance following infection.

Further experiments were performed to phenotypically define the CD8 T cell population following aerosol infection with *M. tuberculosis*. We examined multiple surface markers of activation and costimulation, as well as markers associated with memory in mice infected with *M. tuberculosis* and in memory-immune mice that were infected and subsequently treated using a combination anti-tuberculosis drug regimen. In these experiments, we characterized not only the total CD8 T cell population in the lungs and spleens of mice, but also an antigen-specific CD8 T cell subpopulation using a novel MHC class I tetramer reagent containing a peptide epitope located within the *M. tuberculosis*-derived Mtb32 secreted protein. In subsequent experiments, we characterized the cytokine secretion profile and expression of cytolytic effector molecules by the responding CD8 T cell population following infection. These experiments allowed us to precisely observe the phenotypic changes that occurred following aerosol infection, as well as document the phenotypic changes associated with the emergence of CD8 memory T cells following chemotherapeutic-induced reduction of bacterial numbers.

In chapter three, we utilized the MHC class I tetramer reagent to track Mtb32-specific CD8 T cells in the lungs of mice infected with *M. tuberculosis*. We were able to characterize the antigen-specific response to this protein over time in both infected mice

and mice that were first immunized with the protective candidate Mtb72F vaccine. These experiments revealed an early, robust antigen-specific CD8 T cell response possessing interferon-gamma secreting ability in the lungs after aerosol infection, the size of which temporally correlated with immunologic control of bacterial replication. We were further able to demonstrate the induction of an antigen-specific memory response following immunization with a novel liposomal/protein vaccine adjuvant. Other experiments utilizing this tetramer reagent in conjunction with mice lacking CD4 T cells defined the requirement for CD4 T cell help in augmenting the CD8 T cell response.

Chapter four outlines experiments examining the antigen-specific CD8 T cell response to the Mtb10.3/Mtb10.4 vaccine candidate proteins. Although CD8 T cell-directed immunization with the minimal peptide epitope failed to confer protection in the lungs of mice, an exceptionally large and persistent antigen-specific CD8 T cell response possessing cytolytic activity directed against this single antigenic peptide was observed. The significance of this large but nonprotective CD8 T cell response remains to be determined.

In these studies, we were able to comprehensively characterize the pulmonary recruitment kinetics, surface phenotype and cytokine secretion profile of the CD8 T cells responding to pulmonary tuberculosis infection in a murine model. Importantly, we were able to track and characterize with precision the antigen-specific CD8 T cell response directed against the Mtb32 and Mtb10.3/Mtb10.4 *M. tuberculosis*-derived proteins over the course of infection.

These experiments have further demonstrated that antigen-specific CD8 T cells can be targeted by multiple different immunization regimens, including liposomal, DNA,

and protein in adjuvant combinations containing *M. tuberculosis*-derived antigens that possess CD8 T cell epitopes. In addition, we have shown that the cells elicited by immunization rapidly traffic to the lungs following aerosol infection and secrete interferon-gamma; a cytokine known to be protective during tuberculosis infection. We were able to monitor these cells over the timecourse of infection to determine the magnitude and duration of the CD8 T cell response. We have also shown that CD8 T cells elicited by vaccination can express phenotypic markers associated with a memory phenotype, which is the ultimate goal of a successful vaccine.

These studies have contributed to the collective knowledge of the CD8 T cell response during pulmonary infection with *M. tuberculosis* in the hope that a better understanding of this response will aid in rational vaccine design and selection of candidate antigens for incorporation into future tuberculosis vaccines.

Scott M. Irwin
Department of Microbiology, Immunology, & Pathology
Colorado State University
Fort Collins, CO 80523
Summer, 2006

ACKNOWLEDGEMENTS

First of all, I would like to thank Dr. Ian Orme not only for accepting me into the laboratory and funding my graduate research, but also for allowing me the freedom to examine some of the interesting questions that arise during the course of scientific investigation. Through his hard work, he helped to establish a truly first-rate research facility, with access to all of the reagents and materials necessary to safely investigate the intricacies of a pathogenic organism.

As a good foundation is essential for a successful scientific career, I would like to thank Dr. Joanne Turner for getting me started on the right foot, and for her honest discussions and critical observations which significantly impacted the course of my scientific development.

I would also like to thank Dr. Andre Kipnis for overseeing my training and taking a personal interest in ensuring that my work was both technically proficient as well as conducted safely within the confines of the biosafety level 3 environment. I must also thank him for his endless patience in answering all of the questions a novice researcher could think up, as well as for his insightful discussions and expertise regarding immunity to tuberculosis. As flow cytometry comprised a significant proportion of my graduate work, I would like to thank Ana Paula Junqueira-Kipnis for her expert training in the practice and methodologies of flow cytometry. I am forever indebted to both of the Kipnis researchers, as their strong work ethic and passion for science helped to set the tone of my graduate studies.

Most importantly, I would like to extend my sincerest thanks to Dr. Angelo Izzo; who unselfishly stepped into the role of a mentor, freely donating both his time and considerable expertise to guide not only the direction of my graduate research, but my development as a scientist as well. His constant accessibility and expert knowledge of the field strengthened my experiments and prevented time-consuming mistakes, while his Aussie sense of humor encouraged me to critically evaluate and interpret data in a scientifically sound, defensible manner. Through the course of our many discussions, I was able to acquire and refine the essential skill of critical analysis, as well as engage in scientifically-based speculation, which ultimately provides the basis of rational hypothesis generation. I can honestly say that without his support and encouragement, my tenure as a scientist would have ended prematurely and this work would not have been possible.

Lastly, I would like to thank all of the members of my graduate committee for their insightful comments and for their participation in my graduate studies.

TABLE OF CONTENTS

LIST OF TABLES

LIST OF FIGURES

LIST OF ABBREVIATIONS

AIDS	Acquired Immune Deficiency Syndrome
APC	Antigen Presenting Cell
APC	Allophycocyanin
ATP	Adenosine Triphosphate
β_2-M	β_2-Microglobulin
BCG	Bacille Calmette-Guérin
BSA	Bovine Serum Albumin
C-terminus	Carboxyl Terminus
CCL19	Chemokine Ligand 19
CCR7	Chemokine Receptor 7
CD	Cluster of Differentiation
CFP	Culture Filtrate Protein
CFSE	Carboxyfluorescein Diacetate, Succinimidyl Ester
CFU	Colony Forming Unit
CpG	Hypomethylated Cytosine-Guanine
CTL	Cytotoxic T Lymphocyte
CTLA	Cytotoxic T Lymphocyte-Associated Protein-4
DC	Dendritic Cell
DC-SIGN	Dendritic Cell Specific ICAM-3 Grabbing Nonintegrin
DDA	Dimethyl Dioctadecylammonium Bromide
DMEM	Dulbecco's Modified Eagle Medium
DNA	Deoxyribonucleic Acid
DOTS	Directly Observed Treatment, Short Course
dsRNA	Double-Stranded Ribonucleic Acid
E. coli	*Escherichia coli*
EBV	Epstein Barr Virus
ELISPOT	Enzyme-Linked ImmunoSpot Assay
ER	Endoplasmic Reticulum
ESAT-6	Early Secreted Antigenic Target-6
$F(ab')_2$	Fragment Antigen-Binding, Divalent
Fc	Fragment Crystalizable
FITC	Fluorescein Isothiocyanate
$\gamma\delta$	Gamma-Delta T Cell
G+C	Guanine + Cytosine
GTP	Guanine Triphosphate
HCMV	Human Cytomegalovirus
HEPES	4-(2-Hydroxyethyl)-1-Piperazineethanesulfonic Acid
HIV	Human Immunodeficiency Virus
HLA-E	Human Leukocyte Antigen E
HML-1	Human Mucosal Lymphocyte-1 Antigen
HRP	Horseradish Peroxidase
ICAM	Intracellular Adhesion Molecule
IFN-γ	Gamma Interferon

IgG	Immunoglobulin G
IL	Interleukin
i.m.	Intramuscular
INH	Isoniazid
i.p.	Intraperitoneal
i.v.	Intravenous
kDa	Kilodalton
KO	Knock-out
L. monocytogenes	*Listeria monocytogenes*
LB Broth	Luria-Bertani Broth
LCMV	Lymphocytic Choriomeningitis Virus
LDA	Low Dose Aerosol Infection
LFA-1	Leukocyte Function-Associated Antigen-1
LMP2	Low Molecular Weight Polypeptide 2
LMP7	Low Molecular Weight Polypeptide 7
LMW CFP	Low Molecular Weight Culture Filtrate Protein
LN	Lymph Node
LPAM-1	Leukocyte Peyer's Patch Adhesion Molecule-1
LPS	Lipopolysaccharide
M. avium	*Mycobacterium avium*
M. bovis	*Mycobacterium bovis*
M. leprae	*Mycobacterium leprae*
M. tuberculosis	*Mycobacterium tuberculosis*
MadCAM	Mucosal Addressin Cell Adhesion Molecule
MCP-1	Monocyte Chemoattractant Protein-1
MECL1	Multicatalytic Endopeptidase Complex-Like 1
MHC	Major Histocompatability Complex
MPL-SE	Monophosphoryl Lipid A-Squalene Emulsion
mRNA	Messenger Ribonucleic Acid
N-terminus	Amino Terminus
NK	Natural Killer Cell
OCT	Optimal Cutting Temperature Compound
OVA	Ovalbumin
PA28	Proteasome Activator 28
PAMPs	Pathogen-Associated Molecular Patterns
PAS	para-Aminosalicylic Acid
PBS	Phosphate Buffered Saline
PD-1	Programmed Cell Death-1
pDNA	Plasmid DNA
PE	Phycoerythrin
PerCP	Peridinin Chlorophyll *a* Protein
PG	Peptidoglycan
PMN	Polymorphonuclear Cells
PPD	Purified Protein Derivative
PRR	Pattern Recognition Receptor
PZA	Pyrazinamide

RIF	Rifampin
s.c.	Subcutaneous
S.E.M.	Standard Error of the Means
TAP	Transporter Associated with Antigen Processing
TB	Tuberculosis
T_C	Cytotoxic T Cell
T_{CM}	Central Memory T Cell
TCR	T Cell Receptor
T_{EM}	Effector Memory T Cell
T_H	Helper T Cell
Tim-3	T Cell Immunoglobulin and Mucin Domain-Containing Molecule-3
TLR	Toll-like Receptor
TNF-α	Tumor Necrosis Factor Alpha
T_{reg}	Regulatory T Cell
VCAM	Vascular Cell Adhesion Molecule
VLA-4	Very Late Antigen-4
WHO	World Health Organization

Chapter 1

Literature Review

The Epidemiology of Tuberculosis

It is estimated that one-third of the world is currently infected with *Mycobacterium tuberculosis*, the causative agent of tuberculosis. To define it more precisely, in a world of approximately 6.2 billion people, 1.86 billion are believed to be currently infected. In a recent epidemiological study, there were an estimated 8.3 million new cases of tuberculosis in the year 2000, and approximately 1.8 million people died as the result of infection with *M. tuberculosis* [68]. Of the almost 2 billion people currently infected, approximately 10% of them will at some time during their lives present with active tuberculosis disease [245, 275]. Due to the increased susceptibility of tuberculosis recrudescence in human immunodeficiency virus (HIV) infected individuals, this 10% lifetime risk markedly increases to a 10% annual risk [41, 105, 218]. While the percentage of people who exhibit symptoms of active disease appears quite low when compared to the infectious potential of other diseases, this still translates into almost 3.9 million new cases of active tuberculosis disease per year [290]. On a global scale, these numbers are absolutely staggering.

The fact that greater than 98% of new tuberculosis cases occur in developing countries underscores the disproportionately higher economic and social burden placed upon countries with already severely limited economic resources at their disposal to combat this problem [84]. To further complicate this situation, the majority of new cases of tuberculosis occurred within the healthiest and most productive segment of the population; adults between the ages of 15-49 years of age [68]. Therefore tuberculosis is

not only responsible for a tremendous amount of death and human suffering, it also places an immense drain on the economic productive potential of afflicted nations.

While the incidence of tuberculosis within industrialized nations has been declining at a steady rate, the total number of new tuberculosis cases worldwide increased at a rate of 1.8% per year between 1997 and 2000 [68]. Two factors primarily account for the observed increase in tuberculosis cases: the HIV/AIDS pandemic and the emergence of multidrug-resistant strains of tuberculosis. In 2000, 11% of all new tuberculosis cases within the adult population occurred in persons coinfected with HIV [68]. To further illustrate the magnitude of the growing problem, within the sub-Saharan region of Africa, 31% of adult tuberculosis cases were attributable to HIV [68]. To complicate the situation, multidrug-resistant isolates of *M. tuberculosis* are highly prevalent in some parts of Asia and Eastern Europe. In fact, in some Eastern European countries, the incidence of acquired resistance to at least one anti-tuberculosis drug is 100% [186, 289]. The synergistic effect of HIV infection upon both the incidence and the mortality rate of tuberculosis is certain to fuel more rapid increases in the prevalence of multidrug-resistant tuberculosis unless drastic measures are undertaken to control the pandemic spread of both diseases.

Since the mid 1800s, well before the introduction of effective anti-tuberculosis chemotherapy, the incidence of tuberculosis within the United States began to decline. When nationwide reporting was initiated in 1953, the incidence of tuberculosis within the United States was declining rather dramatically, at a rate of about 5.8% per year [199]. This steady decrease in case numbers can be attributed to a multitude of factors that encompass not only advances in infectious disease research, but social and economic

policies as well. Over two hundred years of economic prosperity have endowed the United States with abundant resources to construct and maintain a social infrastructure that has reduced the conditions that promote the spread not only of tuberculosis, but of many infectious diseases. Increased public sanitation, clean drinking water, pasteurization of milk, and a reduction in homelessness, poverty, malnutrition, and overcrowding combined to reduce the prevalence of tuberculosis even prior to the advent of modern chemotherapeutic agents [287]. Access to unsurpassed medical care, rigorous skin test screening of children, and the implementation of multiple drug chemotherapy in conjunction with effective treatment regimens further served to decrease the incidence of tuberculosis.

These advances in medicine and improvements in living conditions, when seen in the afterglow of milestone medical accomplishments such as the discovery of the broad spectrum antibiotic penicillin, widespread control of diseases such as polio and diphtheria, and the imminent eradication of the smallpox virus; led the Surgeon General, William H. Stewart in 1967 to declare that it was "time to close the book on infectious diseases, declare the war against pestilence won, and shift national resources to such chronic problems as cancer and heart disease" [238]. And for an optimistically blissful but remarkably short period of time, this pronouncement seemed to be entirely accurate.

The high standard of medical treatment within the United States, the decreasing prevalence of tuberculosis, and the fact that developing countries harbor the overwhelming majority of fatal tuberculosis cases created an air of complacency towards a pathogen that has infected more people than any other pathogen since the beginning of mankind [84]. That we were wrong to ignore such a formidable opponent became

obvious fifteen years ago, when outbreaks of multidrug-resistant tuberculosis occurred in New York and Miami. In the period from 1985 to 1992 the annual number of tuberculosis cases in the United States increased by 20% [50]. Social and economic collapse abroad fostered increased transmission of tuberculosis while ineffective or prematurely abrogated treatment regimens generated multidrug-resistant strains. These conditions coincided with the HIV pandemic, fueling the spread of tuberculosis while simultaneously increasing its lethality. With the prevalence of *M. tuberculosis* infection approaching 50% in some southeast Asian countries and considering the ease and rapidity of modern travel, it should have come as no surprise that multidrug-resistant tuberculosis would follow the trail of the HIV pandemic to the shores of North America.

The effect of this resurgence in tuberculosis cases within the United States goes beyond incidence and mortality statistics. It is estimated that each case of tuberculosis costs $25,000 to treat, with each case of multidrug-resistant tuberculosis costing ten times more [230]. Estimates of the current cost of tuberculosis control in the United States range from $700 million to $1 billion per year [40].

If a silver lining can be found within so much death and suffering, it is that the tuberculosis outbreaks of the 1990s served to focus world-wide attention on a disease that had been primarily confined to developing countries. In the past twenty years, remarkable advances have taken place in the fields of genetics, bacteriology, drug development, and immunology. Never before have infectious disease researchers had so many powerful tools at their disposal. With renewed attention and continued funding, it is hoped that the "the captain of all these men of death" can finally be silenced [44].

A Concise History of Tuberculosis

Within the archaeological record, evidence exists that *M. tuberculosis* has infected humans almost since the inception of humanity itself. Mycobacteria have been macroscopically identified from human skeletal remains found in Heidelberg, Germany dated to 5,000 B.C., and Egyptian mummies from 3,500 B.C. possess evidence of skeletal manifestations of tuberculosis known as Pott's Disease [59, 175, 208]. Although it was once believed that the Americas were absent of tuberculosis until European colonization, acid-fast bacilli and *M. tuberculosis* DNA have been isolated from the lungs of 1,800 year old mummies in Peru, and skeletal remains dated to 100 B.C. from native Americans living in Illinois and in the Ohio Valley region possessed evidence consistent with tuberculosis [5, 10, 42, 189, 210].

It is important to understand that for the majority of human existence, tuberculosis was a sporadic disease that played a minor role in the realm of human infectious disease. The available evidence indicates that tuberculosis did not become endemic until approximately 10,000 years ago [169]. Small isolated communal bands of hunter-gatherers could not support the widespread dissemination and high infection rates observed in the more modern tuberculosis pandemic. *M. tuberculosis* is above all a persistent pathogen, and this persistence allowed the bacterium to survive throughout human existence until the conditions required for its pandemic spread emerged. The rise of large agrarian societies eventually followed by the even more crowded, unsanitary, and poverty-stricken conditions of the industrial revolution fueled the epidemic spread of tuberculosis. Malnutrition and overcrowded living conditions created an environment

optimized for the rapid transmission of an aerosolized pathogen, as well as for the maintenance of a sufficiently large reservoir of persons presenting with actively infectious disease.

While there has been much speculation as to the precise evolutionary origins of *M. tuberculosis*, it took the miracles of modern genomics and high-throughput DNA sequencing to ultimately shed some light upon this mystery. Originally, it was believed that *M. tuberculosis* evolved from the related pathogen *Mycobacterium bovis*, and that domestication of cattle by early humans served as the critical link for pathogen transmission and adaptation to human hosts [163]. While this explanation was temporally satisfying, there was no conclusive scientific evidence to support this hypothesis. More recently, detailed phylogenetic analysis of genomic deletion patterns by Brosch *et al.* indicated that *M. bovis* and *M. tuberculosis* diverged from a common evolutionary ancestor that most likely possessed human tropism [37, 159].

The Etiologic Cause of Tuberculosis, and the Dawning of Microbiology

Throughout history, a great deal of mythology and superstition has surrounded the unfortunate individuals who have contracted infectious diseases. Ignorance, fear, and an innate sense of self-preservation have intermingled to promote wild speculation in the absence of scientific reason as to the cause of observable pathologies. The historical record regarding tuberculosis is no exception. Many therapeutic treatments with no scientific basis were performed to treat tuberculosis. These practices ranged from

innocuous treatments such as the supposedly curative touch of a monarch or eating the uncooked liver of a wolf, to more physically injurious treatments such as blood letting and artificial pneumothorax which supposedly promoted pulmonary healing by allowing the infected lung to rest [75, 81]. The eventual discovery of the causative transmissible agent of tuberculosis ultimately dispelled these ineffective treatments by providing a scientifically sound framework with which to test and apply medically relevant treatments.

Although the Greek philosopher Aristotle first postulated that tuberculosis was transmissible, it took more than 2,000 years until the causative agent of tuberculosis was conclusively proven. Benjamin Marten is credited with ascribing tuberculosis to a living microorganism that could be transmitted to other humans by aerosolization from the lungs [80]. However, due to the varied manifestations and pathologies caused by *M. tuberculosis*, it wasn't until the early 1800s, nearly 100 years after Marten's observation, that Theophile Laennec first identified the diverse pathological manifestations of disseminated tuberculosis as being the result of a single disease [144, 161].

It took until the latter half of the 1800s before the first scientifically sound experiments regarding the infectious nature of tuberculosis were performed. In 1868, Jean-Antoine Villemin transferred sputum from an infectious human isolate into healthy rabbits, successfully transmitting the disease and inducing a pathological response that mimicked tuberculosis disease in humans [161]. Although these initial experiments established the infectious nature of tuberculosis, they fell short of ascribing the disease to a specific microbiological pathogen.

In 1881, a brilliant German researcher named Robert Koch began performing experiments to definitively identify the etiologic agent of tuberculosis. At the inception of these experiments, Koch realized that to accomplish this goal, he must be able to visually identify the causative bacterium as well as propagate the bacterium under *in vitro* conditions, in a manner whereby he could isolate pure strains for further study. By exploiting the exotic nature of the mycobacterial cell envelope, Koch developed microscopic staining methods to identify mycobacteria from infectious isolates. In addition, he was the first to utilize solid media to propagate bacteria. In conjunction with this, he developed techniques still being used today for obtaining pure bacterial strains from mixed cultures. With these novel tools, Koch applied the scientific method to develop a simplistic set of rational, stepwise postulates to conclusively identify the infectious agent responsible for a particular disease. These postulates, which bear his name in honor of his scientific contributions, state that in order to determine the etiologic agent responsible for a disease: the agent must be present in every case of disease but not in healthy individuals, one must isolate the organism from a diseased individual, propagate the organism in a pure culture, induce the identical disease state in experimental animals infected with the pure culture, and finally re-isolate the same organism from these infected animals following the appearance of disease. This methodology, along with irrefutable evidence that *M. tuberculosis* was the causative agent of tuberculosis, was presented in 1882 at the Berlin Physiological Society [135]. Thus, with that single historic speech, Robert Koch dispelled the mythology surrounding the infectious nature of disease and simultaneously ushered in the age of microbiology and infectious disease research. This single speech forever changed the course of human

history, for once the infectious nature of tuberculosis had been identified, scientifically sound steps could now be taken to treat infected individuals, prevent further transmission, and systematically search for efficacious vaccines and chemotherapeutic agents to eradicate the disease.

While Koch elucidated the causative agent responsible for tuberculosis, the American physician Edward Trudeau was about to uncover the effect that the environment has on the progression, pathology, and ultimate outcome of tuberculosis infection. Afflicted with tuberculosis himself, Trudeau experienced a miraculous recovery which he attributed to the clean air, healthy food, and rest that he experienced while living in the Adirondack mountains in upstate New York. To test the effect of environmental conditions upon the progression of disease, Trudeau housed uninfected and infected rabbits in a damp, dark cellar with minimal food and water, and simultaneously released infected rabbits on a small island containing ample food, water, sunlight, and fresh air. Six months later, all of the infected rabbits living under poor conditions had died of progressive tuberculosis, while all but one of the infected rabbits living on the island under healthy conditions had survived [258]. These results clearly demonstrated that poor environmental conditions had the ability to impact transmission rates by resulting in higher numbers of infectious cases, as well as impact mortality rates attributed to tuberculosis infection.

Physical Characteristics of the Tubercle Bacillus

The *M. tuberculosis* bacillus that Koch originally identified as the etiologic agent of tuberculosis is taxonomically defined as belonging to the Order Actinomycetales, Suborder Corynebacterineae, Family Mycobacteriaceae [30]. While the majority of mycobacteria are nonpathogenic, saprophytic environmental bacteria found ubiquitously in soil and water, a minority have evolved to become intracellular pathogens of vertebrates. The only members of this family that possess medical significance belong to the Genus *Mycobacterium.* Of these, *M. tuberculosis* is the most relevant pathogen of humans.

M. tuberculosis is a facultative intracellular pathogen that primarily infects mononuclear phagocytes and occasionally pulmonary epithelial cells and other nonprofessional phagocytes of humans and other primates. While it normally prefers an aerobic environment, it possesses the metabolic potential to adapt to microaerophilic and anaerobic environments [36]. It is a pleomorphic, rod-shaped bacillus of approximately 1-4 μm in length. It is nonsporeforming, nonmotile, and is considered a slow growing bacterium, having a generation time of 15-20 hours [23, 277]. *M. tuberculosis* is nonencapsulated, and is not known to possess any transmissible or extrachromosomal plasmid DNA.

M. tuberculosis can be routinely cultured *in vitro* upon solid egg-based media such as Lowenstein-Jensen or upon agar-based media such as Middlebrook 7H11. After incubation at 37°C in an environment of 5-10% CO_2 for 10-20 days, 1-3 mm rough, light buff-colored colonies with irregular edges appear. Growth in liquid media is

characterized by serpentine cording resembling rope-like aggregates of bacilli, due to the presence of trehalose dimycolate in the cell wall of mycobacteria. Being primarily an intracellular pathogen, *M. tuberculosis* can tolerate only minor fluctuations in acidity, from pH 6.5-7.0.

M. tuberculosis possesses an extremely complex bacterial envelope that is composed of 60% lipids by dry weight; the primary constituent being long-chain mycolic acids [35, 74]. Due to this lipid-enriched cellular envelope, mycobacteria fall outside of Hans Christian Gram's traditional classification of bacteria, based upon iodine retention in crystal violet stained cells. Although sometimes referred to as weakly Gram positive, *M. tuberculosis* is more appropriately classified as an acid-fast organism based upon its ability to retain the arylmethane dye; carbol fuchsin, when subjected to aqueous acid-alcohol decolorization [23]. It is believed that the unique properties of the mycobacterial cell envelope are responsible for their characteristic staining properties, as mycobacteria with shorter chain mycolic acids or mycobacteria with disrupted cell envelopes stain only weakly acid-fast [82]. Biochemical characterization has revealed that *M. tuberculosis* possesses a thick peptidoglycan layer consistent with that found in other Gram positive bacteria.

Upon publication of the genome sequence of *M. tuberculosis* H37Rv by Cole *et al.*, it was determined that the genome possessed 65.6% G+C content, and consisted of 4,411,532 base pairs containing 4,043 genes that encode 3,995 predicted proteins [61]. Of the almost 4,000 genomically encoded proteins, only 52% have been assigned a function upon annotation [45]. Completion of the entire genomic sequences for *M. tuberculosis*

strains H37Rv and CDC 1551, *M. bovis* AF2122/97, and *M. leprae* have revealed that the mycobacterial genome is highly conserved, possessing a remarkable stability over time [234].

The Route of Infection

Disease caused by *M. tuberculosis* primarily targets the tissues of the lungs, although under certain circumstances, this organism can disseminate and infect almost any anatomical site within the body. The cycle of transmission begins when virulent bacilli within an infected individual erode through the bronchial walls of the lungs and enter the airways. This is normally the result of a breakdown in the protective architecture of the granuloma, and is characterized by caseation of a Ghon focus followed by central necrosis, liquefaction, cavitation, and erosion of bacilli into the airways. This process is responsible for much of the destructive pathology observed within the lungs. When an infected individual coughs, sneezes, or speaks, bacilli contained within aqueous droplets from 1-10 μm in diameter are aerosolized and released into the environment [103]. Each droplet is estimated to contain 1-10 bacilli, and while a single bacillus is capable of transmitting infection in animal models, more realistic estimates of infectious dose indicate that 5-200 bacilli are required for infectivity [103, 284].

Upon inhalation by a healthy contact, a small percentage of bacilli-containing droplets are deeply inhaled into the terminal bronchioles and alveolar sacs, bypassing many of the innate pulmonary physiological barriers. Within the alveolus, bacilli

encounter resident macrophages, and are internalized by a phagocytic process that fails to initiate a respiratory burst which would otherwise be effective in killing the ingested bacilli [93]. Once inside macrophage cells, the bacilli halt normal phagosome maturation by blocking phagosome-lysosome fusion and subsequent acidification, contributing to the intracellular survival of the bacilli. Here the bacilli begin to replicate until a critical threshold is reached, whereby the adaptive immune response is initiated, which ultimately halts bacterial replication. Concurrently, some bacilli traffic to the draining lymph nodes (LNs) either within pulmonary dendritic cells (DCs) or as free bacilli via the draining lymph [103]. At sites of initial infection, there is an occurrence of localized pneumonia and a chronic granulomatous response. Infected and dying macrophages release a variety of chemotactic factors that recruit activated monocytes and lymphocytes into the lung and initiate formation of a protective granulomatous response that effectively sequesters the bacteria by physically walling it off. The granulomatous response surrounding the primary foci of infection may eradicate the organisms entirely through a process that can involve calcification, or this response may successfully sequester but maintain viable bacilli for the life of the host [103]. These bacilli have the potential to cause recrudescent disease under conditions of decreasing cellular immunity caused by age, stress, infection with HIV, or in response to immunosuppressive drug treatment. In a small percentage of individuals, an alternate scenario develops where there is a failure to initially contain the bacilli at the foci of infection within the lungs. This facilitates dissemination of infectious bacilli to extrapulmonary anatomical sites, and results in a condition termed miliary tuberculosis. This condition has a faster progression and a much poorer prognosis when compared to pulmonary tuberculosis.

These pathological events occurs in the vast majority of infected individuals, with approximately 90% of infected individuals mounting a protective response that will either eliminate or control the bacteria for the lifetime of the host. Of the remaining 10% of cases, approximately one-half will present with progressive disease within three years. The remaining half will recrudesce at some point later in life, which is typically associated with a decrease in cellular immunity [63].

The classical symptoms of tuberculosis infection include an initially dry, nonproductive cough that eventually becomes productive and may or may not contain bloody sputum. In the later stages of active disease, progressive weight loss commonly occurs, which gave rise to the name consumption. Fever, night sweats, malaise, and chest pain also accompany infection to a greater or lesser degree.

While transmission of tuberculosis may also occur through ingestion, this process is significantly less efficient than aerosol transmission. This mode of transmission typically occurs with the related pathogen, *M. bovis*, and was relatively common in industrialized nations until pasteurization of milk became a routine practice.

Current Drug Therapy

The discovery of the first effective anti-tuberculosis drug; streptomycin, by Schatz and Waksman in 1944 initiated the modern era of chemotherapeutic treatment of tuberculosis [213]. Only two years later, para-aminosalicylic acid (PAS) was discovered and shown to be effective against tuberculosis [151]. However, less than four years

following the discovery of streptomycin, the emergence of drug-resistant strains of *M. tuberculosis* was documented [48, 64, 70]. Although ominous in nature, the initial manifestations of drug resistance were largely overshadowed by the discovery of isoniazid (INH) in 1952. This drug was shown to be to be highly active, inexpensive, and had few significant side effects [294]. That same year, pyrazinamide (PZA) was introduced and shown to be a highly effective anti-tuberculosis drug, especially for the treatment of latent tuberculosis [162]. These discoveries were soon followed by the addition of rifampin (RIF), one of the most powerful anti-tuberculosis chemotherapeutic agents. Rifampin rapidly became the primary first-line drug for the treatment of tuberculosis and has been a mainstay in anti-tuberculosis treatment since the 1970s. The period of time spanning the mid 1940s through the mid 1960s was truly the Golden Era of tuberculosis drug discovery, as this period of time encompassed the discovery of the majority of front-line anti-tuberculosis drugs still in use today.

Equally important as having a diverse and highly active arsenal of first-line anti-tuberculosis drugs is the method in which they are administered. Although the stability of mycobacterial genomes makes spontaneous mutations that induce drug resistance a rare event, the persistent nature of this organism and the long course of treatment required effectively facilitate the emergence of drug-resistant strains [48, 64]. It was soon realized that multidrug regimens were an effective countermeasure for limiting the emergence of resistant strains of tuberculosis. Combined treatment with PAS and INH for 18-24 months with the addition of streptomycin for the first two months was found to be highly effective, producing cure rates in excess of 97% [98, 136]. Unfortunately, the long timecourse of therapy fostered patient noncompliance, which aided in the emergence and

spread of drug-resistant strains of tuberculosis. As such, a more powerful, shortened course of multidrug therapy was developed and was shown to maintain cure rates in excess of 95%, improve patient compliance, and consequently limit the generation of drug-resistant strains [55, 292]. Based upon these findings, the World Health Organization (WHO) developed the current recommended tuberculosis chemotherapy, termed Directly Observed Treatment, Short course (DOTS). Treatment consists of INH, RIF, PZA, and ethambutol for two months, followed by four months of INH and RIF [291, 292]. The addition of the powerful drugs RIF and PZA allowed for a reduction in the duration of treatment from greater than 12 months to 6 months.

In industrialized nations possessing adequate tuberculosis funding, proper disease surveillance, medical follow-up after treatment, and correct implementation of DOTS, the emergence and transmission of drug-resistant strains was minimized and the incidence of tuberculosis declined sharply. In contrast, within developing nations, political strife and economic collapse lead to an inadequate supply of drugs, poor infrastructure to support detection and follow-up of tuberculosis cases, and a failure to fully or correctly implement DOTS therapy. Improper implementation of DOTS lead to the generation and spread of drug-resistant strains of tuberculosis, including multidrug-resistant strains, defined as possessing resistance to at least INH and RIF [136, 278]. In situations where multidrug-resistant tuberculosis is present, the cure rate using standard DOTS treatment drops from greater than 90% to approximately 50% [76, 123, 133]. In these situations, short course chemotherapy is no longer recommended [86]. The WHO now recommends a modification of DOTS called DOTS-Plus, which consists of DOTS treatment plus second-line tuberculosis drugs for a period of 24 months [292].

Due to failed treatment regimens and patient noncompliance, many individuals have developed acquired drug-resistant infections, defined as the presence of drug-resistant strains in a patient that has previously been treated for tuberculosis for at least one month [194]. In contrast, primary drug resistance is defined as the presence of resistant strains in newly diagnosed individuals who have never received anti-tuberculosis chemotherapy, or received drug treatment for less than one month [194]. From a purely epidemiological perspective, ineffective drug therapy is worse than no treatment at all, for it extends the lives of chronically infected individuals and increases the likelihood of transmission when compared to the significantly shorter lifespans of untreated individuals. Not only do these individuals spread tuberculosis for a longer period of time, but they serve as a reservoir for the dissemination of primary drug-resistant strains within the community. This creates a current and future problem, by spreading cases of tuberculosis that are both more difficult and more costly to treat. In addition, cure rates of multidrug-resistant tuberculosis are significantly reduced and only approach 50% when properly administered [123, 186]. The longer treatment regimen required by DOTS-Plus therapy significantly decreases patient compliance rates, furthering the spread of the most drug-resistant strains. The problem of drug resistance has become so large, that within some regions such as Ivanovo Oblast in Russia, acquired drug resistance to at least one anti-tuberculosis drug is 100% [186]. Even more unsettling, the incidence of primary multidrug-resistant tuberculosis in Estonia increased from 10% to 14% in only four years [194].

To further compound the problem of drug resistance, multidrug-resistant tuberculosis patients coinfected with HIV have a significantly higher risk of presenting

with active tuberculosis and a faster rate of disease progression. In addition, chemotherapeutic treatment regimens are less effective and mortality rates can approach 80% [29, 123, 136]. Unless significant new resources are devoted to the detection and treatment of tuberculosis in developing countries, the worldwide increase in the incidence of tuberculosis will continue to escalate at an ever faster rate. With the rapidity of modern international travel and the increase in global emigration, this will eventually lead to more epidemics of multidrug-resistant tuberculosis occurring within industrialized nations, compromising once successful anti-tuberculosis programs and resulting in substantial financial and human costs.

The Development of a Vaccine – BCG

Due to the enormous global problem of tuberculosis, there has been an intensive search for an effective vaccine. Vaccination provides many benefits over conventional chemotherapy including reduced cost, higher rates of patient compliance, and persistence of lifelong immunity in many instances. Vaccination also circumvents the ever-growing problem of drug resistance encountered with the majority of anti-tuberculosis drugs currently in use. The smallpox virus, the only disease to ever be successfully eradicated from human circulation, was eliminated through the use of an effective strategy of vaccination.

Upon recognition that heat-killed *M. tuberculosis* failed to induce protective immunity in animal models, Trudeau began experimenting with the related pathogen, *M.*

avium in an attempt to develop a live attenuated tuberculosis vaccine. He observed that live *M. avium* could protect against subsequent challenge with virulent *M. tuberculosis* in animal models, although *M. avium* was too virulent for human use [259]. Trudeau next utilized a strain of *M. tuberculosis* known as R1 that had been serially cultured for 11 years, and had been shown to be attenuated for virulence in animal models. All of the rabbits and guinea pigs that received immunization with the R1 strain followed by challenge with virulent *M. tuberculosis* survived, while all of the nonimmunized controls died [259]. Even though these results were highly encouraging, for unknown reasons Trudeau never pursued clinical applications for this vaccine.

In 1908, based upon the observations of bacterial attenuation following prolonged *in vitro* culture, Albert Calmette and Camille Guérin began a process of bacterial attenuation using a strain of *M. bovis* obtained from an infected cow. In a remarkable demonstration of scientific persistence, after 13 years of subculturing the pathogenic isolate upon a medium composed of potatoes, 5% glycerol, and ox-bile, they successfully demonstrated that the new strain was attenuated for virulence and conferred resistance to infection with *M. tuberculosis* both in animal models and ultimately in humans [108]. The live attenuated vaccine strain was named bacille Calmette-Guérin (BCG), and has since been given to over three billion people worldwide, making it the most widely administered vaccine in history.

Although world-wide usage of the BCG vaccine is high, it is the most controversial vaccine currently in use. Throughout the history of its use, BCG has consistently been shown to be safe in most individuals. Adverse reactions are predominantly confined to minor vaccination site reactions. However in 1929, a

preparation of BCG vaccine became contaminated with virulent *M. tuberculosis*, resulting in the death of 72 children [62]. While more rigorous manufacturing controls have since eliminated the risk of contamination, this incident focused attention on the inherent dangers of live attenuated vaccines. Although no evidence exists of reversion of BCG to its previously virulent state, immunization with BCG can cause disease in individuals who are infected with HIV, or in individuals who possess genetic immunological defects. While the risk is rare, these individuals often contract a disseminated form of BCG infection that is usually fatal [34, 273, 279]. Even in light of these rare, potentially fatal complications, BCG is considered a very safe vaccine [91].

The BCG vaccine possesses many other attributes that foster its continued usage. It is inexpensive to manufacture, stable, can be given at birth, and leaves a small scar at the site of inoculation which can be used in future epidemiological monitoring. Vaccination also results in long lasting sensitization, although the correlation with protective efficacy remains unclear [252].

Aside from the considerations of live attenuated vaccine use in immunocompromised individuals, the BCG vaccine has two major disadvantages – a failure to prevent initial infection and inconsistent protective efficacy in clinical trails. An analysis of multiple BCG vaccination studies revealed that the protective efficacy varied from 0-80% [16, 60, 261]. While the range of efficacy within this study was extremely large, further studies indicated that immunization with BCG conferred approximately 50% protective efficacy [58, 60]. It is also believed that while immunization with BCG has variable efficacy against adult pulmonary disease, it appears to consistently protect

children from severe forms of tuberculosis such as disseminated disease and tuberculosis meningitis, which often have fatal outcomes [203].

While the exact cause of the observed variations in the protective efficacy of BCG is unknown, current hypotheses include the genetic variability inherent in different human populations, variation in the regional prevalence or virulence of *M. tuberculosis* strains, differences in the protective efficacy of the multiple strains of BCG currently in use, and the effect of BCG vaccination on individuals harboring prior subclinical tuberculosis infection [198]. While the cause of the variation in efficacy is most likely multifactorial in nature, the most generally accepted explanation involves regional differences in the prevalence of environmental strains of mycobacteria. It has been postulated that previous exposure to environmental mycobacteria might block subsequent BCG replication, resulting in incomplete induction of protective immunity [33]. It has also been proposed that previous sensitization with environmental mycobacteria might induce some level of protective immunity to infection with *M. tuberculosis*, and that subsequent BCG immunization fails to improve upon this [187].

Due to the immense potential that vaccination holds for control of infectious disease, and in light of the variable protective efficacy observed in clinical BCG vaccination trials, a major effort is currently underway to develop a safe, more effective tuberculosis vaccine. Even though the BCG vaccine has questionable efficacy in human trials, it is still the gold standard to which all new candidate vaccines are compared. The absence of any concrete, definitive laboratory correlate of protection in humans is a major challenge to the discovery of more efficacious vaccines. Current work utilizing animal models is underway to elucidate the protective mechanisms involved in resistance to

tuberculosis infection, so that these mechanisms can be specifically targeted by future vaccines.

The Acquired Immune Response to Tuberculosis

After many unsuccessful attempts to transfer passive immunity through the use of immune serum, it became apparent that protective immunity to tuberculosis was cellular in nature. A formal demonstration of this was performed by Suter, and consisted of adoptive transfer of resistance by immune lymphocytes [244]. Utilizing the mouse model, Lefford demonstrated that splenocytes from mice previously sensitized by immunization with BCG could adoptively protect recipient mice that had been irradiated prior to transfer [150]. Furthermore, treatment with anti-thymus serum, but not treatment with anti-immunoglobulin serum prior to adoptive transfer abolished the observed protection, implicating T cells as the cell type that conferred protection. The formal and conclusive demonstration that T cells mediated protection to tuberculosis was performed by Orme and Collins [183, 184]. Utilizing subset-specific complement-mediated antibody depletion of splenocytes prior to transfer, it was demonstrated that T cells transferred adoptive immunity to tuberculosis in irradiated mice.

With the formal understanding that T cells conferred protection to tuberculosis in place, the next obstacle was to define the precise T cell subsets involved in protective immunity, and characterize their activation status and phenotype. In 1987, Orme demonstrated that CD4 T cells adoptively protected irradiated mice at a level equal to

adoptive transfer of mixed splenocytes [182]. While the CD4 T cell population provided the most protection, CD8 T cells were also shown to protect naïve recipient mice, although to a lesser degree than the protection mediated by CD4 T cells [182]. These experiments hinted at the fact that CD8 T cells may play a protective role during infection with *M. tuberculosis*.

Exactly how CD4 T cells mediated the observed protective effect was unknown, but secretion of protective cytokines was a likely explanation. With the development of a mouse model possessing a gene disruption within the IFN-γ gene, experiments demonstrated that these mice were exquisitely susceptible to infection with *M. tuberculosis* [94]. Infection of IFN-γ knock-out (KO) mice was characterized by uncontrolled bacterial replication within the lungs, and death by 40 days following infection. Subsequent experiments by Cooper *et al.* revealed that following infection, IL-12 mRNA levels were increased in the lungs, and that administration of exogenous IL-12 increased the production of IFN-γ, and had a transient positive effect upon the course of infection in mice [67]. Further experiments using an IL-12 p40 KO mouse model revealed that these mice failed to control bacterial replication within the lung, and that this failure was primarily the result of an inability to activate T lymphocytes to produce IFN-γ [66].

Based upon this body of experimental evidence, a model of adaptive immunity to tuberculosis has been developed. This paradigm consists of phagocytic uptake of infectious bacilli within the lungs by nonactivated alveolar macrophages. Nonactivated macrophage cells are unable to kill ingested bacilli, which begin to replicate intracellularly. Upon reaching a critical threshold of bacterial numbers, adaptive

immunity is initiated in the draining LNs by antigen-primed DCs. Activated, antigen-specific CD4 T cells migrate to the lungs and extravasate into the pulmonary airways. Following a chemokine gradient elicited by infected macrophage cells, CD4 T cells encounter infected macrophages at the sites of initial infection and secrete IFN-γ, which serves to activate infected cells. IFN-γ activated macrophage cells respond by producing IL-12, which promotes further IFN-γ production by responding T cells. Activation of macrophage cells also partially reverses the inhibitory effect intracellular bacilli have on phagosome-lysosome fusion, resulting in increased killing of internalized bacilli.

The Role of CD8 T Cells in Immunity to Tuberculosis

While experimental work has clearly identified CD4 T cells as being essential for host control of infection with *M. tuberculosis*, evidence supporting a clear protective role for CD8 T cells is less compelling and often contradictory. Several studies have shown that CD8 T cells arrive within in the lungs of aerosol-infected mice within one week of infection [88, 219]. These cells possess an activated surface phenotype, consisting of $CD44^{hi}$, $CD62L^{lo}$, $CD45RB^{lo}$, LFA-1^{hi}, and VLA-4^{hi} [88]. Furthermore, it was demonstrated that activated CD8 T cells arriving in the lungs of infected mice could produce IFN-γ as well as TNF-α upon *ex vivo* restimulation, indicating that these cells were actively responding to infection. While the temporal association between the initiation of infection and the arrival, activation status, and cytokine production implied a

protective role for CD8 T cells during pulmonary infection, further research was required to conclusively define a protective role for this subpopulation of cells during infection.

Early work using *in vivo* antibody depletion of specific T cell subsets implicated CD8 T cells as contributing to protection during pulmonary infection with tuberculosis. Experiments by Kaufman's laboratory using an intravenous infection model demonstrated that depletion of CD8 T cells impaired resistance to subsequent challenge with virulent tuberculosis [177]. Further experiments utilizing antibody depletion followed by a more realistic, low dose aerosol challenge with *M. tuberculosis* confirmed these results and noted a shortened lifespan as well as histopathological differences in the pulmonary granulomas of CD8 T cell depleted mice [152]. It was later shown that CD8 T cells also played a protective role following infection with avirulent *M. bovis* BCG [143]. Taken together, these results indicate that while CD8 T cells do contribute to protection as measured by recoverable colony forming unit (CFU) counts, the protective function that these cells exhibit during infection might well be to reduce or limit the destructive pathology associated with pulmonary tuberculosis infection, and therefore the significance of this effect is only revealed upon histological examination or by the use of time-to-death experiments.

Although the T cell depletion data provided a tentative link between CD8 T cells and adaptive immune protection during infection, the adoptive transfer experiments by Orme in 1987 conclusively demonstrated that while CD4 T cells mediate the majority of protection following challenge infection, adoptively transferred CD8 T cells also protect recipient mice [182]. At 10 days following infection, modest reductions in bacterial numbers were observed in irradiated mice that received CD8 T cells from *M. tuberculosis*

infected donors. In a complementary study, both CD4 and CD8 T cell-depleted splenocytes obtained from *M. tuberculosis* infected and antibiotic treated donor mice were able to confer protection [119]. These experiments lent evidence to the idea that not only can CD8 T cells mediate protection, but that protective CD8 memory T cells were generated during infection, and therefore could be targeted by vaccination.

In another study that utilized an aerosol infection-based modified Cornell model of latent infection, antibody depletion of CD8 T cells during acute infection had no discernable effect [268]. Conversely, antibody depletion during the latent stage of infection resulted in a significant increase in the bacterial burden within the lungs. These data support the idea that CD8 T cells exert their greatest protective effect during the chronic stage of infection, and may represent an important mechanism preventing recrudescent disease later in life.

With the advent of techniques for the genetic manipulation of the mouse model, a series of mice with targeted gene disruptions were engineered in an attempt to precisely define the role that CD8 T cells play during infection with tuberculosis. Mice lacking CD8 T cells were first generated through targeted deletion of the β_2-M accessory molecule required for MHC class I expression by antigen presenting cells (APCs) [137]. Flynn *et al.* utilized this model to examine the requirement for CD8 T cells following intravenous infection with *M. tuberculosis* [96]. These studies demonstrated a significantly increased susceptibility to infection in β_2-M KO mice when compared to control mice, as measured by CFU counts in the lungs, spleen, and liver. The survival of these KO mice was also drastically impacted, with all mice succumbing to disease by 10 weeks following infection, compared to no deaths in the control group. Further studies by

D'Souza *et al.* utilizing the low dose aerosol route of infection confirmed the increased susceptibility of the β_2-M KO mouse model and in addition, careful histological examination revealed that the β_2-M KO mice failed to efficiently recruit lymphocytes into pulmonary lesions [83]. Furthermore, this novel β_2-M-associated defect was independent of MHC class I and CD1 molecules.

While these results were initially intriguing and implicated a prominent role for CD8 T cells during infection, an increased understanding of the immune system has revealed significant limitations in the β_2-M KO mouse model. The β_2-M accessory molecule is found not only in the classical MHC class Ia molecules which present antigen to conventional $\alpha\beta$ TCR^+ CD8 T cells, but it is also a component of several nonclassical MHC class Ib molecules and the CD1 molecule, as well as a mammalian transferrin receptor. Disruption of the β_2-M molecule therefore has a broad effect on multiple antigen presentation pathways, as well as adverse effects upon host iron metabolism [211]. In retrospect, utilization of this model does not distinguish between the protective effect of classically restricted CD8 T cells from nonclassically restricted CD8 T cells.

Studies involving mice in which the TAP1 molecule was genetically disrupted were also performed, to circumvent the complications associated with the β_2-M KO mouse model [19, 232]. In experiments using intravenous infection, decreased survival times as well as greater organ bacterial burdens were observed, indicating an increased susceptibility of TAP KO mice to infection [19]. Unfortunately, this mouse model also suffers from an inherent drawback. The TAP molecules transport short peptide fragments into the endoplasmic reticulum (ER) for assembly onto classical MHC class Ia molecules. However, through a process termed ER retrograde transport, certain specific peptides

such as signal sequence fragments can be transported out of the ER, for TAP-mediated reentry and assembly onto nonclassical MHC class Ib molecules such as H2-M3 or Qa-1. Similar to the β_2-M KO mouse model, the TAP KO model also fails to ascribe the increased susceptibility of these mice to either classically or nonclassically restricted CD8 T cells.

To overcome the inherent limitations present in the β_2-M and TAP KO mouse models, mice lacking the CD8α coreceptor were generated. Using an intravenous infection model, the susceptibility of β_2-M KO and CD8α KO mice was directly compared [232]. It was noted that the β_2-M KO mice had approximately 1-$\log_{10}$ CFU more bacteria in the lungs at 80 days following infection and survived two months less than the CD8α KO mice. Importantly, while β_2-M KO mice clearly possessed an increased susceptibility to infection, the CD8α KO mice also possessed an increased susceptibility when compared to wild-type control mice. CD8α KO mice had approximately 0.5-$\log_{10}$ more bacterial lung burden and survived on average two months less than controls. These results were confirmed and extended by Turner *et al.* who showed that mice lacking the CD8α coreceptor can initially contain infection as well as control mice, but that this control is gradually lost beyond 50 days following infection, even in the presence of IFN-γ at levels equal to or greater than control mice [262].

Although the CD8α KO mouse model confirmed the increased susceptibility of mice lacking CD8 T cells following infection, there are inherent problems with this mouse model as well. The CD8 and CD4 coreceptor molecules serve to increase the overall avidity of TCR-MHC class I molecule interactions, and facilitate increased signaling at the immunological synapse. During thymic selection within normal mice, T

cells of intermediate avidity are selected for survival while T cells that possess very low or exceedingly high avidity are deleted. In the absence of the CD4 coreceptor, it appears that an increased TCR-MHC class I avidity can compensate for the lack of this coreceptor, permitting thymic survival of cells destined to become CD4 positive T cells, but which fail to express the CD4 molecule [263]. This same scenario is likely to occur during thymic selection in the CD8α KO model. Therefore the CD4 and CD8α mouse KO models may possess cells that are functionally CD4 or CD8 T cells, but that phenotypically lack the expression of the these surface molecules.

The conclusive experiments ascribing a protective role to the CD8 T cell population were performed in MHC class I KO mice, and in the H-2K^b/H-2D^b double KO mouse models [171, 205, 264]. These studies are in agreement that CD8 T cells, while not as effective as CD4 T cells, aid in adaptive immunological control of bacterial numbers in the lung. In addition, work using the H-2K^b/H-2D^b KO mouse model confirmed the histological findings of D'Sousa *et al.*, further implicating MHC class I molecules as playing a central role in the organization and construction of protective granulomas and/or recruitment of lymphocytes into infectious foci [83, 264]. Collectively, these studies demonstrated that classically restricted CD8 T cells participate in the protective immune response in the lungs of mice infected with tuberculosis [171, 205, 232, 264].

The Effector Functions of CD8 T Cells

With the understanding that CD8 T cells contribute to the ability of the adaptive immune system to control bacterial replication in the lungs, significant progress has been made in defining how CD8 T cells mediate this protective effect, and in specifically targeting the induction of CD8 T cells by vaccination.

CD8 T cells possess two primary effector mechanisms: lysis of cells by the granule exocytosis pathway or through contact-dependent Fas-FasL interactions, and secretion of protective cytokines. CD8 T cells play an essential role during many viral infections, and current evidence suggests that the primary effector mechanism involves the granule exocytosis pathway. After CD8 T cell recognition of an infected cell, endosomes containing cytotoxic molecules such as perforin and serine proteases termed granzymes are mobilized and released in a directional fashion to the immunological synapse between the cytotoxic lymphocyte (CTL) and the infected target cell. It is currently believed that the secretory endosomes released by the CTL are endocytosed by the target cell, where perforin molecules polymerize within the endosomal membrane, facilitating the release of granzymes into the cytoplasm of the target cell [52]. Granzymes then act upon caspase 3 to initiate mitochondrial damage, DNA fragmentation, and ultimately apoptosis [256].

Based upon viral infection models, the search for the effector function of mycobacteria-specific CD8 T cells initially began by examination of cytolytic activity. Early experiments by De Libero *et al.* generated cell lines from mice infected with *M. tuberculosis*, and identified cytolytic CTLs that were able to lyse mycobacteria-primed

macrophage cells [77]. Subsequently, many other groups identified CD8 T cells possessing cytolytic activity both in humans and in the mouse model [145, 220, 227, 237].

While these results seemed to indicate that CD8 T cells mediate their anti-mycobacterial activity by lysing infected cells, experiments by Cooper *et al.* using perforin KO and granzyme KO mice clearly demonstrated that within the first 80 days of infection these cytolytic molecules did not affect the bacterial numbers in the lungs [65]. Similar experiments by multiple groups failed to observe any decrease in protection in perforin KO mice [46, 147, 232].

Contact-dependent cytolytic activity is also an important cytotoxic mechanism utilized by CD8 T cells. Multiple cell types express the Fas molecule. Upon ligation of Fas by CTL expressing FasL, intracellular signaling events are initiated, ultimately resulting in target cell apoptosis. Similar experiments were therefore performed to examine the contribution of CTL-mediated Fas-FasL induced cell death during infection with tuberculosis. Turner *et al.* examined the progression of disease in both Fas and FasL KO mice, and while these KO mice were not different from wild-type controls within the first 30 days following infection, the bacterial numbers in the lungs of both KO strains significantly increased during the chronic phase of infection [262]. In addition, histological examination of the granulomatous response revealed an uncharacteristic necrotic degeneration of infectious foci and an influx of neutrophils in the absence of an intact Fas-FasL apoptotic pathway.

Cytokine secretion by activated CD8 T cells is an important, although underappreciated mechanism of CTL function. In fact, CD8 T cells have been shown to

produce IFN-γ and TNF-α, both of which are known to have anti-mycobacterial activity [94, 95]. Following the successful demonstration that adoptively transferred CD8 T cells can protect a recipient host, Orme postulated that the most likely protective mechanism was via production of IFN-γ [185]. As previously noted, CD8 T cells capable of rapidly producing IFN-γ are recruited to the lungs within one week following aerosol infection [88, 182, 219]. In a series of elegant experiments by Tascon *et al.*, adoptive transfer of CD8 T cells from IFN-γ KO donor mice, but not from control donor mice, failed to protect recipient athymic mice following intraperitoneal infection [250]. However, on average CD8 T cells produce one-half to one-tenth the amount of IFN-γ as CD4 T cells, making them rather inefficient at IFN-γ production [47]. These experiments confirmed that the primary role of CD8 T cells during acute tuberculosis infection is exerted through production of IFN-γ. That the mechanism by which CD8 T cells protect may revert to a cytolytic mechanism during the chronic phase of infection was indicated by the perforin and Fas KO studies and the chronic phase CD8 T cell depletion experiments previously described [262, 268]. Thus, it appears that rapid accumulation of IFN-γ-secreting CD8 T cells into the lungs may augment CD4 T cell-derived IFN-γ, aiding in early adaptive control of bacterial replication. However, during the chronic phase of infection, immunosurveillance by activated, antigen-specific CD8 T cells may serve to lyse infected macrophage cells that attempt to escape the confines of the protective granuloma.

Due to the increasing evidence that CD8 T cells play a protective role in adaptive control of pulmonary infection with *M. tuberculosis*, there has been a directed effort to identify *M. tuberculosis*-specific CD8 T cell epitopes for inclusion in candidate tuberculosis vaccines. Currently, a number of murine CD8 T cell epitopes have been

discovered and characterized, underscoring the fact that CD8 T cells have the ability to recognize a diverse array of *M. tuberculosis*-specific antigens (Table 1.1).

The Classical MHC Class I Antigen Processing Pathway

In the past 30 years, a vast amount of information has been added to our understanding of how CD8 T cells recognize infected cells, since the discovery of MHC class I restriction of CD8 T cells by Zinkernagel and Doherty in 1974 [298]. The requirement for antigen processing prior to antigen presentation was elucidated by Ziegler and Unanue, to be followed shortly by the discovery that CD8 T cells recognized virally infected cells by their surface expression of small virus-derived peptide fragments rather than whole protein molecules [255, 297]. Since these seminal discoveries, the majority of players in the sequence of events known as antigen processing and antigen presentation have been elucidated, and their functional significance revealed.

CD8 T cells evolved to identify malignant cells or cells infected with viruses or intracellular bacteria. They accomplish this by constantly surveilling small peptide epitopes bound to MHC class I antigen presentation molecules expressed on the surface of all nucleated cells in the body. Recognition of a foreign peptide epitope by CD8 T cells results in T cell activation, clonal proliferation, and initiation of cytokine secretion and/or cytolytic activity. These mechanisms serve to increase the number of antigen-specific cells capable of responding to a particular pathogenic organism and allow for the secretion of cytokines capable of warning nearby cells of the infection and halting viral

replication. In the event that cytokine activation of infected cells fails to eliminate the pathogen, CD8 T cells are equipped with a more deadly arsenal composed of perforin and associated granzyme molecules that have the ability to lyse infected cells.

Critical factors influencing the repertoire of epitopes presented by a cell include the efficiency of liberating the peptide epitope from the parent protein, the relative abundance of the antigenic protein, resistance of the epitope to cytosolic endopeptidase attack, efficiency of peptide transport into the ER, MHC class I-peptide affinity, and levels of MHC class I/peptide complexes expressed upon the surface of cells [178]. The combination of these factors ultimately determines the efficiency of pathogen recognition by CD8 T cells following infection.

The Proteasome - Generation of Peptides

The major function of the proteasome is to degrade cytosolic proteins to generate a pool of peptides from which immunodominant epitopes can be selected for transport into the ER. Targeting of cytosolic proteins for degradation is based upon the ATP-dependent ubiquitin-proteasome pathway [57]. Ligation of the poly-ubiquitin peptide motif to a target protein acts as a molecular tag for proteolytic destruction within the proteasome complex. Both the ubiquitin-protein ligase and the proteasome require ATP for substrate degradation to occur.

The constitutively active 26S proteasome is a hollow, barrel-shaped multisubunit cytosolic protease found within eukaryotic cells. It is composed of a 20S core attached to

two 19S regulatory subunits which aid in substrate recognition. The 20S core is composed of four heptameric rings of approximately equal diameter, stacked atop each other. The two identical outer rings are constructed of seven different α subunits, and the two identical inner rings are constructed of seven different β subunits. Three of the β subunits possess proteolytic activity responsible for the catabolic function of this complex. The outer rings serve to restrict proteolytic activity to the interior of the complex, and form a gate to prevent access of non-ubiquitinated substrates. The 19S regulatory complexes are attached to the outer rings of the 20S core, and facilitate recognition of the poly-ubiquitinated substrates and subsequent opening of the central gate in an ATP-dependent manner. The 19S complexes also possess reverse-chaperone activity to unfold proteins into the linear conformation necessary for entrance into the proteasome.

Although the 26S proteasome is constitutively active, the presence of IFN-γ has been shown to dramatically upregulate this system [39, 106]. The three proteolytically active β subunits have corresponding IFN-γ-inducible homologs (LMP2, LMP7, MECL1) that possess proteolytic activity and replace their constitutive partner upon IFN-γ induction. The presence of IFN-γ also upregulates expression of the proteasome activator complex PA28, which increases the efficiency of antigen processing by an as yet undefined mechanism. It has been speculated that the addition of PA28 facilitates substrate entry into or product exit from the proteasome, or that it may preferentially generate slightly longer peptides of 8-11 amino acids in length which more readily bind to MHC class I molecules [239, 243]. The addition of these IFN-γ-inducible components to the proteasome generates a complex called the immunoproteasome. IFN-γ-inducible

immunoproteasomes have been associated with altered cleavage site preferences and an improved ability to generate peptides that are more favorable for MHC class I binding [225, 267, 295].

Although some controversy still exists, it is believed that the exact C-terminus of the peptide epitope is generated by proteasomal cleavage, while the exact N-terminus may or may not be proteasomally generated [69, 85, 179, 231]. When N-terminally extended peptide fragments are generated by the proteasome, the extra amino acids are removed by ER or cytoplasmic endopeptidases that perform N-terminal trimming to generate the exact epitope sequence required for optimal MHC class I binding [179, 181]. Upon release from the proteasome, peptide fragments are protected from cytosolic degradation by chaperone molecules until they reach the ER [142].

That proteasome activity is essential for the generation of the majority of peptides required for antigen presentation was established by Rock *et al.* through the use of highly-specific proteasome inhibitors [201, 202]. These results demonstrated that the proteasome and not other cellular proteases was responsible for the majority of peptide generation. The fact that the Epstein-Barr virus (EBV) specifically targets the proteasome degradation portion of the antigen presentation pathway to avoid CTL recognition underscores the important role this organelle plays in recognition of virally-infected infected cells. The EBV nuclear antigen 1 protein contains a repeated Gly-Gly-Ala motif that has been shown to become ubiquitinated, but is degraded much less efficiently by the proteasome complex [153]. Thus, avoidance of viral protein degradation may facilitate pathogen persistence by preventing antigen presentation and ultimately CTL detection.

The TAP Complex - Transport of Peptides

The TAP proteins belong to the ATP-binding cassette family of transporter proteins. They are transmembrane proteins embedded within the membrane surrounding the ER in the form of a heterodimeric complex composed of TAP1 and TAP2 subunits. They contribute to antigen presentation by shuttling small peptide fragments generated within the cytosol into the lumen of the ER where they can be loaded into the peptide binding groove of newly synthesized MHC class I molecules. As such, they not only serve as a peptide transport mechanism, but their inherent specificity for peptide length and peptide charge characteristics modifies the composition of the available peptide pool within the ER, and therefore contributes to the repertoire of peptides that can be expressed on the surface of a given cell.

TAP proteins normally transport peptides in the range of 15 amino acids or less with a higher efficiency, as these peptides are the optimally suited length for binding to MHC class I molecules [173, 266]. Because the TAP proteins are encoded within the MHC locus, there are suggestions of coevolution in transporter peptide specificity and MHC class I polymorphic binding patterns to cooperatively optimize the display of antigenic epitopes [168]. In fact, it is believed that the proteasome, TAP proteins, and MHC class I molecules co-evolved for the efficient generation, transport, and presentation of peptide fragments to more readily facilitate the detection of infected or transformed cells.

TAP proteins serve a vital link in the antigen presentation pathway required for the detection of intracellular pathogens by CD8 T cells. The observation that some

viruses have evolved immune subversion mechanisms that specifically target TAP proteins is an indication of their importance in the overall antigen presentation process. For example, the herpes simplex viral protein ICP47 binds to the cytosolic face of the TAP complex, physically blocking importation of peptides into the ER lumen [101]. The human cytomegalovirus (HCMV) adopts a similar strategy to prevent the surface display of its antigenic proteins by encoding a protein that blocks TAP transporter function, although this occurs on the luminal side of the ER rather than on the cytosolic side [3]. Thus, the targets of viral subversion mechanisms serve as an indication of the critical importance of these components within the overall antigen presentation pathway.

Generation of MHC class I Molecules - Antigen Presentation

MHC class I molecules are expressed on the surface of virtually all nucleated cells. Therefore, their expression is not confined solely to professional antigen presenting cells. MHC class I molecules are a trimolecular complex composed of a class I heavy chain, the β_2-M accessory molecule, and a cognate peptide that may be either self- or nonself-derived. All three of these components are required for proper folding, stability, and surface expression of the MHC class I molecule. MHC class I heavy chain molecules are encoded by three loci in the mouse, identified by the designation K, D, and L. These regions code for the MHC class I heavy chain, which is composed of $\alpha 1$, $\alpha 2$, and $\alpha 3$ globular domains, a transmembrane domain, and a short cytoplasmic tail. Although the cytoplasmic tail is too short to support intracellular signaling, recent evidence suggests

that it is involved in endosomal trafficking [155]. The two most distal globular domains, α1 and α2, are known be highly polymorphic and constitute the peptide binding groove. The peptide binding groove is structurally defined by two parallel α-helices resting atop a flat base composed of β-pleated sheet structure. This binding groove possesses multiple, highly polymorphic pockets that interact in a noncovalent manner with the side chains of a bound peptide [158]. Degeneracy in the location and size of these pockets results in the promiscuous binding patterns for a wide range of short peptide fragments characteristic of each MHC class I allele. The size range of MHC class I peptides is typically from 8-11 amino acids in length, with nonamers being particularly prevalent [192].

Construction of the MHC class I complex begins as it is co-translationally inserted into the ER immediately following ribosomal synthesis. Inside the ER, the membrane-bound chaperone molecule calnexin binds to and stabilizes the heavy chain and initiates proper folding in a step-wise manner. This is followed by binding of the soluble chaperone molecule calreticulin, binding of the thiol oxidoreductase molecule ERp57, and binding of β_2-M. It is believed that calreticulin continues the heavy chain folding process, while ERp57 catalyzes disulfide bond formation within the α2 and α3 globular domains. Incorporation of the β_2-M accessory molecule is believed to stabilize the partially-folded heavy chain. Binding of these three components allows for the dissociation of calnexin, and promotes binding to the membrane-bound molecule, tapasin which normally associates with the TAP complex and serves as a noncovalent bridge that connects the TAP proteins with peptide-deficient MHC class I molecules. Localization of awaiting MHC molecules in close proximity to the transporter that supplies the requisite peptide fragments serves to optimize the loading efficiency of peptides into the MHC

class I peptide binding groove. Physical association with tapasin may facilitate peptide binding and may allow for peptide exchange to encourage binding and retention of peptides with the highest affinities [174, 285]. It should be noted that not all MHC class I molecules bind to tapasin or require physical association with the TAP complex. While the efficiency of peptide loading of these molecules is most likely reduced, this mechanism probably serves as a backup pathway to preserve antigen presentation following infection with viruses that encode proteins which bind to tapasin and inhibit antigen presentation, such as the US3 protein encoded by HCMV [188].

Once the MHC class I molecule has been properly folded and has acquired β_2-M and an appropriate peptide, ERp57, tapasin, and calreticulin are released and the trimeric MHC class I complex can be exported via the trans Golgi network (Figure 1.1). By utilizing conserved motifs located within the cytoplasmic tail, MHC class I molecules can be targeted to the endosomal trafficking network or directly targeted to the surface of the cell for presentation of the peptide fragment to MHC class I-restricted CD8 T cells [155]. Surface expression of foreign peptide fragments is the first step in the activation of the CD8 T cell component of the adaptive immune response.

Mycobacterial Access to the MHC Class I Pathway

Early investigations into the mechanisms by which *M. tuberculosis* persists within macrophage cells indicated that virulent bacilli were maintained within the phagsomal membrane. Studies by D'Arcy Hart demonstrated that phagosomes containing live but

not dead *M. tuberculosis* failed to fuse with lysosomes and were halted at an early stage of phagosome maturation [9, 38]. Blocking normal phagosome maturation prevents the acquisition of toxic hydrolases, proteases, lipases, and other molecules that would otherwise facilitate the destruction of intraphagosomal pathogens. Thus, actively metabolizing bacteria produce products that modulate host endocytic trafficking patterns, to the benefit of the pathogen.

It is also known that upon phagocytic uptake, *M. tuberculosis* is able to inhibit recruitment of proton ATPase pumps to prevent acidification of the phagosome and maintain an intraphagosomal pH conducive for mycobacterial viability [240]. Normal phagosomal maturation proceeds via acquisition of Rab5, a small GTPase molecule. This facilitates the binding of Vps34, which is a class III phosphatidylinositol 3-kinase (PI 3-K) that generates PI 3-P. Production of PI 3-P allows for recruitment of EEA1, which binds calmodulin. This complex then has the ability to acquire the Rab 7 GTPase. It has been shown that infection with *M. tuberculosis* blocks normal phagosomal progression, and is characterized by a failure to acquire EEA1 as well as Rab7 [99]. Although the precise mechanism is not currently known, bacterial products such as lipoarabinomannan and trehalose dimycolate have been implicated in the disruption of normal phagosome maturation. Both of these products have been shown to alter endosomal trafficking when coated upon latex microspheres [100, 121]. Regardless of the exact mechanism, premature termination of phagosome maturation prevents recruitment of lysosomes containing bactericidal hydrolases, and facilitates intracellular survival of this organism.

Since *M. tuberculosis* is believed to reside only within the phagosome and not escape into the cytosol, the question arises as to how pathogen-derived antigens escape

the confines of the phagosomal membrane and enter the MHC class I antigen presentation pathway. It is known that *M. tuberculosis* as well as other intracellular pathogens confined to intraphagosomal survival can initiate an antigen-specific CD8 T cell response [73, 122, 130, 207, 247]. There are two major hypotheses to explain how antigens from these membrane-enclosed pathogens possess the ability to access the cytosol.

The first hypothesis involves the observation by Bloom's group that infection of macrophage cells with live but not dead *M. tuberculosis* in conjunction with soluble ovalbumin (OVA) resulted in cytoplasmic access of the internalized OVA in a TAP-dependent manner [167]. Further studies revealed that macrophage cells infected with live BCG possessed phagosomes permeable to proteins up to 70 kDa in size, whereas macrophages that had taken up dead BCG possessed membrane-impermeable phagosomes [251]. The implications of this study are that live, metabolically active *M. tuberculosis* and *M. bovis* BCG have the ability to modify the host phagosomal membrane, resulting in size-restricted permeability. Phagosomal access to the cytoplasm may provide nutrients to the internalized bacilli, or may allow for the egress of bacterial virulence factors and immunomodulatory molecules into the host cell cytoplasm. Fortunately for the host, bacterially-induced permeability of the phagosome concurrently allows bacterial antigens to enter the cytoplasm and enter the classical MHC class I antigen presentation pathway.

The second hypothesis involves active, host-mediated translocation of bacterial antigens out of the phagosomal compartment and into the cytosol where they intersect the

classical MHC class I antigen processing pathway (Figure 1.2). This is a process termed cross-presentation, and is discussed in detail below.

Cross-Presentation of Exogenous Antigen

For a time, there existed an antigen processing paradigm whereby exogenous antigens that entered a cell would be processed and presented upon MHC class II molecules, and endogenous antigens generated within the cytoplasm would be processed and presented upon MHC class I molecules. However, this rigid separation of the MHC class I and class II antigen presentation pathways led to an interesting conundrum: since only professional antigen presenting cells are able to stimulate naïve T cells and initiate a primary adaptive immune response, how does the immune system recognize viruses that possess a solely nonhematopoietic tropism? Early work performed by Bevan *et al.* demonstrated that in some instances, exogenously-derived antigen could be presented upon MHC class I molecules [24, 25]. This was followed by an elegant series of experiments by Sigal *et al.* demonstrating that infected nonhematopoietic cells are unable to stimulate a primary CD8 T cell response, and that the generation of virus-specific CTLs required the cross-presentation of exogenous antigen on MHC class I molecules by bone marrow-derived APCs [226].

Because of these observations, a series of models based upon ER retrograde protein transport, endosomal peptide exchange, peptide regurgitation, or phagosome to cytosol transport were developed to explain this apparent overlap of the class I and class

II pathways [56, 113, 139, 180, 204]. Until recently, these models were collectively termed 'alternate' MHC class I antigen processing pathways, and were believed to be either *in vitro* artifacts, or occur only under very specialized conditions. With the simultaneous discovery of the exogenous antigen cross-presentation pathway by three separate groups, the importance of this pathway for MHC class I antigen presentation has been elucidated [1, 110, 117].

Although a direct phagosome to cytosol pathway for the delivery of exogenous antigens into the classical MHC class I antigen processing pathway had been described 10 years earlier, it wasn't until 2004 that the mechanisms behind this phenomenon and its functional relevance were fully realized [110, 139]. Guermonperez *et al.* demonstrated that upon phagocytosis, for a short period of time the ER membrane fuses with the phagosomal membrane, delivering all of the necessary MHC class I antigen processing components to the phagosome, including TAP proteins, newly synthesized MHC class I molecules, β_2-M, and the requisite stabilizing chaperone molecules necessary for class I peptide loading [110]. Antigens within the phagosome are then transported from the phagosome to the cytosol by a mechanism similar to ER retrograde protein translocation. Although the exact transport molecule has yet to be conclusively identified, it is believed to be Sec61. Furthermore, it has been shown that proteasomes are recruited to and associate with the cytoplasmic face of the phagosomal membrane [117]. This most likely increases the efficiency of cross-presentation. Experimental evidence indicates that most exogenously-derived antigens destined for class I expression must reach the cytosol and intersect the classical MHC class I pathway [139, 180, 200].

The exact outline of events involves exogenous antigen uptake by endocytosis, followed by phagosome to cytosol transport of exogenous antigen mediated by Sec61 (Figure 1.2). These proteins are then degraded by proteasomes physically associated with the cytoplasmic side of the phagosomal membrane, and the antigenic peptides are transported back into the phagosome by TAP molecules. Within the phagosome, naïve MHC class I molecules can be loaded with exogenously-derived antigenic peptides, and the mature MHC class I molecules can then be targeted to the surface of the cell via a conserved motif in the cytoplasmic tail of the class I molecule [155].

Further research indicates that cross-presentation of exogenous antigen is limited primarily to DCs of the $CD8\alpha^+$ subtype, although evidence exists that macrophages and B cells may utilize this pathway under specialized circumstances although with reduced efficiency [78, 190]. How these DCs obtain exogenous, bacterially-derived antigens is currently a matter of debate, although there is considerable evidence that the apoptotic remains of dead infected cells can readily be taken up by sentinel DCs and their antigenic peptides cross-presented [212]. Evidence also exists that heat shock proteins released from necrotic cells bind to bacterial protein fragments, and that these complexes can be internalized by DCs using receptor-mediated endocytosis and their antigenic cargo efficiently cross-presented [27].

Intuitively, confining cross-presentation to DCs makes immunological sense. Dendritic cells are the only cell type that can readily initiate a naïve T cell response, and this cell type is highly equipped to survey the environment for the antigenic signals of infection. It would be more efficient for DCs to actively acquire and present the antigens of other infected cells, rather than to simply present endogenous antigens which would

necessitate infection of the DC before class I presentation could occur. Utilization of the cross-presentation pathway by DCs would also reduce the expression of primarily self-derived antigens upon a cell type that has the ability to readily prime a naïve T cell response. Cross-presentation therefore has implications involving the reduction of autoimmunity as well as the induction of infectious immunity. The fact that cross-presentation is primarily confined to DCs would also limit the destruction of bystander cells in the proximity of virally infected cells. For example, if epithelial cells could cross-present antigen from a nearby virally-infected cell, it would be difficult for responder CD8 T cells to distinguish the cells that were actually infected from the cells cross-presenting exogenous viral antigens, and the amount of unnecessary bystander killing would be enormous.

While the vast majority of cells in the body processes endogenous antigens through the classical MHC class I antigen processing pathway, DC cross-presentation of exogenously-derived antigens may represent a major component of CD8 T cell antigen priming. Although this mechanism is likely to significantly contribute to the antigenic peptide repertoire expressed on the surface of DCs, the exact contribution of exogenous antigen cross-presentation still remains to be determined.

Alternate MHC Class I Antigen Processing Mechanisms

Although the proteasome is responsible for generating the majority of peptides destined for antigen presentation, other proteasome-independent processes have been

implicated in the generation of antigenic peptides (Figure 1.3). Within the endocytic pathway, lysosomal degradation of exogenous antigens may produce peptide fragments possessing the correct binding motifs for MHC class I molecules. It has been postulated that when portions of the plasma membrane are incorporated into the phagosome, some MHC class I molecules displayed on the exterior surface of the cell are internalized and line the interior of the phagosome [134]. Upon lysosomal acidification, the nascent peptides from these class I molecules could be released and exchanged with newly degraded peptides derived from exogenous antigens. Alternately, it has been proposed that newly synthesized MHC class I molecules could be transported from the Golgi network and intersect the endocytic pathway, supplying MHC class I molecules that could exchange their bound ER-derived peptide for an exogenously-derived one [56].

Leader sequences which are proteolytically cleaved as polypeptides are co-translationally transported into the lumen of the ER can be presented by nonclassical MHC class Ib molecules such as HLA-E (humans) and Qa1 (mice) [15]. Surface expression of these peptides has been shown to be TAP-dependent, but proteasome-independent. It appears that these signal sequences are transported out of the ER by an as yet undefined transport protein, and then re-enter the ER by TAP-mediated transport. Since the requisite MHC class I antigen presentation molecules are present in the ER, this may seem to be an unnecessarily cumbersome process, however some viruses efficiently block TAP proteins to subvert antigen presentation. TAP-dependent presentation of these signal sequences may provide a mechanism for testing TAP function as a means to detect these viral infections.

Other peptides derived from signal sequences have been shown to directly bind to MHC class I molecules in a TAP-independent manner, and there is an example of a signal sequence derived from a lymphocytic choriomeningitis virus (LCMV) protein that is TAP-dependent and proteasome-dependent [102, 112, 149]. In these cases, it appears that if the correct epitope can be generated in the ER by resident endopeptidases, it can directly bind to MHC class I molecules, however larger proteins can be shuttled out of the ER utilizing retrograde protein translocation, and undergo normal cytosolic processing [260].

Although these novel alternate MHC class I antigen processing mechanisms are interesting from a purely immunological point of view, the exact biological significance of these pathways remains to be determined. In all likelihood, the inherent inefficiency of these processes means that they normally contribute only minimally to the antigenic peptide pools generated by the proteasome, and so have little effect upon adaptive immunity. However under conditions of active viral subversion of normal host antigen processing pathways, these pathways may serve a critical backup role for viral detection and elimination.

CD8 T Cell Priming and the Requirement for CD4 T Cell Help

The components of innate immunity are part of a highly conserved, evolutionarily ancient system that specializes in pathogen identification and clearance through the use of germline-encoded receptors. The adaptive immune system is a more recent evolutionary

advancement that possesses an almost infinite flexibility for pathogen recognition through the use of antigen-specific receptors generated by random gene rearrangements. Although the adaptive immune system possesses a much greater degree of specificity, random rearrangement of receptors occasionally permits the generation of self-reactive cells that could potentially initiate autoimmune disease. It is therefore of paramount importance that adaptive immunity be initiated only in situations where it is absolutely required, and that the development and termination of this response be carefully regulated. Dendritic cells reside at the critical juncture of the innate and adaptive immune responses, for only they possess the ability to initiate, orchestrate, and ultimately terminate adaptive immunity.

The hallmark of immunity is the ability to distinguish foreign pathogens from self molecules and to mount an appropriate response resulting in pathogen clearance. Dendritic cells occupy this critical niche within host immunity. After hematopoiesis in the bone marrow, DC precursors circulate within the blood and eventually enter the tissues where they become resident immature DCs. These cells preferentially accumulate in tissues that interface with the external environment, where they continuously migrate and sample antigen via endocytosis and macropinocytosis. Immature DCs normally possess a high endocytic ability although they express low levels of MHC class I and class II antigen presentation molecules and low levels of costimulatory molecules such as B7.1 and B7.2 [111]. Dendritic cells become activated upon encountering specific warning signals during antigenic sampling. These warning signals include not only pathogen-derived immunostimulatory molecules such as lipopolysaccharide (LPS), peptidoglycan (PG), hypomethylated CpG DNA motifs, and dsRNA but also host-derived

indicators of cellular damage or necrosis such as heat shock proteins and uric acid as originally described by Matzinger's 'danger signal' hypothesis [17, 166, 223].

While normally being unresponsive to host antigens, DCs have a remarkable ability to detect and react to foreign antigens through the use of pattern recognition receptors (PRRs) that identify conserved, pathogen-associated molecular patterns (PAMPs) [124]. Dendritic cells possess a multitude of PRRs which include cytosolic proteins such as protein kinase R and 2',5'-oligoadenylate synthase, secreted proteins such as mannose binding lectin and C-reactive protein, as well as surface-expressed receptors such as the mannose receptor, complement receptors, DEC205, DC-SIGN, scavenger receptors, and toll-like receptors (TLRs) [111, 124]. By recognizing evolutionarily conserved motifs expressed by pathogenic organisms, ligand binding to PRRs (especially TLRs) serves as a critical signal of infection that initiates a carefully orchestrated genetic DC maturation program. Upon TLR-mediated pathogen recognition, DCs dramatically upregulate surface expression of CD1, MHC class I, and MHC class II antigen presentation molecules, while simultaneously increasing the rate of antigen processing [53]. Phagocytic ability is also shut down, to limit the concomitant expression of pathogen-derived and host-derived peptides on the surface of activated APCs. Dendritic cells also upregulate surface expression of costimulatory molecules of the B7 family (CD80, CD86), which are critical for initiation of a naïve T cell response. Furthermore, DC maturation results in the secretion of chemokines (MCP-1, IL-8, etc.) to recruit neutrophils and monocytes as well as the production of proinflammatory cytokines (IL-1β, IL-6, IL-12, TNF-α, etc.) that activate innate host defense mechanisms [111]. Lastly, activated DCs upregulate integrin molecules and chemokine receptors such as CCR7

which allow the DCs to migrate out of peripheral tissues and traffic to regional draining LNs. Once they reach the LN, DCs migrate to T cell rich regions and initiate an adaptive immune response through a process called T cell priming.

Due to the efficient antigen processing capabilities and high-level surface expression of CD1, MHC class I, MHC class II, and costimulatory molecules, DCs are the most potent APC known and are the only cell type that normally has the capability of stimulating a primary immune response. In addition, DCs possess the ability to orchestrate the magnitude and direction that the ensuing adaptive immune response will take. Dendritic cells have a remarkable capacity to integrate and process a vast array of signals within an inflammatory environment to ultimately determine the type of immune response that will be successful in elimination of the invading pathogen. Since different TLRs are activated by different classes of pathogens, this signaling information not only activates the DC, but helps shape the resulting adaptive immune response. Other signals such as the site of DC encounter with antigen and the local cytokine milieu also help determine the magnitude and type of immune response to initiate. This ability to translate a multitude of diverse signals into a coherent, pathogen-specific response allows DCs to correctly prime the appropriate T cell subsets that will efficiently clear an invading pathogen. Based upon differences in signaling patterns, DCs can either initiate no response, prime effector or memory T_H1 or T_H2 biased lymphocytes, prime CTLs, or tolerize recruited T cells through the generation of regulatory T (T_{reg}) cells.

In contrast to CD4 T cell priming, DCs require additional activation and maturation signals to initiate a strong CD8 T cell response in order to prevent the induction of a pathogenic self-reactive CD8 T cell response [216]. This process, termed

'licensing' endows a DC with the ability to prime naïve CD8 T cells [109]. The signals required to properly license a DC include CD40-CD40L interactions with CD4 T helper cells, triggering of Fc receptors by antigen-antibody complexes, and the presence of various cytokines including IL-4, IL-12, and IFN-α/β [21, 148, 235].

Early work investigating the requirement for CD4 T cell help demonstrated that for non-inflammatory stimuli such as immunization with OVA, CD4 T cell help was required for the efficient initiation of a CD8 T cell response. A further requirement was that the licensing CD4 T cell and the naïve CD8 T cell must recognize their cognate antigenic epitopes displayed upon the surface of the same APC [22, 51]. Other experiments have shown that CD4 and CD8 T cell epitopes occurring within the same antigen induce more efficient CD8 T cell immunity [126, 224]. Although the exact mechanism by which physical epitope linkage increases CD8 T cell responses is unknown, it has broad implications in the field of vaccinology for explaining the superior efficacy of fusion protein constructs in inducing strong T cell responses. Exactly how CD4 T cells license a DC was unknown until experiments by multiple groups demonstrated that agonistic CD40 antibodies could bypass the need for CD4 T cell help, uncovering the pivotal role that CD40-CD40L interactions play in DC licensing and subsequent DC activation [21, 197, 215]. Binding of CD40 on an APC to its cognate ligand (CD40L) was shown to upregulate the costimulatory molecules B7.1 and B7.2, and to initiate the production of IL-12, which promotes full activation of a CD8 T cell response [71, 191, 214].

Recent studies examining the highly inflammatory conditions following active infection and utilizing more sensitive assay conditions such as MHC class I tetramer

reagents and ELISPOT assays have come to a different conclusion as to the requirement for CD4 T cell help. These experiments indicate that the initiation of a primary CD8 T cell response and the generation of protective CD8 effector T cells in response to pathogenic organisms is CD4 T cell help independent [43, 154, 222]. It appears that in an infectious context, pathogen-derived molecules interacting with host TLRs, in conjunction with proinflammatory cytokines such as TNF-α and IFN-α/β have the ability to overcome the requirement for CD4 T cell help.

An important observation from these experiments was that CD8 T cells generated in the absence of CD4 T cell help failed to form long lasting, competent memory cells [125, 221, 241]. Upon secondary encounter with the same antigen, CD8 memory T cells generated in the absence of CD4-mediated help responded poorly, as indicated by an inferior proliferative response, decreased production of IFN-γ, and compromised protection to the secondary challenge [20, 31, 221, 241, 272]. Even more controversial than the requirement for CD4 T cell help is the issue of exactly when CD4 help is required. Elegant experiments by Bevan's laboratory confirmed that the initial priming of most CD8 T cell responses in an infectious context was CD4 help-independent, but that CD4 T cells were required for the maintenance of memory CD8 T cells [242]. Intriguingly, these experiments also indicated that the nature of the CD4 T cell help in memory CD8 T cell maintenance is most likely antigen-independent. An explanation for this observed phenomenon awaits further study.

Thus, it appears that under noninflammatory conditions, initiation of a CD8 T cell response is dependent upon CD4 T cell help in the form of CD40-CD40L interactions with the APC. Dendritic cells endocytose antigen and present it in conjunction with MHC

class II molecules to CD4 T cells. Upon activation, CD4 T cells upregulate CD40L, which interacts with CD40 expressed on the DC and effectively licenses the DC to upregulate the expression of requisite costimulatory molecules that enable it to efficiently prime a naïve CD8 T cell response. Presentation of CD8 T cell epitopes in the context of adequate costimulation then leads to the initiation of a robust CD8 effector T cell response. Conversely, if a naïve CD8 T cell encountered its cognate antigen expressed on an unlicensed DC, it would fail to receive the necessary costimulatory signals for activation and instead would become tolerized. Thus, dual recognition of an antigenic stimulus by both CD4 and CD8 T cells provides a mechanism to ensure that the displayed antigen is indeed foreign, in order to prevent the induction of autoimmunity.

However, in the highly immunostimulatory context of an infection, the requirement for DC licensing by CD4 T cells can be overcome by pathogen-derived signals. This allows for the efficient generation of a primary CD8 T cell response in the absence of CD4 T cell help. It is important to note that under both scenarios, CD4 T cells are still required for the maintenance of the CD8 memory T cell population.

While CD40-CD40L interactions mediated by CD4 T cells are the predominant DC licensing mechanism under noninflammatory conditions, cytokine regulation of CD8 T cell priming has the ability to shape the resultant polarization of the CD8 response, and in some instances may be sufficient to overcome the requirement for CD4 T cell-derived help. Experiments utilizing IL-4 KO mice demonstrated that IL-4 negatively impacted the resultant CD8 T cell response to LCMV infection [271]. However, other experiments have shown that IL-4 possesses an adjuvant-like activity that promotes a strong T_H1 response, most likely by initiating a cytokine cascade that triggered the release of large

amounts of IL-12 [26]. IL-4 has also been shown to promote differentiation of CD8 T cells into long-lived memory cells when it is present early in T cell priming [118]. As IL-4 normally has a strong association with T_H2 polarization, further experiments are required to elucidate the exact role that this cytokine plays during initiation of a T_H1 response and its role in memory cell differentiation.

Although the exact requirements for IL-4 during T cell priming are unclear, the presence of IL-12 or the type I interferons has been shown to promote DC activation and licensing of a strong CD8 T cell response, especially in the context of viral infections [140, 156]. While the type I interferons possess the ability to act at the DC-CD8 T cell level during initiation of a CD8 T cell response, they also act upon clonally-expanded CD8 T cells to promote T_H1 cytokine production, differentiation, and survival [72, 165, 280]. Recent experiments utilizing IFN-α/βR KO donor cells adoptively transferred into wild-type recipient mice demonstrated the requirement for type I interferon recognition by CD8 T cells during the antigen-driven clonal proliferation phase [138]. In the absence of type I interferon receptor signaling, CD8 T cell survival during clonal expansion was markedly reduced, resulting in a greater than 99% reduction in the number of CD8 T cells surviving antigen-specific proliferation. Interestingly, the T_H1 cytokine IL-12 has the ability to reverse this survival defect during the antigen-specific proliferative phase [72]. Therefore, the presence, absence, or balance of these two cytokines during the inflammatory process may ultimately control the magnitude of the CD8 T cell response to different infectious pathogens.

Generation of Competent CD8 T Cells

CD8 T cell responses can be divided into four distinct phases: activation, expansion, contraction, and memory cell maintenance. Following TCR-mediated recognition of its cognate peptide antigen, the activation phase initiates a modifiable genetic program of differentiation that directs the expansion and effector function of the resulting CD8 T cells. The expansion phase is responsible for the massive clonal proliferation of activated T cells, which is composed primarily of effector cells capable of combating infection. The contraction phase encompasses the elimination of 90-95% of the effector cell population, and occurs following pathogen control as antigen levels decrease. Following contraction, the surviving memory cell population is actively maintained through slow, homeostatic proliferative renewal during the maintenance phase. Progression through each of these stages is critical for protective CD8 T cell immunity to pathogenic organisms, and there is evidence that the dynamics of each of these phases is controlled, at least in part, by the initial encounter with antigen.

CD8 T Cell Activation

As previously described, the initial activation of naïve CD8 T cells occurs within the lymphoid tissues and is mediated by an activated DC that has been properly licensed to initiate a CD8 T cell response. Classical activation of T lymphocytes involves a sequential series of interactions that must occur within a time-dependent context. Initial

recognition of an antigenic peptide presented by a MHC class I molecule has been termed Signal 1, and results in intracellular signaling through the CD3 protein complex [107]. This is immediately followed by binding of the CD8αβ heterodimer to a conserved region on the MHC class I molecule. Binding by the CD8 coreceptor increases the overall avidity of the TCR-MHC class I interaction and prolongs the duration of contact to allow for formation of the immunological synapse and to facilitate continued intracellular signaling. Following TCR-MHC class I interaction, CD28 expressed on the CD8 T cell must interact with one of the B7 family of costimulatory molecules expressed by the APC in an event termed Signal 2 [115]. Failure to receive Signal 2 in temporal association to Signal 1 results in abortive activation of the CD8 T cell and the induction of anergy.

While these two signals comprise a large part of lymphocyte activation, a third signal has recently been identified. Signal 3 is mediated by soluble cytokine molecules, and serves to direct the polarization of a CD4 T cell response towards a predominantly T_H1 or T_H2 bias [131]. Priming of CD8 T cells is also influenced by soluble factors, with IL-12 or IFN-α/β being the predominant Signal 3 molecules [72, 265]. In the absence of Signal 3, CD8 T cells proliferate but fail to develop classical effector functions such as cytolytic activity. This third signal for CD8 T cell activation not only serves as a molecular switch regulating activation and tolerance, but also regulates the resulting CD8 effector T cell function through T_C1 or T_C2 polarization.

In addition, other surface molecule interactions serve to increase the activation status of the CD8 T cell, or modify the proliferative program or effector function of the resulting response. While the precise role of many of these molecules has yet to be elucidated, expression of CD27, 4-1BB, CD40, and LFA-1 have been shown to be

important in shaping the resultant CD8 T cell response to a greater or lesser degree [11, 32, 49, 114].

Expansion Phase

There is increasing evidence that the initial duration of antigenic stimulation has a profound effect upon the resulting characteristics of the CD8 T cell response. The effects of the duration of exposure to antigenic stimulation have been investigated by adoptive transfer at various timepoints during infection, premature termination of infection by antibiotic treatment, as well as through the use of a novel *ex vivo* membrane antigen presentation system [269, 286]. Multiple studies have shown that a brief encounter with antigen of approximately 24 hours in duration is sufficient to initiate an antigen-independent proliferation, differentiation, and effector function program within CD8 T cells [127, 170, 270]. Following this 24 hour period, activated CD8 T cells begin to rapidly proliferate in the presence of IL-7, IL-15, and IL-2. Cell division occurs every 5-6 hours and it has been shown that cells undergo approximately 14 cycles of division [28, 288]. This rapid proliferation cycle allows the initial pool of antigen-specific CD8 T cells to increase greater than 50,000-fold by the peak of infection, when examined in a murine LCMV infection model [28]. These newly-generated effector cells begin to leave the LN after 3-4 days, and migrate to the sites of active infection [87].

While the duration of antigenic stimulation clearly has a profound impact upon subsequent CD8 T cell proliferation, the amount of antigen also plays a role in the

ultimate size of the responding antigen-specific effector cell response, as well as the total number of memory cells generated. An elegant study utilizing vaccinia constructs expressing differing amounts of OVA demonstrated a correlation between the amount of antigen and the size of the resulting antigen-specific CD8 T cell population [282]. Similarly, others have shown that the burst size of the CD8 effector T cell response ultimately determined the size of the CD8 memory T cell pool [116]. The implications from these two studies are that the amount of antigen controls the size of the effector cell population, which in turn governs the size of the memory T cell pool that persists following the contraction phase.

Although the effect of the initial priming conditions on the magnitude and quality of the effector cell population is well defined, the degree to which initial priming events impact the differentiation of the population of cells destined to become long-lived memory cells is less certain. Kaech *et al.* utilized microarray analysis to characterize genes indicative of the memory cell population [128]. Through this analysis, they discovered that although naïve CD8 T cells express high levels of the alpha chain of the IL-7 receptor (IL-7Rα), effector cells rapidly lost expression of this molecule. More importantly, CD8 memory precursor T cells reacquired expression of IL-7Rα and could be identified at the peak of active viral infection [129]. While these cells were at an early stage of memory cell differentiation and possessed effector cell-like functions, they could gradually acquire the characteristics of memory cells upon antigen clearance. Further studies by Wherry *et al.* utilizing purified murine LCMV-derived central memory (T_{CM}) and effector memory (T_{EM}) subpopulations as defined by CD62L expression determined that T_{EM} converted to T_{CM} cells while the reverse ($T_{CM} \rightarrow T_{EM}$) was not observed in the

absence of antigen [283]. Together, these results indicated that cells destined to become memory cells diverged in their cellular differentiation patterns at an early stage following activation, implicating the conditions of initial priming upon subsequent memory cell development and demonstrated that CD8 T cell differentiation was a linear process that ultimately culminated in the generation of a protective CD8 T_{CM} subpopulation. These observations led Ahmed's group to propose a linear and progressive model for CD8 memory T cell generation. This model incorporates initiation of a CD8 T cell proliferation and effector function acquisition program following a brief period of antigenic stimulation, and the gradual transition of CD8 T cells through a linear naïve $\rightarrow$ $T_{effector} \rightarrow T_{EM} \rightarrow T_{CM}$ progressive differentiation program.

Similarly, Williams *et al.* showed that antibiotic treatment 24 hours following infection with *Listeria monocytogenes* generated similar effector CD8 T cell responses when compared to mice without antibiotic treatment, however alterations in memory cell development that did not impact protective efficacy were observed [286]. Taken together, these experiments indicate that the initial priming events contribute to and modify the early differentiation program of memory cells, and that the development of this population of cells diverges soon after antigenic exposure. It is also evident that the initial imprinting events may be more important for the generation of immunological memory than for the generation of the effector T cell response.

In contrast to the linear and progressive model, an alternate theory proposed by Lanzavecchia and Sallusto advocates that the signal strength received by a lymphocyte through its TCR is the primary factor determining the state of differentiation and the acquisition of T cell characteristics [146]. This divergent model of T cell activation states

that differential signaling results in the differential attainment of T cell attributes on a progressively increasing scale.

The first part of this model identifies differences in the strength of stimulus that T cells receive as being the result of antigen dose (which affects the rate of TCR stimulation), the amount of costimulation (which affects the amplification of TCR signaling), and the duration of TCR signaling (which determines the accumulation of TCR signals). Collectively, these signaling attributes result in a specific level of signaling through an additive effect.

The second part of this model relates distinct cellular processes such as cell cycle progression, the ability to respond to cytokines, migratory potential, effector function, etc. to individual transcriptional programs. The acquisition of each of these programs would require a sequentially increasing amount of TCR signaling. Therefore, the specific level of signal received by a lymphocyte during DC priming would determine how many transcriptional programs the cell could enact. For example, weak signaling results in proliferation, but a failure to acquire effector functions and cellular fitness, culminating in tolerance or apoptosis (i.e. peripherally silenced cells). Intermediate signaling results in proliferation and fitness acquisition, but a failure to acquire effector function (i.e. memory cells). Strong signaling results in the acquisition of proliferation, fitness, and effector function (i.e. effector cells). Within this model, extremely weak signals induce anergy, while excessively strong signals trigger activation-induced cell death.

This model advocates the idea that CD8 T cells possess various activation thresholds, and that different combinations of costimulatory signals, duration of contact, or the presence of cytokines can additively combine to attain a particular threshold level

of signaling. Once this threshold has been reached, CD8 T cells initiate an antigen-independent program that governs proliferation, effector function, and memory cell generation. This program can be subtly modified by activation signals either prior to or during initiation of the program, which serves to shape the resultant CD8 T cell response. Therefore this model differs from the linear and progressive model by suggesting that effector cells, T_{EM}, and T_{CM} subpopulations arise separately from the initial DC-CD8 T cell contact, rather than progress through distinct stages of cellular differentiation culminating in the generation of a T_{CM} subpopulation.

While the divergent model of T cell activation possesses many appealing characteristics that explain the existence of different T cell subsets as well as the acquisition of function, by definition it relegates the generation of memory cells to a somewhat random, stochastic process based entirely upon DC-T cell encounters of variable length to reproducibly generate consistent memory T cell responses. In addition, although not addressed by the authors, the implications of this model are that the memory cell population would be generated from T cell clones of intermediate avidity, rather than from the highest avidity clones. While this at first seems counterintuitive, one could argue that in a secondary immune response, memory cells possessing lower thresholds of activation are consequently less dependent upon high-avidity TCR interactions as compared to naïve T cells. The actual explanation for the development of heterogeneous T cell responses will most likely contain elements from the linear and progressive differentiation model, as well as from the divergent differentiation model to completely describe the complexities of T cell differentiation and memory cell generation.

Contraction Phase

Upon pathogen clearance and in conjunction with decreasing antigen levels, the effector cell population undergoes a massive contraction phase, resulting in 90-95% of the effector cells dying through the induction of apoptosis. The remaining 5-10% of activated cells differentiate into long-lived memory cells. The mechanisms for effector cell death are complex and interrelated, but primarily involve a reduction in anti-apoptotic molecules of the Bcl-2 family, which result from a failure to sustain high-level pro-survival signaling in a progressively less inflammatory environment following pathogen clearance.

It has been demonstrated that signaling through CD28, as well as 4-1BB induces expression of the anti-apoptotic protein; Bcl-x_L [233, 236]. However upon activation, T cells concurrently upregulate surface expression of CTLA-4. CTLA-4 competes with CD28 for binding to B7 molecules on APCs, effectively increasing the requirement for T cell costimulation. In addition, signaling through the common chain of the IL-2 family of cytokine receptors (IL-2R, IL-4R, IL-7R, IL-9R, IL-15R) induces expression of a related anti-apoptotic protein; Bcl-2. In fact, reductions on the levels of IL-2 are known to result in the death of effector cells by a mechanism termed activation-induced cell death [193]. Therefore, costimulatory signals as well as cytokine signaling trigger pro-survival pathways that actively inhibit apoptosis. However, as the inflammatory process is resolved, a lack of T cell costimulation in conjunction with decreasing cytokine levels results in a reduction of intracellular anti-apoptotic molecules, followed by apoptosis. In effect, these inhibitory signaling pathways serve to increase the survival threshold for

activated effector cells, shifting the delicate survival balance towards apoptosis. As long as a strongly pro-inflammatory environment exists, the induction of anti-apoptotic molecules continues and effector cells can persist. However, in the absence of continued proinflammatory signaling, the elevated survival requirements can no longer be met, triggering apoptosis.

Two recently discovered mechanisms regulating effector cell survival may also have a significant impact upon the contraction phase. As previously described, Kaech *et al.* observed that naïve cells expressed high levels of the IL-7R, which facilitates survival through the induction of Bcl-2 [129]. Effector cells rapidly downregulate IL-7R expression following activation, rendering them insensitive to *in vivo* levels of IL-7; a critical regulator of CD8 T cell survival. Thus, in the absence of other compensatory pro-survival signals, the effector population rapidly succumbs to apoptosis. Another cytokine involved in the CD8 T cell contraction phase is IFN-γ. While normally associated with its antiviral and cellular activation properties, IFN-γ has also been implicated in the regulation of the CD8 T cell contraction phase. Although the exact mechanism by which IFN-γ mediates this effect is unknown, it has been observed that following infection with *L. monocytogenes*, activated CD8 T cells in IFN-γ KO mice fail to undergo the T cell contraction characteristic of wild-type mice [14]. Taken together, these two mechanisms contribute significantly to effector cell death following antigen clearance, and as such play a major role in CD8 T cell homeostasis.

Other mechanisms may also contribute to the massive death of effector cells during the contraction phase. Increased expression of Fas and upregulation of molecules of the TNF family, especially the TNF p50 receptor have all been shown to induce

apoptosis through the caspase-mediated death pathway [193]. That these mechanisms are unlikely to play a major role in the decline of effector cells following antigen clearance is indicated by a failure to observe large differences in apoptosis using mouse KO models [164]. Conversely, this might indicate that redundancy within this system exists, due to the central importance of these mechanisms for regulation of lymphocyte numbers following pathogen clearance.

A model of lymphocyte contraction can be outlined where activation of naïve CD8 T cells triggers a series of mechanisms that increases the threshold required for survival of effector cells. In the presence of active infection and in the context of a proinflammatory environment, effector cells receive an abundance of pro-survival signals and are able to achieve this increased level of signaling. However, upon pathogen clearance, effector cells are at a competitive disadvantage as compared to naïve and memory cell populations and rapidly die under conditions of reduced activation signals. In effect, upon cellular activation the lifespan of effector cells is governed by a molecular clock that can be continually reset in response to proinflammatory stimuli, but begins to wind down in the absence or reduction of these stimuli.

The question then arises as to how a small percentage of cells manages to escape the massive apoptosis characteristic of the contraction phase. Survival of CD8 T cells destined to become long-lived memory cells is critically dependent upon phenotypic changes that confer resistance to apoptosis.

Even though the contraction phase seems tied to the loss of antigenic stimuli, evidence exists that the contraction phase is also imprinted upon the CD8 T cell during the initial priming phase [13]. Early priming events such as the programming of cytokine

receptor expression patterns or the production of IFN-γ during early infection may define the scope and magnitude of the contraction phase [12]. In contrast to models of increased memory cell fitness and competitive survival advantage, regulation of cytokine receptor expression provides a passive model based upon the ability or inability to respond to IL-7, explaining CD8 memory T cell survival and concurrent effector cell death.

While there has been significant progress in understanding the cellular mechanisms responsible for the generation of memory CD8 T cells, further research needs to be performed to determine the precise signaling events required for optimal memory cell formation. These signaling pathways are attractive targets for immunological adjuvants, to boost the protective efficacy of modern subunit vaccines.

Maintenance of CD8 Memory T Cells

While survival of the CD8 memory T cell population is based primarily upon cytokine receptor expression, persistence of the memory cell population involves two separate but interrelated mechanisms: phenotypic changes that increase the fitness of the memory cell population, and a resource-limiting environment within which these memory cells possess a competitive advantage.

It has been shown that while the lifespan of a CD8 memory T cell is significantly longer than an effector cell, it is still finite in length. Therefore a slow, homeostatic proliferation rate equal to the natural death rate is necessary to maintain constant numbers of CD8 memory T cells [141, 254]. Homeostatic proliferation is primarily dependent

upon the constant presence of basal levels of IL-15, and to a lesser degree IL-7 [18, 249]. Although the functions of these two pro-survival cytokines overlap to some extent, IL-7 is responsible for the continued survival and fitness of CD8 memory T cells, while IL-15 induces homeostatic proliferation by triggering cell cycle progression. In addition, the total amount of available IL-15 regulates the size of the CD8 T cell memory pool. Competition for IL-15, therefore selects the most fit memory cells for retention.

While a basal level of IL-15 efficiently regulates the ultimate size of the CD8 memory cell pool, it also dictates that newly generated memory cells must compete with existing memory cells for available IL-15. This creates a situation where newly generated memory cells proportionally reduce the existing memory cell populations to previously encountered infections [217]. The result is progressive attrition of existing memory cells at the expense of newly generated memory cells. Therefore, competition for a finite amount of available IL-15 drives the continued maintenance and survival of memory CD8 T cell numbers at relatively constant homeostatic levels.

The CD8 T Cell Memory Response

The ability to mount a more rapid and qualitatively superior pathogen-specific response to a secondary challenge is the hallmark of immunological memory. As such, the generation of durable immunological memory is the primary target of vaccinology, and therefore our understanding of the dynamic process of memory cell generation and maintenance is of paramount importance.

Memory cells collectively possess several attributes that give them superior abilities in clearing pathogenic organisms. The primary characteristic that defines a memory cell is the ability to persist for long periods of time in the absence of antigen; in many cases for the lifetime of the host. In addition, when compared to naïve cells, memory cells respond more quickly to pathogens as the result of three characteristics: greater initial numbers of antigen-specific memory cells compared to the numbers of antigen-specific naïve cells in a primary infection, a reduced dependence upon costimulation resulting in a lower threshold of activation, and more rapid cytokine production. In combination, these characteristics allow memory cells to mount a rapid, highly effective secondary immune response that in many cases prevents reinfection.

There is increasing evidence that the cells comprising the memory pool are in fact a heterogeneous population, and that these subsets differentially contribute to protection upon infectious challenge with a diversity of pathogenic organisms. Recent work by Lanzavecchia and Sallusto identified two populations of memory cells, as defined by their effector functions and migratory patterns [209]. Central memory T cells are phenotypically characterized by surface expression of CCR7 and CD62L molecules, and reside primarily within the LNs, spleen, and blood. In contrast, effector memory T cells express low levels of CCR7 and low or variable levels of CD62L and reside primarily within nonlymphoid tissues [209]. In addition to these phenotypic and tissue homing differences, T_{EM} cells possess a low proliferative potential, high cytotoxic activity, and rapidly secrete IFN-γ, TNF-α, or IL-4 upon restimulation. T_{CM} cells possess a rapid proliferative capacity, immediately secrete IL-2, and exhibit delayed secretion of effector molecules such as IFN-γ and TNF-α [195]. These functional differences suggest that the

T_{EM} population provides an initial defense mechanism to quickly constrain pathogen replication at the sites of initial infection, while the T_{CM} population rapidly proliferates, providing a newly-generated source of pathogen-specific effector cells that can migrate to the periphery and mediate pathogen clearance.

While the effector functions of these subsets have been well-defined, the generation of these populations and their lineage relationships are not completely understood. Most evidence; however, favors a progressive linear differentiation model, where naïve cells differentiate into activated effector cells following antigenic stimulation. Upon antigen clearance, a small proportion of effector cells that survives the contraction phase differentiates into the T_{EM} population. Further differentiation in the absence of antigen leads to the generation of the T_{CM} population [196, 257, 283]. Upon secondary challenge, the T_{CM} population rapidly proliferates and these newly generated cells differentiate into effector cells that home to infected tissues.

The generation of functional memory cells begins soon after initial contact with an activated APC. Evidence indicates that upon stimulation for as little as 24 hours, memory CD8 T cells can be programmed to develop in the absence of further antigenic stimulation or additional costimulation [127]. These early priming events trigger a memory cell developmental program that can be modified by stimulatory events during its initiation. Importantly, this memory cell developmental program is heritable, as all of the daughter cells produced following cell division retain this imprinted program. Signaling events during priming initiate a series of transcription factors that not only upregulate or downregulate important effector functions, but also initiate chemical and structural modifications to the DNA, many of which can be passed on during mitosis. For

example, within CD4 T cells, TCR triggering in conjunction with IL-12R or IL-4R signaling induces the transcription factors T-bet or GATA-3, which promote the differentiation of T_H1 or T_H2 biased cells, respectively [120, 176, 248]. These transcription factors then induce chromatin remodeling events such as histone acetylation and demethylation of DNA, which increases the accessibility of a specific subset of genes [2, 6]. In particular, demethylation of the IFN-γ locus in T_H1 biased cells and demethylation of the IL-4 locus in T_H2 biased cells allows for increased accessibility of these genes for their respective transcription factors, and may account for the shortened time and increased amount of cytokine production characteristic of memory cells upon restimulation [6, 92]. Similar events are believed to occur within CD8 T cells, which demethylate DNA regions preceding the IFN-γ, perforin, and granzyme loci.

Further evidence for the importance of these early signaling events upon the imprintation of the memory cell differentiation program occurs in CD8 enhancer ($E8_I$) KO mice, which have the ability to express the heterodimeric CD8αβ molecule, but fail to express the CD8αα homodimer. Upon antigen encounter, $E8_I$ KO mice generated a normal functioning primary immune response, but antigen-specific CD8 T cells failed to upregulate the IL-7R and consequently these mice failed to generate memory cells [157]. The explanation for this involves the spatial localization of the CD8αα molecule within the plasma membrane. In contrast to the CD8αβ molecule, CD8αα fails to enter cellular membrane lipid rafts, and therefore decreases TCR signaling by sequestering tyrosine kinase molecules away from the TCR-CD3 signaling apparatus located within cholesterol-rich lipid rafts [8, 54]. This lends support to Sallusto's signal strength model of memory cell formation, whereby the expression of CD8αα weakens the otherwise

strong TCR signaling required for effector cell generation, resulting in intermediate level signaling which promotes the generation of memory cells [104].

While these early events are crucial for initiation of the memory cell developmental program, subsequent signaling events during the ensuing inflammatory process have the ability to modify this program and ultimately shape its outcome. Following experimental infection of mice with LCMV, a gradual acquisition of memory cell characteristics was observed. This differentiation was detectable by the peak of infection, and continued well beyond the clearance of antigen. In fact, changes in gene profiles could still be observed 100 days following infection [128]. The exact post-priming stimuli are unknown, but are most likely tied to the amount of inflammation and the levels of cytokines to which developing memory cells are exposed.

Therefore a complex series of events serves to initiate and further shape the resultant memory cell developmental program. This process may take months following antigen clearance for complete memory cell differentiation and acquisition of the full complement of memory cell attributes to occur. The signaling events that contribute to memory cell formation include the initial priming events, the amount and type of costimulatory molecules present, the cytokine environment, the amount of antigen, the duration of antigen persistence, as well as the presence or absence of CD4 T cell help. Together, these signals serve to imprint a unique, durable level of differentiation that makes a recipient cell competent for memory cell generation. While the exact contribution of each of these stimuli to the complete memory cell differentiation program is unknown, it appears that the initial priming events occurring within the first 24 hours following T cell activation have the largest impact, while secondary stimuli occurring

during the inflammatory process and following antigen clearance have the ability to subtly modify the program established during priming. It is therefore becoming clear that the acquisition and development of memory T cell properties is a progressive differentiation event that occurs for weeks following pathogen clearance.

Protective Memory Cell Subsets

From a vaccinology standpoint, the existence of multiple memory cell subsets invokes the question of which of these subpopulations provides the most durable, longest-lasting protective efficacy, and how this subset can be effectively targeted by vaccination. In an elegant paper by Zaph *et al.*, CD4 T_{CM} and T_{EM} populations were directly examined for their ability to mediate protection upon infection with *Leishmania major* [293]. They determined that while the T_{EM} population provided some amount of initial protection to infection, these memory cells failed to persist following antigenic clearance. In contrast, the T_{CM} population took longer to develop, but rapidly proliferated in response to secondary challenge and afforded significant protection.

In a related study Wherry *et al.* examined the development of CD8 T_{CM} and T_{EM} populations during acute and chronic infection with LCMV [281]. Importantly, it was demonstrated that following acute infection accompanied by antigen clearance, CD8 memory T cells fully differentiate and progressively acquire the hallmarks of memory immune cells. However, in the presence of continued antigenic stimulation during chronic infection, functional defects in CD8 memory T cell development and survival

were noted. In addition, the amount of functional decline directly correlated with the duration and intensity of the antigenic stimulus. This decline ultimately resulted in functional exhaustion and clonal deletion of antigen-specific CD8 T cells that were subjected to uninterrupted antigenic stimulation. That these functional defects are long lasting was demonstrated by transfer of memory cells generated under conditions of chronic antigenic stimulation. When adoptively transferred into antigen-free naïve mice, the T_{CM} population gradually declined in numbers, indicating a fundamental defect in acquisition of the hallmark memory cell characteristic of persistence [281]. Lastly, these experiments also concluded that the T_{CM} population, due to its rapid proliferative potential and long-term persistence following antigen clearance, should be targeted by vaccines.

Together, these experiments have important implications for the development of vaccines. Both studies determined that for long-term protection, vaccines should specifically target the generation of the T_{CM} subpopulation, as this population of cells possesses rapid proliferative potential and long-term persistence following antigen-clearance, and ultimately results in the greatest amount of durable protection. These experiments also revealed a major difference between the CD4 T_{CM} and CD8 T_{CM} populations. While protective CD4 T_{CM} cells can be generated in the presence of persistent antigen, functionally competent CD8 T_{CM} cells required the elimination of antigen for completion of their functional differentiation program and ultimate persistence.

Table 1.1. Murine MHC Class I Epitope List

Protein	Rv #	Epitope	Allele	Reference
Mtb10.3$_{20-28}$	Rv3019c	GYAGTLQSL	H-2K^d	[160]
Mtb10.4$_{20-28}$	Rv0288	GYAGTLQSL	H-2K^d	[160]
Ag85A$_{144-152}$	Rv3804c	VYAGAMSGL	H-2K^d	[79]
PstS-1$_{326-333}$	Rv0934	INYEYAIV	H-2K^b	[274]
PstS-1$_{129-138}$	Rv0934	AQQVNYNLPG	H-2D^b	[296]
PstS-1$_{225-234}$	Rv0934	ALGENGNGGM	H-2D^b	[296]
PstS-1$_{166-175}$	Rv0934	IAALNPGVNL	H-2D^b	[97, 276]
PstS-3$_{285-293}$	Rv0928	SGVGNDLVL	H-2D^b	[206]
Mtb32A$_{309-318}$	Rv0125	GAPINSATAM	H-2D^b	[122, 228]
Mtb8.4$_{33-41}$	Rv1174c	ASPVAQSYL	H-2D^b	[4]
Mtb8.4$_{46-55}$	Rv1174c	AAPPPQRAAM	H-2D^b	[4]
Mtb41$_{43-52}$	Rv0915c	VSYGSVVSTL	H-2D^b	[4, 229]
MPT70$_{96-105}$	Rv2875	YTVFAPTNAA	ND	[253]
MPT64$_{190-198}$	Rv1980c	FAVTNDGVI	H-2D^b	[89, 90, 276]
MPT51$_{24-32}$	Rv3803c	GGPHAVYLL	H-2D^d	[7, 246]
GmdA$_{36-45}$	Rv1511	TFNTSRIDHL	H-2K^d	[172]
GmdA$_{67-76}$	Rv1511	TRLVTLLSTI	H-2K^d	[172]
GmdA$_{135-143}$	Rv1511	ASPPPQNEL	H-2K^d	[172]
GmdA$_{146-155}$	Rv1511	FYPRSPYGAA	H-2K^d	[172]
GmdA$_{190-199}$	Rv1511	TFVTRKITRA	H-2K^d	[172]
GmdA$_{211-219}$	Rv1511	VYMGNLDAV	H-2K^d	[172]
GmdA$_{271-280}$	Rv1511	QYVKFDQRYL	H-2K^d	[172]
	Rv2520c	DPNTIKQEI	H-2L^d	[172]
	Rv2520c	RVIAFLRKPI	H-2K^d	[172]
	Rv3407	IPARRPQNL	H-2L^d	[172]
	Rv3407	RPQNLLDVT	H-2L^d	[172]
CFP10$_{32-39}$	Rv3874	VESTAGSL	H-2K^k	[132]

Note: Predicted MHC class I anchor residues are underlined
ND = Not Determined

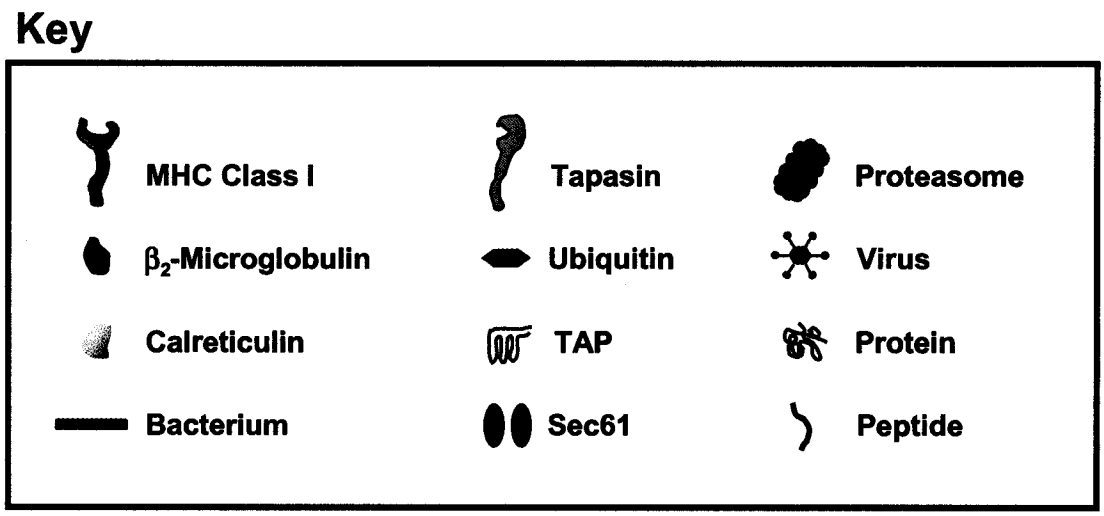

Key for Figures 1.1-1.3. N = Nucleus, ER = Endoplasmic Reticulum, G = Golgi Apparatus, ES = Endosome, PS = Phagosome.

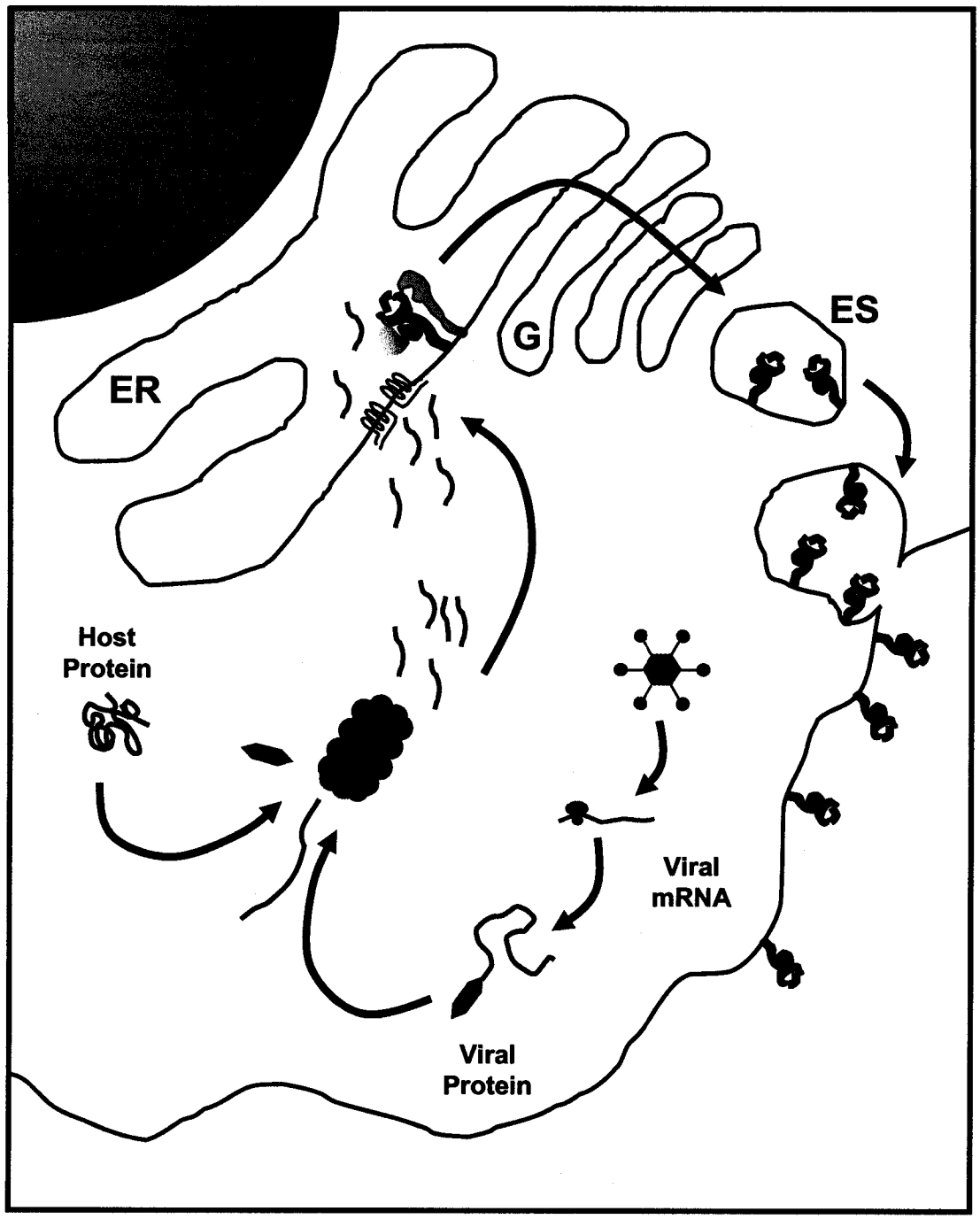

Figure 1.1. The classical MHC class I antigen processing and presentation pathway. Host-derived as well as pathogen-derived proteins are ubiquinated within the cytosol and targeted for destruction by the proteasome. These proteins are degraded into peptide fragments which are transported into the ER by the TAP proteins. Once inside the ER, peptide fragments combine with empty MHC class I molecules, releasing the associated chaperone molecules. The complete MHC class I complex is then targeted to the Golgi network where it is exported to the plasma membrane for surface display.

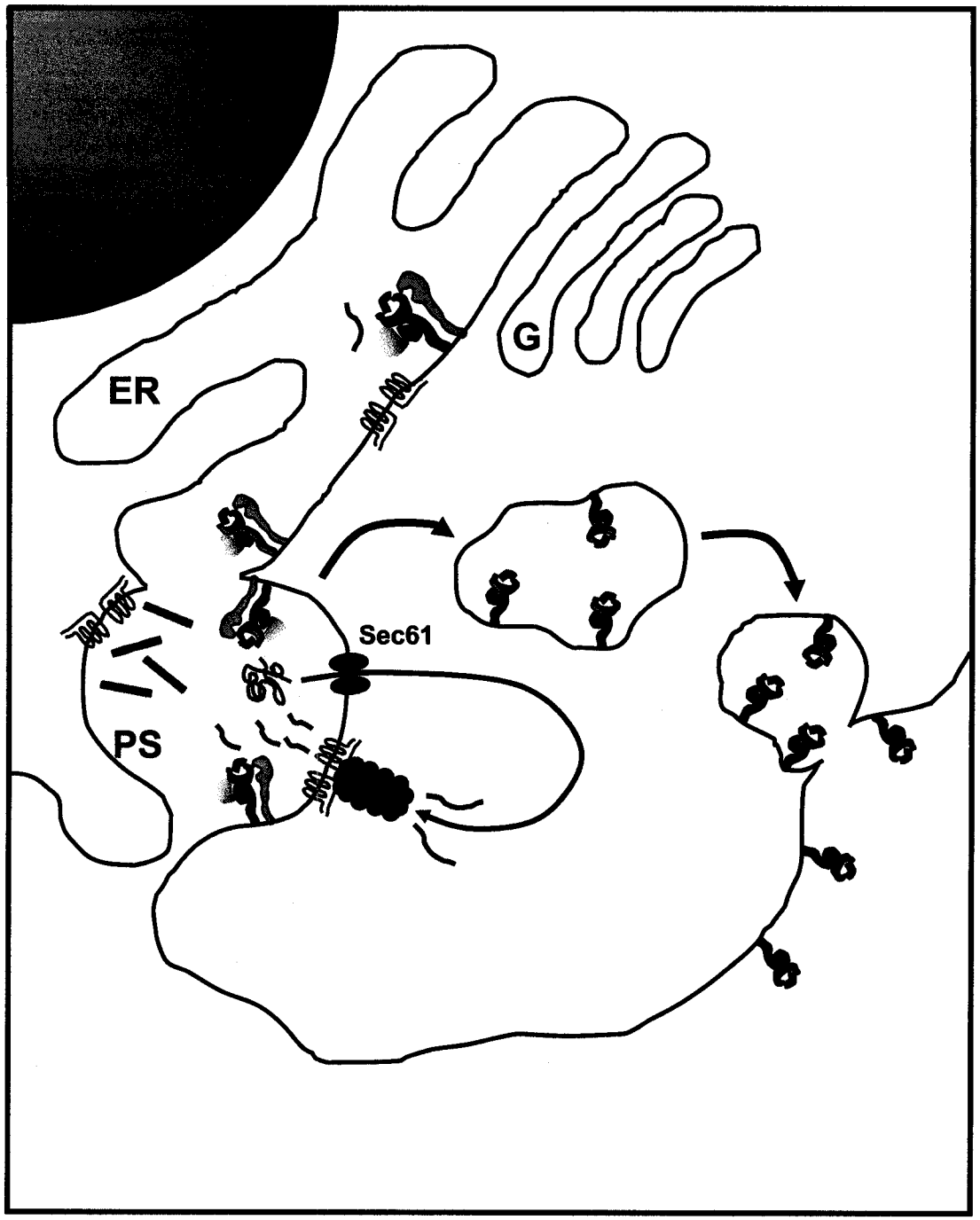

Figure 1.2. The exogenous antigen MHC class I cross-presentation pathway. During phagosome formation, portions of the ER fuse with the phagosome, delivering all of the associated MHC class I antigen processing components. Exogenously-derived protein antigen is then transported out of the phagosome where it is degraded by phagosome-associated proteasome complexes. The resulting peptide fragments are then transported into the phagosome by TAP proteins, where they associate with empty MHC class I molecules. MHC class I-peptide complexes then traffic through the endocytic system and are targeted for surface expression.

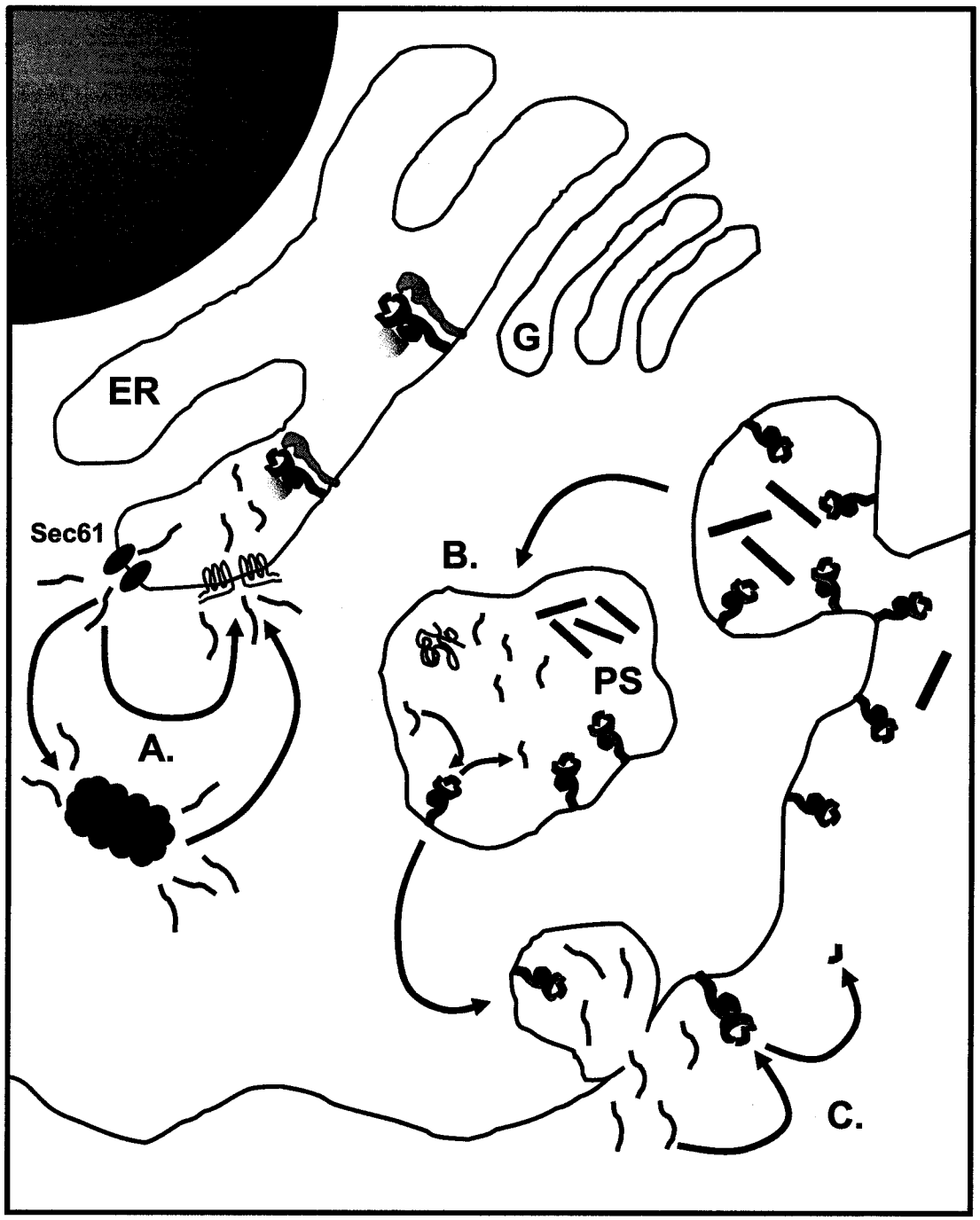

Figure 1.3. Alternate MHC class I antigen processing and presentation pathways. Multiple alternative processing pathways exist, which include retrograde transport of ER proteins via Sec61, which may or may not utilize proteasome-mediated protein cleavage; MHC class I recycling and intraphagosomal peptide exchange following proteolytic breakdown of exogenous proteins; and peptide regurgitation and exchange following exocytosis of degraded exogenous antigens. A = ER Retrograde Transport, B = MHC Recycling and Intraphagosomal Peptide Exchange, C = Peptide Regurgitation and Exchange.

References

1. **Ackerman, A. L., C. Kyritsis, R. Tampe, and P. Cresswell.** 2003. Early phagosomes in dendritic cells form a cellular compartment sufficient for cross presentation of exogenous antigens. Proc Natl Acad Sci U S A **100:**12889-94.

2. **Agarwal, S., and A. Rao.** 1998. Modulation of chromatin structure regulates cytokine gene expression during T cell differentiation. Immunity **9:**765-75.

3. **Ahn, K., A. Gruhler, B. Galocha, T. R. Jones, E. J. Wiertz, H. L. Ploegh, P. A. Peterson, Y. Yang, and K. Fruh.** 1997. The ER-luminal domain of the HCMV glycoprotein US6 inhibits peptide translocation by TAP. Immunity **6:**613-21.

4. **Alderson, M. R.** 2004. Personal Communication.

5. **Allison, M. J., D. Mendoza, and A. Pezzia.** 1973. Documentation of a case of tuberculosis in Pre-Columbian America. Am Rev Respir Dis **107:**985-91.

6. **Ansel, K. M., D. U. Lee, and A. Rao.** 2003. An epigenetic view of helper T cell differentiation. Nat Immunol **4:**616-23.

7. **Aoshi, T., M. Suzuki, M. Uchijima, T. Nagata, and Y. Koide.** 2005. Expression mapping using a retroviral vector for $CD8^+$ T cell epitopes: definition of a *Mycobacterium tuberculosis* peptide presented by H2-D^d. J Immunol Methods **298:**21-34.

8. **Arcaro, A., C. Gregoire, N. Boucheron, S. Stotz, E. Palmer, B. Malissen, and I. F. Luescher.** 2000. Essential role of CD8 palmitoylation in CD8 coreceptor function. J Immunol **165:**2068-76.

9. **Armstrong, J. A., and P. D. Hart.** 1971. Response of cultured macrophages to *Mycobacterium tuberculosis*, with observations on fusion of lysosomes with phagosomes. J Exp Med **134:**713-40.

10. **Arriaza, B. T., W. Salo, A. C. Aufderheide, and T. A. Holcomb.** 1995. Pre-Columbian tuberculosis in northern Chile: molecular and skeletal evidence. Am J Phys Anthropol **98:**37-45.

11. **Bachmann, M. F., K. McKall-Faienza, R. Schmits, D. Bouchard, J. Beach, D. E. Speiser, T. W. Mak, and P. S. Ohashi.** 1997. Distinct roles for LFA-1 and CD28 during activation of naive T cells: adhesion versus costimulation. Immunity **7:**549-57.

12. **Badovinac, V. P., B. B. Porter, and J. T. Harty.** 2004. $CD8^+$ T cell contraction is controlled by early inflammation. Nat Immunol **5:**809-17.

13. **Badovinac, V. P., B. B. Porter, and J. T. Harty.** 2002. Programmed contraction of $CD8^+$ T cells after infection. Nat Immunol **3:**619-26.

14. **Badovinac, V. P., A. R. Tvinnereim, and J. T. Harty.** 2000. Regulation of antigen-specific $CD8^+$ T cell homeostasis by perforin and interferon-γ. Science **290:**1354-8.

15. **Bai, A., J. Broen, and J. Forman.** 1998. The pathway for processing leader-derived peptides that regulate the maturation and expression of Qa-1b. Immunity **9:**413-21.

16. **Baily, G. V.** 1980. Tuberculosis prevention trial, Madras. Indian J Med Res **72 Suppl:**1-74.

17. **Basu, S., R. J. Binder, R. Suto, K. M. Anderson, and P. K. Srivastava.** 2000. Necrotic but not apoptotic cell death releases heat shock proteins, which deliver a partial maturation signal to dendritic cells and activate the NF-κB pathway. Int Immunol **12:**1539-46.

18. **Becker, T. C., E. J. Wherry, D. Boone, K. Murali-Krishna, R. Antia, A. Ma, and R. Ahmed.** 2002. Interleukin 15 is required for proliferative renewal of virus-specific memory CD8 T cells. J Exp Med **195:**1541-8.

19. **Behar, S. M., C. C. Dascher, M. J. Grusby, C. R. Wang, and M. B. Brenner.** 1999. Susceptibility of mice deficient in CD1D or TAP1 to infection with *Mycobacterium tuberculosis*. J Exp Med **189:**1973-80.

20. **Belz, G. T., D. Wodarz, G. Diaz, M. A. Nowak, and P. C. Doherty.** 2002. Compromised influenza virus-specific $CD8^+$-T-cell memory in $CD4^+$-T-cell-deficient mice. J Virol **76:**12388-93.

21. **Bennett, S. R., F. R. Carbone, F. Karamalis, R. A. Flavell, J. F. Miller, and W. R. Heath.** 1998. Help for cytotoxic-T-cell responses is mediated by CD40 signaling. Nature **393:**478-80.

22. **Bennett, S. R., F. R. Carbone, F. Karamalis, J. F. Miller, and W. R. Heath.** 1997. Induction of a $CD8^+$ cytotoxic T lymphocyte response by cross-priming requires cognate $CD4^+$ T cell help. J Exp Med **186:**65-70.

23. **Bergey, D. H., and American Society for Microbiology.** 1994. *Bergey's Manual of Determinative Bacteriology*, 9th ed. Williams and Wilkins, Baltimore.

24. **Bevan, M. J.** 1976. Cross-priming for a secondary cytotoxic response to minor H antigens with H-2 congenic cells which do not cross-react in the cytotoxic assay. J Exp Med **143:**1283-8.

25. **Bevan, M. J.** 1976. Minor H antigens introduced on H-2 different stimulating cells cross-react at the cytotoxic T cell level during *in vivo* priming. J Immunol **117:**2233-8.

26. **Biedermann, T., S. Zimmermann, H. Himmelrich, A. Gumy, O. Egeter, A. K. Sakrauski, I. Seegmuller, H. Voigt, P. Launois, A. D. Levine, H. Wagner, K. Heeg, J. A. Louis, and M. Rocken.** 2001. IL-4 instructs T_H1 responses and resistance to *Leishmania major* in susceptible BALB/c mice. Nat Immunol **2:**1054-60.

27. **Binder, R. J., and P. K. Srivastava.** 2005. Peptides chaperoned by heat-shock proteins are a necessary and sufficient source of antigen in the cross-priming of $CD8^+$ T cells. Nat Immunol **6:**593-9.

28. **Blattman, J. N., R. Antia, D. J. Sourdive, X. Wang, S. M. Kaech, K. Murali-Krishna, J. D. Altman, and R. Ahmed.** 2002. Estimating the precursor frequency of naive antigen-specific CD8 T cells. J Exp Med **195:**657-64.

29. **Bloom, B. R., and C. J. Murray.** 1992. Tuberculosis: commentary on a reemergent killer. Science **257:**1055-64.

30. **Boone, D. R., R. W. Castenholz, and G. M. Garrity.** 2001. *Bergey's Manual of Systematic Bacteriology*, 2nd ed. Springer, New York.

31. **Borrow, P., A. Tishon, S. Lee, J. Xu, I. S. Grewal, M. B. Oldstone, and R. A. Flavell.** 1996. CD40L-deficient mice show deficits in antiviral immunity and have an impaired memory $CD8^+$ CTL response. J Exp Med **183:**2129-42.

32. **Bourgeois, C., B. Rocha, and C. Tanchot.** 2002. A role for CD40 expression on $CD8^+$ T cells in the generation of $CD8^+$ T cell memory. Science **297:**2060-3.

33. **Brandt, L., J. Feino Cunha, A. Weinreich Olsen, B. Chilima, P. Hirsch, R. Appelberg, and P. Andersen.** 2002. Failure of the *Mycobacterium bovis* BCG vaccine: some species of environmental mycobacteria block multiplication of BCG and induction of protective immunity to tuberculosis. Infect Immun **70:**672-8.

34. **Braun, M. M., and G. Cauthen.** 1992. Relationship of the human immunodeficiency virus epidemic to pediatric tuberculosis and bacillus Calmette-Guérin immunization. Pediatr Infect Dis J **11:**220-7.

35. **Brennan, P., and P. Draper.** 1994. Ultrastructure of *Mycobacterium tuberculosis*, p. 271-306. *In* B. R. Bloom (ed.), *Tuberculosis: Pathogenesis, Protection, and Control.* ASM Press, Washington, D.C.

36. **Brodin, P., C. Demangel, and S. T. Cole.** 2005. Introduction to Functional Genomics of the *Mycobacterium tuberculosis* Complex, p. 143-153. *In* S. T. Cole (ed.), *Tuberculosis and the Tubercle Bacillus.* ASM Press, Washington, DC.

37. **Brosch, R., S. V. Gordon, M. Marmiesse, P. Brodin, C. Buchrieser, K. Eiglmeier, T. Garnier, C. Gutierrez, G. Hewinson, K. Kremer, L. M. Parsons, A. S. Pym, S. Samper, D. van Soolingen, and S. T. Cole.** 2002. A new evolutionary scenario for the *Mycobacterium tuberculosis* complex. Proc Natl Acad Sci U S A **99:**3684-9.

38. **Brown, C. A., P. Draper, and P. D. Hart.** 1969. Mycobacteria and lysosomes: a paradox. Nature **221:**658-60.

39. **Brown, M. G., J. Driscoll, and J. J. Monaco.** 1991. Structural and serological similarity of MHC-linked LMP and proteasome (multicatalytic proteinase) complexes. Nature **353:**355-7.

40. **Brown, R. E., B. Miller, W. R. Taylor, C. Palmer, L. Bosco, R. M. Nicola, J. Zelinger, and K. Simpson.** 1995. Health-care expenditures for tuberculosis in the United States. Arch Intern Med **155:**1595-600.

41. **Bucher, H. C., L. E. Griffith, G. H. Guyatt, P. Sudre, M. Naef, P. Sendi, and M. Battegay.** 1999. Isoniazid prophylaxis for tuberculosis in HIV infection: a meta-analysis of randomized controlled trials. Aids **13:**501-7.

42. **Buikstra, J. E., and D. C. Cook.** 1981. Pre-Columbian tuberculosis in West-Central Illinois: prehistoric disease in biocultural perspective. Northwestern University Archaeological Program, Evanston.

43. **Buller, R. M., K. L. Holmes, A. Hugin, T. N. Frederickson, and H. C. Morse, 3rd.** 1987. Induction of cytotoxic T-cell responses *in vivo* in the absence of CD4 helper cells. Nature **328:**77-9.

44. **Bunyan, J.** 1900. *The Life and Death of Mr. Badman.* R.H. Russel, New York.

45. **Camus, J. C., M. J. Pryor, C. Medigue, and S. T. Cole.** 2002. Re-annotation of the genome sequence of *Mycobacterium tuberculosis* H37Rv. Microbiology **148:**2967-73.

46. **Canaday, D. H., R. J. Wilkinson, Q. Li, C. V. Harding, R. F. Silver, and W. H. Boom.** 2001. $CD4^+$ and $CD8^+$ T cells kill intracellular *Mycobacterium tuberculosis* by a perforin and Fas/Fas ligand-independent mechanism. J Immunol **167:**2734-42.

47. **Canaday, D. H., C. Ziebold, E. H. Noss, K. A. Chervenak, C. V. Harding, and W. H. Boom.** 1999. Activation of human $CD8^+$ $\alpha\beta$ TCR^+ cells by *Mycobacterium tuberculosis* via an alternate class I MHC antigen-processing pathway. J Immunol **162:**372-9.

48. **Canetti, G.** 1965. Present aspects of bacterial resistance in tuberculosis. Am Rev Respir Dis **92:**687-703.

49. **Cannons, J. L., P. Lau, B. Ghumman, M. A. DeBenedette, H. Yagita, K. Okumura, and T. H. Watts.** 2001. 4-1BB ligand induces cell division, sustains survival, and enhances effector function of CD4 and CD8 T cells with similar efficacy. J Immunol **167:**1313-24.

50. **Cantwell, M. F., D. E. Snider, Jr., G. M. Cauthen, and I. M. Onorato.** 1994. Epidemiology of tuberculosis in the United States, 1985 through 1992. Jama **272:**535-9.

51. **Cassell, D., and J. Forman.** 1988. Linked recognition of helper and cytotoxic antigenic determinants for the generation of cytotoxic T lymphocytes. Ann N Y Acad Sci **532:**51-60.

52. **Catalfamo, M., and P. A. Henkart.** 2003. Perforin and the granule exocytosis cytotoxicity pathway. Curr Opin Immunol **15:**522-7.

53. **Caux, C., C. Massacrier, B. Vanbervliet, B. Dubois, C. Van Kooten, I. Durand, and J. Banchereau.** 1994. Activation of human dendritic cells through CD40 cross-linking. J Exp Med **180:**1263-72.

54. **Cawthon, A. G., H. Lu, and M. A. Alexander-Miller.** 2001. Peptide requirement for CTL activation reflects the sensitivity to CD3 engagement: correlation with CD8αβ versus CD8αα expression. J Immunol **167:**2577-84.

55. **Centers for Disease Control.** 1993. Initial therapy for tuberculosis in the era of multidrug-resistance. Recommendations of the Advisory Council for the Elimination of Tuberculosis. MMWR Recomm Rep **42:**1-8.

56. **Chefalo, P. J., and C. V. Harding.** 2001. Processing of exogenous antigens for presentation by class I MHC molecules involves post-Golgi peptide exchange influenced by peptide-MHC complex stability and acidic pH. J Immunol **167:**1274-82.

57. **Ciechanover, A.** 1994. The ubiquitin-proteasome proteolytic pathway. Cell **79:**13-21.

58. **Clemens, J. D., J. J. Chuong, and A. R. Feinstein.** 1983. The BCG controversy. A methodological and statistical reappraisal. Jama **249:**2362-9.

59. **Cockburn, A., E. Cockburn, and T. A. Reyman.** 1998. *Mummies, Disease & Ancient Cultures*, 2nd ed. Cambridge University Press, Cambridge, New York.

60. **Colditz, G. A., T. F. Brewer, C. S. Berkey, M. E. Wilson, E. Burdick, H. V. Fineberg, and F. Mosteller.** 1994. Efficacy of BCG vaccine in the prevention of tuberculosis. Meta-analysis of the published literature. Jama **271:**698-702.

61. **Cole, S. T., R. Brosch, J. Parkhill, T. Garnier, C. Churcher, D. Harris, S. V. Gordon, K. Eiglmeier, S. Gas, C. E. Barry, 3rd, F. Tekaia, K. Badcock, D.**

Basham, D. Brown, T. Chillingworth, R. Connor, R. Davies, K. Devlin, T. Feltwell, S. Gentles, N. Hamlin, S. Holroyd, T. Hornsby, K. Jagels, A. Krogh, J. McLean, S. Moule, L. Murphy, K. Oliver, J. Osborne, M. A. Quail, M. A. Rajandream, J. Rogers, S. Rutter, K. Seeger, J. Skelton, R. Squares, S. Squares, J. E. Sulston, K. Taylor, S. Whitehead, and B. G. Barrell. 1998. Deciphering the biology of *Mycobacterium tuberculosis* from the complete genome sequence. Nature **393:**537-44.

62. **Collins, F. M.** 1998. Mycobacterial pathogenesis: a historical perspective. Front Biosci **3:**e123-32.

63. **Comstock, G. W.** 1982. Epidemiology of tuberculosis. Am Rev Respir Dis **125:**8-15.

64. **Conway, H.** 1964. Prevalence of drug resistance in previously untreated patients. United States Public Health Service Cooperative Investigation. Am Rev Respir Dis **89:**327-36.

65. **Cooper, A. M., C. D'Souza, A. A. Frank, and I. M. Orme.** 1997. The course of *Mycobacterium tuberculosis* infection in the lungs of mice lacking expression of either perforin- or granzyme-mediated cytolytic mechanisms. Infect Immun **65:**1317-20.

66. **Cooper, A. M., J. Magram, J. Ferrante, and I. M. Orme.** 1997. Interleukin 12 (IL-12) is crucial to the development of protective immunity in mice intravenously infected with *Mycobacterium tuberculosis*. J Exp Med **186:**39-45.

67. **Cooper, A. M., A. D. Roberts, E. R. Rhoades, J. E. Callahan, D. M. Getzy, and I. M. Orme.** 1995. The role of interleukin-12 in acquired immunity to *Mycobacterium tuberculosis* infection. Immunology **84:**423-32.

68. **Corbett, E. L., C. J. Watt, N. Walker, D. Maher, B. G. Williams, M. C. Raviglione, and C. Dye.** 2003. The growing burden of tuberculosis: global trends and interactions with the HIV epidemic. Arch Intern Med **163:**1009-21.

69. **Craiu, A., T. Akopian, A. Goldberg, and K. L. Rock.** 1997. Two distinct proteolytic processes in the generation of a major histocompatibility complex class I-presented peptide. Proc Natl Acad Sci U S A **94:**10850-5.

70. **Crofton, J., and D. A. Mitchison.** 1948. Streptomycin resistance in pulmonary tuberculosis. BMJ **2:**1009-15.

71. **Curtsinger, J. M., D. C. Lins, and M. F. Mescher.** 2003. Signal 3 determines tolerance versus full activation of naive CD8 T cells: dissociating proliferation and development of effector function. J Exp Med **197:**1141-51.

72. **Curtsinger, J. M., J. O. Valenzuela, P. Agarwal, D. Lins, and M. F. Mescher.** 2005. Type I IFNs provide a third signal to CD8 T cells to stimulate clonal expansion and differentiation. J Immunol **174:**4465-9.

73. **da Conceicao-Silva, F., B. L. Perlaza, J. A. Louis, and P. Romero.** 1994. *Leishmania major* infection in mice primes for specific major histocompatibility complex class I-restricted $CD8^+$ cytotoxic T cell responses. Eur J Immunol **24:**2813-7.

74. **Daffe, M., and P. Draper.** 1998. The envelope layers of mycobacteria with reference to their pathogenicity. Adv Microb Physiol **39:**131-203.

75. **Daniel, T. M.** 1997. *Captain of Death: The Story of Tuberculosis*. University of Rochester Press, Rochester, NY, USA.

76. **De Cock, K. M., and R. E. Chaisson.** 1999. Will DOTS do it? A reappraisal of tuberculosis control in countries with high rates of HIV infection. Int J Tuberc Lung Dis **3:**457-65.

77. **De Libero, G., I. Flesch, and S. H. Kaufmann.** 1988. Mycobacteria-reactive Lyt-2^+ T cell lines. Eur J Immunol **18:**59-66.

78. **den Haan, J. M., S. M. Lehar, and M. J. Bevan.** 2000. $CD8^+$ but not $CD8^-$ dendritic cells cross-prime cytotoxic T cells *in vivo*. J Exp Med **192:**1685-96.

79. **Denis, O., A. Tanghe, K. Palfliet, F. Jurion, T. P. van den Berg, A. Vanonckelen, J. Ooms, E. Saman, J. B. Ulmer, J. Content, and K. Huygen.** 1998. Vaccination with plasmid DNA encoding mycobacterial antigen 85A stimulates a $CD4^+$ and $CD8^+$ T-cell epitopic repertoire broader than that stimulated by *Mycobacterium tuberculosis* H37Rv infection. Infect Immun **66:**1527-33.

80. **Doetsch, R. N.** 1978. Benjamin Marten and his "New Theory of Consumptions". Microbiol Rev **42:**521-8.

81. **Dormandy, T.** 2000. *The White Death: A History of Tuberculosis*. New York University Press, New York.

82. **Draper, P.** 1982. The Anatomy of Mycobacteria, p. 9-52. *In* C. Ratledge and J. Stanford (ed.), *The Biology of the Mycobacteria*, vol. 1. Academic Press, London; New York.

83. **D'Souza, C. D., A. M. Cooper, A. A. Frank, S. Ehlers, J. Turner, A. Bendelac, and I. M. Orme.** 2000. A novel nonclassic β_2-microglobulin-restricted mechanism influencing early lymphocyte accumulation and subsequent resistance to tuberculosis in the lung. Am J Respir Cell Mol Biol **23:**188-93.

84. **Dye, C., S. Scheele, P. Dolin, V. Pathania, and M. C. Raviglione.** 1999. Consensus statement. Global burden of tuberculosis: estimated incidence, prevalence, and mortality by country. WHO Global Surveillance and Monitoring Project. Jama **282:**677-86.

85. **Elliott, T., A. Willis, V. Cerundolo, and A. Townsend.** 1995. Processing of major histocompatibility class I-restricted antigens in the endoplasmic reticulum. J Exp Med **181:**1481-91.

86. **Espinal, M. A., S. J. Kim, P. G. Suarez, K. M. Kam, A. G. Khomenko, G. B. Migliori, J. Baez, A. Kochi, C. Dye, and M. C. Raviglione.** 2000. Standard short-course chemotherapy for drug-resistant tuberculosis: treatment outcomes in 6 countries. Jama **283:**2537-45.

87. **Fazekas de St Groth, B., A. L. Smith, W. P. Koh, L. Girgis, M. C. Cook, and P. Bertolino.** 1999. Carboxyfluorescein diacetate succinimidyl ester and the virgin lymphocyte: a marriage made in heaven. Immunol Cell Biol **77:**530-8.

88. **Feng, C. G., A. G. Bean, H. Hooi, H. Briscoe, and W. J. Britton.** 1999. Increase in gamma interferon-secreting $CD8^+$, as well as $CD4^+$, T cells in lungs following aerosol infection with *Mycobacterium tuberculosis*. Infect Immun **67:**3242-7.

89. **Feng, C. G., T. J. Blanchard, G. L. Smith, A. V. Hill, and W. J. Britton.** 2001. Induction of $CD8^+$ T-lymphocyte responses to a secreted antigen of *Mycobacterium tuberculosis* by an attenuated vaccinia virus. Immunol Cell Biol **79:**569-75.

90. **Feng, C. G., C. Demangel, A. T. Kamath, M. Macdonald, and W. J. Britton.** 2001. Dendritic cells infected with *Mycobacterium bovis* bacillus Calmette Guérin activate $CD8^+$ T cells with specificity for a novel mycobacterial epitope. Int Immunol **13:**451-8.

91. **Fine, P. E.** 1989. The BCG story: lessons from the past and implications for the future. Rev Infect Dis **11 Suppl 2:**S353-9.

92. **Fitzpatrick, D. R., K. M. Shirley, and A. Kelso.** 1999. Cutting edge: stable epigenetic inheritance of regional IFN-γ promoter demethylation in $CD44^{high}CD8^+$ T lymphocytes. J Immunol **162:**5053-7.

93. **Flynn, J. L., and J. Chan.** 2001. Immunology of tuberculosis. Annu Rev Immunol **19:**93-129.

94. **Flynn, J. L., J. Chan, K. J. Triebold, D. K. Dalton, T. A. Stewart, and B. R. Bloom.** 1993. An essential role for interferon-γ in resistance to *Mycobacterium tuberculosis* infection. J Exp Med **178:**2249-54.

95. **Flynn, J. L., M. M. Goldstein, J. Chan, K. J. Triebold, K. Pfeffer, C. J. Lowenstein, R. Schreiber, T. W. Mak, and B. R. Bloom.** 1995. Tumor necrosis factor-α is required in the protective immune response against *Mycobacterium tuberculosis* in mice. Immunity **2:**561-72.

96. **Flynn, J. L., M. M. Goldstein, K. J. Triebold, B. Koller, and B. R. Bloom.** 1992. Major histocompatibility complex class I-restricted T cells are required for resistance to *Mycobacterium tuberculosis* infection. Proc Natl Acad Sci U S A **89:**12013-7.

97. **Fonseca, D. P., B. Benaissa-Trouw, M. van Engelen, C. A. Kraaijeveld, H. Snippe, and A. F. Verheul.** 2001. Induction of cell-mediated immunity against *Mycobacterium tuberculosis* using DNA vaccines encoding cytotoxic and helper T-cell epitopes of the 38-kilodalton protein. Infect Immun **69:**4839-45.

98. **Fox, W.** 1981. Whither short-course chemotherapy? Br J Dis Chest **75:**331-57.

99. **Fratti, R. A., J. M. Backer, J. Gruenberg, S. Corvera, and V. Deretic.** 2001. Role of phosphatidylinositol 3-kinase and Rab5 effectors in phagosomal biogenesis and mycobacterial phagosome maturation arrest. J Cell Biol **154:**631-44.

100. **Fratti, R. A., J. Chua, I. Vergne, and V. Deretic.** 2003. *Mycobacterium tuberculosis* glycosylated phosphatidylinositol causes phagosome maturation arrest. Proc Natl Acad Sci U S A **100:**5437-42.

101. **Fruh, K., K. Ahn, H. Djaballah, P. Sempe, P. M. van Endert, R. Tampe, P. A. Peterson, and Y. Yang.** 1995. A viral inhibitor of peptide transporters for antigen presentation. Nature **375:**415-8.

102. **Gallimore, A., K. Schwarz, M. van den Broek, H. Hengartner, and M. Groettrup.** 1998. The proteasome inhibitor lactacystin prevents the generation of an endoplasmic reticulum leader-derived T cell epitope. Mol Immunol **35:**581-91.

103. **Garay, S. M.** 2004. Pulmonary Tuberculosis, p. 345-394. *In* W. N. Rom and S. M. Garay (ed.), *Tuberculosis*, 2nd ed. Lippincott Williams & Wilkins, Philadelphia.

104. **Gett, A. V., F. Sallusto, A. Lanzavecchia, and J. Geginat.** 2003. T cell fitness determined by signal strength. Nat Immunol **4:**355-60.

105. **Girardi, E., M. C. Raviglione, G. Antonucci, P. Godfrey-Faussett, and G. Ippolito.** 2000. Impact of the HIV epidemic on the spread of other diseases: the case of tuberculosis. Aids **14 Suppl 3:**S47-56.

106. **Glynne, R., S. H. Powis, S. Beck, A. Kelly, L. A. Kerr, and J. Trowsdale.** 1991. A proteasome-related gene between the two ABC transporter loci in the class II region of the human MHC. Nature **353:**357-60.

107. **Grakoui, A., S. K. Bromley, C. Sumen, M. M. Davis, A. S. Shaw, P. M. Allen, and M. L. Dustin.** 1999. The immunological synapse: a molecular machine controlling T cell activation. Science **285:**221-7.

108. **Grange, J. M., J. Gibson, T. W. Osborn, C. H. Collins, and M. D. Yates.** 1983. What is BCG? Tubercle **64:**129-39.

109. **Guerder, S., and P. Matzinger.** 1992. A fail-safe mechanism for maintaining self-tolerance. J Exp Med **176:**553-64.

110. **Guermonprez, P., L. Saveanu, M. Kleijmeer, J. Davoust, P. Van Endert, and S. Amigorena.** 2003. ER-phagosome fusion defines an MHC class I cross-presentation compartment in dendritic cells. Nature **425:**397-402.

111. **Guermonprez, P., J. Valladeau, L. Zitvogel, C. Thery, and S. Amigorena.** 2002. Antigen presentation and T cell stimulation by dendritic cells. Annu Rev Immunol **20:**621-67.

112. **Hammond, S. A., R. C. Bollinger, T. W. Tobery, and R. F. Silliciano.** 1993. Transporter-independent processing of HIV-1 envelope protein for recognition by $CD8^+$ T cells. Nature **364:**158-61.

113. **Harding, C. V., and R. Song.** 1994. Phagocytic processing of exogenous particulate antigens by macrophages for presentation by class I MHC molecules. J Immunol **153:**4925-33.

114. **Hendriks, J., Y. Xiao, and J. Borst.** 2003. CD27 promotes survival of activated T cells and complements CD28 in generation and establishment of the effector T cell pool. J Exp Med **198:**1369-80.

115. **Hochweller, K., and S. M. Anderton.** 2005. Kinetics of costimulatory molecule expression by T cells and dendritic cells during the induction of tolerance versus immunity *in vivo*. Eur J Immunol **35:**1086-96.

116. **Hou, S., L. Hyland, K. W. Ryan, A. Portner, and P. C. Doherty.** 1994. Virus-specific $CD8^+$ T-cell memory determined by clonal burst size. Nature **369:**652-4.

117. **Houde, M., S. Bertholet, E. Gagnon, S. Brunet, G. Goyette, A. Laplante, M. F. Princiotta, P. Thibault, D. Sacks, and M. Desjardins.** 2003. Phagosomes are competent organelles for antigen cross-presentation. Nature **425:**402-6.

118. **Huang, L. R., F. L. Chen, Y. T. Chen, Y. M. Lin, and J. T. Kung.** 2000. Potent induction of long-term $CD8^+$ T cell memory by short-term IL-4 exposure during T cell receptor stimulation. Proc Natl Acad Sci U S A **97:**3406-11.

119. **Hubbard, R. D., C. M. Flory, and F. M. Collins.** 1991. Memory T cell-mediated resistance to *Mycobacterium tuberculosis* infection in innately susceptible and resistant mice. Infect Immun **59:**2012-6.

120. **Iezzi, G., E. Scotet, D. Scheidegger, and A. Lanzavecchia.** 1999. The interplay between the duration of TCR and cytokine signaling determines T cell polarization. Eur J Immunol **29:**4092-101.

121. **Indrigo, J., R. L. Hunter, Jr., and J. K. Actor.** 2003. Cord factor trehalose 6,6'-dimycolate (TDM) mediates trafficking events during mycobacterial infection of murine macrophages. Microbiology **149:**2049-59.

122. **Irwin, S. M., A. A. Izzo, S. W. Dow, Y. A. Skeiky, S. G. Reed, M. R. Alderson, and I. M. Orme.** 2005. Tracking antigen-specific CD8 T lymphocytes in the lungs of mice vaccinated with the Mtb72F polyprotein. Infect Immun **73:**5809-16.

123. **Iseman, M. D., and L. A. Madsen.** 1989. Drug-resistant tuberculosis. Clin Chest Med **10:**341-53.

124. **Janeway, C. A., Jr., and R. Medzhitov.** 2002. Innate immune recognition. Annu Rev Immunol **20:**197-216.

125. **Janssen, E. M., E. E. Lemmens, T. Wolfe, U. Christen, M. G. von Herrath, and S. P. Schoenberger.** 2003. $CD4^+$ T cells are required for secondary expansion and memory in $CD8^+$ T lymphocytes. Nature **421:**852-6.

126. **Juretic, A., B. Malenica, E. Juretic, J. Klein, and Z. A. Nagy.** 1985. Helper effects required during *in vivo* priming for a cytolytic response to the H-Y antigen in nonresponder mice. J Immunol **134:**1408-14.

127. **Kaech, S. M., and R. Ahmed.** 2001. Memory $CD8^+$ T cell differentiation: initial antigen encounter triggers a developmental program in naive cells. Nat Immunol **2:**415-22.

128. **Kaech, S. M., S. Hemby, E. Kersh, and R. Ahmed.** 2002. Molecular and functional profiling of memory CD8 T cell differentiation. Cell **111:**837-51.

129. **Kaech, S. M., J. T. Tan, E. J. Wherry, B. T. Konieczny, C. D. Surh, and R. Ahmed.** 2003. Selective expression of the interleukin 7 receptor identifies effector CD8 T cells that give rise to long-lived memory cells. Nat Immunol **4:**1191-8.

130. **Kaleab, B., T. Ottenoff, P. Converse, E. Halapi, G. Tadesse, M. Rottenberg, and R. Kiessling.** 1990. Mycobacterial-induced cytotoxic T cells as well as nonspecific killer cells derived from healthy individuals and leprosy patients. Eur J Immunol **20:**2651-9.

131. **Kalinski, P., C. M. Hilkens, E. A. Wierenga, and M. L. Kapsenberg.** 1999. T-cell priming by type-1 and type-2 polarized dendritic cells: the concept of a third signal. Immunol Today **20:**561-7.

132. **Kamath, A. B., J. Woodworth, X. Xiong, C. Taylor, Y. Weng, and S. M. Behar.** 2004. Cytolytic $CD8^+$ T cells recognizing CFP10 are recruited to the lung after *Mycobacterium tuberculosis* infection. J Exp Med **200:**1479-89.

133. **Kimerling, M. E., H. Kluge, N. Vezhnina, T. Iacovazzi, T. Demeulenaere, F. Portaels, and F. Matthys.** 1999. Inadequacy of the current WHO re-treatment regimen in a central Siberian prison: treatment failure and MDR-TB. Int J Tuberc Lung Dis **3:**451-3.

134. **Kleijmeer, M. J., J. M. Escola, F. G. UytdeHaag, E. Jakobson, J. M. Griffith, A. D. Osterhaus, W. Stoorvogel, C. J. Melief, C. Rabouille, and H. J. Geuze.** 2001. Antigen loading of MHC class I molecules in the endocytic tract. Traffic **2:**124-37.

135. **Koch, R.** 1882. Die Aetiologie der Tuberculose. Berlin Klin Wochenchr **19:**221-30.

136. **Kochi, A., B. Vareldzis, and K. Styblo.** 1993. Multidrug-resistant tuberculosis and its control. Res Microbiol **144:**104-10.

137. **Koller, B. H., P. Marrack, J. W. Kappler, and O. Smithies.** 1990. Normal development of mice deficient in β_2M, MHC class I proteins, and $CD8^+$ T cells. Science **248:**1227-30.

138. **Kolumam, G. A., S. Thomas, L. J. Thompson, J. Sprent, and K. Murali-Krishna.** 2005. Type I interferons act directly on CD8 T cells to allow clonal expansion and memory formation in response to viral infection. J Exp Med **202:**637-50.

139. **Kovacsovics-Bankowski, M., and K. L. Rock.** 1995. A phagosome-to-cytosol pathway for exogenous antigens presented on MHC class I molecules. Science **267:**243-6.

140. **Krug, A., R. Veeraswamy, A. Pekosz, O. Kanagawa, E. R. Unanue, M. Colonna, and M. Cella.** 2003. Interferon-producing cells fail to induce proliferation of naive T cells but can promote expansion and T helper 1 differentiation of antigen-experienced unpolarized T cells. J Exp Med **197:**899-906.

141. **Ku, C. C., M. Murakami, A. Sakamoto, J. Kappler, and P. Marrack.** 2000. Control of homeostasis of $CD8^+$ memory T cells by opposing cytokines. Science **288:**675-8.

142. **Kunisawa, J., and N. Shastri.** 2003. The group II chaperonin TRiC protects proteolytic intermediates from degradation in the MHC class I antigen processing pathway. Mol Cell **12:**565-76.

143. **Ladel, C. H., S. Daugelat, and S. H. Kaufmann.** 1995. Immune response to *Mycobacterium bovis* bacille Calmette Guérin infection in major histocompatibility complex class I- and II-deficient knock-out mice: contribution of CD4 and CD8 T cells to acquired resistance. Eur J Immunol **25:**377-84.

144. **Laennec, R. T. H.** 1821. *A Treatise on Diseases of the Chest*, Special ed. T. and G. Underwood, London.

145. **Lalvani, A., R. Brookes, R. J. Wilkinson, A. S. Malin, A. A. Pathan, P. Andersen, H. Dockrell, G. Pasvol, and A. V. Hill.** 1998. Human cytolytic and interferon γ-secreting $CD8^+$ T lymphocytes specific for *Mycobacterium tuberculosis*. Proc Natl Acad Sci U S A **95:**270-5.

146. **Lanzavecchia, A., and F. Sallusto.** 2000. Dynamics of T lymphocyte responses: intermediates, effectors, and memory cells. Science **290:**92-7.

147. **Laochumroonvorapong, P., J. Wang, C. C. Liu, W. Ye, A. L. Moreira, K. B. Elkon, V. H. Freedman, and G. Kaplan.** 1997. Perforin, a cytotoxic molecule which mediates cell necrosis, is not required for the early control of mycobacterial infection in mice. Infect Immun **65:**127-32.

148. **Le Bon, A., N. Etchart, C. Rossmann, M. Ashton, S. Hou, D. Gewert, P. Borrow, and D. F. Tough.** 2003. Cross-priming of $CD8^+$ T cells stimulated by virus-induced type I interferon. Nat Immunol **4:**1009-15.

149. **Lee, S. P., W. A. Thomas, N. W. Blake, and A. B. Rickinson.** 1996. Transporter (TAP)-independent processing of a multiple membrane-spanning protein, the Epstein-Barr virus latent membrane protein 2. Eur J Immunol **26:**1875-83.

150. **Lefford, M. J.** 1975. Transfer of adoptive immunity to tuberculosis in mice. Infect Immun **11:**1174-81.

151. **Lehmann, J.** 1946. Para-aminosalicylic acid in the treatment of tuberculosis. The Lancet **247:**15-16.

152. **Leveton, C., S. Barnass, B. Champion, S. Lucas, B. De Souza, M. Nicol, D. Banerjee, and G. Rook.** 1989. T-cell-mediated protection of mice against virulent *Mycobacterium tuberculosis*. Infect Immun **57:**390-5.

153. **Levitskaya, J., A. Sharipo, A. Leonchiks, A. Ciechanover, and M. G. Masucci.** 1997. Inhibition of ubiquitin/proteasome-dependent protein degradation by the Gly-Ala repeat domain of the Epstein-Barr virus nuclear antigen 1. Proc Natl Acad Sci U S A **94:**12616-21.

154. **Liu, Y., and A. Mullbacher.** 1989. The generation and activation of memory class I MHC restricted cytotoxic T cell responses to influenza A virus *in vivo* do not require $CD4^+$ T cells. Immunol Cell Biol **67 (Pt 6):**413-20.

155. **Lizee, G., G. Basha, and W. A. Jefferies.** 2005. Tails of wonder: endocytic-sorting motifs key for exogenous antigen presentation. Trends Immunol **26:**141-9.

156. **Luft, T., K. C. Pang, E. Thomas, P. Hertzog, D. N. Hart, J. Trapani, and J. Cebon.** 1998. Type I IFNs enhance the terminal differentiation of dendritic cells. J Immunol **161:**1947-53.

157. **Madakamutil, L. T., U. Christen, C. J. Lena, Y. Wang-Zhu, A. Attinger, M. Sundarrajan, W. Ellmeier, M. G. von Herrath, P. Jensen, D. R. Littman, and H. Cheroutre.** 2004. CD8αα-mediated survival and differentiation of CD8 memory T cell precursors. Science **304:**590-3.

158. **Madden, D. R.** 1995. The three-dimensional structure of peptide-MHC complexes. Annu Rev Immunol **13:**587-622.

159. **Mahairas, G. G., P. J. Sabo, M. J. Hickey, D. C. Singh, and C. K. Stover.** 1996. Molecular analysis of genetic differences between *Mycobacterium bovis* BCG and virulent *M. bovis*. J Bacteriol **178:**1274-82.

160. **Majlessi, L., M. J. Rojas, P. Brodin, and C. Leclerc.** 2003. $CD8^+$ T-cell responses of mycobacterium-infected mice to a newly identified major histocompatibility complex class I-restricted epitope shared by proteins of the ESAT-6 family. Infect Immun **71:**7173-7.

161. **Major, R. H.** 1945. *Classic Descriptions of Disease, with Biographical Sketches of the Authors*, 3rd ed. C. C. Thomas, Springfield, Illinois.

162. **Malone, L., A. Schurr, H. Lindh, K. D. Mc, J. S. Kiser, and J. H. Williams.** 1952. The effect of pyrazinamide (aldinamide) on experimental tuberculosis in mice. Am Rev Tuberc **65:**511-8.

163. **Manchester, K.** 1984. Tuberculosis and leprosy in antiquity: an interpretation. Med Hist **28:**162-73.

164. **Marrack, P., and J. Kappler.** 2004. Control of T cell viability. Annu Rev Immunol **22:**765-87.

165. **Marrack, P., J. Kappler, and T. Mitchell.** 1999. Type I interferons keep activated T cells alive. J Exp Med **189:**521-30.

166. **Matzinger, P.** 1994. Tolerance, danger, and the extended family. Annu Rev Immunol **12:**991-1045.

167. **Mazzaccaro, R. J., M. Gedde, E. R. Jensen, H. M. van Santen, H. L. Ploegh, K. L. Rock, and B. R. Bloom.** 1996. Major histocompatibility class I presentation of soluble antigen facilitated by *Mycobacterium tuberculosis* infection. Proc Natl Acad Sci U S A **93:**11786-91.

168. **McCluskey, J., J. Rossjohn, and A. W. Purcell.** 2004. TAP genes and immunity. Curr Opin Immunol **16:**651-9.

169. **McGrath, J. W.** 1988. Social networks of disease spread in the lower Illinois valley: a simulation approach. Am J Phys Anthropol **77:**483-96.

170. **Mercado, R., S. Vijh, S. E. Allen, K. Kerksiek, I. M. Pilip, and E. G. Pamer.** 2000. Early programming of T cell populations responding to bacterial infection. J Immunol **165:**6833-9.

171. **Mogues, T., M. E. Goodrich, L. Ryan, R. LaCourse, and R. J. North.** 2001. The relative importance of T cell subsets in immunity and immunopathology of airborne *Mycobacterium tuberculosis* infection in mice. J Exp Med **193:**271-80.

172. **Mollenkopf, H. J., L. Grode, J. Mattow, M. Stein, P. Mann, B. Knapp, J. Ulmer, and S. H. Kaufmann.** 2004. Application of mycobacterial proteomics to vaccine design: improved protection by *Mycobacterium bovis* BCG prime-Rv3407 DNA boost vaccination against tuberculosis. Infect Immun **72:**6471-9.

173. **Momburg, F., and G. J. Hammerling.** 1998. Generation and TAP-mediated transport of peptides for major histocompatibility complex class I molecules. Adv Immunol **68:**191-256.

174. **Momburg, F., and P. Tan.** 2002. Tapasin-the keystone of the loading complex optimizing peptide binding by MHC class I molecules in the endoplasmic reticulum. Mol Immunol **39:**217-33.

175. **Morse, D., D. R. Brothwell, and P. J. Ucko.** 1964. Tuberculosis in ancient Egypt. Am Rev Respir Dis **90:**524-41.

176. **Mullen, A. C., F. A. High, A. S. Hutchins, H. W. Lee, A. V. Villarino, D. M. Livingston, A. L. Kung, N. Cereb, T. P. Yao, S. Y. Yang, and S. L. Reiner.** 2001. Role of T-bet in commitment of T_H1 cells before IL-12-dependent selection. Science **292:**1907-10.

177. **Muller, I., S. P. Cobbold, H. Waldmann, and S. H. Kaufmann.** 1987. Impaired resistance to *Mycobacterium tuberculosis* infection after selective *in vivo* depletion of $L3T4^+$ and $Lyt\text{-}2^+$ T cells. Infect Immun **55:**2037-41.

178. **Niedermann, G., E. Geier, M. Lucchiari-Hartz, N. Hitziger, A. Ramsperger, and K. Eichmann.** 1999. The specificity of proteasomes: impact on MHC class I processing and presentation of antigens. Immunol Rev **172:**29-48.

179. **Niedermann, G., G. King, S. Butz, U. Birsner, R. Grimm, J. Shabanowitz, D. F. Hunt, and K. Eichmann.** 1996. The proteolytic fragments generated by vertebrate proteasomes: structural relationships to major histocompatibility complex class I binding peptides. Proc Natl Acad Sci U S A **93:**8572-7.

180. **Norbury, C. C., L. J. Hewlett, A. R. Prescott, N. Shastri, and C. Watts.** 1995. Class I MHC presentation of exogenous soluble antigen via macropinocytosis in bone marrow macrophages. Immunity **3:**783-91.

181. **Nussbaum, A. K., T. P. Dick, W. Keilholz, M. Schirle, S. Stevanovic, K. Dietz, W. Heinemeyer, M. Groll, D. H. Wolf, R. Huber, H. G. Rammensee, and H. Schild.** 1998. Cleavage motifs of the yeast 20S proteasome β subunits deduced from digests of enolase 1. Proc Natl Acad Sci U S A **95:**12504-9.

182. **Orme, I. M.** 1987. The kinetics of emergence and loss of mediator T lymphocytes acquired in response to infection with *Mycobacterium tuberculosis*. J Immunol **138:**293-8.

183. **Orme, I. M., and F. M. Collins.** 1984. Adoptive protection of the *Mycobacterium tuberculosis*-infected lung. Dissociation between cells that passively transfer protective immunity and those that transfer delayed-type hypersensitivity to tuberculin. Cell Immunol **84:**113-20.

184. **Orme, I. M., and F. M. Collins.** 1983. Protection against *Mycobacterium tuberculosis* infection by adoptive immunotherapy. Requirement for T cell-deficient recipients. J Exp Med **158:**74-83.

185. **Orme, I. M., E. S. Miller, A. D. Roberts, S. K. Furney, J. P. Griffin, K. M. Dobos, D. Chi, B. Rivoire, and P. J. Brennan.** 1992. T lymphocytes mediating protection and cellular cytolysis during the course of *Mycobacterium tuberculosis* infection. Evidence for different kinetics and recognition of a wide spectrum of protein antigens. J Immunol **148:**189-96.

186. **Pablos-Mendez, A., M. C. Raviglione, A. Laszlo, N. Binkin, H. L. Rieder, F. Bustreo, D. L. Cohn, C. S. Lambregts-van Weezenbeek, S. J. Kim, P. Chaulet, and P. Nunn.** 1998. Global surveillance for antituberculosis-drug resistance, 1994-1997. World Health Organization-International Union against Tuberculosis and Lung Disease Working Group on Anti-Tuberculosis Drug Resistance Surveillance. N Engl J Med **338:**1641-9.

187. **Palmer, C. E., and M. W. Long.** 1966. Effects of infection with atypical mycobacteria on BCG vaccination and tuberculosis. Am Rev Respir Dis **94:**553-68.

188. **Park, B., Y. Kim, J. Shin, S. Lee, K. Cho, K. Fruh, and K. Ahn.** 2004. Human cytomegalovirus inhibits tapasin-dependent peptide loading and optimization of the MHC class I peptide cargo for immune evasion. Immunity **20:**71-85.

189. **Perzigian, A. J., and L. Widmer.** 1979. Evidence for tuberculosis in a prehistoric population. Jama **241:**2643-6.

190. **Pooley, J. L., W. R. Heath, and K. Shortman.** 2001. Cutting edge: intravenous soluble antigen is presented to CD4 T cells by CD8- dendritic cells, but cross-presented to CD8 T cells by $CD8^+$ dendritic cells. J Immunol **166:**5327-30.

191. **Prilliman, K. R., E. E. Lemmens, G. Palioungas, T. G. Wolfe, J. P. Allison, A. H. Sharpe, and S. P. Schoenberger.** 2002. Cutting edge: a crucial role for B7-CD28 in transmitting T help from APC to CTL. J Immunol **169:**4094-7.

192. **Rammensee, H. G., T. Friede, and S. Stevanoviic.** 1995. MHC ligands and peptide motifs: first listing. Immunogenetics **41:**178-228.

193. **Rathmell, J. C., and C. B. Thompson.** 2002. Pathways of apoptosis in lymphocyte development, homeostasis, and disease. Cell **109 Suppl:**S97-107.

194. **Raviglione, M. C., R. Gupta, C. M. Dye, and M. A. Espinal.** 2001. The burden of drug-resistant tuberculosis and mechanisms for its control. Ann N Y Acad Sci **953:**88-97.

195. **Ravkov, E. V., C. M. Myrick, and J. D. Altman.** 2003. Immediate early effector functions of virus-specific $CD8^+CCR7^+$ memory cells in humans defined by HLA and CC chemokine ligand 19 tetramers. J Immunol **170:**2461-8.

196. **Razvi, E. S., R. M. Welsh, and H. I. McFarland.** 1995. *In vivo* state of antiviral CTL precursors. Characterization of a cycling cell population containing CTL precursors in immune mice. J Immunol **154:**620-32.

197. **Ridge, J. P., F. Di Rosa, and P. Matzinger.** 1998. A conditioned dendritic cell can be a temporal bridge between a $CD4^+$ T-helper and a T-killer cell. Nature **393:**474-8.

198. **Rieder, H.** 2003. BCG Vaccination, p. 337-353. *In* P. D. O. Davies (ed.), *Clinical Tuberculosis*, 2nd ed. Arnold, London.

199. **Rieder, H. L., G. M. Cauthen, G. W. Comstock, and D. E. Snider, Jr.** 1989. Epidemiology of tuberculosis in the United States. Epidemiol Rev **11:**79-98.

200. **Rock, K. L.** 1996. A new foreign policy: MHC class I molecules monitor the outside world. Immunol Today **17:**131-7.

201. **Rock, K. L., C. Gramm, L. Rothstein, K. Clark, R. Stein, L. Dick, D. Hwang, and A. L. Goldberg.** 1994. Inhibitors of the proteasome block the degradation of most cell proteins and the generation of peptides presented on MHC class I molecules. Cell **78:**761-71.

202. **Rock, K. L., I. A. York, T. Saric, and A. L. Goldberg.** 2002. Protein degradation and the generation of MHC class I-presented peptides. Adv Immunol **80:**1-70.

203. **Rodrigues, L. C., V. K. Diwan, and J. G. Wheeler.** 1993. Protective effect of BCG against tuberculous meningitis and miliary tuberculosis: a meta-analysis. Int J Epidemiol **22:**1154-8.

204. **Rodriguez, A., A. Regnault, M. Kleijmeer, P. Ricciardi-Castagnoli, and S. Amigorena.** 1999. Selective transport of internalized antigens to the cytosol for MHC class I presentation in dendritic cells. Nat Cell Biol **1:**362-8.

205. **Rolph, M. S., B. Raupach, H. H. Kobernick, H. L. Collins, B. Perarnau, F. A. Lemonnier, and S. H. Kaufmann.** 2001. MHC class Ia-restricted T cells partially account for β_2-microglobulin-dependent resistance to *Mycobacterium tuberculosis*. Eur J Immunol **31:**1944-9.

206. **Romano, M., O. Denis, S. D'Souza, X. M. Wang, T. H. Ottenhoff, J. M. Brulet, and K. Huygen.** 2004. Induction of *in vivo* functional D^b-restricted cytolytic T cell activity against a putative phosphate transport receptor of *Mycobacterium tuberculosis*. J Immunol **172:**6913-21.

207. **Romero, P., J. L. Maryanski, G. Corradin, R. S. Nussenzweig, V. Nussenzweig, and F. Zavala.** 1989. Cloned cytotoxic T cells recognize an epitope in the circumsporozoite protein and protect against malaria. Nature **341:**323-6.

208. **Sager, P., M. Schalimtzer, and V. Moller-Christensen.** 1972. A case of spondylitis tuberculosa in the Danish Neolithic Age. Dan Med Bull **19:**176-80.

209. **Sallusto, F., D. Lenig, R. Forster, M. Lipp, and A. Lanzavecchia.** 1999. Two subsets of memory T lymphocytes with distinct homing potentials and effector functions. Nature **401:**708-12.

210. **Salo, W. L., A. C. Aufderheide, J. Buikstra, and T. A. Holcomb.** 1994. Identification of *Mycobacterium tuberculosis* DNA in a pre-Columbian Peruvian mummy. Proc Natl Acad Sci U S A **91:**2091-4.

211. **Schaible, U. E., H. L. Collins, F. Priem, and S. H. Kaufmann.** 2002. Correction of the iron overload defect in β-2-microglobulin knockout mice by lactoferrin abolishes their increased susceptibility to tuberculosis. J Exp Med **196:**1507-13.

212. **Schaible, U. E., F. Winau, P. A. Sieling, K. Fischer, H. L. Collins, K. Hagens, R. L. Modlin, V. Brinkmann, and S. H. Kaufmann.** 2003. Apoptosis facilitates antigen presentation to T lymphocytes through MHC-I and CD1 in tuberculosis. Nat Med **9:**1039-46.

213. **Schatz, A. B., and S. Waksman.** 1944. Streptomycin, a substance exhibiting antibiotic activity against gram-positive and gram-negative bacteria. Proc. Soc. Exp. Biol. Med. **55:**66-69.

214. **Schmidt, C. S., and M. F. Mescher.** 1999. Adjuvant effect of IL-12: conversion of peptide antigen administration from tolerizing to immunizing for $CD8^+$ T cells *in vivo*. J Immunol **163:**2561-7.

215. **Schoenberger, S. P., R. E. Toes, E. I. van der Voort, R. Offringa, and C. J. Melief.** 1998. T-cell help for cytotoxic T lymphocytes is mediated by CD40-CD40L interactions. Nature **393:**480-3.

216. **Schuurhuis, D. H., S. Laban, R. E. Toes, P. Ricciardi-Castagnoli, M. J. Kleijmeer, E. I. van der Voort, D. Rea, R. Offringa, H. J. Geuze, C. J. Melief, and F. Ossendorp.** 2000. Immature dendritic cells acquire $CD8^+$ cytotoxic T lymphocyte priming capacity upon activation by T helper cell-independent or -dependent stimuli. J Exp Med **192:**145-50.

217. **Selin, L. K., M. Y. Lin, K. A. Kraemer, D. M. Pardoll, J. P. Schneck, S. M. Varga, P. A. Santolucito, A. K. Pinto, and R. M. Welsh.** 1999. Attrition of T cell memory: selective loss of LCMV epitope-specific memory CD8 T cells following infections with heterologous viruses. Immunity **11:**733-42.

218. **Selwyn, P. A., D. Hartel, V. A. Lewis, E. E. Schoenbaum, S. H. Vermund, R. S. Klein, A. T. Walker, and G. H. Friedland.** 1989. A prospective study of the risk of tuberculosis among intravenous drug users with human immunodeficiency virus infection. N Engl J Med **320:**545-50.

219. **Serbina, N. V., and J. L. Flynn.** 1999. Early emergence of $CD8^+$ T cells primed for production of type 1 cytokines in the lungs of *Mycobacterium tuberculosis*-infected mice. Infect Immun **67:**3980-8.

220. **Serbina, N. V., C. C. Liu, C. A. Scanga, and J. L. Flynn.** 2000. $CD8^+$ CTL from lungs of *Mycobacterium tuberculosis*-infected mice express perforin *in vivo* and lyse infected macrophages. J Immunol **165:**353-63.

221. **Shedlock, D. J., and H. Shen.** 2003. Requirement for CD4 T cell help in generating functional CD8 T cell memory. Science **300:**337-9.

222. **Shedlock, D. J., J. K. Whitmire, J. Tan, A. S. MacDonald, R. Ahmed, and H. Shen.** 2003. Role of CD4 T cell help and costimulation in CD8 T cell responses during *Listeria monocytogenes* infection. J Immunol **170:**2053-63.

223. **Shi, Y., J. E. Evans, and K. L. Rock.** 2003. Molecular identification of a danger signal that alerts the immune system to dying cells. Nature **425:**516-21.

224. **Shirai, M., C. D. Pendleton, J. Ahlers, T. Takeshita, M. Newman, and J. A. Berzofsky.** 1994. Helper-cytotoxic T lymphocyte (CTL) determinant linkage required for priming of anti-HIV $CD8^+$ CTL *in vivo* with peptide vaccine constructs. J Immunol **152:**549-56.

225. **Sibille, C., K. G. Gould, K. Willard-Gallo, S. Thomson, A. J. Rivett, S. Powis, G. W. Butcher, and P. De Baetselier.** 1995. $LMP2^+$ proteasomes are required for the presentation of specific antigens to cytotoxic T lymphocytes. Curr Biol **5:**923-30.

226. **Sigal, L. J., S. Crotty, R. Andino, and K. L. Rock.** 1999. Cytotoxic T-cell immunity to virus-infected non-haematopoietic cells requires presentation of exogenous antigen. Nature **398:**77-80.

227. **Silva, C. L., and D. B. Lowrie.** 2000. Identification and characterization of murine cytotoxic T cells that kill *Mycobacterium tuberculosis*. Infect Immun **68:**3269-74.

228. **Skeiky, Y. A., M. R. Alderson, P. J. Ovendale, J. A. Guderian, L. Brandt, D. C. Dillon, A. Campos-Neto, Y. Lobet, W. Dalemans, I. M. Orme, and S. G. Reed.** 2004. Differential immune responses and protective efficacy induced by components of a tuberculosis polyprotein vaccine, Mtb72F, delivered as naked DNA or recombinant protein. J Immunol **172:**7618-28.

229. **Skeiky, Y. A., M. R. Alderson, P. J. Ovendale, Y. Lobet, W. Dalemans, I. M. Orme, S. G. Reed, and A. Campos-Neto.** 2005. Protection of mice and guinea pigs against tuberculosis induced by immunization with a single *Mycobacterium tuberculosis* recombinant antigen, MTB41. Vaccine **23:**3937-45.

230. **Snider, D.** 1990. Outbreak of multidrug-resistant tuberculosis --Texas, California, and Pennsylvania. MMWR **39:**369-372.

231. **Snyder, H. L., J. W. Yewdell, and J. R. Bennink.** 1994. Trimming of antigenic peptides in an early secretory compartment. J Exp Med **180:**2389-94.

232. **Sousa, A. O., R. J. Mazzaccaro, R. G. Russell, F. K. Lee, O. C. Turner, S. Hong, L. Van Kaer, and B. R. Bloom.** 2000. Relative contributions of distinct MHC class I-dependent cell populations in protection to tuberculosis infection in mice. Proc Natl Acad Sci U S A **97:**4204-8.

233. **Sperling, A. I., J. A. Auger, B. D. Ehst, I. C. Rulifson, C. B. Thompson, and J. A. Bluestone.** 1996. CD28/B7 interactions deliver a unique signal to naive T cells that regulates cell survival but not early proliferation. J Immunol **157:**3909-17.

234. **Sreevatsan, S., X. Pan, K. E. Stockbauer, N. D. Connell, B. N. Kreiswirth, T. S. Whittam, and J. M. Musser.** 1997. Restricted structural gene polymorphism in the *Mycobacterium tuberculosis* complex indicates evolutionarily recent global dissemination. Proc Natl Acad Sci U S A **94:**9869-74.

235. **Stager, S., J. Alexander, A. C. Kirby, M. Botto, N. V. Rooijen, D. F. Smith, F. Brombacher, and P. M. Kaye.** 2003. Natural antibodies and complement are endogenous adjuvants for vaccine-induced $CD8^+$ T-cell responses. Nat Med **9:**1287-92.

236. **Starck, L., C. Scholz, B. Dorken, and P. T. Daniel.** 2005. Costimulation by CD137/4-1BB inhibits T cell apoptosis and induces Bcl-x_L and c-$FLIP_{short}$ via phosphatidylinositol 3-kinase and AKT/protein kinase B. Eur J Immunol **35:**1257-66.

237. **Stenger, S., R. J. Mazzaccaro, K. Uyemura, S. Cho, P. F. Barnes, J. P. Rosat, A. Sette, M. B. Brenner, S. A. Porcelli, B. R. Bloom, and R. L. Modlin.** 1997. Differential effects of cytolytic T cell subsets on intracellular infection. Science **276:**1684-7.

238. **Stewart, W. H.** 1967. A Mandate for State Action. Presented at the Association of State and Territorial Health Officers, Washington, D.C., Dec. 4, 1967.

239. **Stohwasser, R., U. Salzmann, J. Giesebrecht, P. M. Kloetzel, and H. G. Holzhutter.** 2000. Kinetic evidences for facilitation of peptide channelling by the proteasome activator PA28. Eur J Biochem **267:**6221-30.

240. **Sturgill-Koszycki, S., P. H. Schlesinger, P. Chakraborty, P. L. Haddix, H. L. Collins, A. K. Fok, R. D. Allen, S. L. Gluck, J. Heuser, and D. G. Russell.** 1994. Lack of acidification in mycobacterium phagosomes produced by exclusion of the vesicular proton-ATPase. Science **263:**678-81.

241. **Sun, J. C., and M. J. Bevan.** 2003. Defective CD8 T cell memory following acute infection without CD4 T cell help. Science **300:**339-42.

242. **Sun, J. C., M. A. Williams, and M. J. Bevan.** 2004. $CD4^+$ T cells are required for the maintenance, not programming, of memory $CD8^+$ T cells after acute infection. Nat Immunol **5:**927-33.

243. **Sun, Y., A. J. Sijts, M. Song, K. Janek, A. K. Nussbaum, S. Kral, M. Schirle, S. Stevanovic, A. Paschen, H. Schild, P. M. Kloetzel, and D. Schadendorf.** 2002. Expression of the proteasome activator PA28 rescues the presentation of a cytotoxic T lymphocyte epitope on melanoma cells. Cancer Res **62:**2875-82.

244. **Suter, E.** 1961. Passive transfer of acquired resistance to infection with *Mycobacterium tuberculosis* by means of cells. Am Rev Respir Dis **83:**535-43.

245. **Sutherland, I.** 1976. Recent studies in the epidemiology of tuberculosis, based on the risk of being infected with tubercle bacilli. Adv Tuberc Res **19:**1-63.

246. **Suzuki, M., T. Aoshi, T. Nagata, and Y. Koide.** 2004. Identification of murine H2-D^d- and H2-A^b-restricted T-cell epitopes on a novel protective antigen, MPT51, of *Mycobacterium tuberculosis*. Infect Immun **72:**3829-37.

247. **Szalay, G., J. Hess, and S. H. Kaufmann.** 1994. Presentation of *Listeria monocytogenes* antigens by major histocompatibility complex class I molecules to CD8 cytotoxic T lymphocytes independent of listeriolysin secretion and virulence. Eur J Immunol **24:**1471-7.

248. **Takemoto, N., Y. Kamogawa, H. Jun Lee, H. Kurata, K. I. Arai, A. O'Garra, N. Arai, and S. Miyatake.** 2000. Cutting edge: chromatin remodeling at the IL-4/IL-13 intergenic regulatory region for Th2-specific cytokine gene cluster. J Immunol **165:**6687-91.

249. **Tan, J. T., B. Ernst, W. C. Kieper, E. LeRoy, J. Sprent, and C. D. Surh.** 2002. Interleukin (IL)-15 and IL-7 jointly regulate homeostatic proliferation of memory phenotype $CD8^+$ cells but are not required for memory phenotype $CD4^+$ cells. J Exp Med **195:**1523-32.

250. **Tascon, R. E., E. Stavropoulos, K. V. Lukacs, and M. J. Colston.** 1998. Protection against *Mycobacterium tuberculosis* infection by $CD8^+$ T cells requires the production of gamma interferon. Infect Immun **66:**830-4.

251. **Teitelbaum, R., M. Cammer, M. L. Maitland, N. E. Freitag, J. Condeelis, and B. R. Bloom.** 1999. Mycobacterial infection of macrophages results in membrane-permeable phagosomes. Proc Natl Acad Sci U S A **96:**15190-5.

252. **ten Dam, H. G.** 1984. Research on BCG vaccination. Adv Tuberc Res **21:**79-106.

253. **Tollefsen, S., J. M. Pollock, T. Lea, M. Harboe, and H. G. Wiker.** 2003. T- and B-cell epitopes in the secreted *Mycobacterium bovis* antigen MPB70 in mice. Scand J Immunol **57:**151-61.

254. **Tough, D. F., and J. Sprent.** 1994. Turnover of naive- and memory-phenotype T cells. J Exp Med **179:**1127-35.

255. **Townsend, A. R., J. Rothbard, F. M. Gotch, G. Bahadur, D. Wraith, and A. J. McMichael.** 1986. The epitopes of influenza nucleoprotein recognized by cytotoxic T lymphocytes can be defined with short synthetic peptides. Cell **44:**959-68.

256. **Trapani, J. A., and V. R. Sutton.** 2003. Granzyme B: pro-apoptotic, antiviral and antitumor functions. Curr Opin Immunol **15:**533-43.

257. **Tripp, R. A., S. Hou, and P. C. Doherty.** 1995. Temporal loss of the activated L-selectin-low phenotype for virus-specific $CD8^+$ memory T cells. J Immunol **154:**5870-5.

258. **Trudeau, E. L.** 1887. Environment in its relation to the progress of bacterial invasion in tuberculosis. Amer J Med Sci **94:**118-23.

259. **Trudeau, E. L.** 1893. Eye tuberculosis and antitubercular inoculation in the rabbit. New York Med J **58:**97-101.

260. **Tsai, B., Y. Ye, and T. A. Rapoport.** 2002. Retro-translocation of proteins from the endoplasmic reticulum into the cytosol. Nat Rev Mol Cell Biol **3:**246-55.

261. **Tuberculosis Research Centre (ICMR) Chennai.** 1999. Fifteen year follow up of trial of BCG vaccines in south India for tuberculosis prevention. Indian J Med Res **110:**56-69.

262. **Turner, J., C. D. D'Souza, J. E. Pearl, P. Marietta, M. Noel, A. A. Frank, R. Appelberg, I. M. Orme, and A. M. Cooper.** 2001. CD8- and CD95/95L-dependent mechanisms of resistance in mice with chronic pulmonary tuberculosis. Am J Respir Cell Mol Biol **24:**203-9.

263. **Tyznik, A. J., J. C. Sun, and M. J. Bevan.** 2004. The CD8 population in CD4-deficient mice is heavily contaminated with MHC class II-restricted T cells. J Exp Med **199:**559-65.

264. **Urdahl, K. B., D. Liggitt, and M. J. Bevan.** 2003. $CD8^+$ T cells accumulate in the lungs of *Mycobacterium tuberculosis*-infected $K^{b-/-}D^{b-/-}$ mice, but provide minimal protection. J Immunol **170:**1987-94.

265. **Valenzuela, J., C. Schmidt, and M. Mescher.** 2002. The roles of IL-12 in providing a third signal for clonal expansion of naive CD8 T cells. J Immunol **169:**6842-9.

266. **van Endert, P. M.** 1996. Peptide selection for presentation by HLA class I: a role for the human transporter associated with antigen processing? Immunol Res **15:**265-79.

267. **Van Kaer, L., P. G. Ashton-Rickardt, M. Eichelberger, M. Gaczynska, K. Nagashima, K. L. Rock, A. L. Goldberg, P. C. Doherty, and S. Tonegawa.** 1994. Altered peptidase and viral-specific T cell response in LMP2 mutant mice. Immunity **1:**533-41.

268. **van Pinxteren, L. A., J. P. Cassidy, B. H. Smedegaard, E. M. Agger, and P. Andersen.** 2000. Control of latent *Mycobacterium tuberculosis* infection is dependent on CD8 T cells. Eur J Immunol **30:**3689-98.

269. **van Stipdonk, M. J., G. Hardenberg, M. S. Bijker, E. E. Lemmens, N. M. Droin, D. R. Green, and S. P. Schoenberger.** 2003. Dynamic programming of $CD8^+$ T lymphocyte responses. Nat Immunol **4:**361-5.

270. **van Stipdonk, M. J., E. E. Lemmens, and S. P. Schoenberger.** 2001. Naive CTLs require a single brief period of antigenic stimulation for clonal expansion and differentiation. Nat Immunol **2:**423-9.

271. **Villacres, M. C., and C. C. Bergmann.** 1999. Enhanced cytotoxic T cell activity in IL-4-deficient mice. J Immunol **162:**2663-70.

272. **von Herrath, M. G., M. Yokoyama, J. Dockter, M. B. Oldstone, and J. L. Whitton.** 1996. CD4-deficient mice have reduced levels of memory cytotoxic T

lymphocytes after immunization and show diminished resistance to subsequent virus challenge. J Virol **70:**1072-9.

273. **von Reyn, C. F., C. J. Clements, and J. M. Mann.** 1987. Human immunodeficiency virus infection and routine childhood immunisation. Lancet **2:**669-72.

274. **Vordermeier, H. M., X. Zhu, and D. P. Harris.** 1997. Induction of $CD8^+$ CTL recognizing mycobacterial peptides. Scand J Immunol **45:**521-6.

275. **Vynnycky, E., and P. E. Fine.** 1997. The natural history of tuberculosis: the implications of age-dependent risks of disease and the role of reinfection. Epidemiol Infect **119:**183-201.

276. **Wang, Q. M., S. H. Sun, Z. L. Hu, F. J. Zhou, M. Yin, C. J. Xiao, and J. C. Zhang.** 2004. Epitope DNA vaccines against tuberculosis: spacers and ubiquitin modulates cellular immune responses elicited by epitope DNA vaccine. Scand J Immunol **60:**219-25.

277. **Wayne, L. G.** 1976. Dynamics of submerged growth of *Mycobacterium tuberculosis* under aerobic and microaerophilic conditions. Am Rev Respir Dis **114:**807-11.

278. **Weis, S. E., P. C. Slocum, F. X. Blais, B. King, M. Nunn, G. B. Matney, E. Gomez, and B. H. Foresman.** 1994. The effect of directly observed therapy on the rates of drug resistance and relapse in tuberculosis. N Engl J Med **330:**1179-84.

279. **Weltman, A. C., and D. N. Rose.** 1993. The safety of bacille Calmette-Guérin vaccination in HIV infection and AIDS. Aids **7:**149-57.

280. **Wenner, C. A., M. L. Guler, S. E. Macatonia, A. O'Garra, and K. M. Murphy.** 1996. Roles of IFN-γ and IFN-α in IL-12-induced T helper cell-1 development. J Immunol **156:**1442-7.

281. **Wherry, E. J., D. L. Barber, S. M. Kaech, J. N. Blattman, and R. Ahmed.** 2004. Antigen-independent memory CD8 T cells do not develop during chronic viral infection. Proc Natl Acad Sci U S A **101:**16004-9.

282. **Wherry, E. J., K. A. Puorro, A. Porgador, and L. C. Eisenlohr.** 1999. The induction of virus-specific CTL as a function of increasing epitope expression: responses rise steadily until excessively high levels of epitope are attained. J Immunol **163:**3735-45.

283. **Wherry, E. J., V. Teichgraber, T. C. Becker, D. Masopust, S. M. Kaech, R. Antia, U. H. von Andrian, and R. Ahmed.** 2003. Lineage relationship and protective immunity of memory CD8 T cell subsets. Nat Immunol **4:**225-34.

284. **Wiegeshaus, E., V. Balasubramanian, and D. W. Smith.** 1989. Immunity to tuberculosis from the perspective of pathogenesis. Infect Immun **57:**3671-6.

285. **Williams, A. P., C. A. Peh, A. W. Purcell, J. McCluskey, and T. Elliott.** 2002. Optimization of the MHC class I peptide cargo is dependent on tapasin. Immunity **16:**509-20.

286. **Williams, M. A., and M. J. Bevan.** 2004. Shortening the infectious period does not alter expansion of CD8 T cells but diminishes their capacity to differentiate into memory cells. J Immunol **173:**6694-702.

287. **Wilson, L. G.** 1990. The historical decline of tuberculosis in Europe and America: its causes and significance. J Hist Med Allied Sci **45:**366-96.

288. **Wong, P., and E. G. Pamer.** 2001. Cutting edge: antigen-independent CD8 T cell proliferation. J Immunol **166:**5864-8.

289. **World Health Organization.** 1997. Anti-tuberculosis drug resistance. The WHO/IUATLD Global Project on Anti-Tuberculosis Drug Resistance Surveillance.

290. **World Health Organization.** 2005. Global Tuberculosis Control: Surveillance, Planning, Financing. Presented at the World Health Organization, Geneva, Switzerland.

291. **World Health Organization.** 1997. Treatment of tuberculosis: guidelines for national programmes. World Health Organization, Global Tuberculosis Programme.

292. **World Health Organization.** 2003. The World Health Organization Global Tuberculosis Program. http://www.who.int/gtb/.

293. **Zaph, C., J. Uzonna, S. M. Beverley, and P. Scott.** 2004. Central memory T cells mediate long-term immunity to *Leishmania major* in the absence of persistent parasites. Nat Med **10:**1104-10.

294. **Zhang, Y.** 2004. Isoniazid, p. 739-758. *In* W. N. Rom and S. M. Garay (ed.), *Tuberculosis*, 2nd ed. Lippincott Williams & Wilkins, Philadelphia.

295. **Zhou, X., F. Momburg, T. Liu, U. M. Abdel Motal, M. Jondal, G. J. Hammerling, and H. G. Ljunggren.** 1994. Presentation of viral antigens restricted by H-2K^b, D^b or K^d in proteasome subunit LMP2- and LMP7-deficient cells. Eur J Immunol **24:**1863-8.

296. **Zhu, X., H. J. Stauss, J. Ivanyi, and H. M. Vordermeier.** 1997. Specificity of CD8$^+$ T cells from subunit-vaccinated and infected H-2^b mice recognizing the 38 kDa antigen of *Mycobacterium tuberculosis*. Int Immunol **9:**1669-76.

297. **Ziegler, K., and E. R. Unanue.** 1981. Identification of a macrophage antigen-processing event required for I-region-restricted antigen presentation to T lymphocytes. J Immunol **127:**1869-75.

298. **Zinkernagel, R. M., and P. C. Doherty.** 1974. Restriction of *in vitro* T cell-mediated cytotoxicity in lymphocytic choriomeningitis within a syngeneic or semiallogeneic system. Nature **248:**701-2.

Chapter 2

Phenotypic Characterization of the CD8 T Cell Response Following Aerosol Infection with *Mycobacterium tuberculosis*

Introduction

Infection with *Mycobacterium tuberculosis*, the causative agent of tuberculosis, is arguably responsible for more lost productivity, human suffering, illness, and death than any other bacterial pathogen in the history of mankind. Although improved social and economic conditions in conjunction with effective monitoring and improved access to health care have contributed to long-term control of this disease in many industrialized countries, tuberculosis remains a significant problem in underdeveloped nations.

The emergence and dissemination of multidrug-resistant strains of tuberculosis, and the pandemic spread of the human immunodeficiency virus have combined to fuel a resurgence of disease, and ultimately threaten to subvert successful tuberculosis control programs, even within industrialized nations. Although a live attenuated strain of *M. bovis* has been used for decades as a tuberculosis vaccine, *M. bovis* bacille Calmette-Guérin (BCG) has proven to have variable protective efficacy in populations most susceptible to infection [4, 12]. In addition, it often fails to prevent adult pulmonary infection and the protective efficacy of the vaccine declines with time [12, 60]. Due to the shortcomings of the BCG vaccine, there has been a major effort to develop novel vaccine candidates with increased protective efficacy.

In order to aid rational vaccine design, there has been an increase in research to define the immunological correlates of protection to pulmonary tuberculosis infection. One of the leading questions in this area of research is whether CD8 T cells mediate protection to tuberculosis, and if so, to define the protective mechanisms involved. While the evidence for a protective role for CD8 T cells is often contradictory, it is known that

CD8 T cells having an activated phenotype arrive in the lung within one week following aerosol infection, and that following *ex vivo* restimulation, these cells possess the ability to secrete IFN-γ and TNF-α; two cytokines known to mediate resistance to mycobacterial infection [16, 18, 19, 54]. Using *in vivo* antibody depletion of previously thymectomized mice, it was demonstrated that CD8 T cells can confer protection in a mouse model of tuberculosis infection [39]. Furthermore, adoptive transfer of cell populations enriched for CD8 T cells conferred protection to a low dose aerosol challenge [42]. Memory cell populations generated by *M. tuberculosis* infection and subsequent drug treatment, when depleted of CD4 T cells conferred protection to recipient mice upon adoptive transfer, demonstrating that protective CD8 T cell populations can be targeted by vaccination [31]. In addition, various mouse knock-out models having no or significantly reduced numbers of CD8 T cells support a protective role for CD8 T cells during tuberculosis infection, although the relative amount of protection, as measured by pulmonary bacterial load, is often small [7, 15, 20, 37, 46, 56, 61]. We therefore began our inquiry into the role of CD8 T cells during tuberculosis infection with a phenotypic survey of these cells, and an examination of the protective mechanisms that they commonly employ. There are four primary functional attributes that protective immune cells must possess in order to effectively combat infectious pathogens. These attributes are lymphocyte activation, recruitment and migration into sites of infection, effector function, and memory cell generation. Therefore, we wanted to examine CD8 T cell expression of various cell adhesion molecules, markers of cellular activation, costimulatory/inhibitory molecules, and memory-associated markers to phenotypically characterize the CD8 T cell response following aerosol infection with *M. tuberculosis*. We also utilized intracellular antibody

staining coupled with flow cytometric analysis to characterize the cytokine secretion profile and cytolytic capacity of CD8 T cells following infection.

Previous work by Gonzalez-Juarrero *et al.* demonstrated that CD8 T cells preferentially localize around the periphery of murine granulomas [22]. In fact, it has been speculated that CD8 T cells may provide a critical immunosurveillance role during the chronic phase of infection, to prevent infected macrophages from escaping the protective confines of the granuloma [39]. Since adhesion molecules play a prominent role in cell migration and retention within the lung environment, we wanted to examine whether the failure to penetrate murine granulomas was the result of poor integrin expression. We initiated these studies by examining the expression patterns of four relevant integrin molecules (VLA-4, LFA-1, LPAM-1, HML-1) following aerosol infection with *M. tuberculosis* to determine if CD8 T cells were able to efficiently upregulate these molecules and maintain their expression during the course of infection (Table 2.1).

To better understand the dynamics of the CD8 T cell response that occurs following aerosol infection with tuberculosis, we next performed a broad phenotypic characterization of these cells in the lungs and spleens of naïve mice, mice chronically infected with *M. tuberculosis*, and mice infected with *M. tuberculosis* and subsequently drug-treated using a combination chemotherapeutic regimen that reduces bacterial burden to undetectable levels following prolonged administration. Examination of naïve mice allowed us to establish baseline expression levels for these molecules, while examination of cells elicited following active infection allowed us to characterize the effector cell population responding to infection. Examination of the CD8 T cell population remaining

following drug treatment of bacterial infection allowed us to examine the memory cell population that persists following the contraction phase.

In these studies, we examined a series of activation-associated markers (CD44, CD69, CD11a, CD122, CD132) and memory-associated markers (CCR7, CD62L, IL-7Rα, CD45RB, Ly6C, IL-15Rα) at multiple timepoints following low dose aerosol infection (Table 2.2). In addition to examining the total CD8 T cell response, we utilized a MHC class I tetramer reagent specific for a previously identified peptide epitope located within the *M. tuberculosis*-derived Mtb32 protein. Examination of an antigen-specific population allowed us to precisely observe the dynamic phenotypic changes that occurred during the progression of infection, as well as visualize the transition to a memory phenotype following chemotherapeutic-induced reduction in pathogen numbers.

In addition to classical T cell activation and memory markers, we also wanted to examine a series of costimulatory and/or immunoregulatory molecules (CD27, CD43, 4-1BB, PD-1, Tim-3) commonly expressed on CD8 T cells to better characterize and understand the multitude of secondary signals available to cells actively responding to infection and to cells transitioning to a state of memory (Table 2.2).

The costimulatory molecule CD27 is a member of the tumor necrosis factor receptor (TNFR) family, and has been shown to have multiple effects upon T cell activation and differentiation following T cell receptor (TCR) stimulation. Early following T cell activation, CD27 signaling is known to promote the survival and clonal expansion of primed CD8 T cells by protecting activated cells from apoptosis, as well as control the accumulation of CD8 effector T cells at the sites of infection [23, 28, 30, 48]. In addition, signaling through CD27 promotes the formation of the memory cell

population, either by increasing T cell survival during the contraction phase following antigen clearance, or by providing signals required for further differentiation into functional memory cells [2, 27]. Repetitive TCR stimulation results in a downregulation of the surface expression of CD27, and this loss of CD27 correlates with increased CD8 effector T cell function [25].

CD43 is a complex molecule that can exhibit both adhesive and anti-adhesive effects, as well as costimulatory functions [41]. Differential glycosylation patterns may explain the contradictory effects of this molecule. In these experiments, we utilized the S7 monoclonal antibody, which is specific for the 115 kDa low molecular mass form of CD43. Due to its role in trafficking and costimulation, we wanted to examine the expression patterns of this receptor on CD8 T cells.

4-1BB is a member of the TNFR superfamily, and is an inducible costimulatory receptor on T cells. On CD8 T cells, 4-1BB appears to function by enhancing the survival of activated cells, thereby contributing to an increased CD8 T cell proliferative response [11]. This pro-survival effect is mediated by the induction of anti-apoptotic factors of the Bcl-2 family, such as Bcl-x_L and Bfl-1 [32, 35]. Although 4-1BB is transiently upregulated immediately following CD8 T cell activation and evidence exists that 4-1BB–4-1BBL interactions may augment or in some cases even replace CD28 costimulatory signaling, effects upon transition into and maintenance of the CD8 memory cell pool appear to be the primary functions of this receptor [24, 53]. Ligation of 4-1BB allows cells to avoid the massive clonal deletion that occurs following pathogen clearance, ultimately increasing the number of antigen-specific CD8 T cells transitioning into the memory cell pool [8, 58]. Recently, 4-1BB has been shown to be reexpressed on

activated CD8 T cells in an IL-15-dependent manner within several weeks following antigen clearance [44]. These studies also demonstrated that 4-1BB-dependent signaling positively impacted the survival and maintenance of memory CD8 T cells in the absence of antigen. There is also evidence suggesting that 4-1BB may imprint memory cell characteristics into T cells during the primary response that are required for optimal CD8 T cell expansion upon secondary challenge [29]. Therefore this molecule appears to possess early costimulatory and pro-survival signals overlapping with CD28 costimulatory activity, as well as nonredundant, late-acting signaling effects aiding CD8 memory T cell survival and maintenance following antigenic clearance.

In addition to the previously identified costimulatory molecules, we also wanted to examine CD8 T cell expression of Tim-3 and PD-1; two immunoregulatory molecules whose functional significance have recently been elucidated.

T cell immunoglobulin and mucin domain-containing molecule-3 (Tim-3) is a recently identified T_H1-specific type I membrane protein [38]. Surface expression of Tim-3 is confined to activated, T_H1-polarized CD4 and CD8 T cells under conditions of repetitive stimulation. Interaction of Tim-3 with its ligand; galectin-9, initiates inhibitory signaling resulting in the death of T_H1-biased cells and the reduction or termination of an inflammatory response [66]. As such, this molecule may be a key regulator in the induction of peripheral tolerance, the expansion of effector T_H1 cells, and resolution of the inflammatory process upon pathogen clearance. Since galectin-9 is highly expressed in mucosal environments, and given the fact that upregulation of this molecule is IFN-γ-inducible, we speculated that the Tim-3–galectin-9 pathway may serve as a critical negative feedback mechanism to dampen or control the inflammatory response during

pulmonary infection with *M. tuberculosis* [66]. Due to its central role in T_H1 immunity, we wanted to examine the expression of Tim-3 on CD8 T cells during the course of infection with *M. tuberculosis*, and following drug-treatment of active tuberculosis infection.

The inhibitory receptor programmed cell death-1 (PD-1) is a member of the immunoglobulin superfamily, and functions primarily to prevent aberrant immune responses to self antigens. PD-1 acts to dampen TCR signaling to reduce T cell responsiveness to persistent antigen, as in the case of peripheral tolerance to self antigens. While this molecule is normally upregulated following T cell activation, it is rapidly downregulated following antigenic clearance. In a recent paper, it was shown that high PD-1 expression correlated with functional exhaustion of CD8 T cells during chronic viral infection [5]. Antibody blockade of the ligands for PD-1 (PD-L1 and PD-L2) resulted in restoration of proliferative ability and cytokine secretion in these previously exhausted CD8 T cells. Given the fact that during pulmonary infection with *M. tuberculosis* the majority of activated CD8 T cells fail to exhibit cytolytic activity and fail to readily produce cytokines following *ex vivo* stimulation, we wanted to examine PD-1 expression as an indication of functional exhaustion.

While the expression patterns of extracellular molecules on CD8 T cells can give important insights into the activation status and migrational abilities of responding cells, examination of the effector functions of these cells ultimately reveals whether the responding population of cells has the capacity to mediate protection following infectious aerosol challenge. As cytolytic activity and cytokine secretion are prominent CD8 T cell effector mechanisms, we used intracellular staining in conjunction with flow cytometric

analysis to examine the cellular capacity to produce cytolytic molecules (perforin, granzyme B) and cytokines (IL-2, IL-4, IL-10, IFN-γ, TNF-α) following *ex vivo* restimulation.

Materials & Methods

Mice. Studies were performed using 8-10 week old specific pathogen-free female C56BL/6 mice purchased from Charles River Laboratories (Wilmington, MA). All mice were maintained within a biosafety level III facility at Colorado State University for the duration of the experiments, and had free access to sterile water and standard mouse chow. The specific pathogen-free nature of the mouse colonies was demonstrated by testing sentinel animals, which were shown to be negative for 13 known mouse pathogens. All experimental procedures were approved by the Colorado State University Animal Care and Use Committee.

Bacterial Strains. *M. tuberculosis* strain H37Rv, originally obtained from the Trudeau Mycobacteria Collection (TMCC #102), was grown from low passage seed lots in Proskauer-Beck liquid media containing 0.05% Tween 80 to mid-log phase, and 1.5 ml aliquots were frozen at -70°C until use.

Aerosol Infections. Mice were infected via the aerosol route using a Glas-Col aerosol generator (Glas-Col, Terre Haute, IN), such that ~100 viable bacteria were deposited in

the lungs of each animal. The number of viable bacteria in the lungs was determined at specific time points by plating 10-fold serial dilutions of individual whole organ homogenates on nutrient Middlebrook 7H11 agar, and counting bacterial colonies after 21 days of incubation at 37°C.

Antimicrobial Treatment. For experiments utilizing combination drug treatment, animals were treated with 100 mg/l of rifampicin (Sigma-Aldrich, St. Louis, MO) and isoniazid (MP Biochemicals, Solon, OH) administered in the drinking water. This concentration has previously been demonstrated to deliver ~25 mg/kg animal weight (A. Lenaerts, unpublished data). Treatment was initiated 40 days following low dose aerosol infection and was continued for the duration of the experiments. After 40 days following the initiation of drug treatment, viable bacteria were enumerated by plating undiluted whole organ homogenates on nutrient Middlebrook 7H11 agar.

Single-Cell Suspension Preparation. Animals were sacrificed by carbon dioxide asphyxiation and were perfused through the heart with 10 ml cold PBS containing 3 U/ml heparin (Sigma-Aldrich). The lungs were removed from the pulmonary cavity and placed in cold Dulbecco's minimal essential medium (DMEM; Cellgro, Herndon, VA). The lung tissue was disrupted using sterile razor blades and incubated for 30 minutes at 37°C in a final volume of 2 ml DMEM containing 0.7 mg/ml collagenase D (Roche Applied Science, Indianapolis, IN) and 30 μg/ml deoxyribonuclease (Sigma-Aldrich). Following incubation, the digested lung tissue was gently passed through a sterile 70 μm nylon screen, rinsed using 8 ml cold DMEM supplemented with 10% heat-inactivated

endotoxin low fetal bovine serum (Atlas Biologicals, Fort Collins, CO), 10 mM HEPES buffer (Sigma-Aldrich), 2 mM L-glutamine (Sigma-Aldrich), 2% MEM-nonessential amino acids (100x; Sigma-Aldrich), 50 μM 2-mercaptoethanol (Sigma-Aldrich) and centrifuged at 200 × *g*. Red blood cells were lysed using Gey's solution (0.15 M NH_4Cl, 10 mM $KHCO_3$) and the samples were centrifuged and resuspended in DMEM plus supplements. Cells were counted using a hemacytometer and aliquots were taken for flow cytometric analysis.

Flow Cytometry. Single-cell suspensions from individual mice were resuspended in PBS containing 0.1% sodium azide (Fisher Chemicals, Fairlawn, NJ). Cells were incubated in the dark for 20 minutes at 4°C with specific antibody (directly conjugated to fluorescein isothiocyanate [FITC], phycoerythrin [PE], peridinin chlorophyll *a* protein [PerCP], or allophycocyanin [APC] at 3 μg/ml), followed by 2 washes using PBS with sodium azide. Cells were analyzed immediately using a FACSCalibur dual laser flow cytometer (BD Biosciences, Mountain View, CA) and the data were analyzed using CellQwest software (BD Biosciences, San Jose, CA) and Summit software (DakoCytomation, Fort Collins, CO). Viable lymphocytes were gated based upon their forward- and side-scatter characteristics and cell populations were analyzed by expression of fluorochrome-labeled markers. All analyses were performed with a minimum acquisition of 100,000 events.

Cell surface markers were analyzed with the following specific antibodies: FITC anti-CD29 (clone Ha2/5), anti-β_7 (clone M293), anti-CD18 (clone C71/16), anti-CD44 (clone IM7), anti-CD62L (clone MEL-14), anti-CD45RB (clone 16A), anti-CD122 (clone TM-β1), anti-CD11a (clone 2D7), anti-CD137 (clone 1AH2), anti-CD69 (clone H1.2F3),

anti-CD43 (clone S7); PE anti-CD49d (clone R1-2), anti-CD11a (clone 2D7), anti-CD103 (clone M290); PerCP anti-CD3ε (clone 145-2C11), anti-CD8α (clone 53-6.7); APC anti-CD8α (clone 53-6.7), anti-CD127 (clone A7R34; eBioscience, San Diego, CA); biotin-conjugated anti-Ly6C (clone AL-21), anti-CD27 (clone LG.7F9; eBioscience), and anti-CD132 (clone TUGm2). To stain IL-15Rα, biotin conjugated polyclonal goat anti-IL-15Rα antibodies (R&D Systems, Minneapolis, MN) were used. Streptavidin-APC (eBioscience) was used to label all biotin-conjugated antibodies. Cell suspensions were also stained with a PE-Mtb32 H-2D^b MHC class I tetramer (Beckman Coulter Immunomics, San Diego, CA) containing the peptide GAPINSATAM. Background staining with this tetramer reagent was less than 0.15% when staining cells from naïve mice or from MHC mismatched (Balb/c, H-2^d) mice.

For staining PD-1, Tim-3, and CCR7, cells were stained with either anti-PD-1 (clone RMP1-14; BioLegend, San Diego, CA), anti-Tim-3 (clone RMT3-23; eBioscience), or anti-CCR7 (clone 4B12; BioLegend) followed by biotin conjugated goat anti-rat IgG (Caltag, Burlingame, CA) followed by labeling with streptavidin-APC (eBioscience). Cells were sequentially incubated in the dark for 20 minutes at 4°C with specific primary antibody, biotin conjugated secondary antibody, and streptavidin-APC with appropriate washes using PBS with azide between steps.

For intracellular cytokine staining, single-cell suspensions were resuspended in DMEM with supplements and stimulated with 0.1 μg/ml anti-CD3ε (clone 145-2C11) and 1 μg/ml anti-CD28 (clone 37.51), in the presence of 3 μM monensin for 4 hours at 37°C, 5% CO_2. Cells were stained with antibodies for cell-surface molecules as described above, before fixation and permeabilization with BD Cytoperm/Cytofix (BD

PharMingen, San Diego, CA) according to the manufacturer's instructions. Cells were incubated with FITC anti-IFN-γ (clone XMG1.2), anti-IL-2 (clone JES6-5H4), anti-granzyme B (clone 16G6; eBioscience), anti-TNF-α (clone MP6-XTL2); APC anti-IL-4 (clone 11B11; eBioscience), anti-IL-10 (clone JES5-16E3; eBioscience), or anti-perforin (clone eBioOMAK-D; eBioscience) for 20 minutes at 4°C, washed twice, and resuspended in PBS with sodium azide before analysis. Appropriate isotype controls were prepared simultaneously and were included in each analysis. Unless otherwise noted, all antibodies were purchased from BD PharMingen.

Histology. Individual lung lobes were first perfused and then immersed in 10% phosphate-buffered formalin solution and embedded in paraffin wax. Sections of 5 μm thickness were prepared and stained using hematoxylin and eosin, and examined by a trained pathologist in a double-blinded fashion.

Data & Results

Bacterial replication following low dose aerosol infection with *M. tuberculosis*. In order to accurately assess the amount of bacterial replication within the lungs, spleen, and liver of C57BL/6 mice following low dose aerosol infection with *M. tuberculosis* H37Rv, serial dilutions of whole organ homogenates were plated onto Middlebrook 7H11 agar and colonies were enumerated after 2-3 weeks of incubation at 37°C. Based upon the data obtained in Figure 2.1, bacterial replication within all three organs could be divided into

three phases: log-phase growth from day 0 to day 30, immunological control of bacterial replication from day 30 to day 50, and a plateau phase from day 50 through day 120 which was the last timepoint examined in this experiment. Log-phase growth was characterized by relatively uncontrolled bacterial replication within target organs prior to initiation of the adaptive immune response. With the initiation of adaptive immunity, bacterial replication was halted and the number of viable bacilli began to decrease in the lungs by approximately 0.5-$\log_{10}$. Following this small decline, bacterial numbers remained relatively constant during the plateau phase, through 120 days following aerosol infection.

The kinetics of CD4 and CD8 T cell recruitment into the lungs following aerosol infection. Since the point of immunological control of infection temporally coincides with the onset of adaptive immunity, we next wanted to quantify the recruitment of both CD4 and CD8 T cells into the lungs following low dose aerosol infection. As shown in Figure 2.2, the point at which bacterial growth is controlled occurred when approximately 1-2 $\times$ 10^6 CD4 and CD8 T cells arrived in the lungs, although the number of these cells continued to increase until day 50. At the peak of T cell influx into the lungs, the number of these cells increased 3-4-fold over baseline numbers of these cells present in the lungs of naïve mice. Overall, the kinetics of both CD4 and CD8 T cell recruitment roughly paralleled the number of bacteria in the lungs, although the kinetics of the T cell response was delayed by approximately 20 days.

Integrin expression by CD4 and CD8 T cells in the lungs of mice following aerosol infection. Since integrin molecules are required by lymphocytes to efficiently traffic to the sites of pulmonary inflammation, extravasate into the pulmonary intersitium, migrate to infectious foci, and be retained at sites of inflammation, we wanted to examine the expression of these molecules by CD4 and CD8 T cells in the lungs. As shown in Figure 2.3, CD4 T cells upregulated expression of both VLA-4 and LFA-1 integrin molecules following infection. CD8 T cells also upregulated these integrin molecules to a similar magnitude in response to infection (Figure 2.4). As shown in Figures 2.5 and 2.6, both CD4 and CD8 T cells upregulated these integrins with similar kinetics and similar total numbers. In addition, the total number of CD4 or CD8 T cells expressing VLA-4 is very similar to the total number of CD4 or CD8 T cells expressing LFA-1, indicating that expression of these molecules may be coordinately regulated at the cellular level following T cell activation.

We next wanted to examine the expression of two mucosal-associated integrin molecules; LPAM-1 and HML-1, on CD4 and CD8 T cells. Figure 2.7 shows that while CD4 T cells do express LPAM-1, they failed to upregulate expression of this molecule to a LPAM-1^{hi} phenotype in response to infection. Additionally, small but detectable numbers of CD4 T cells expressed the HML-1 integrin (Figure 2.7). In contrast to CD4 T cell expression of these integrin molecules, significant numbers of CD8 T cells upregulated expression of LPAM-1 and/or HML-1 (Figure 2.8). The kinetics of CD8 T cell expression of LPAM-1^{hi} are shown in Figure 2.9, demonstrating that the population of CD8 T cells expressing high levels of this integrin increased in response to infection. Although few CD4 T cells expressed the HML-1 integrin, the number of these cells

increased slightly over the course of infection (Figure 2.10). In contrast, a large number of CD8 T cells expressed the HML-1 integrin molecule in the lungs following infection.

Phenotypic characterization of CD8 T cells. In order to better understand the CD8 T cell response generated following infection with *M. tuberculosis*, we wanted to perform a comprehensive phenotypic analysis of various extracellular markers of activation, costimulation, and memory at multiple timepoints following infection (Table 2.2). To accomplish this, at each timepoint we examined naïve mice to determine baseline expression patterns, mice infected with *M. tuberculosis* H37Rv to characterize the CD8 effector T cell population, and mice infected with H37Rv and subsequently drug-treated to reduce bacterial numbers to undetectable levels to examine the CD8 memory T cell population. Figure 2.11 is a pictorial representation of the experimental design used for the phenotypic characterization experiments.

For these experiments we utilized a low dose aerosol infection model to infect C57BL/6 mice with approximately 100 CFU of *M. tuberculosis* H37Rv. At 40 days following infection, we treated the naïve and drug-treated groups of mice with approximately 25 mg/kg of rifampicin/isoniazid combination drug treatment in the drinking water. To verify that the drug treatment regimen was effective at reducing bacterial burden in treated mice, lungs and spleens were harvested after 40 days of treatment and undiluted whole organ homogenates were plated to examine the number of recoverable viable bacilli in these organs. As shown in Figure 2.12, the bacterial load in the spleen was reduced to undetectable levels (< 50 CFU). Although a small number (~150 CFU) of viable bacteria were still present in the lungs, a greater than 4-$\log_{10}$

reduction in bacterial numbers was observed following 40 days of combination drug treatment. Once initiated, drug treatment was continued throughout the duration of these experiments.

In these experiments we examined the total CD8 T cell population in the lungs and spleens at multiple timepoints following infection. In addition, we examined a clonal antigen-specific CD8 T cell response as a means to phenotypically characterize a subset of CD8 T cells actually responding to *M. tuberculosis* infection. We utilized a MHC class I tetramer reagent containing the 10-mer peptide sequence GAPINSATAM, previously shown to be an immunogenic CD8 T cell epitope located within the *M. tuberculosis*-derived Mtb32 secreted protein [55].

Figures 2.13-2.28 illustrate the relative expression levels over the timecourse of infection for various markers expressed on the surface of CD8 T cells isolated from the lungs and spleens of mice. CD8 T cells were identified and gated by characteristic size, granularity, and expression of CD8α. For extracellular markers that exhibited discrete populations, we analyzed the percentage of CD8 T cells at each timepoint falling within an indicated region (Figures 2.29-2.31). For markers that exhibited only a minor change in expression levels, the mean fluorescence intensity was analyzed for each group (Figures 2.32-2.33).

Examination of classical markers of activation revealed pronounced upregulation of the integrin molecule CD44, with high-level expression retained on both effector and memory cells (Figure 2.13). CD69, a marker of early activation associated with recent TCR stimulation, was also upregulated on the majority of the CD8 T cells in the lung (Figure 2.14). Another integrin molecule; CD11a, was rapidly upregulated on effector

cells in the lung, and subsequently downregulated in the tetramer-positive memory cell population (Figure 2.15). These three markers of activation were upregulated early following infection, and persistently expressed throughout the course of infection by CD8 effector T cells. Upregulation of the IL-2Rβ (CD122) and IL-2Rγ (CD132) components of the IL-2 receptor is a classical consequence of T cell activation, and was clearly observed in the spleen, while effector cells in the lung downregulated expression of both of these molecules (Figures 2.16, 2.17). Although the number of Mtb32 tetramer-positive events in the drug-treated group at day 150 was too small for accurate analysis, the data suggest that at least CD122 is reexpressed on the CD8 memory T cell population.

We next examined the expression patterns of a series of memory-associated markers. Although the overall expression of CCR7 was low, CD8 effector T cells in the lungs and spleen expressed higher levels of this molecule (Figure 2.18). Memory cells in the spleen retained this higher level of expression, while the memory population in the lungs exhibited decreased CCR7 expression. The cell adhesion molecule L-selectin (CD62L) is another marker whose expression is associated with both activation and memory. Upon T cell activation and egress from the spleen, CD62L is rapidly shed resulting in a population of tissue-restricted $CD62L^{lo}$ effector cells (Figure 2.19). Following drug treatment, the remaining antigen-specific memory cells in the lung reexpressed the CD62L molecule. The expression of CD45RB has also been commonly used as an effector cell and memory cell marker. Following proliferation, CD45RB expression is progressively reduced on activated effector cells, and this trend was clearly observed in these studies as a transition from $CD45RB^{hi}$ naïve cells, to $CD45RB^{int/lo}$ effector cells (Figure 2.20). Interestingly, CD45RB appeared to be reexpressed at high

levels on the majority of antigen-specific CD8 memory T cells in the lung. Ly6C expression has also been utilized as a CD8 T cell memory marker, however in our hands we could not differentiate between effector and memory cell populations during the course of infection. Expression of this molecule was predominantly Ly6C^{int} in the spleen, and Ly6C^{hi} within the lung for both the effector and memory cell populations (Figure 2.21).

Two cytokine receptors, IL-7Rα and IL-15Rα have recently been identified as CD8 memory T cell markers. Interleukin 7 is a T cell pro-survival cytokine, responsible for the maintenance of both naïve T cells and memory T cells. Naïve CD8 T cells express high levels of IL-7Rα, but immediately downregulate expression of this receptor following activation. However, by the peak of the infectious process, memory precursor cells can be identified by reexpression of the IL-7Rα [34]. While the range of expression of this receptor is small, the emergence of an IL-7Rα^{hi} tetramer-positive memory cell population was observed in these experiments (Figure 2.22). Interleukin 15 is a cytokine responsible for maintenance of the CD8 memory T cell population via homeostatic proliferative renewal of resting memory cells. Interestingly, in these experiments we observed a marked increase in IL-15Rα expression on activated CD8 effector T cells, and a memory cell-associated decrease in IL-15Rα expression to levels intermediate between effector cell and naïve cell expression levels (Figure 2.23).

The process of lymphocyte activation, acquisition of effector cell characteristics, and memory cell differentiation is a complex process, shaped by multiple stimuli derived from antigen presenting cells as well as the external environment. Since costimulatory and inhibitory receptors play a critical role in modulating and shaping this response, we

wanted to examine the expression of some of the key molecules involved in the CD8 T cell response during tuberculosis infection. The expression of the costimulatory molecule CD27 resembled that of CD45RB, in that cells from naïve mice expressed high levels of this receptor, while expression was progressively reduced on the activated effector cell population (Figure 2.24). This molecule was then reexpressed on splenic memory CD8 T cells. Although the number of antigen-specific events was small, this trend appeared to be duplicated on memory cells within the lung. The expression of CD43, a molecule implicated in cellular adhesion and activation, was upregulated in the lungs following infection, and the data suggested a possible downregulation of this molecule on pulmonary memory cells (Figure 2.25). Although the expression patterns of the costimulatory molecule 4-1BB are known to be transient following activation, we observed consistently high 4-1BB expression on effector and memory cells within the spleen (Figure 2.26). Within the lung, no 4-1BB expression was observed on effector CD8 T cells; however following drug treatment memory cells reexpressed this molecule.

Since T cell activation is often the result of a carefully orchestrated balance of activating and inhibitory signaling, we wanted to examine the expression of two key inhibitory receptors recently identified as having a significant impact upon the T cell response. Although PD-1 is rapidly upregulated following T cell activation, it has recently been observed that persistent expression of this molecule correlates with functional exhaustion of CD8 T cells under conditions of chronic antigenic stimulation [5]. In these studies, we observed pronounced expression of PD-1 following infection, with a rapid decline in expression following drug treatment (Figure 2.27). We also examined the expression of Tim-3, a T_H1-associated inhibitory molecule. Again, we

observed a marked increase of effector cell-associated Tim-3 expression following infection, accompanied by a rapid decrease in expression on memory cells following drug treatment (Figure 2.28).

Characterization of CD8 T cell effector function. In order to characterize the effector function of the CD8 T cell population, we examined cytokine production of lung-derived cells using intracellular antibody staining and flow cytometric analysis (Figures 2.34-2.35). Interestingly, in these experiments we could not detect the presence of perforin or granzyme B, two molecules that comprise the cytolytic repertoire of cytotoxic CD8 T cells. In addition, we could detect no CD8 T cell IL-2, IL-4, or IL-10 production above background levels by intracellular staining following *ex vivo* restimulation. We were able to detect significant numbers of CD8 T cells producing IFN-γ and significant numbers of CD8 T cells producing TNF-α, two protective cytokines known to have critical anti-mycobacterial properties. The percentage of CD8 T cells expressing these molecules is shown in Figure 2.36.

Discussion

Integrin molecules are important for recruitment, extravasation, migration, and retention of leukocytes within the tissues following an infectious challenge. Given their prominent role in the inflammatory response, we investigated the expression of four of these molecules to determine if defects in integrin expression by CD8 T cells could

explain the predominantly peripheral localization of these cells around murine pulmonary granulomas.

Analysis of integrin expression on CD8 and CD4 T cells revealed that in the lungs of infected mice, CD8 T cells are able to upregulate LFA-1 and VLA-4 to a similar extent and with similar kinetics when compared to CD4 T cells. Additionally, the percentage of CD8 and CD4 T cells expressing these two integrin molecules was similar and expression of these two integrin molecules was stably maintained over the timecourse of infection. We also examined two integrin molecules predominantly expressed by CD8 T cells; LPAM-1 and HML-1. CD8 T cells upregulated these molecules following infection, and fairly constant numbers of cells expressing these integrins were maintained during the infectious process.

In these experiments, we were not able to identify any defects in CD8 T cell integrin upregulation or expression following low dose aerosol challenge with *M. tuberculosis*. In addition to integrin expression, lymphocytes responding to infectious stimuli require a chemokine gradient sensed through chemokine receptors to migrate to the origin of infection. Further experiments examining the complement of chemokine receptors expressed by CD8 T cells, as well as an examination of secreted chemokine molecules within the lung may provide insights into the migration patterns resulting in the observed distribution patterns. The recent commercial availability of monoclonal antibodies for many of the chemokine receptors now makes this approach feasible.

These experiments examining the CD8 T cell response in the lungs of mice infected with *M. tuberculosis* documented the early pulmonary influx and sustained maintenance of activated CD8 T cells possessing the ability to secrete IFN-γ and TNF-α,

and as such confirm the published results of other researchers [16, 54, 59]. The ability to track *M. tuberculosis* antigen-specific CD8 T cells over time provided a powerful tool to precisely examine and characterize phenotypic changes in receptor expression patterns following aerosol infection, and during the transition to a state of memory following chemotherapeutic-induced reduction of bacterial numbers.

We have been able to extend these results by demonstrating that a portion of the CD8 T cell influx into the lung is in fact antigen-specific, and therefore elicited in response to pulmonary infection with *M. tuberculosis*. In examining markers of CD8 T cell activation, it was interesting to note that the majority of CD8 T cells in the lung express high levels of CD44, indicating a high level of CD8 T cell activation in the lungs. In addition, the majority of CD8 T cells also express CD69; a marker of recent T cell receptor stimulation. These data strongly suggest that a large proportion of CD8 T cells present in the lung are actively participating in the host anti-mycobacterial response. In addition, examination of the activation-associated integrin molecule CD11a revealed that antigen-specific CD8 T cells in the spleen expressed intermediate levels of this molecule, while pulmonary tissue-resident CD8 T cells expressed high levels of CD11a. Although the number of Mtb32 tetramer-positive cells was small by day 150, it appeared that CD11a expression was downregulated on the Mtb32-specific memory cell population, and as such, a reduction in CD11a expression may serve as a marker of CD8 T cell memory.

We observed high-level CD122 and CD132 expression in the spleen, and low expression of these molecules on the activated pulmonary-resident effector cell population. These results might indicate a shift from splenic IL-2 dependence of antigen-

specific but antigen-inexperienced cells, towards a dependence upon other inflammatory pro-survival signals by the antigen-experienced effector cell population. Since IL-2 is required for T cell proliferation, the lack of a functional IL-2 receptor on pulmonary effector cells implies that proliferation of CD8 T cells within the lung is minimal. Therefore these cells must be constantly renewed by continued recruitment from the sites of T cell priming.

Examination of memory markers expressed by CD8 T cells in the lung revealed CD8 T cells expressing a $CCR7^{lo}$ $CD62L^{hi}$ phenotype, consistent with the formation of an effector memory population as originally described by Lanzavecchia and Sallusto [50]. Additionally, within the spleen a population of $CCR7^{hi}$ $CD62L^{hi}$ antigen-specific CD8 T cells was identified, consistent with the emergence of a central memory cell population. Importantly, examination of CD45RB expression by antigen-specific memory cells revealed that the memory cell population reexpressed the CD45RB molecule. These results are reminiscent of an earlier study by Andersen and Smedegaard that identified $CD45RB^{hi}$ CD4 T cells as the memory cell population conferring protection following adoptive transfer in a mouse model of tuberculosis [1]. Reexpression of the IL-7Rα chain by antigen-specific CD8 memory T cells confirms the utility of this receptor for use in identification of memory cells, and extends the original observation to CD8 memory T cells formed following a bacterial infection [33, 34]. Although it is known that CD8 memory T cells require IL-15 for homeostatic proliferation and maintenance in the absence of antigen, we observed a gradual decrease in IL-15Rα expression levels on memory CD8 T cells as compared to expression levels on effector cells [6, 21, 57]. Understanding the role of IL-15 in CD8 memory cell maintenance and survival has been

complicated by the fact that IL-15Rα expression on memory CD8 T cells may play no role in the memory response [10]. Instead, memory CD8 T cells require IL-15Rα-dependent transpresentation of IL-15 by an as yet unidentified cell type for survival [9, 52]. Recent work indicates that in addition to its role during CD8 memory cell maintenance, IL-15 may also play a role in CD8 T cell survival during the contraction phase [65]. These studies also demonstrated that this pro-survival effect was independent of CD8 T cell IL-15Rα expression, but dependent upon IL-15Rα transpresentation of IL-15. Therefore, the precise function of IL-15Rα expression on CD8 T cells awaits elucidation.

While the previous results have helped to paint a more complete picture of the CD8 T cell response, perhaps the most interesting portion of these studies involved the examination of costimulatory and inhibitory receptors expressed on CD8 T cells during infection. We observed constitutive expression of CD43 on both naïve and effector CD8 T cells as previously described by others [26]. We extend these observations by demonstrating that effector CD8 T cells preferentially upregulated CD43 expression, as indicated by the Mtb32-specific subpopulation of CD8 T cells. Although few Mtb32 tetramer-positive cells persist by day 150, tetramer staining suggested that CD43 may be downregulated on the CD8 memory T cell population following a decrease in antigenic load. Further examination revealed that CD8 effector T cells progressively downregulated CD27 expression, while memory cells appeared to reexpress this molecule, with this effect being most pronounced in the spleen. These results are consistent with a previous report demonstrating that mycobacterial infection causes a reduction in CD27 expression on CD4 effector T cells, and identifying the IFN-γ

producing CD4 T cell subset as predominantly $CD27^{lo}$ [36]. Our results extend these observations to the CD8 T cell population.

The transient expression patterns of the costimulatory molecule 4-1BB are indicative of the dynamic environment in which CD8 T cells function. Within the spleen, the majority of antigen-specific CD8 T cells expressed 4-1BB. Since this receptor is upregulated shortly following T cell priming, this implies that at least some *M. tuberculosis*-specific CD8 T cells are being generated in the spleen. While the CD8 effector cell population in the lungs failed to express 4-1BB, most of the memory cells generated following drug treatment constitutively expressed this molecule. Further experiments will need to be conducted to determine whether 4-1BB expression is a genuine memory cell marker following tuberculosis infection.

In these experiments, we observed a significant and persistent increase in expression of the inhibitory receptor PD-1 on chronically activated CD8 effector T cells which was maintained throughout the course of infection. Following chemotherapeutic-induced reduction in bacterial numbers, PD-1 expression decreased on the remaining CD8 memory T cell population. It is interesting to speculate that the continued presence of high antigenic burden during chronic infection with *M. tuberculosis* may negatively impact the effector functions of CD8 T cells responding to pulmonary infection, similar to CD8 effector T cell defects observed by Barber *et al.* using a murine lymphocytic choriomeningitis virus infection model [5]. Given the fact that no significant cytolytic activity was observed in these studies and that greater than 70% of the pulmonary CD8 T cells failed to produce IFN-γ or TNF-α, high-level PD-1 expression may be indicative of functional exhaustion of the majority CD8 T cells within the lung, as is seen during

chronic viral infections [13, 45, 63]. It remains to be determined whether blockade of the ligands for PD-1 will restore CD8 T cell function and result in enhanced bacterial clearance within the lung in this model of infection.

Due to the fact that expression of the inhibitory receptor Tim-3 is restricted to activated, T_H1-polarized T lymphocytes, and since blocking the ligand for Tim-3 has been shown to abrogate tolerance induction and to result in T_H1 effector cell hyperproliferation, we wanted to characterize the expression patterns of this receptor on pulmonary CD8 T cells [49, 51]. Low dose aerosol infection initiated high-level CD8 effector T cell expression of Tim-3, which persisted throughout the course of infection. Since tuberculosis infection results in large amounts of IFN-γ production within the lung environment, and since IFN-γ induces expression of galectin-9; the recently identified ligand for Tim-3, it is plausible to postulate that CD8 T cells localized around infectious foci are subjected to continuous inhibitory stimuli through the Tim-3–galectin-9 pathway [66]. While this is a tempting explanation for the lack of effector function in the majority of lung-derived CD8 T cells during chronic infection, the underlying cause for this phenomenon is still unresolved. As Tim-3–galectin-9 interaction has been shown to result in antigen-specific T cell apoptosis of T_H1-polarized lymphocytes, it is interesting to note that this interaction may explain the high level of IFN-γ-induced T cell apoptosis observed in the lungs of *M. avium* infected and BCG immunized mice, as well as explain the failure of IFN-γ KO mice to eliminate T lymphocytes during the contraction phase following the resolution of infection [3, 14, 17, 66].

Upon examination of the cytokine-producing ability of CD8 T cells following infection, it was somewhat surprising that lung-derived cells failed to produce any

detectable IL-2, IL-4, or IL-10. In addition, spleen-derived CD8 T cells also failed to produce these cytokines (data not shown). These results can be interpreted in two ways. Although mixed T_H1/T_H2 responses are common even during strongly polarized inflammatory responses, the exceptionally strong T_H1-polarized response to *M. tuberculosis* may counter-regulate and prevent the induction of a detectable T_H2 response following infection. This effect may be more pronounced in the C57BL/6 mouse model used in these experiments, as this strain of mouse often preferentially exhibits a strong T_H1 bias. Alternately, IL-4 has been documented to be a difficult cytokine to detect, as this molecule has biological activity at very low concentrations [47]. Perhaps the intracellular concentration of IL-4 was too low to be detectable by the intracellular flow cytometric methods used in these studies.

While the lack of IL-2 production by pulmonary-resident effector cells was not surprising, we would have expected to observe splenic CD8 T cell production of this molecule. Either production of this molecule was below the limit of detection of our assay, or IL-2 producing CD8 T cells may be primarily confined to the draining lymph nodes as opposed to the spleen following infection with *M. tuberculosis*. Further characterization of the CD8 T cell population within draining lymph nodes should resolve this issue.

Even more surprising was the failure of pulmonary CD8 T cells from *M. tuberculosis*-infected mice to produce detectable levels of the cytolytic effector molecules granzyme B and perforin. Although we cannot rule out the possibility that these molecules were present at levels undetectable by our intracellular staining assay, the

results presented here support the idea that the primary protective function of CD8 T cells is to produce IFN-γ, rather than employ cytolytic mechanisms [43, 59].

The integrin expression studies and phenotypic characterization experiments have allowed us to develop a profile of the expression patterns of CD8 T cells over the course of aerosol infection with *M. tuberculosis* (Table 2.3). Examination of antigen-specific CD8 T cells recognizing the Mtb32 protein allowed us to precisely quantify expression levels of various markers on a population of cells actively responding to tuberculosis infection. It is unknown whether this single antigen-specific population is representative of other antigen-specific CD8 T cells. In the future, elucidation of novel murine CD8 T cell epitopes will allow us to determine the amount of heterogeneity within the CD8 T cell population responding to *M. tuberculosis* infection.

Drug treatment administered following infection with *M. tuberculosis* allowed us to examine the CD8 memory T cell population remaining after contraction and death of the effector cell population. Although combination chemotherapeutic treatment is unable to consistently achieve complete sterilization in the murine model of tuberculosis infection, prolonged treatment does result in a reduction of bacterial numbers to undetectable levels. While the effect of any remaining antigen on CD8 memory T cell development in this model is unknown, the gradual phenotypic divergence of the Mtb32-specific CD8 memory T cell population from the Mtb32-specific CD8 effector T cell population suggests that reducing antigenic burden can promote memory cell differentiation and the gradual acquisition of a memory cell phenotype. These results are consistent with previous work by Wherry *et al.* demonstrating that full acquisition of CD8 memory T cell characteristics can only occur upon viral clearance [62, 64]. As

viable organisms can be detected for approximately 5 months in some anatomical locations following immunization of mice with the *M. bovis* BCG vaccine, it is important to determine the exact impact of persistent antigen upon the generation and maintenance of durable, functional memory cells [40].

The phenotypic characterization experiments presented in these studies have provided an important stepping-stone in our understanding of the CD8 T cell response and the role that these cells play during pulmonary infection with *M. tuberculosis*. Importantly, we have identified several markers indicative of CD8 memory T cells that can be utilized to evaluate the effectiveness of novel experimental vaccine and adjuvant combinations. Importantly, critical examination of phenotypic T cell expression patterns following successful drug treatment may ultimately lead to the identification of several key biomarkers which could be utilized to create a phenotypic profile to monitor the effectiveness of drug therapy in a clinical setting. Additionally, the identification of high-level surface expression of several inhibitory receptors provides a tantalizing explanation for the lack of observable effector function of the majority of T lymphocytes following infection with *M. tuberculosis*.

A better understanding of the mechanisms involved in the generation of memory cells is an urgently needed adjunct to vaccine research, screening, and development. Further elucidation of memory-associated markers coupled with flow cytometric cell sorting will allow us to functionally determine memory cell subpopulations that confer protection to *M. tuberculosis*, ultimately allowing us to screen candidate vaccines for their potential to elicit such cells.

Table 2.1. A cross-reference of integrin molecules examined in subsequent experiments, including their abbreviations, heterodimeric binding partners, and extracellular ligands.

Name	Acronym	α/β #	CD #	Ligand
Very Late Antigen-4	VLA-4	$\alpha_4\beta_1$	CD49d/CD29	Fibronectin VCAM-1 MadCAM-1
Leukocyte Function-Associated Antigen-1	LFA-1	$\alpha_L\beta_2$	CD11a/CD18	ICAM-1 ICAM-2 ICAM-3
Leukocyte Peyer's Patch Adhesion Molecule-1	LPAM-1	$\alpha_4\beta_7$	CD49d/β_7	Fibronectin VCAM-1 MadCAM-1
Human Mucosal Lymphocyte-1 Antigen	HML-1	$\alpha_E\beta_7$	CD103/β_7	E-Cadherin

Table 2.2. A cross-reference of cell surface molecules examined in CD8 T cell phenotypic characterization experiments.

Name	Acronym	CD Number	Ligand
Programmed Cell Death-1	PD-1	CD279	PD-L1, PD-L2
IL-7 Receptor, α-Chain	IL-7Rα	CD127	IL-7
Chemokine Receptor 7	CCR7	CD197	CCL19, CCL21
L-Selectin	LECAM-1	CD62L	CD34, GlyCAM-1, MAdCAM-1
Leukosialin		CD43	CD54
IL-2 Receptor, β-Chain	IL-2Rβ	CD122	IL-2, 15
IL-15 Receptor, α-Chain	IL-15Rα		IL-15
Alpha-L Integrin Chain	α_L	CD11a	ICAM-1, 2, 3
IL-2 Receptor, γ-Chain	IL-2Rγ	CD132	IL-2, 4, 7, 9, 15
	4-1BB	CD137	4-1BBL
		CD44	Hyaluronan
Activation-Inducer Molecule	AIM	CD69	
	Ly6C		
Leukocyte Common Antigen		CD45RB	
		CD27	CD70
T Cell Immunoglobulin and Mucin Domain-Containing Molecule-3	Tim-3		Galectin-9

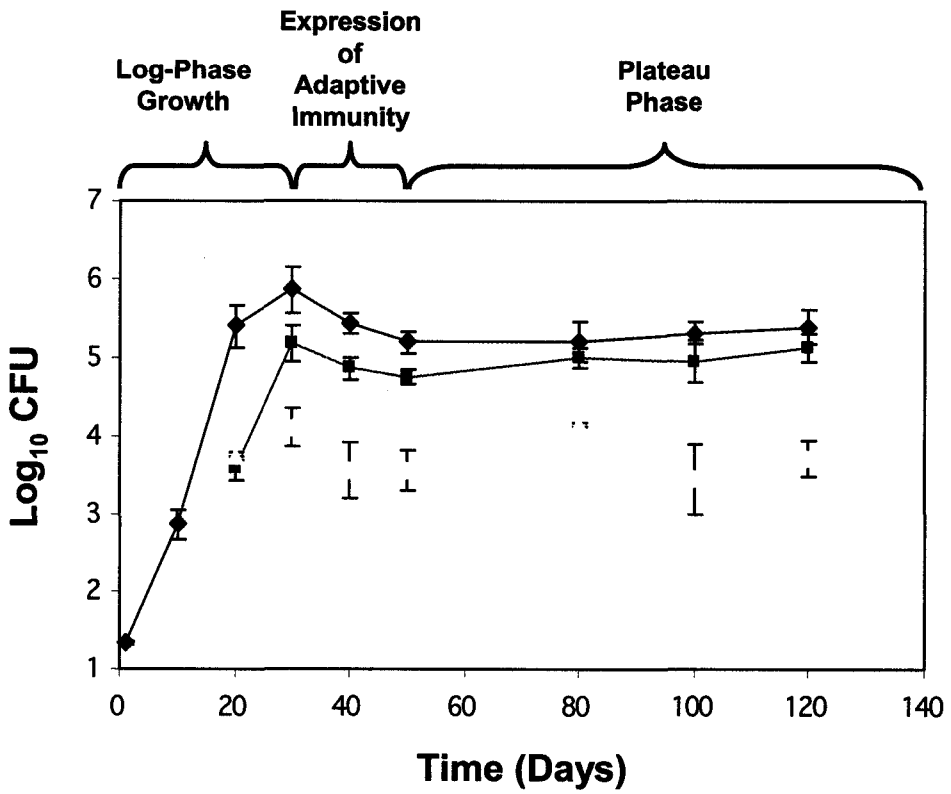

Figure 2.1. Total number viable bacteria in the lungs, spleen, and liver of C57BL/6 mice infected with *M. tuberculosis* H37Rv by the aerosol route. At the indicated timepoints, serial dilutions of lung, spleen, and liver whole organ homogenates were plated on to Middlebrook 7H11 agar and colonies were enumerated after 2-3 weeks of incubation. Data are expressed as the means ± the standard deviation and are from n=4 mice per timepoint. ♦ - Lung, ■ - Spleen, - Liver.

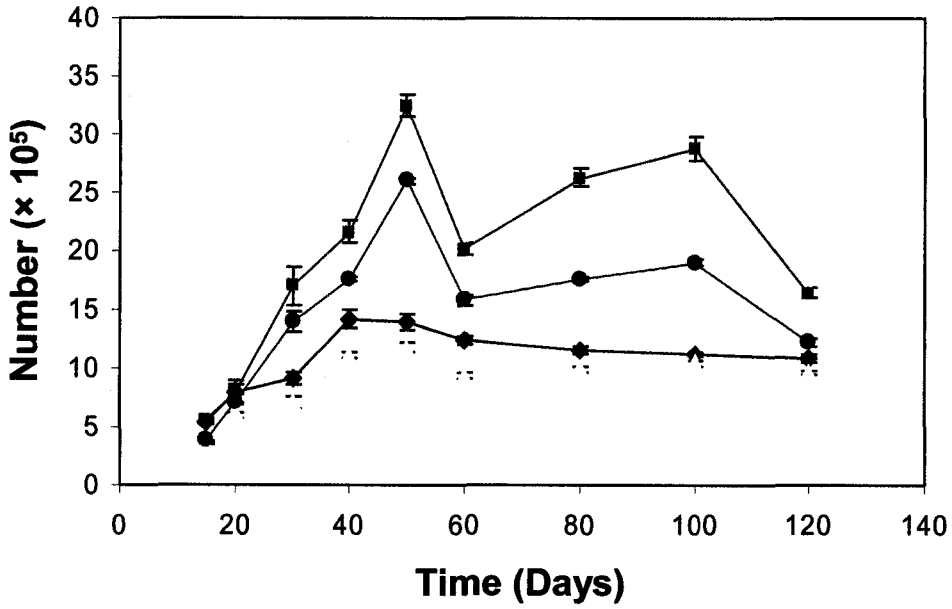

Figure 2.2. Total number of CD4 and CD8 T cells in the lungs of naïve C57BL/6 mice and mice infected with *M. tuberculosis* H37Rv. Data are expressed as the means ± the standard errors of the means and are from n=4 mice per timepoint. ♦ - CD4 T cells, naive mice; ■ - CD4 T cells, infected mice; - CD8 T cells, naive mice; ● - CD8 T cells, infected mice.

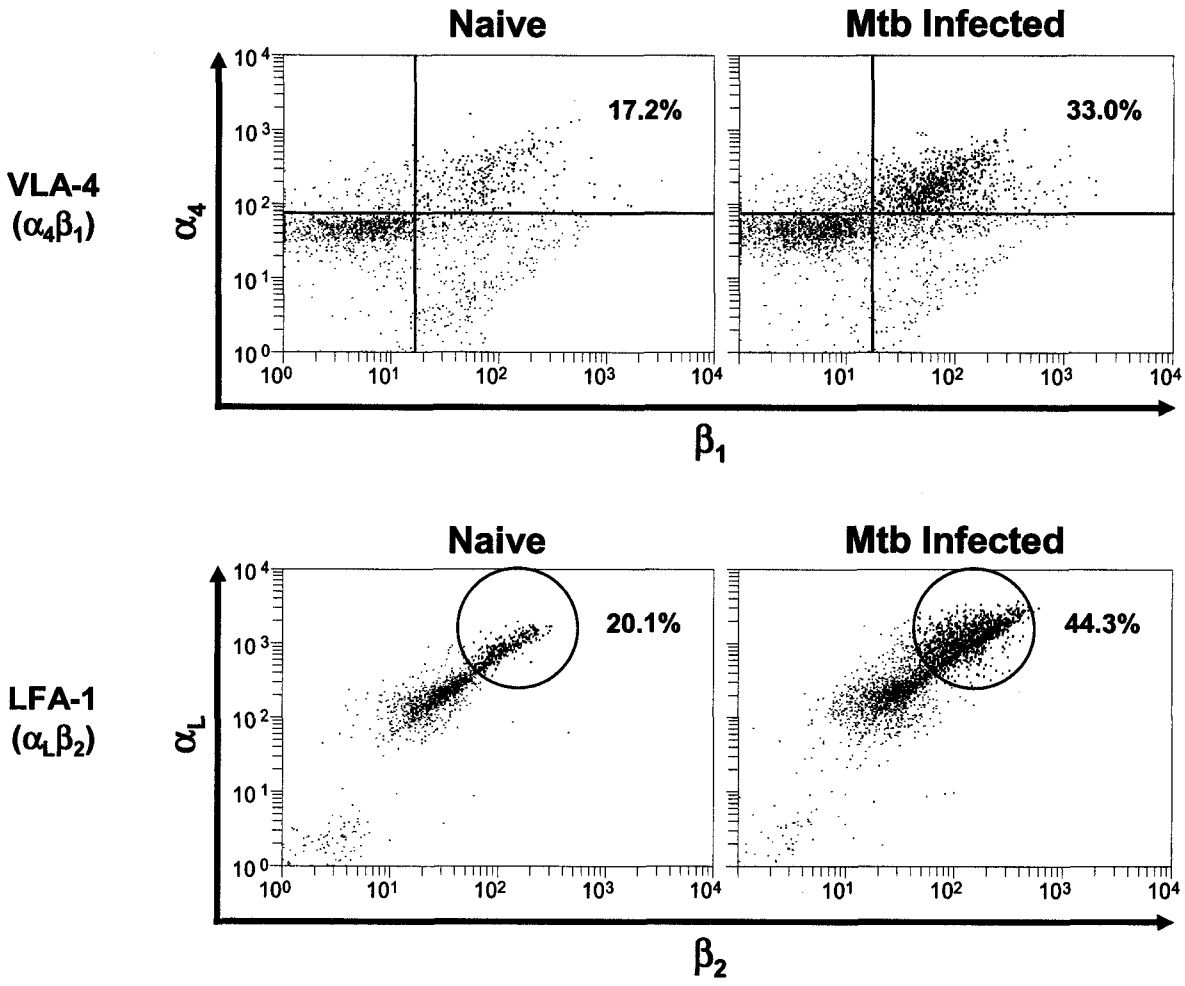

Figure 2.3. VLA-4 and LFA-1 expression by CD4 T cells in the lungs of naïve mice and mice infected for 60 days with *M. tuberculosis* H37Rv. Following aerosol infection, CD4 T cells upregulated expression of both integrin molecules. Percentages represent the number of cells falling within the indicated regions as compared to the total number of CD4 T cells. Dot plots were previously gated upon CD4-expressing T cells.

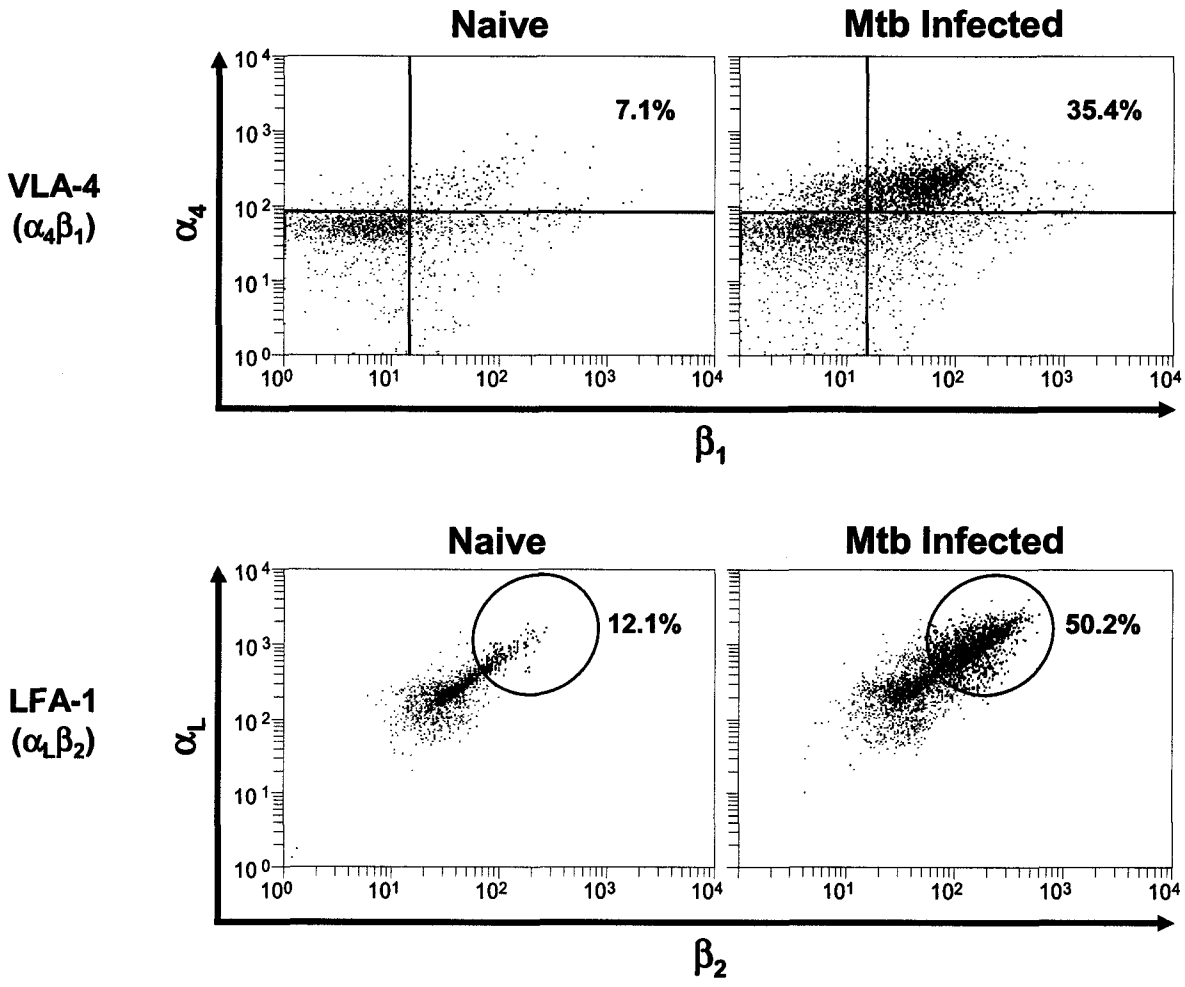

Figure 2.4. VLA-4 and LFA-1 expression by CD8 T cells in the lungs of naïve mice and mice infected for 60 days with *M. tuberculosis* H37Rv. Following aerosol infection, CD8 T cells upregulated expression of both integrin molecules. Percentages represent the number of cells falling within the indicated regions as compared to the total number of CD8 T cells. Dot plots were previously gated upon CD8-expressing T cells.

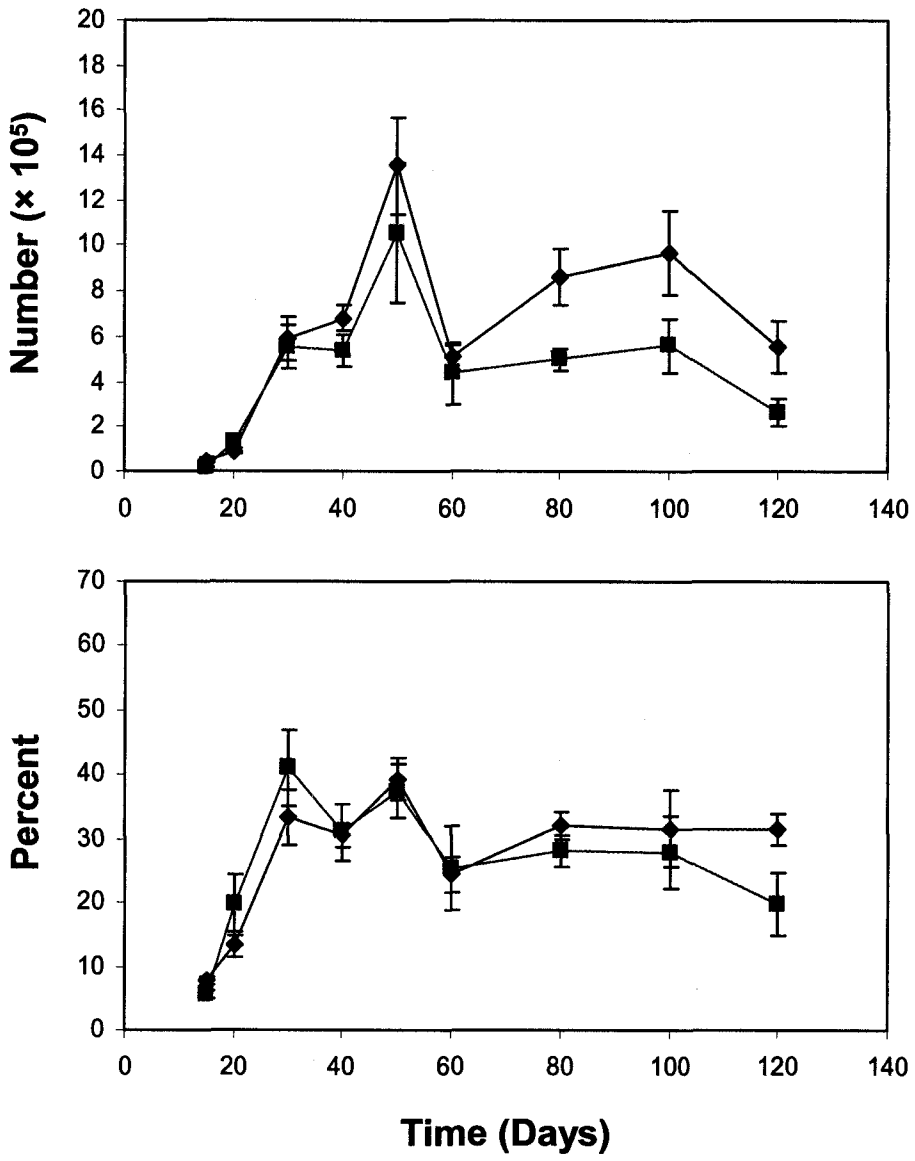

Figure 2.5. Total number of VLA-4^{hi} ($\alpha_4\beta_1$) CD4 and CD8 T cells in the lungs of mice infected with *M. tuberculosis* H37Rv. Percentages represent the number of VLA-4^{hi}-expressing CD4 or CD8 T cells as compared to the total number of CD4 or CD8 T cells, respectively. Data are expressed as the means ± the standard errors of the means and are from n=4 mice per timepoint. ♦ - CD4 T cells, ■ - CD8 T cells.

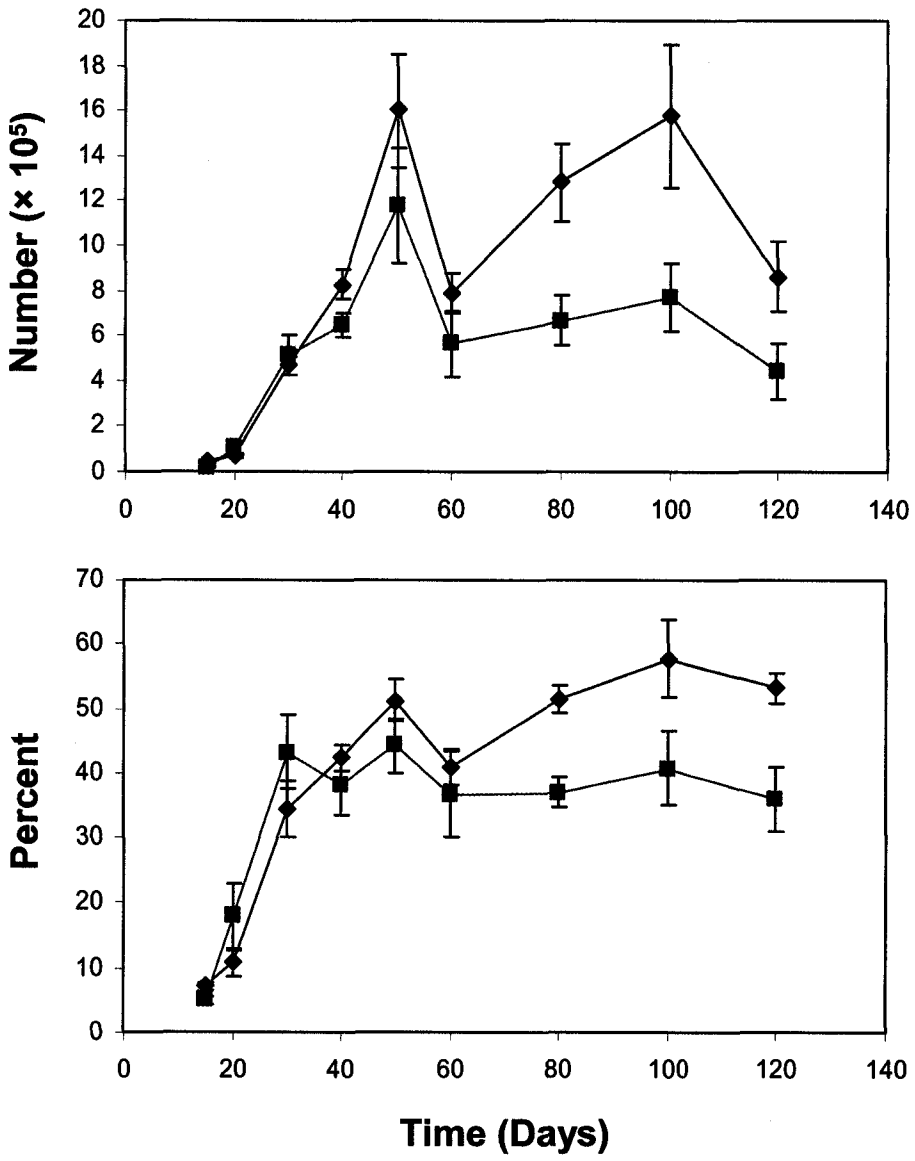

Figure 2.6. Total number of LFA-1^{hi} ($\alpha_L\beta_2$) CD4 and CD8 T cells in the lungs of mice infected with *M. tuberculosis* H37Rv. Percentages represent the number of VLA-4^{hi}-expressing CD4 or CD8 T cells as compared to the total number of CD4 or CD8 T cells, respectively. Data are expressed as the means ± the standard errors of the means and are from n=4 mice per timepoint. ♦ - CD4 T cells, ■ - CD8 T cells.

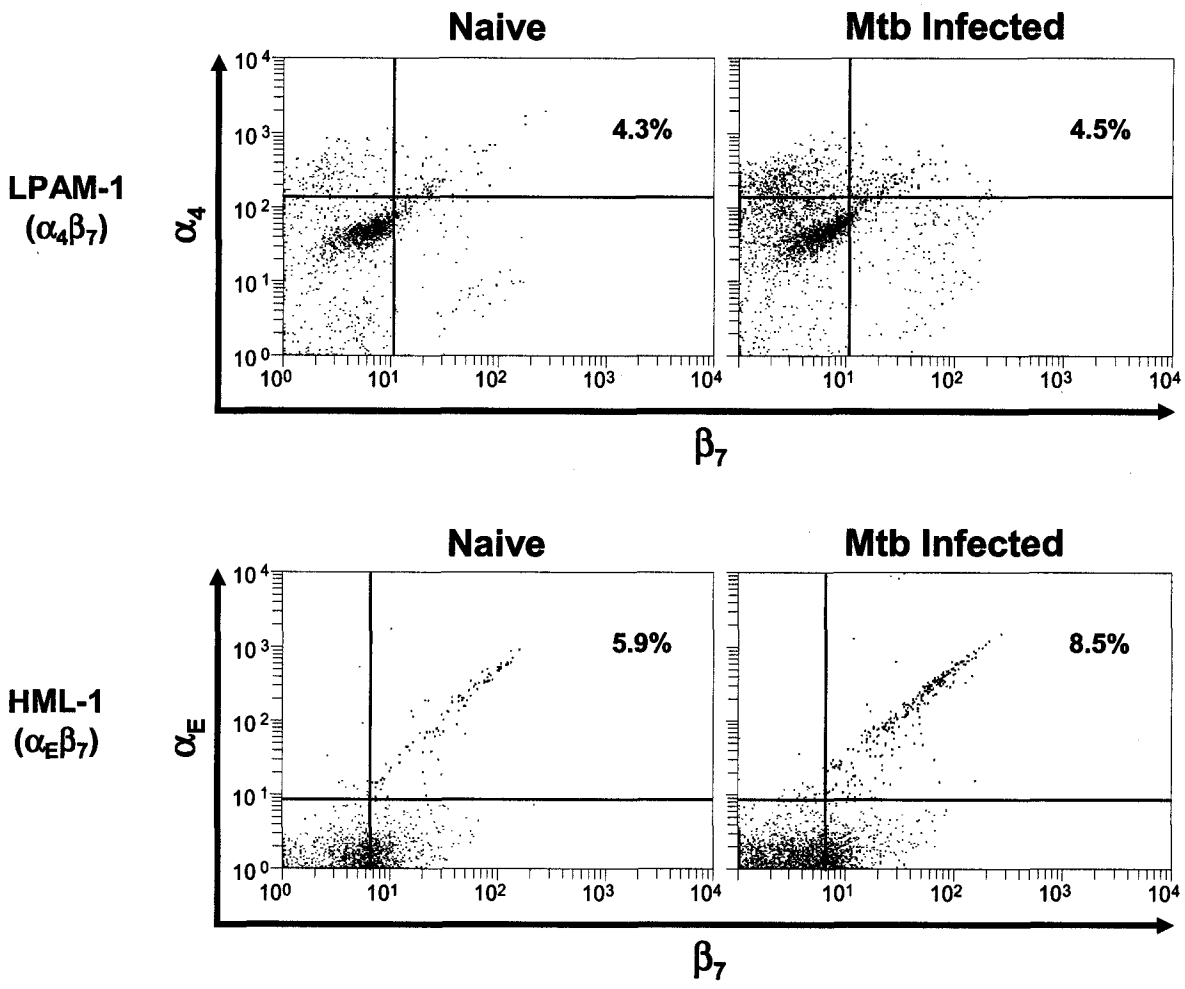

Figure 2.7. LPAM-1 and HML-1 integrin expression by CD4 T cells in the lungs of naïve mice and mice infected for 60 days with *M. tuberculosis* H37Rv. CD4 T cells did not upregulate LPAM-1 expression following infection. In addition, few CD4 T cells expressed HML-1, and the percentage of HML-1-expressing cells did not significantly increase after infection. Percentages represent the number of cells falling within the indicated regions as compared to the total number of CD4 T cells. Dot plots were previously gated upon CD4-expressing T cells.

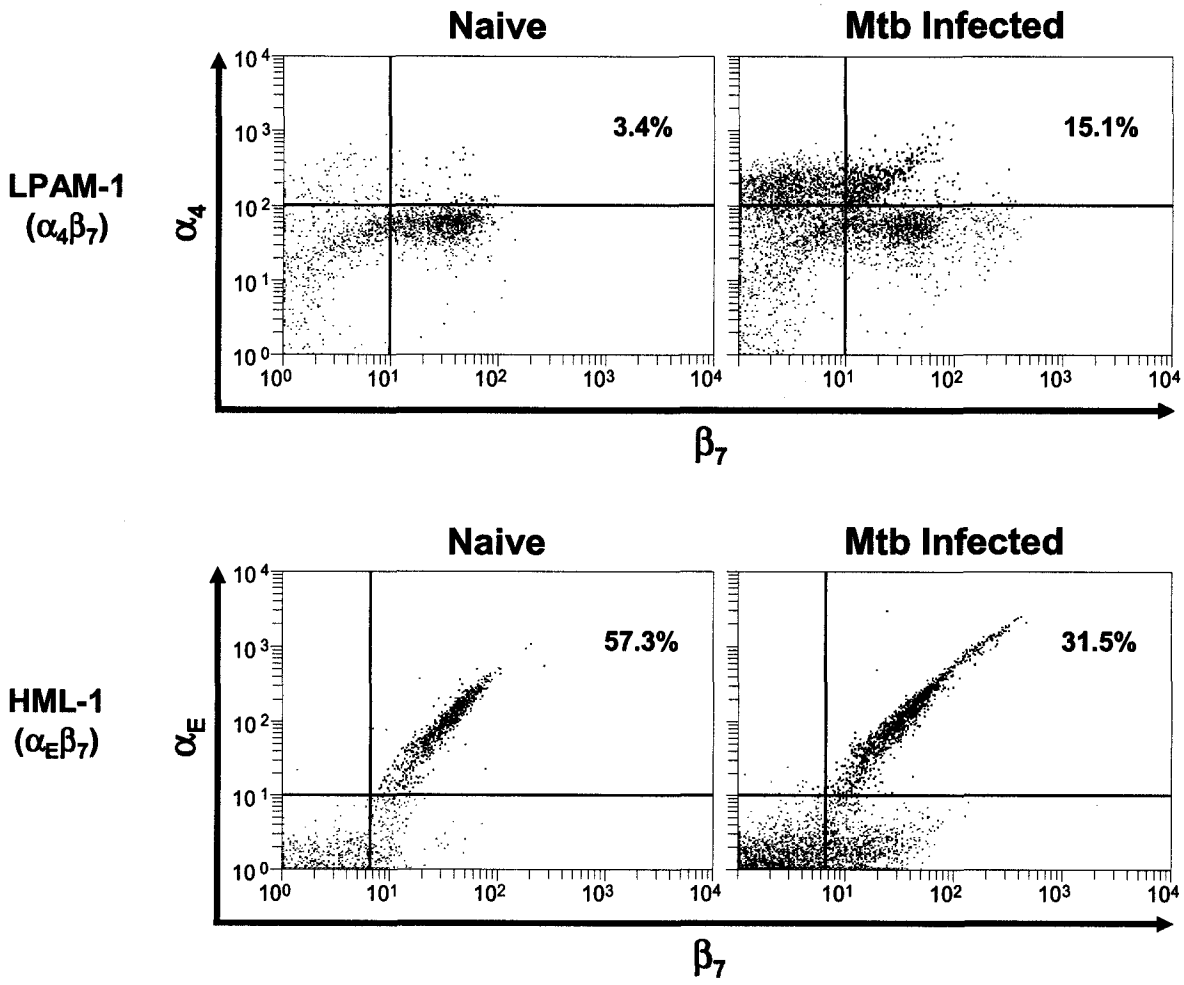

Figure 2.8. LPAM-1 and HML-1 integrin expression by CD8 T cells in the lungs of naïve mice and mice infected for 60 days with *M. tuberculosis* H37Rv. CD8 T cells upregulated expression of LPAM-1 and HML-1 following infection. Percentages represent the number of cells falling within the indicated regions as compared to the total number of CD8 T cells. Dot plots were previously gated upon CD8-expressing T cells.

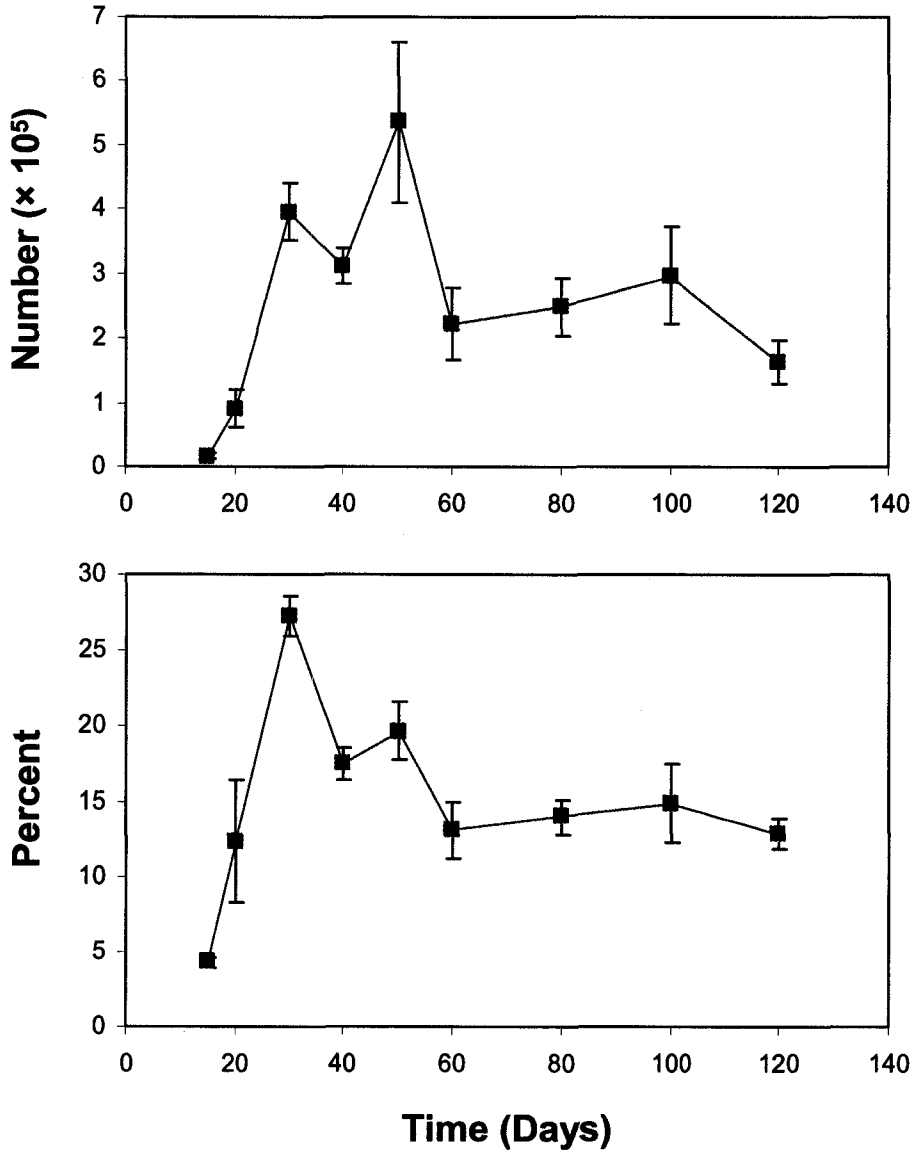

Figure 2.9. Total number of LPAM-1^{hi} ($\alpha_4\beta_7$) CD8 T cells in the lungs of mice infected with *M. tuberculosis* H37Rv. Percentages represent the number of VLA-4^{hi}-expressing CD8 T cells as compared to the total number of CD8 T cells. Data are expressed as the means ± the standard errors of the means and are from n=4 mice per timepoint. ■ - CD8 T cells.

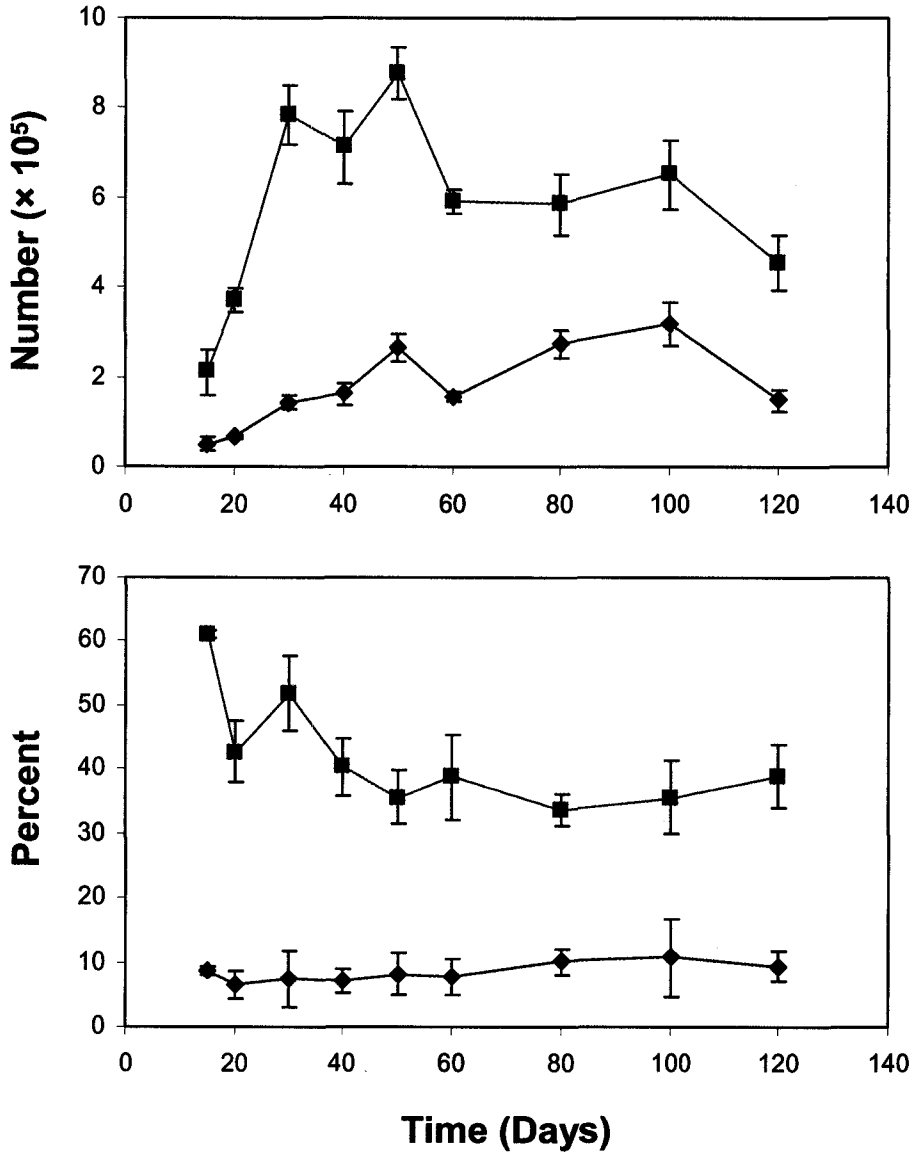

Figure 2.10. Total number of HML-1$^+$ ($\alpha_E\beta_7$) CD4 and CD8 T cells in the lungs of mice infected with *M. tuberculosis* H37Rv. Percentages represent the number of VLA-4^{hi}-expressing CD4 or CD8 T cells as compared to the total number of CD4 or CD8 T cells, respectively. Data are expressed as the means ± the standard errors of the means and are from n=4 mice per timepoint. ♦ - CD4 T cells, ■ - CD8 T cells.

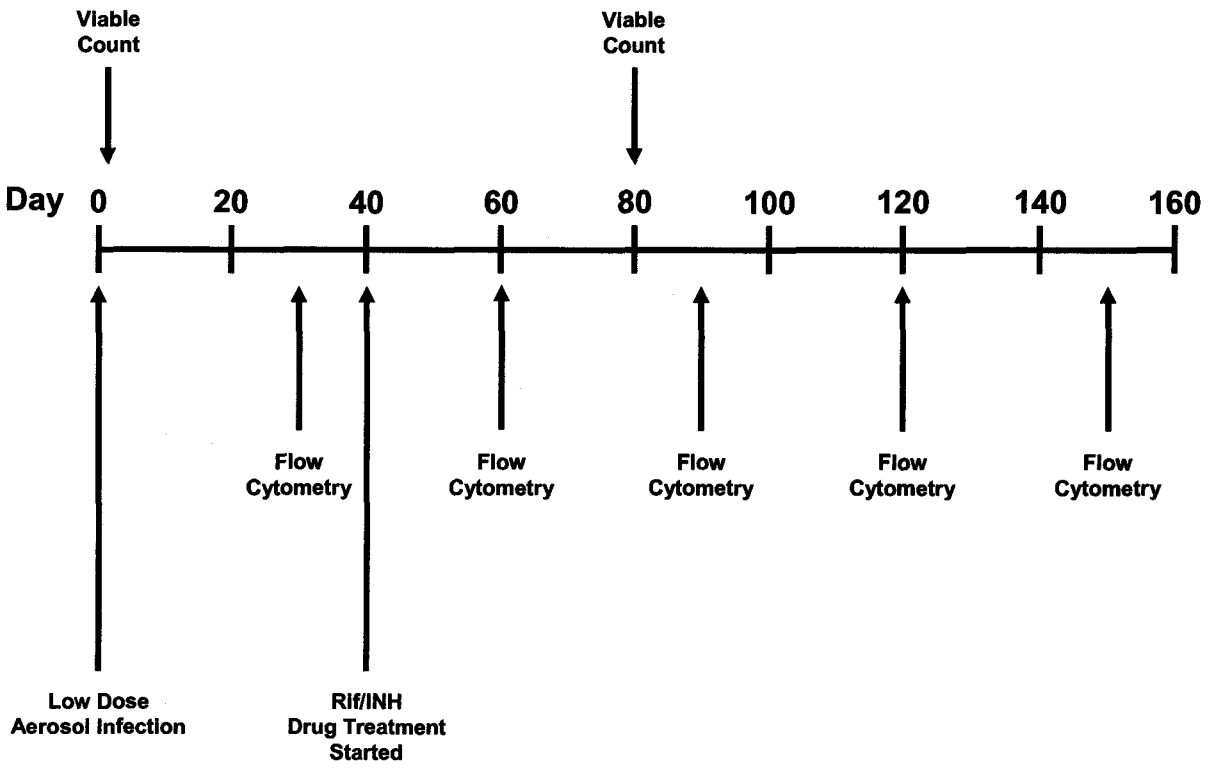

Figure 2.11. Experimental outline for CD8 T cell phenotypic characterization experiments.

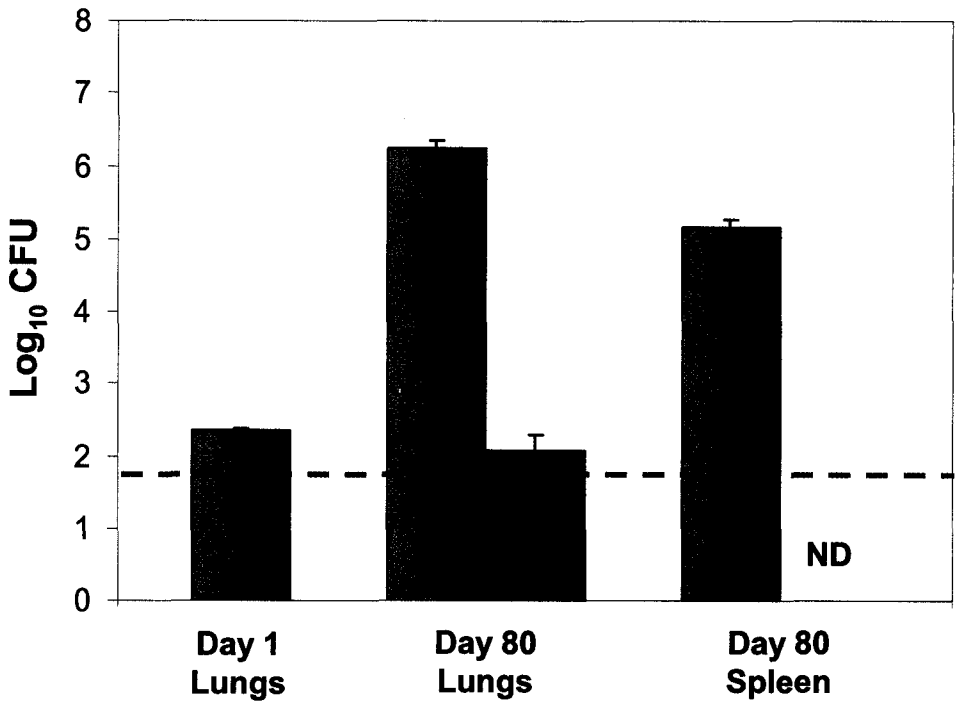

Figure 2.12. Total number of viable bacteria in the lungs and spleens of infected mice and mice infected and treated with rifampicin/isoniazid. Drug treatment was initiated at 40 days following infection and continued for the duration of the experiments. Note that combination drug treatment for 40 days reduced bacterial burden in the lungs by greater than 4-$\log_{10}$, and reduced bacterial burden in the spleen to undetectable numbers (detection limit = 50 CFU; dashed red line). Data are expressed as the means ± the standard deviation and are from n=5 mice per timepoint. ND - Not detectable, ■ - Infected, ■ - Infected and rifampicin/INH treated.

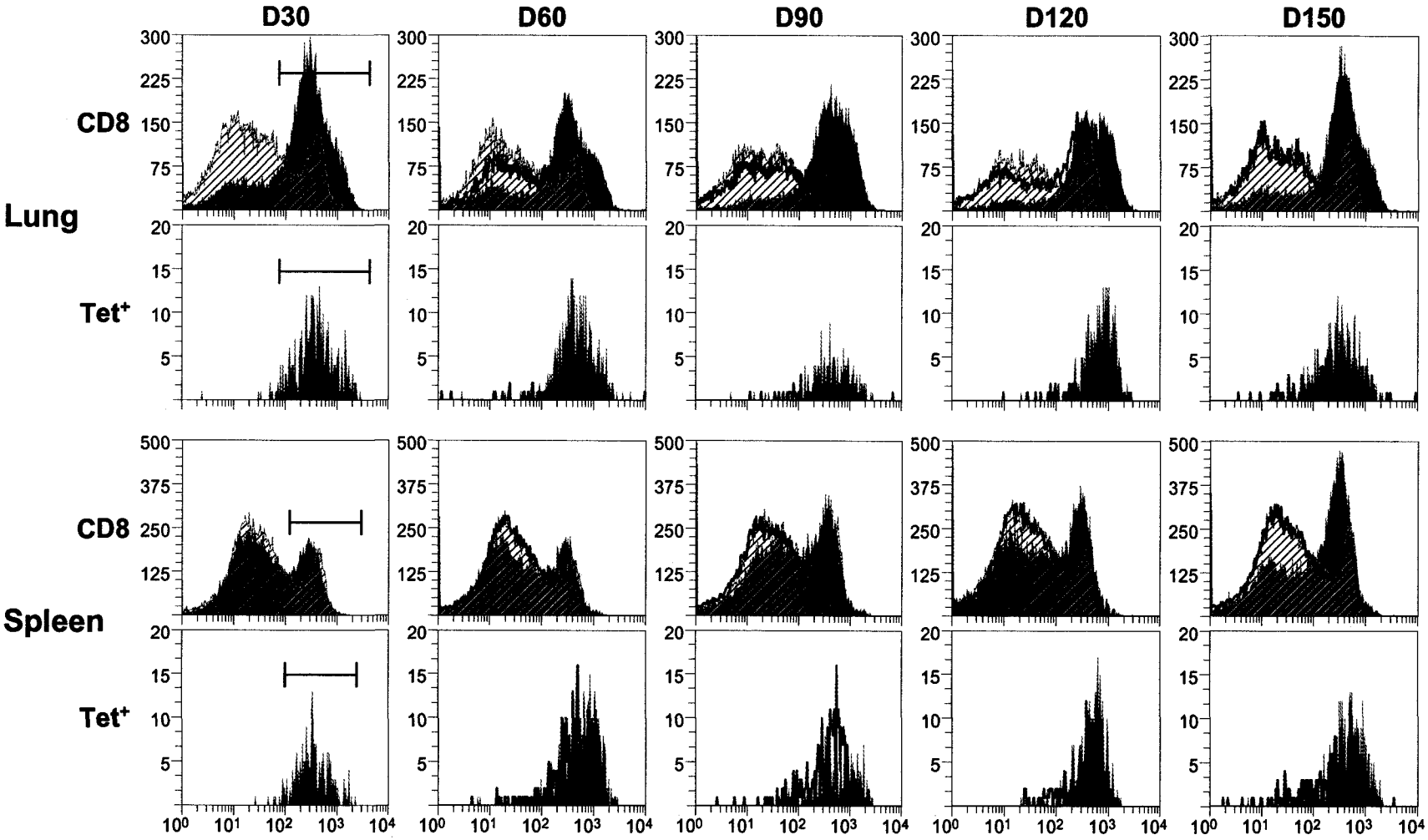

Figure 2.13. CD44 expression by CD8 T cells and Mtb32 tetramer-positive CD8 T cells. Each histogram represents a single mouse representative of n=4. At each timepoint and within each histogram, all data were normalized to the sample containing the largest number of gated events. The indicated region was used for subsequent analysis. ▨ - Naïve CD8 T cells, ■ - Infected CD8 T cells, □ - Infected/treated CD8 T cells.

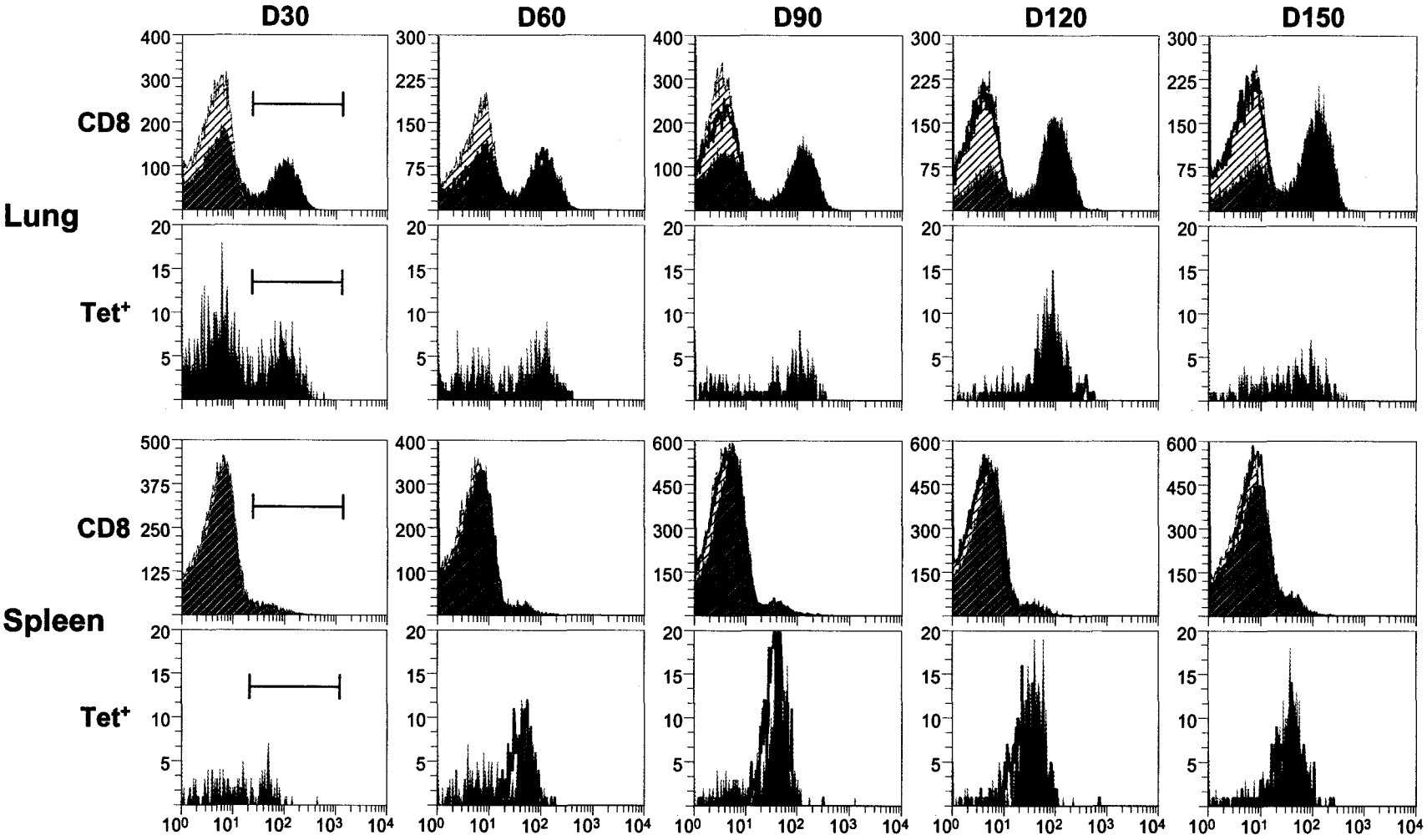

Figure 2.14. CD69 expression by CD8 T cells and Mtb32 tetramer-positive CD8 T cells. Each histogram represents a single mouse representative of n=4. At each timepoint and within each histogram, all data were normalized to the sample containing the largest number of gated events. The indicated region was used for subsequent analysis. ▨ - Naïve CD8 T cells, ■ - Infected CD8 T cells, □ - Infected/treated CD8 T cells.

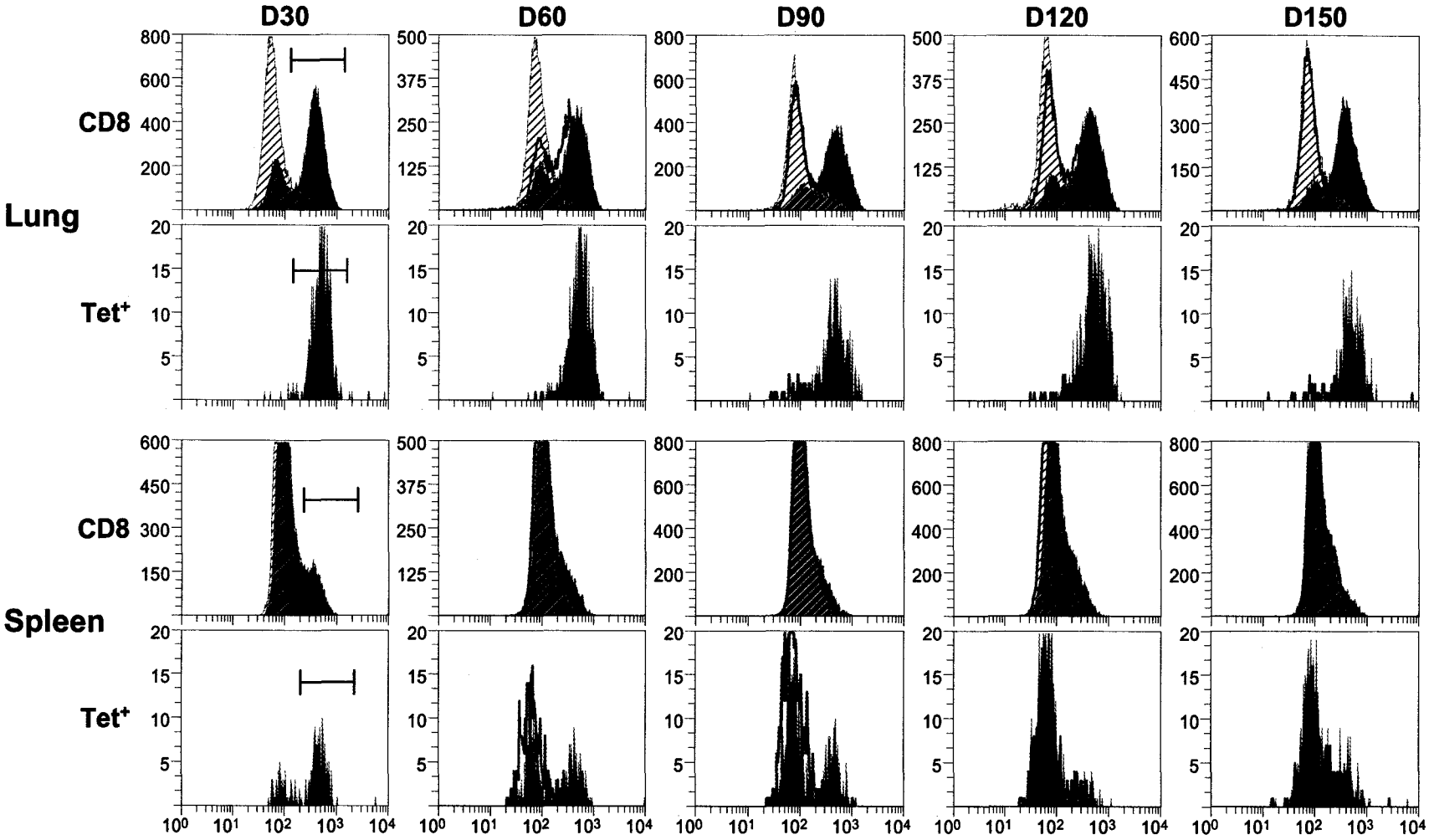

Figure 2.15. CD11a expression by CD8 T cells and Mtb32 tetramer-positive CD8 T cells. Each histogram represents a single mouse representative of n=4. At each timepoint and within each histogram, all data were normalized to the sample containing the largest number of gated events. The indicated region was used for subsequent analysis. ▨ - Naïve CD8 T cells, ■ - Infected CD8 T cells, □ - Infected/treated CD8 T cells.

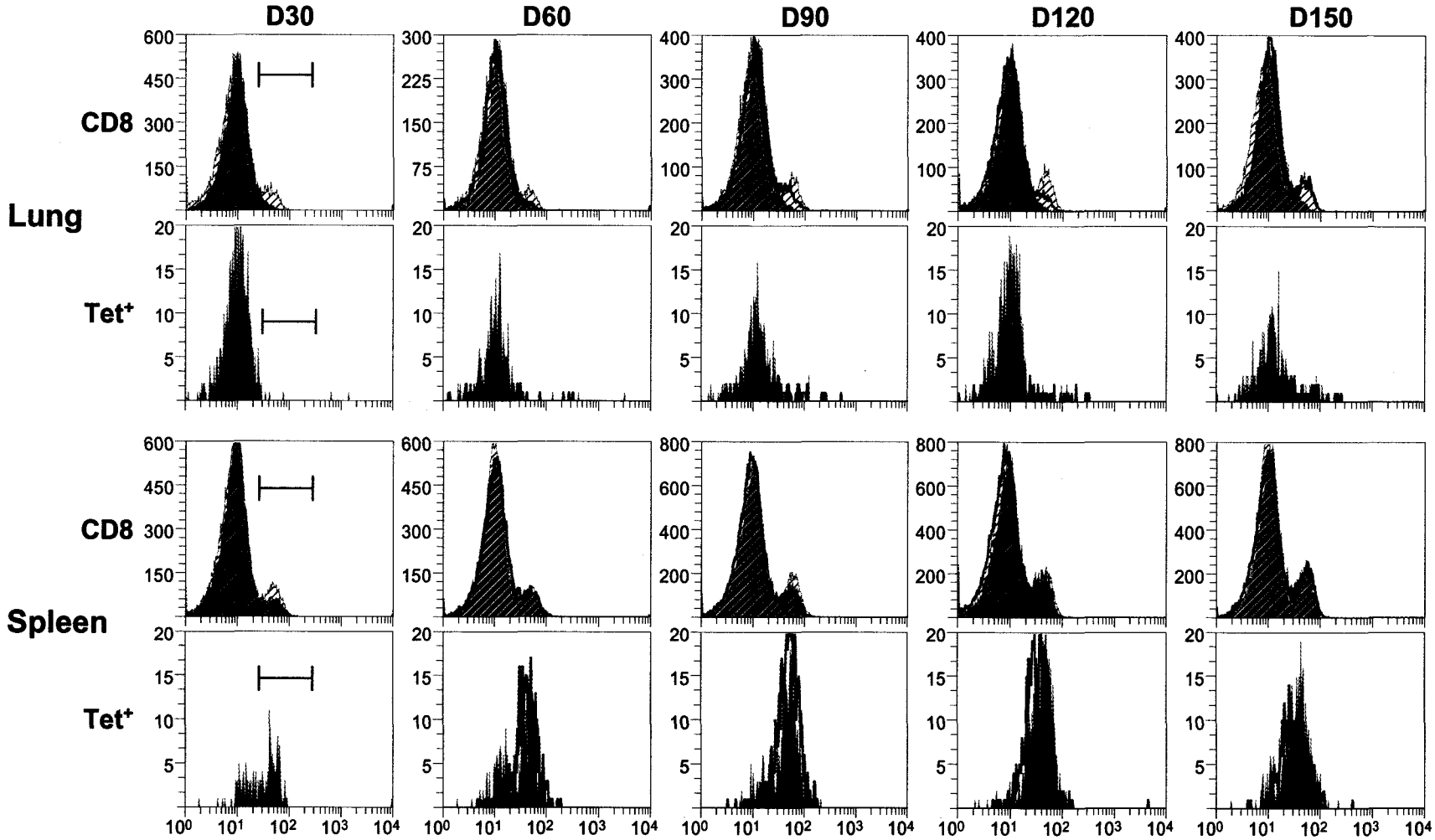

Figure 2.16. CD122 expression by CD8 T cells and Mtb32 tetramer-positive CD8 T cells. Each histogram represents a single mouse representative of n=4. At each timepoint and within each histogram, all data were normalized to the sample containing the largest number of gated events. The indicated region was used for subsequent analysis. ▨ - Naïve CD8 T cells, ■ - Infected CD8 T cells, □ - Infected/treated CD8 T cells.

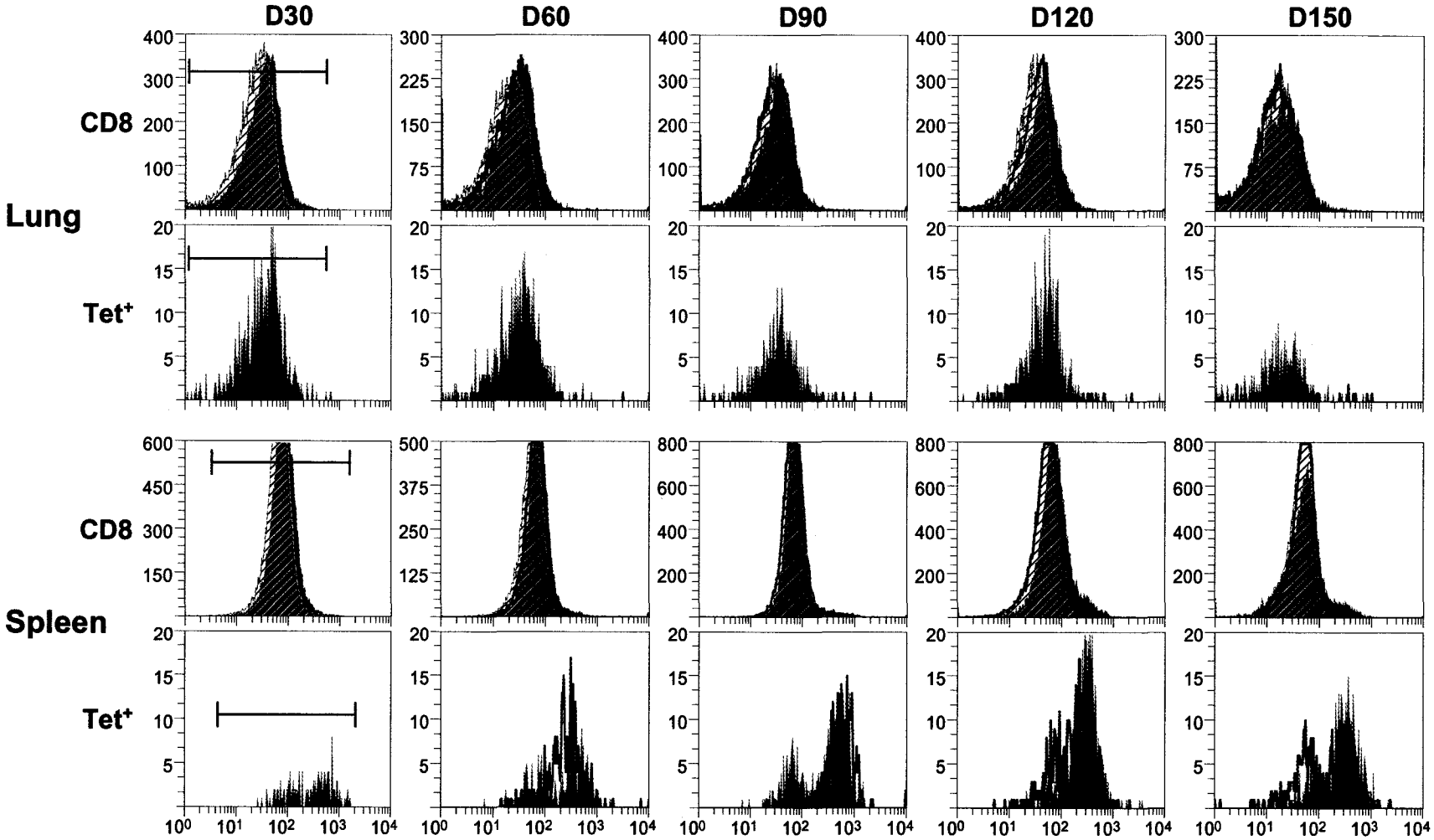

Figure 2.17. CD132 expression by CD8 T cells and Mtb32 tetramer-positive CD8 T cells. Each histogram represents a single mouse representative of n=4. At each timepoint and within each histogram, all data were normalized to the sample containing the largest number of gated events. The indicated region was used for subsequent analysis. ▨ - Naïve CD8 T cells, ■ - Infected CD8 T cells, □ - Infected/treated CD8 T cells.

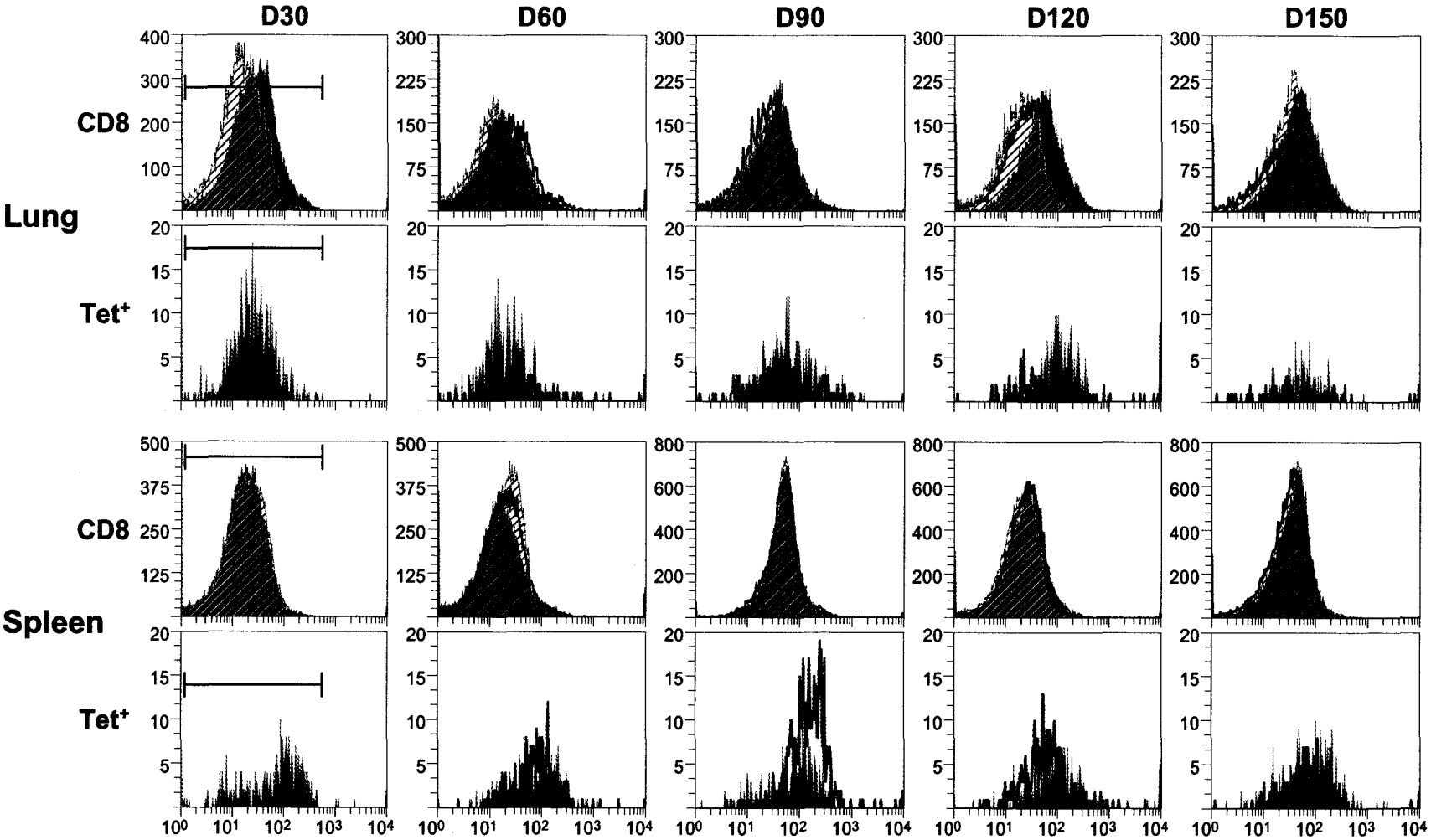

Figure 2.18. CCR7 expression by CD8 T cells and Mtb32 tetramer-positive CD8 T cells. Each histogram represents a single mouse representative of n=4. At each timepoint and within each histogram, all data were normalized to the sample containing the largest number of gated events. The indicated region was used for subsequent analysis. ▨ - Naïve CD8 T cells, ■ - Infected CD8 T cells, □ - Infected/treated CD8 T cells.

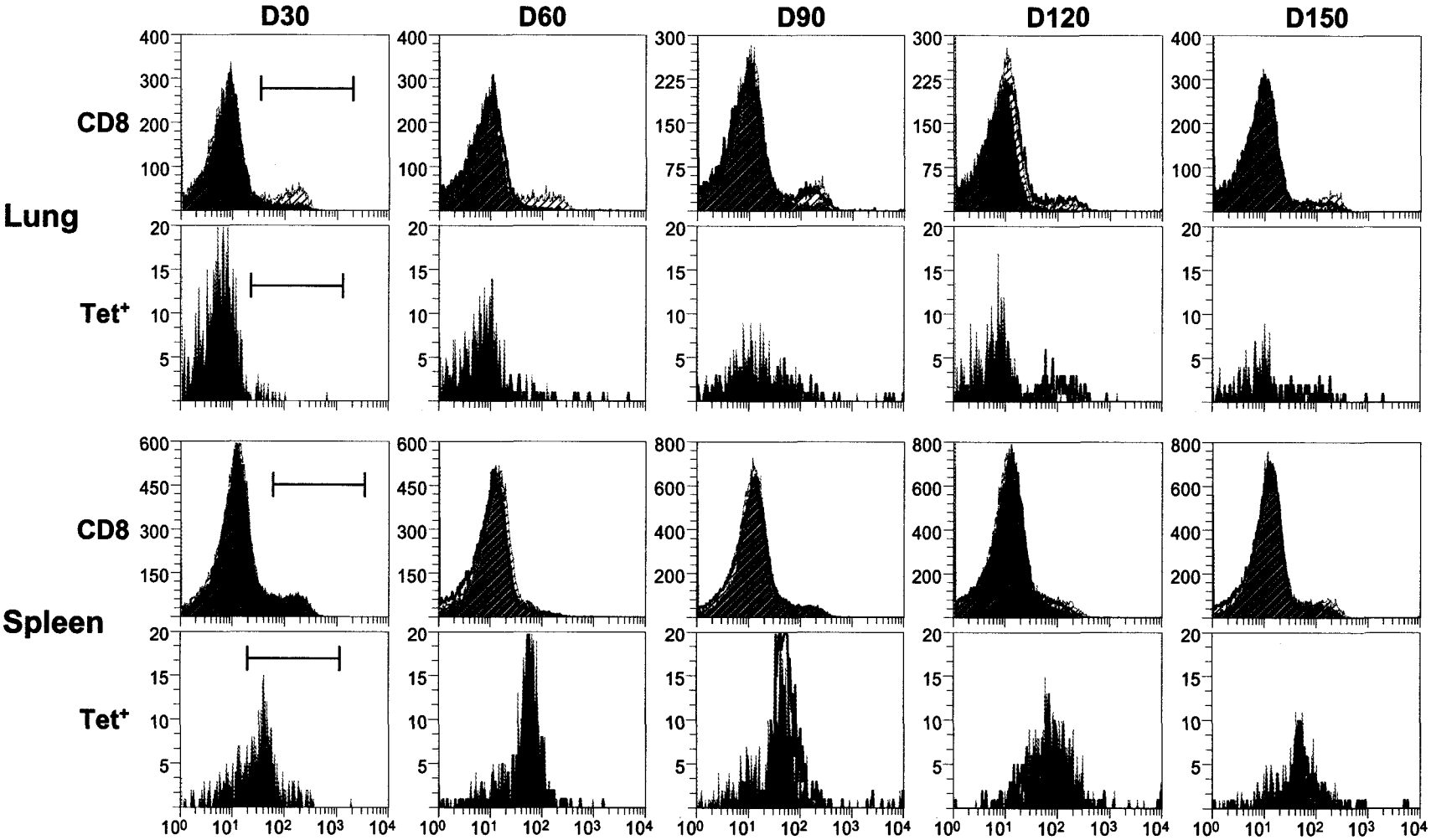

Figure 2.19. CD62L expression by CD8 T cells and Mtb32 tetramer-positive CD8 T cells. Each histogram represents a single mouse representative of n=4. At each timepoint and within each histogram, all data were normalized to the sample containing the largest number of gated events. The indicated region was used for subsequent analysis. ▨ - Naïve CD8 T cells, ■ - Infected CD8 T cells, □ - Infected/treated CD8 T cells.

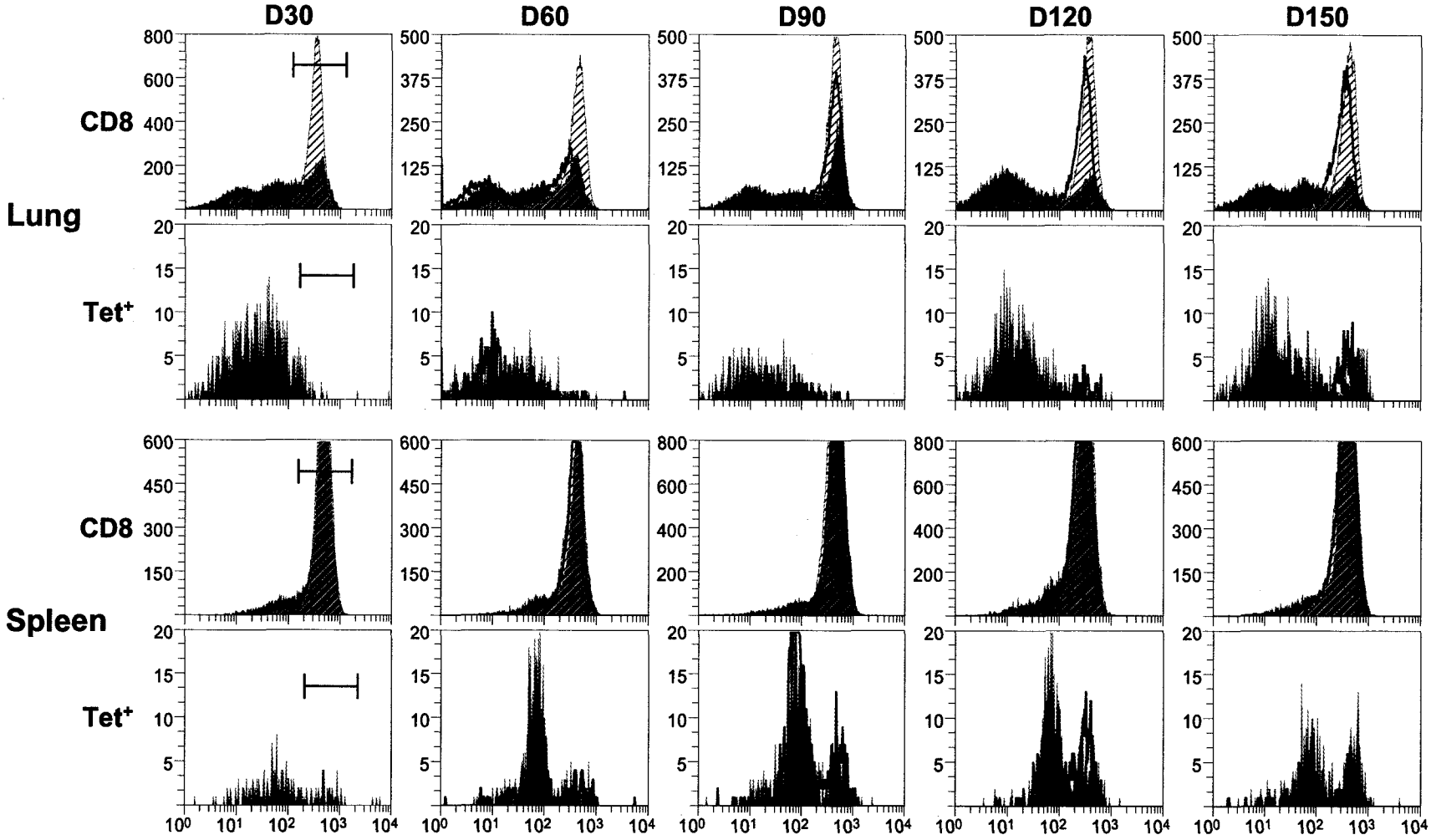

Figure 2.20. CD45RB expression by CD8 T cells and Mtb32 tetramer-positive CD8 T cells. Each histogram represents a single mouse representative of n=4. At each timepoint and within each histogram, all data were normalized to the sample containing the largest number of gated events. The indicated region was used for subsequent analysis. ▨ - Naïve CD8 T cells, ■ - Infected CD8 T cells, □ - Infected/treated CD8 T cells.

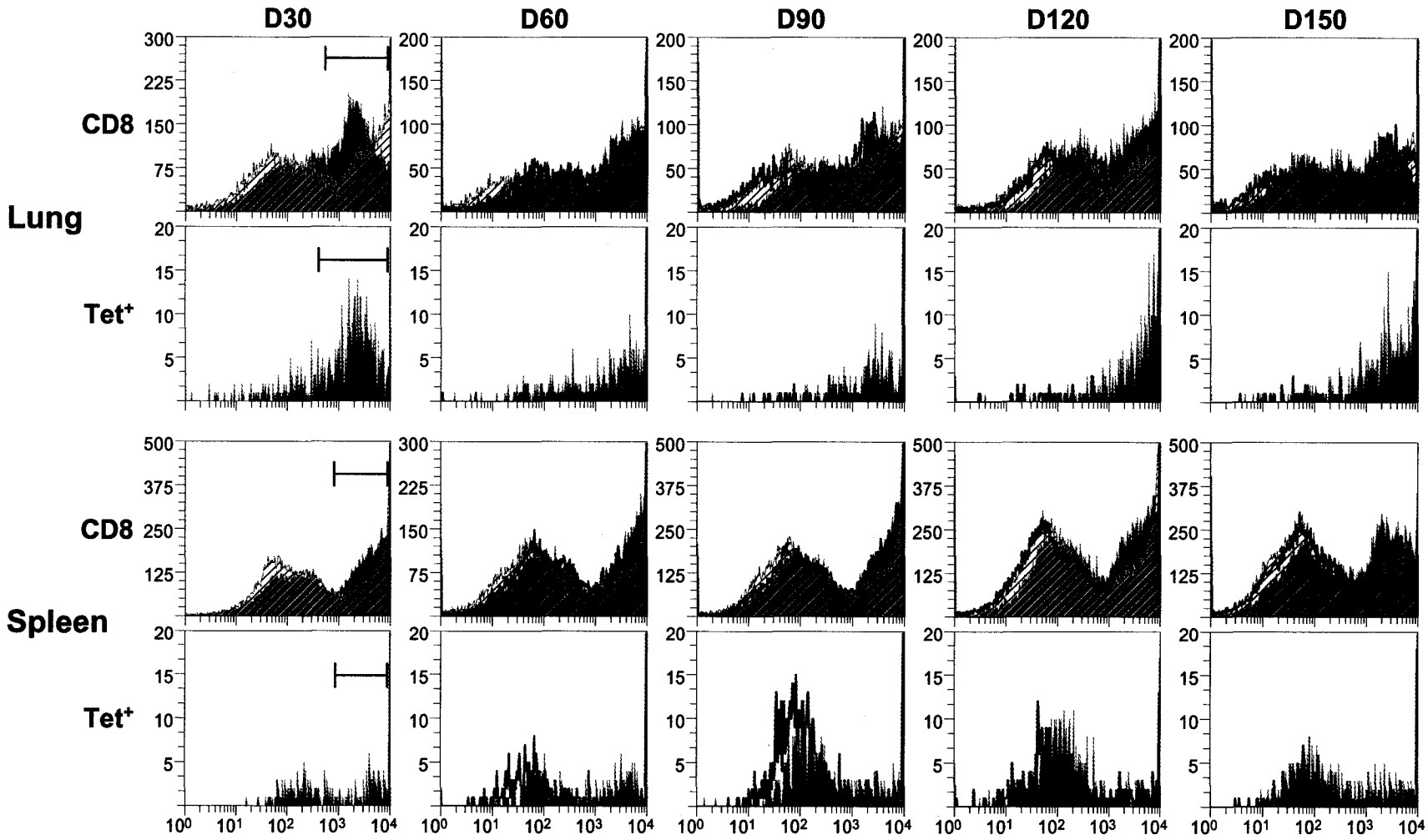

Figure 2.21. Ly6C expression by CD8 T cells and Mtb32 tetramer-positive CD8 T cells. Each histogram represents a single mouse representative of n=4. At each timepoint and within each histogram, all data were normalized to the sample containing the largest number of gated events. The indicated region was used for subsequent analysis. ▨ - Naïve CD8 T cells, ■ - Infected CD8 T cells, □ - Infected/treated CD8 T cells.

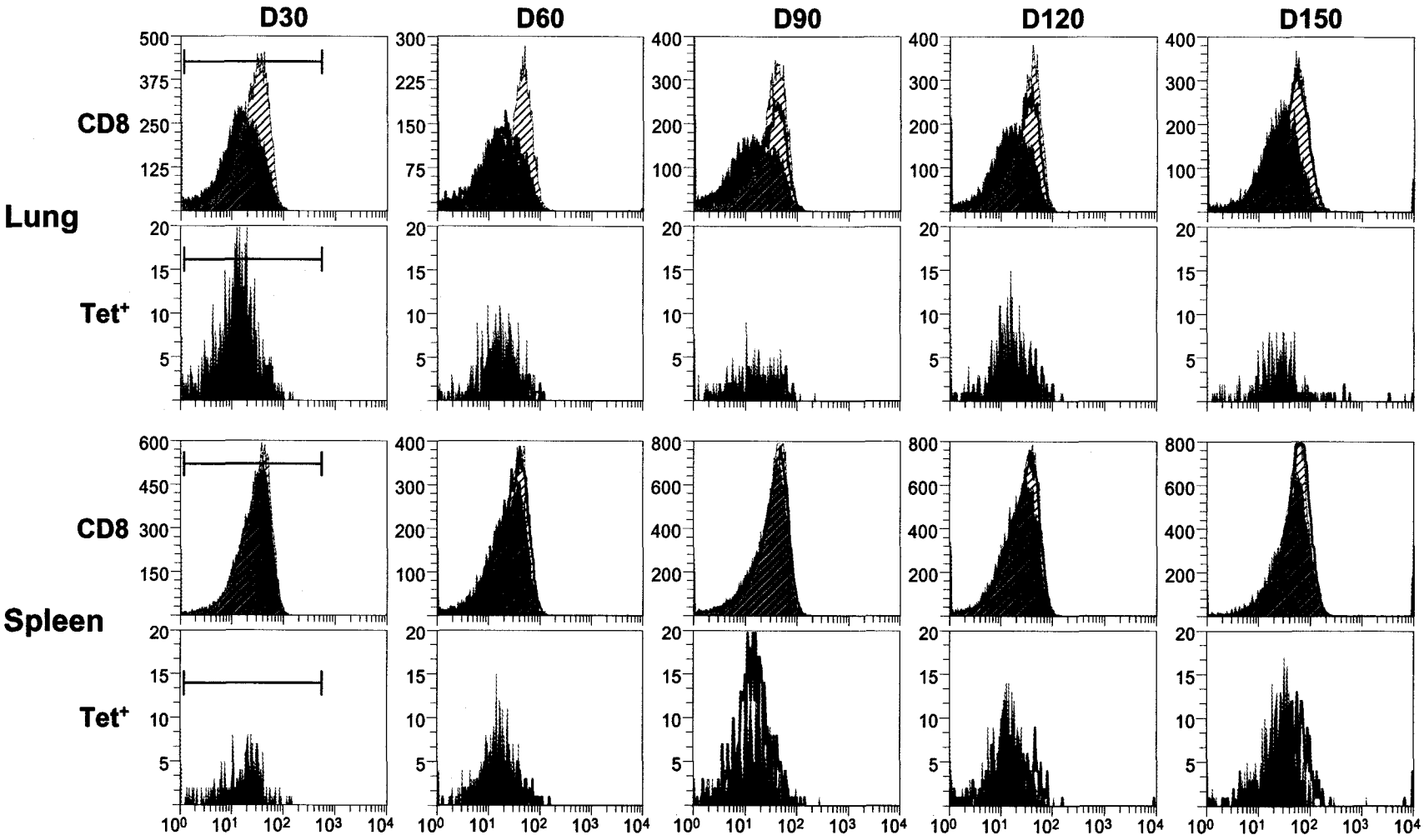

Figure 2.22. IL-7Rα expression by CD8 T cells and Mtb32 tetramer-positive CD8 T cells. Each histogram represents a single mouse representative of n=4. At each timepoint and within each histogram, all data were normalized to the sample containing the largest number of gated events. The indicated region was used for subsequent analysis. ▨ - Naïve CD8 T cells, ■ - Infected CD8 T cells, □ - Infected/treated CD8 T cells.

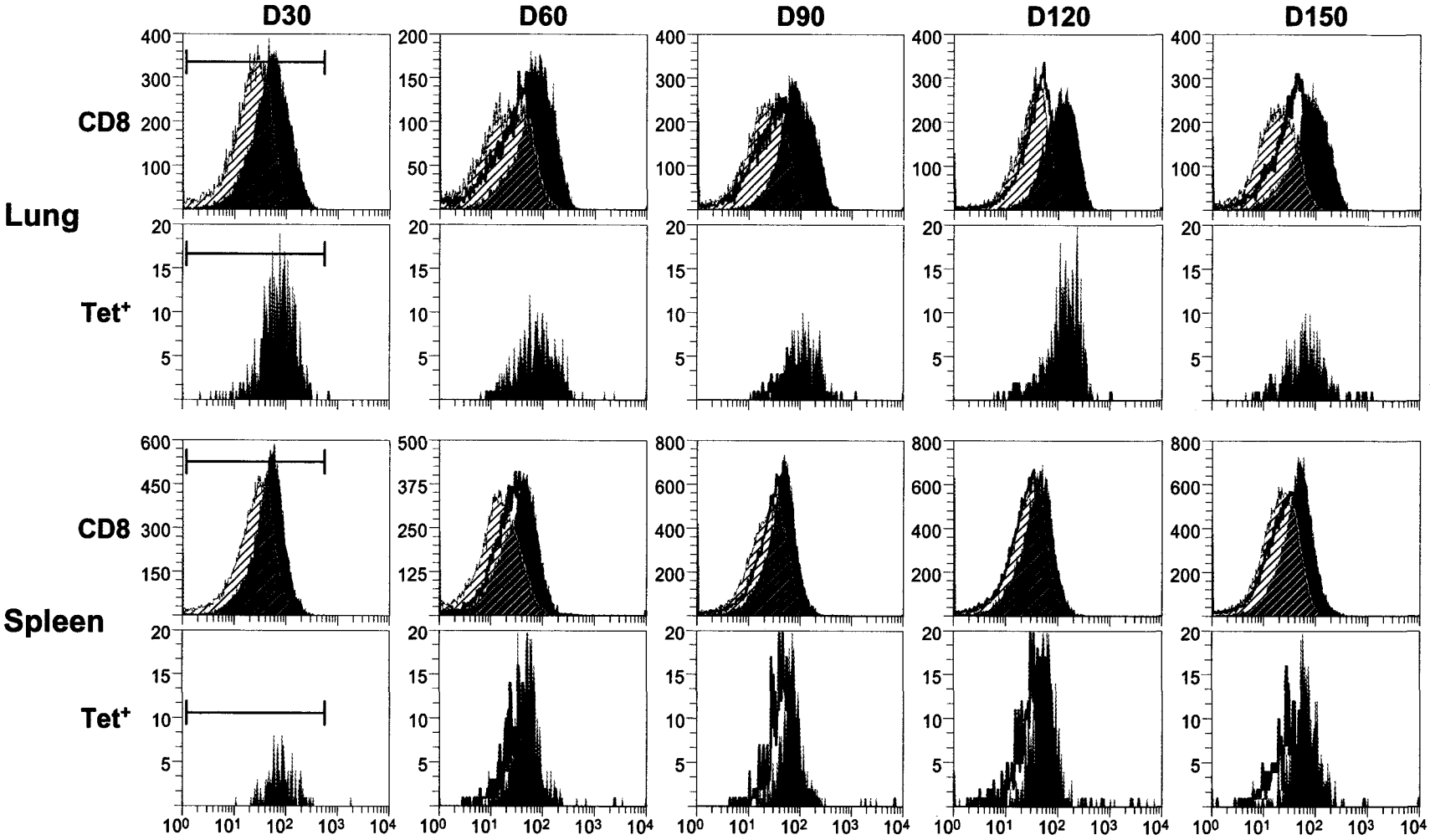

Figure 2.23. IL-15Rα expression by CD8 T cells and Mtb32 tetramer-positive CD8 T cells. Each histogram represents a single mouse representative of n=4. At each timepoint and within each histogram, all data were normalized to the sample containing the largest number of gated events. The indicated region was used for subsequent analysis. ▨ - Naïve CD8 T cells, ■ - Infected CD8 T cells, □ - Infected/treated CD8 T cells.

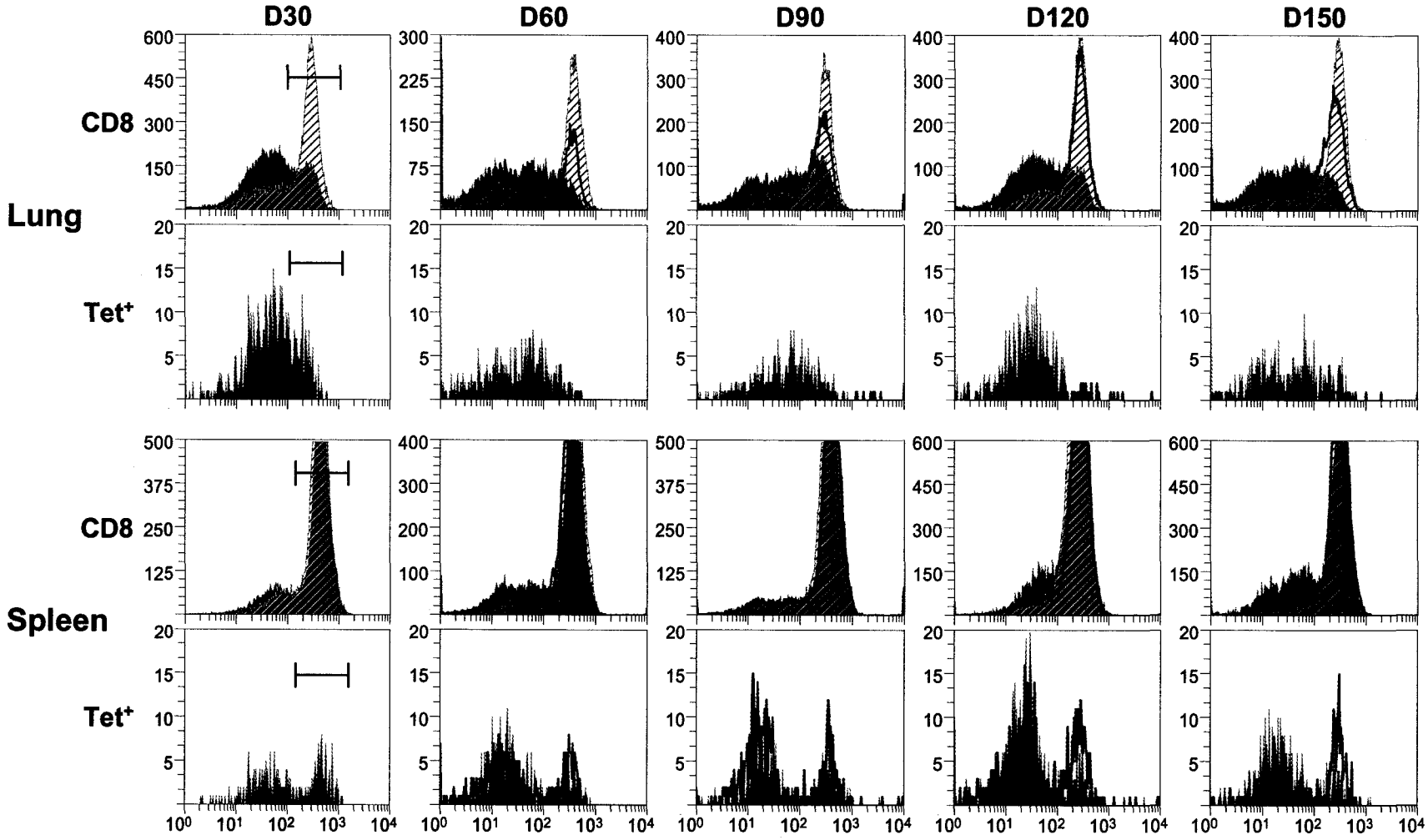

Figure 2.24. CD27 expression by CD8 T cells and Mtb32 tetramer-positive CD8 T cells. Each histogram represents a single mouse representative of n=4. At each timepoint and within each histogram, all data were normalized to the sample containing the largest number of gated events. The indicated region was used for subsequent analysis. ▨ - Naïve CD8 T cells, ■ - Infected CD8 T cells, □ - Infected/treated CD8 T cells.

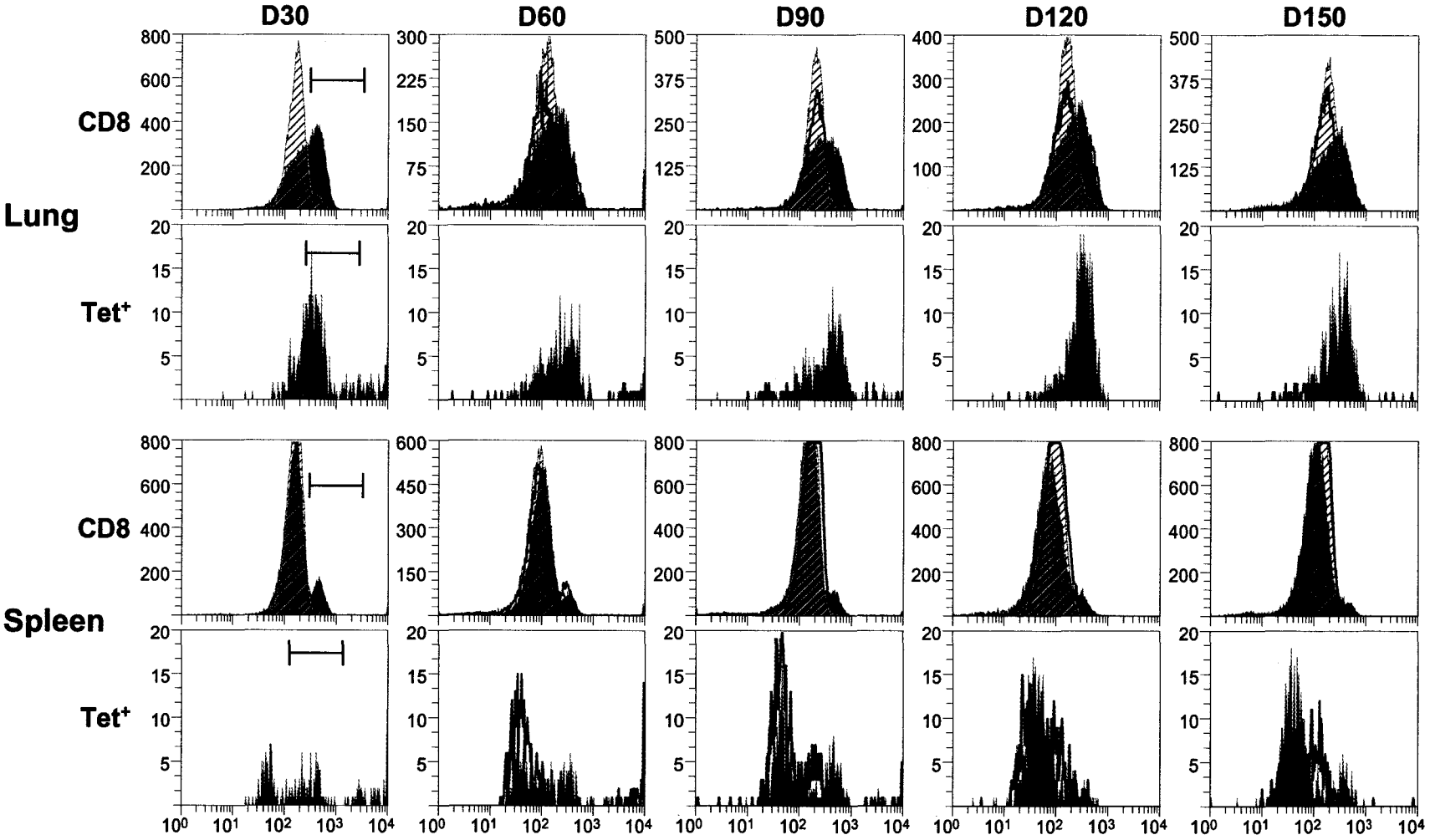

Figure 2.25. CD43 expression by CD8 T cells and Mtb32 tetramer-positive CD8 T cells. Each histogram represents a single mouse representative of n=4. At each timepoint and within each histogram, all data were normalized to the sample containing the largest number of gated events. The indicated region was used for subsequent analysis. ▨ - Naïve CD8 T cells, ■ - Infected CD8 T cells, □ - Infected/treated CD8 T cells.

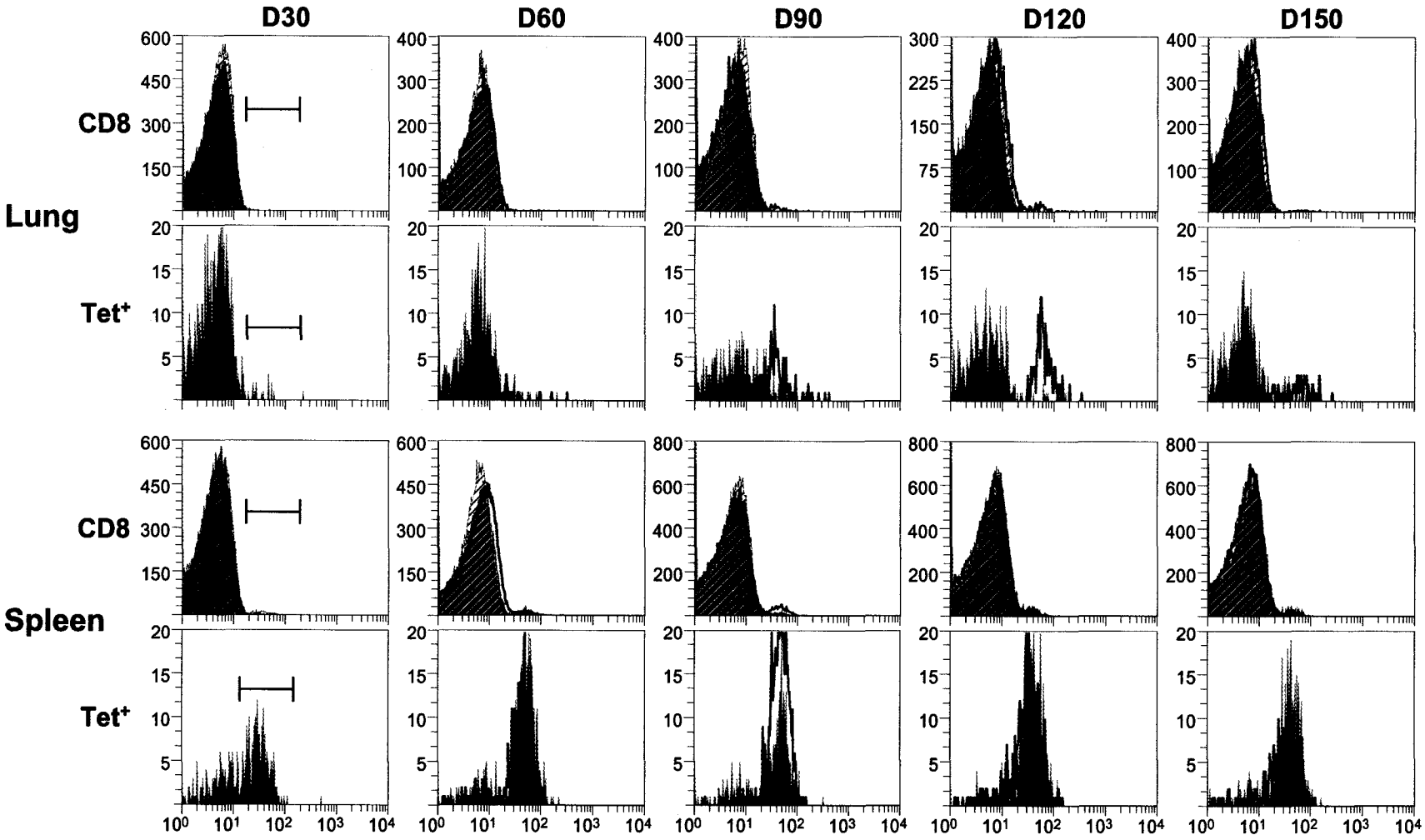

Figure 2.26. 4-1BB expression by CD8 T cells and Mtb32 tetramer-positive CD8 T cells. Each histogram represents a single mouse representative of n=4. At each timepoint and within each histogram, all data were normalized to the sample containing the largest number of gated events. The indicated region was used for subsequent analysis. ▨ - Naïve CD8 T cells, ■ - Infected CD8 T cells, □ - Infected/treated CD8 T cells.

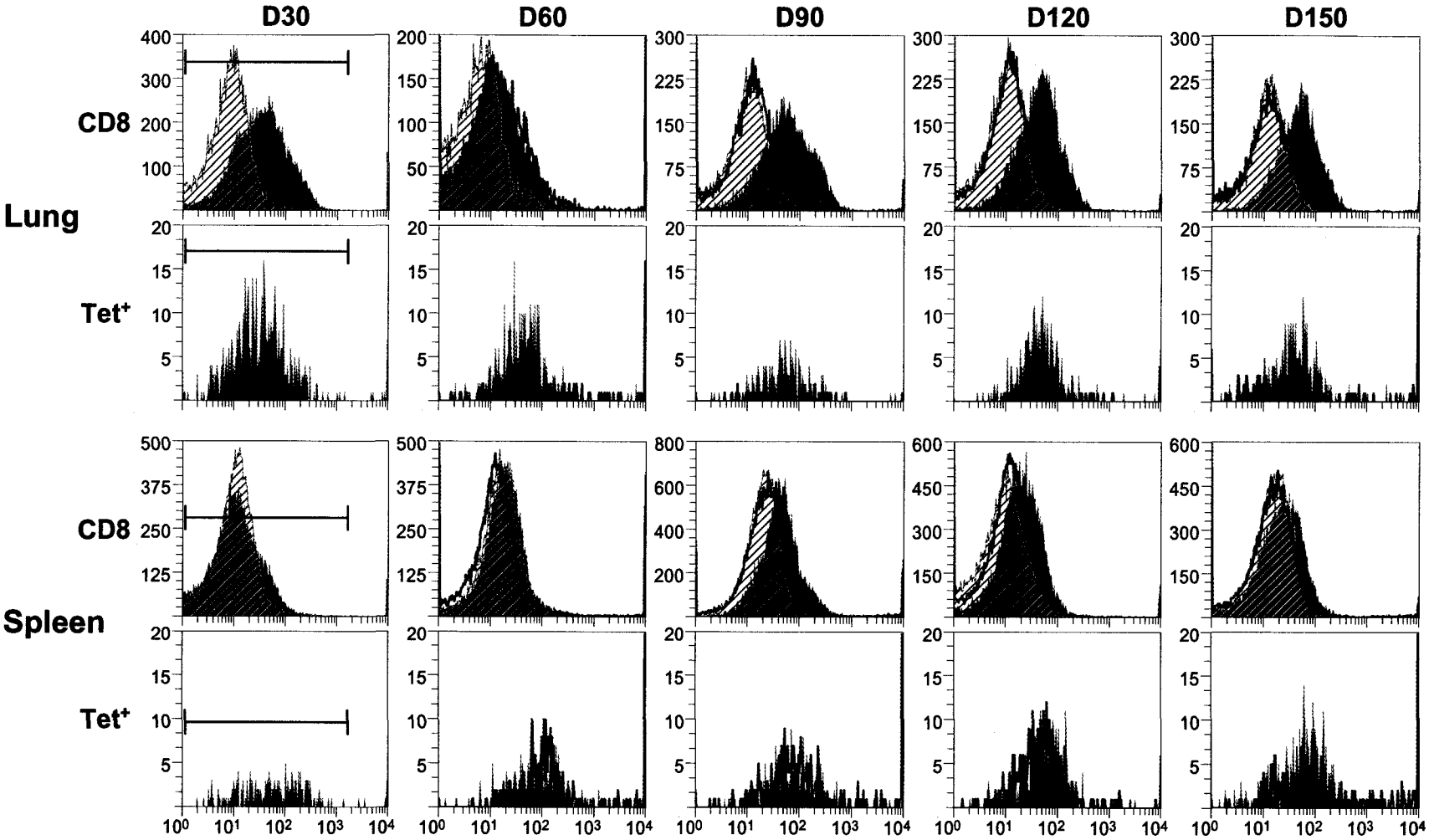

Figure 2.27. PD-1 expression by CD8 T cells and Mtb32 tetramer-positive CD8 T cells. Each histogram represents a single mouse representative of n=4. At each timepoint and within each histogram, all data were normalized to the sample containing the largest number of gated events. The indicated region was used for subsequent analysis. ▨ - Naïve CD8 T cells, ■ - Infected CD8 T cells, □ - Infected/treated CD8 T cells.

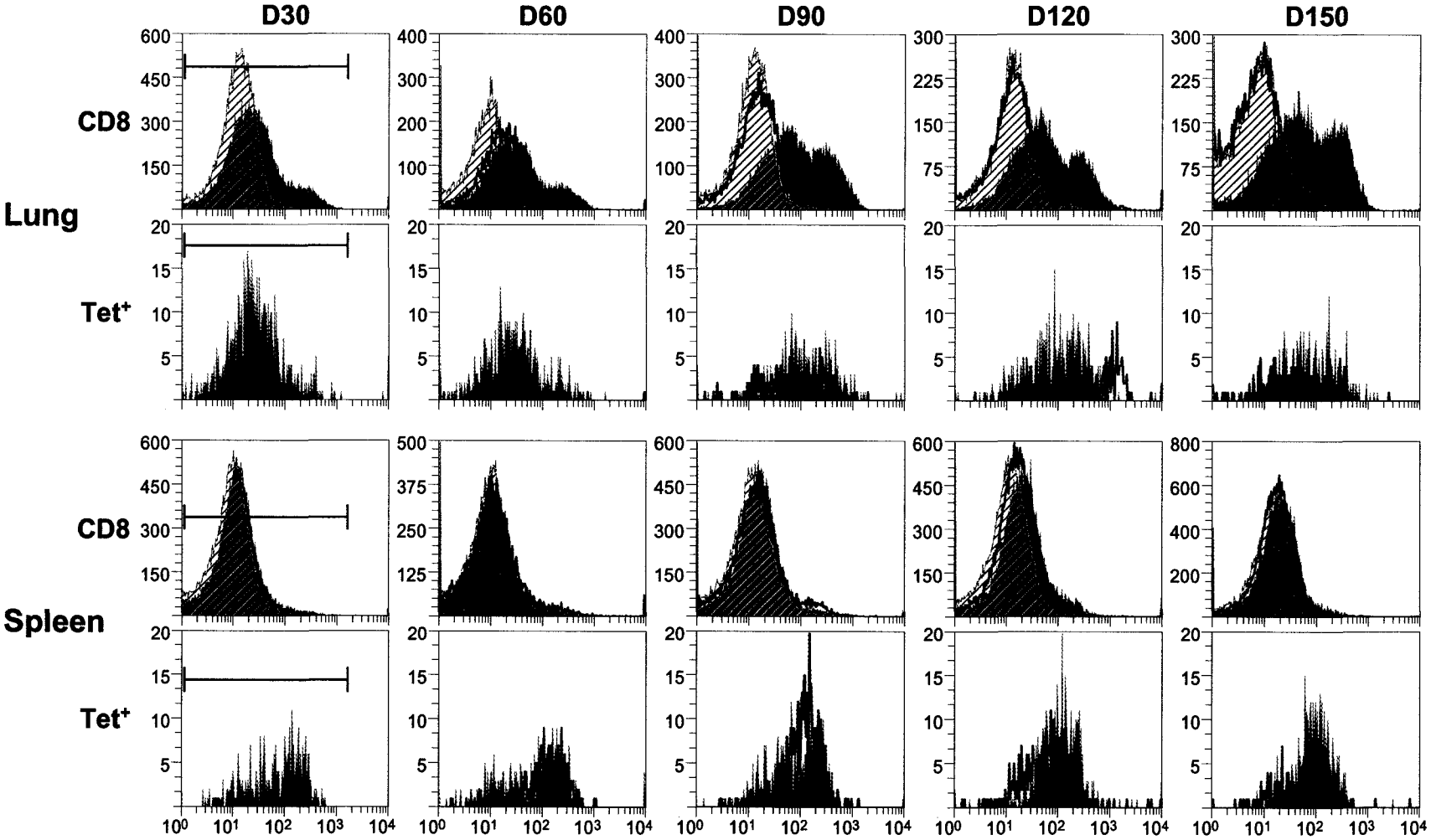

Figure 2.28. Tim-3 expression by CD8 T cells and Mtb32 tetramer-positive CD8 T cells. Each histogram represents a single mouse representative of n=4. At each timepoint and within each histogram, all data were normalized to the sample containing the largest number of gated events. The indicated region was used for subsequent analysis. ▨ - Naïve CD8 T cells, ■ - Infected CD8 T cells, □ - Infected/treated CD8 T cells.

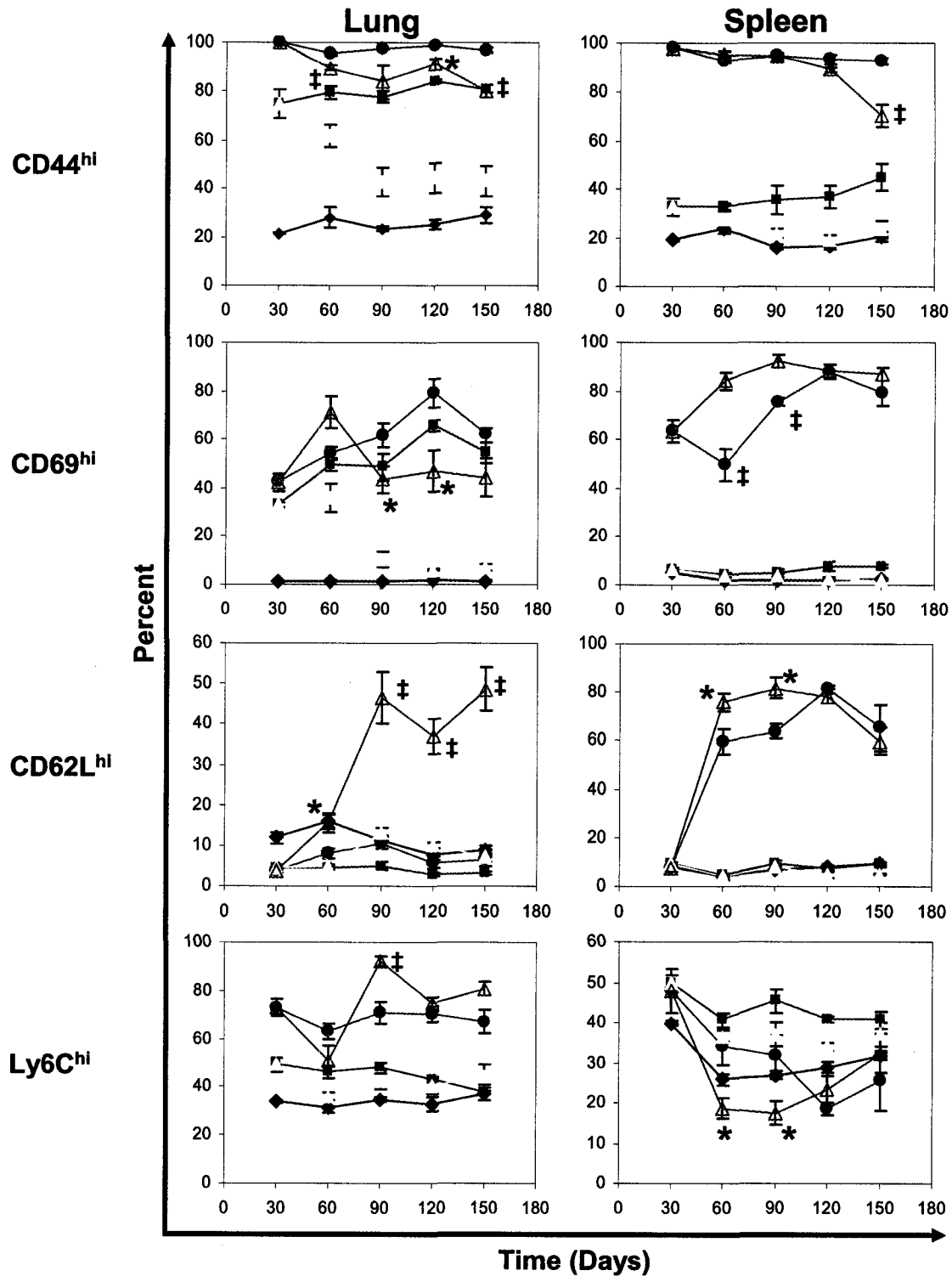

Figure 2.29. Percentage of CD8 T cells expressing phenotypic markers over time. Data represent the means ± the standard errors of the means and are from n=4 mice per timepoint. Statistical significance based upon a comparison of tetramer$^+$ Mtb infected and tetramer$^+$ Mtb infected/drug treated mice was determined using Student's t test (* = $P <$ 0.05, ‡ = $P < 0.01$). ♦ - Naive, ■ - Mtb infected, - Mtb infected/drug treated, ● - Mtb infected, Mtb32 tetramer positive, △ - Mtb infected/drug treated, Mtb32 tetramer positive.

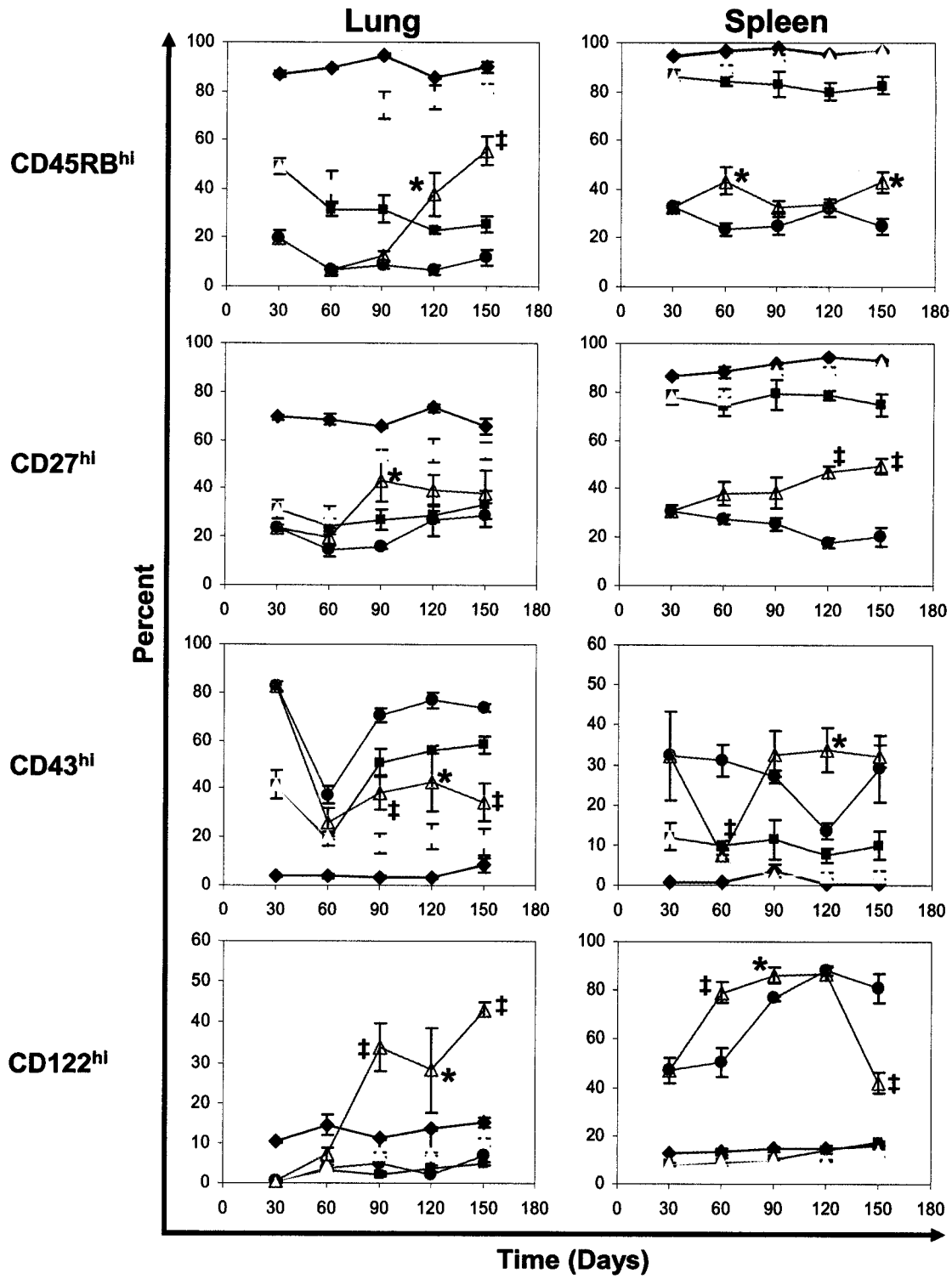

Figure 2.30. Percentage of CD8 T cells expressing phenotypic markers over time. Data represent the means ± the standard errors of the means and are from n=4 mice per timepoint. Statistical significance based upon a comparison of tetramer$^+$ Mtb infected and tetramer$^+$ Mtb infected/drug treated mice was determined using Student's t test (* = $P <$ 0.05, ‡ = $P < 0.01$). ♦ - Naive, ■ - Mtb infected, - Mtb infected/drug treated, ● - Mtb infected, Mtb32 tetramer positive, △ - Mtb infected/drug treated, Mtb32 tetramer positive.

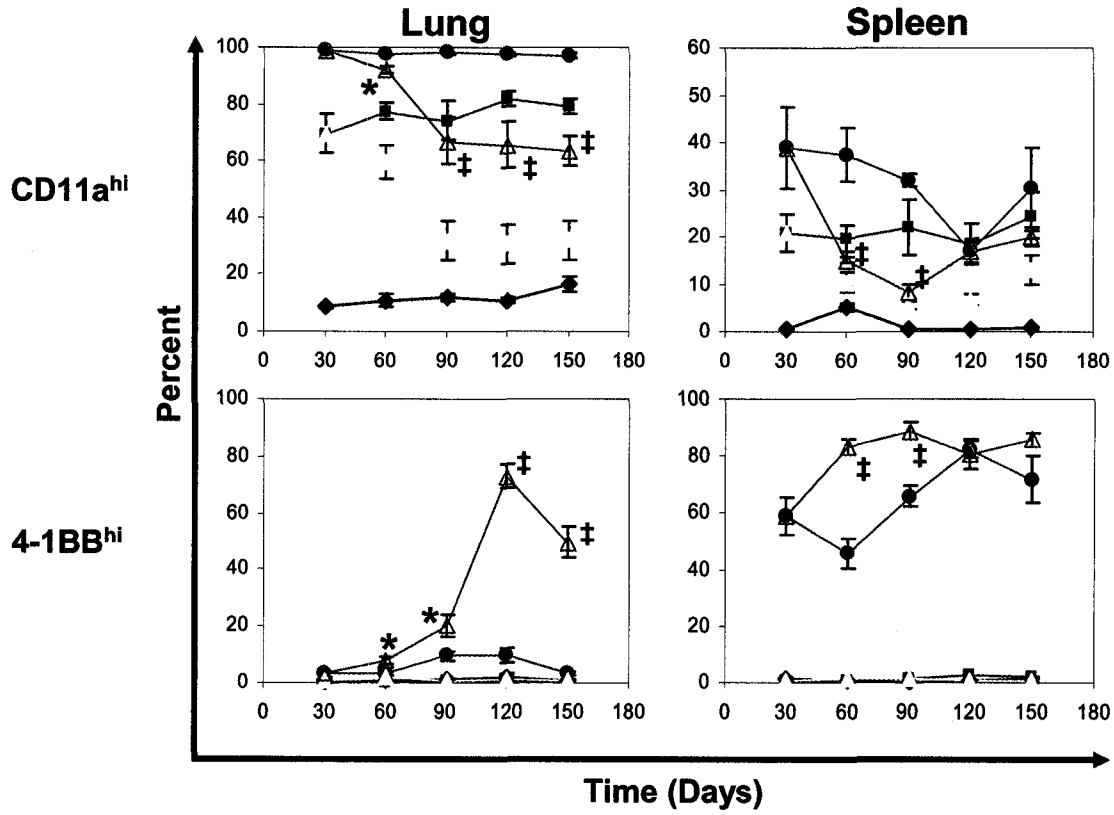

Figure 2.31. Percentage of CD8 T cells expressing phenotypic markers over time. Data represent the means ± the standard errors of the means and are from n=4 mice per timepoint. Statistical significance based upon a comparison of tetramer$^+$ Mtb infected and tetramer$^+$ Mtb infected/drug treated mice was determined using Student's t test (* = $P <$ 0.05, ‡ = $P < 0.01$). ♦ - Naive, ■ - Mtb infected, - Mtb infected/drug treated, ● - Mtb infected, Mtb32 tetramer positive, △ - Mtb infected/drug treated, Mtb32 tetramer positive.

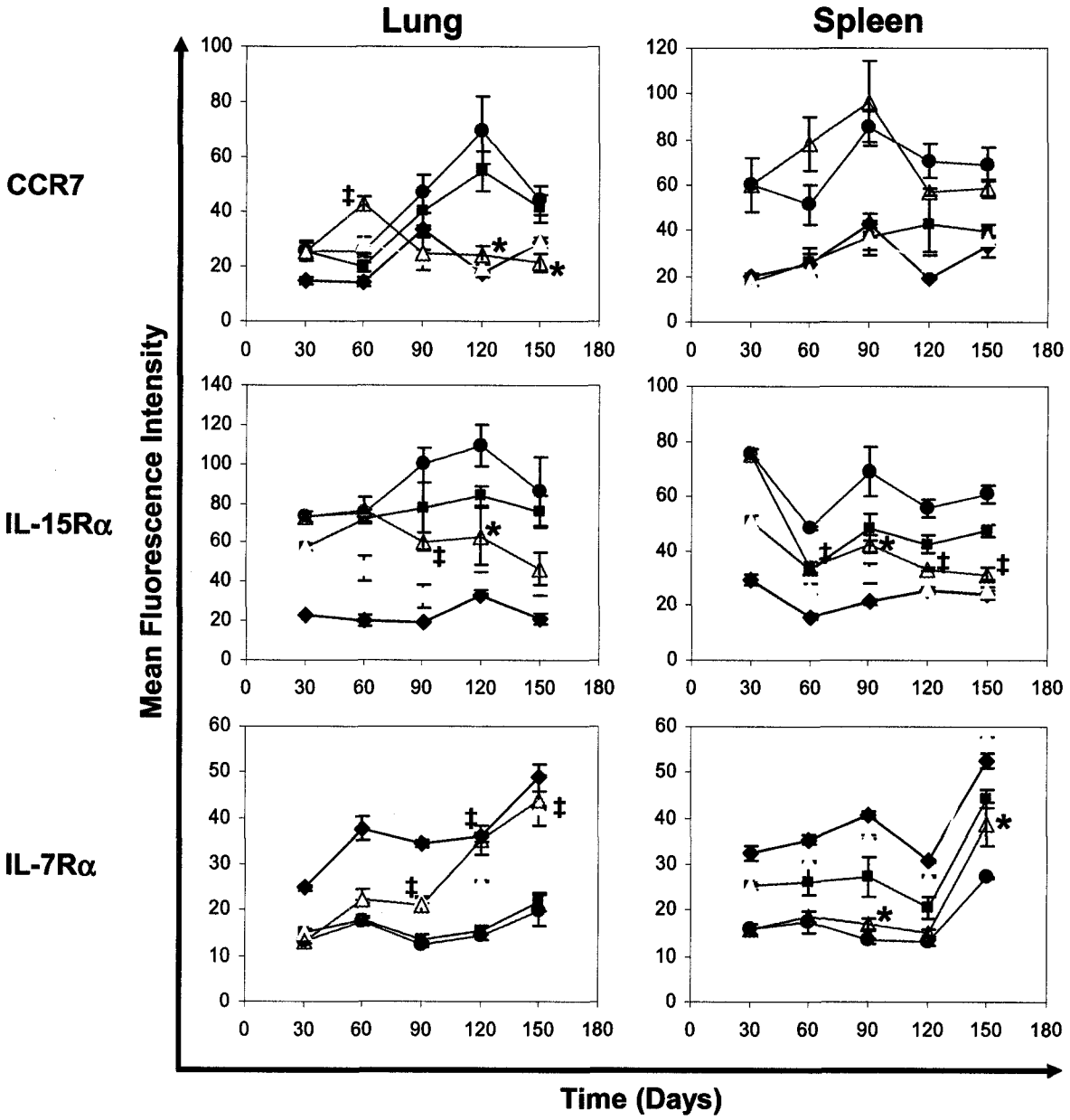

Figure 2.32. The mean fluorescence intensity of phenotypic markers on CD8 T cells over time. Data represent the means ± the standard errors of the means and are from n=4 mice per timepoint. Statistical significance based upon a comparison of tetramer$^+$ Mtb infected and tetramer$^+$ Mtb infected/drug treated mice was determined using Student's t test (* = $P < 0.05$, ‡ = $P < 0.01$). ♦ - Naive, ■ - Mtb infected, - Mtb infected/drug treated, ● - Mtb infected, Mtb32 tetramer positive, △ - Mtb infected/drug treated, Mtb32 tetramer positive.

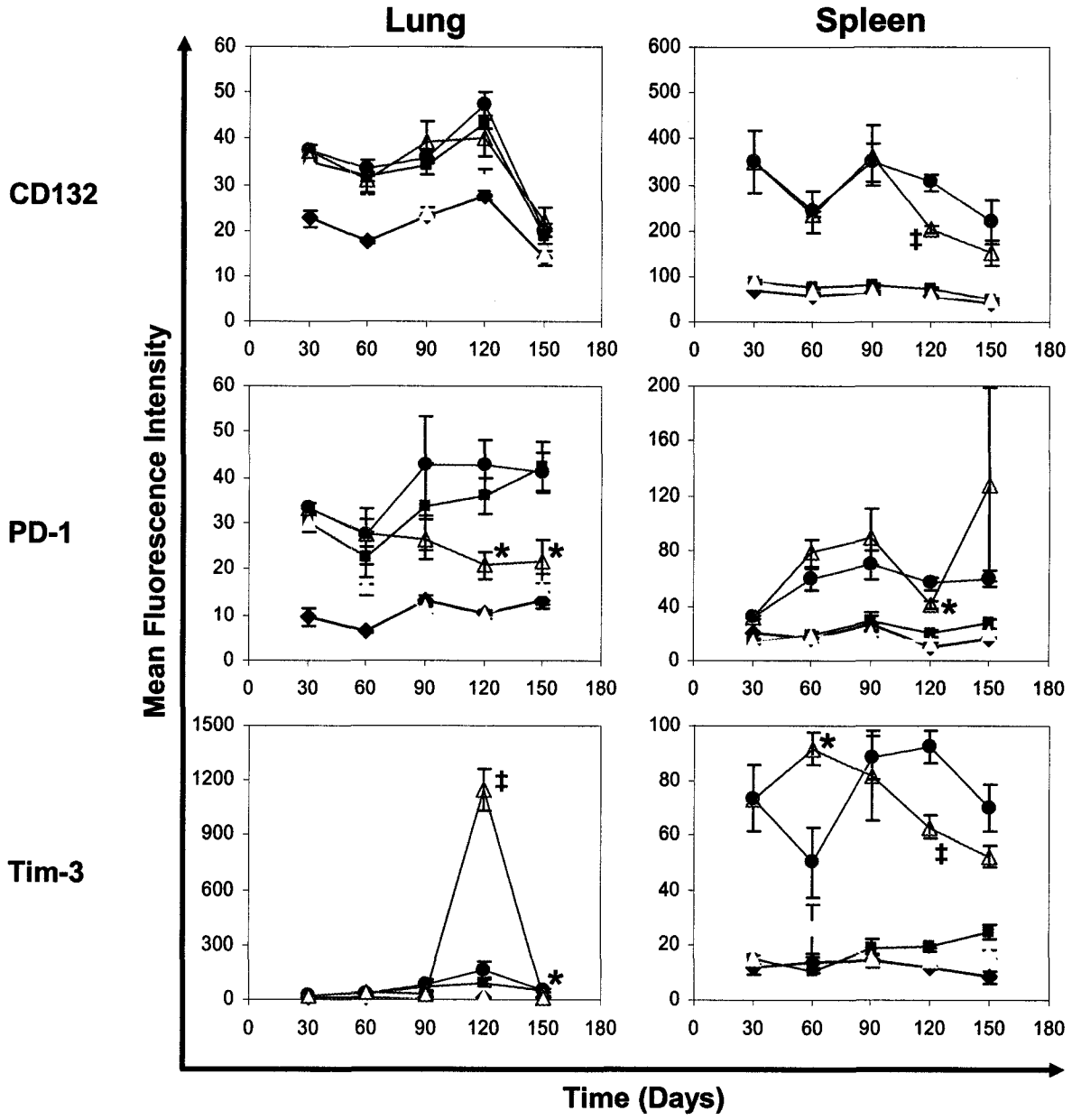

Figure 2.33. The mean fluorescence intensity of phenotypic markers on CD8 T cells over time. Data represent the means ± the standard errors of the means and are from n=4 mice per timepoint. Statistical significance based upon a comparison of tetramer$^+$ Mtb infected and tetramer$^+$ Mtb infected/drug treated mice was determined using Student's t test (* = $P < 0.05$, ‡ = $P < 0.01$). ♦ - Naive, ■ - Mtb infected, - Mtb infected/drug treated, ● - Mtb infected, Mtb32 tetramer positive, △ - Mtb infected/drug treated, Mtb32 tetramer positive.

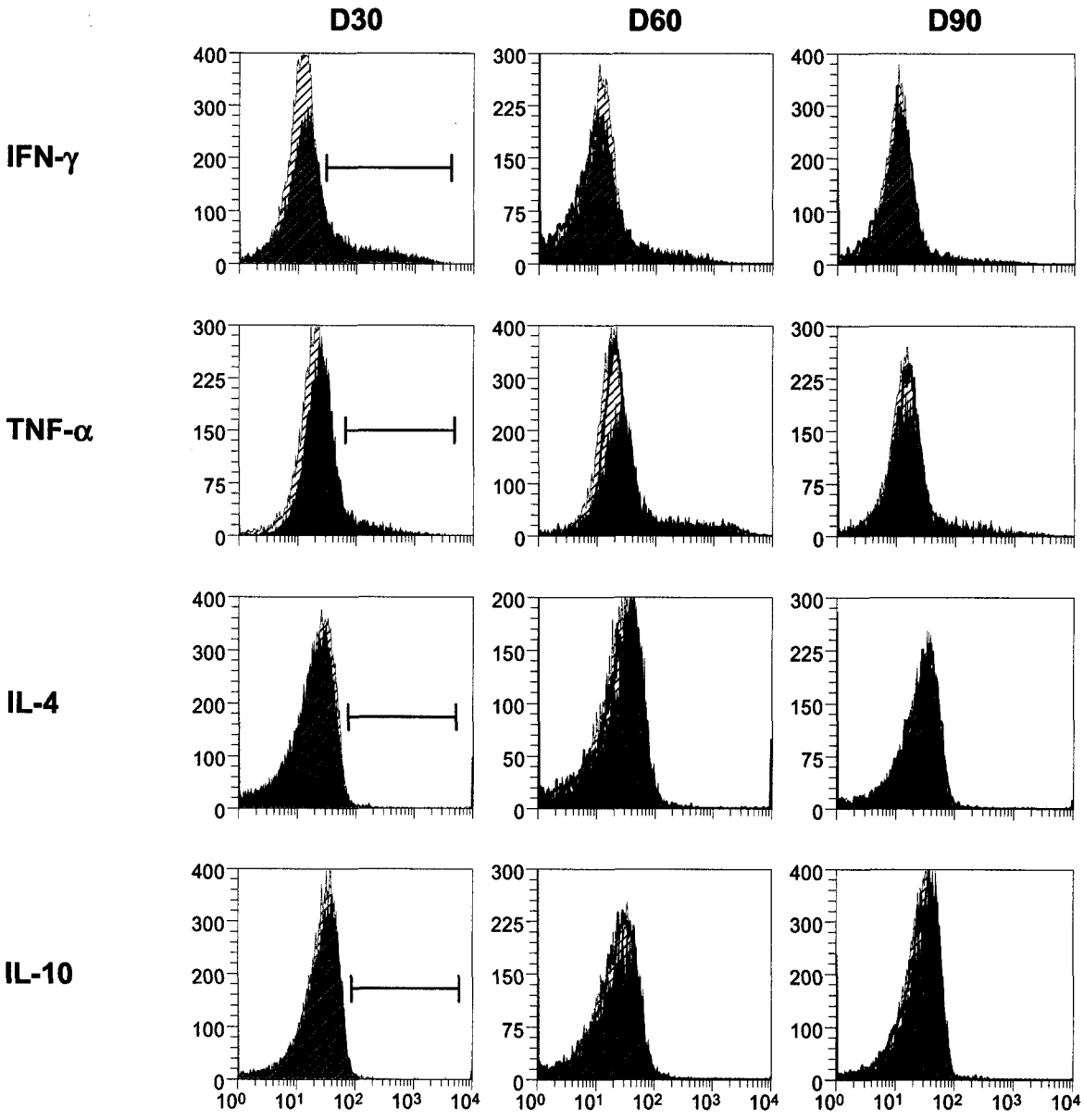

Figure 2.34. Cytokine production by pulmonary-derived CD8 T cells. Each histogram represents a single mouse representative of n=4. At each timepoint and within each histogram, all data were normalized to the sample containing the largest number of gated events. The indicated region was used for subsequent analysis. ▨ - Naïve CD8 T cells, ■ - Infected CD8 T cells, □ - Infected/treated CD8 T cells.

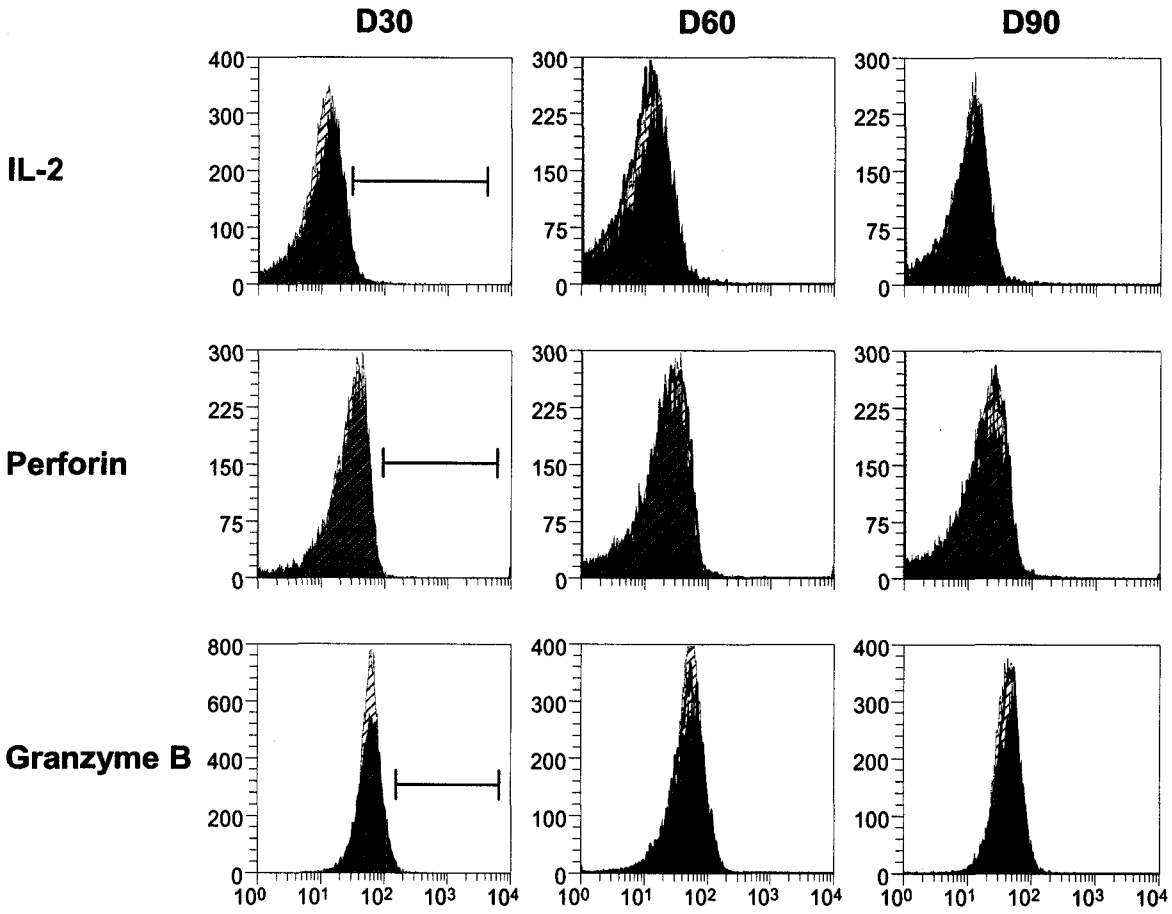

Figure 2.35. Cytokine and cytolytic effector molecule production by pulmonary-derived CD8 T cells. Each histogram represents a single mouse representative of n=4. At each timepoint and within each histogram, all data were normalized to the sample containing the largest number of gated events. The indicated region was used for subsequent analysis. ▨ - Naïve CD8 T cells, ■ - Infected CD8 T cells, □ - Infected/treated CD8 T cells.

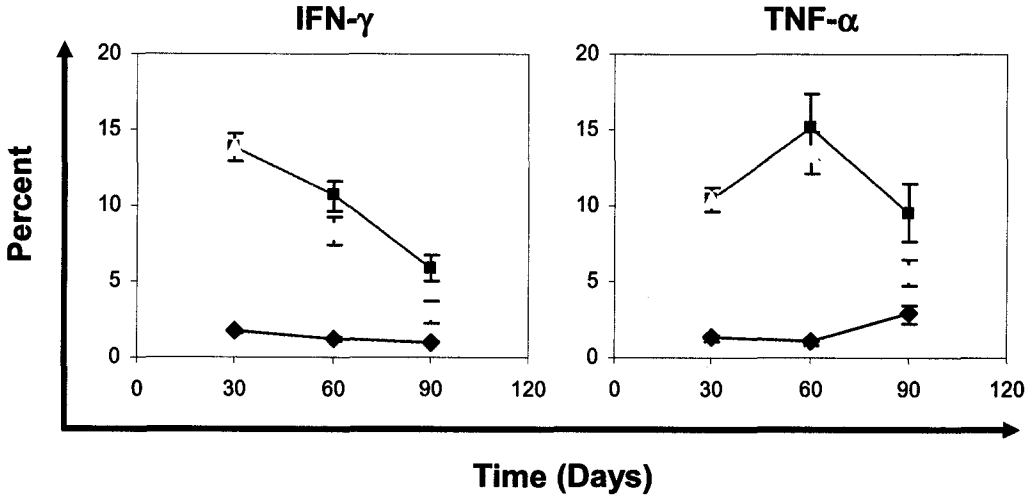

Figure 2.36. Percentage of pulmonary-derived CD8 T cells producing IFN-γ or TNF-α over time. Data represent the means ± the standard errors of the means and are from n=4 mice per timepoint. ♦ - Naive, ■ - Mtb infected, - Mtb infected/drug treated.

Table 2.3. A summary of the relative phenotypic expression patterns on naïve, effector, and memory CD8 T cells in the lungs and spleens of mice. Expression levels are classified as low, intermediate, or high.

Marker	Lung			Spleen		
	Naïve	Effector	Memory	Naïve	Effector	Memory
CD44	lo	hi	hi	lo	hi	hi
CD69	lo	lo/hi	hi	lo	lo/hi	hi
CCR7	lo	hi	lo	lo	hi	hi
CD62L	lo	lo	hi	lo	hi	hi
Ly6C	int/hi	hi	hi	int/hi	int/hi	int
CD45RB	hi	lo/int	hi	hi	int/hi	int/hi
CD27	hi	lo/int	int/hi	hi	int/hi	int/hi
CD43	int	hi	int/hi	int	int	hi
IL-7Rα	hi	lo	hi	hi	lo	hi
IL-15Rα	lo	hi	int	lo	hi	int
CD122	lo	lo	lo	lo	hi	hi
CD132	lo	int	int	int	hi	int/hi
CD11a	int	hi	int/hi	int	int/hi	int
PD-1	lo	hi	lo	lo	hi	int
Tim-3	lo	int/hi	lo	lo	int/hi	int
4-1BB	lo	lo	hi	lo	hi	hi

References

1. **Andersen, P., and B. Smedegaard.** 2000. $CD4^+$ T-cell subsets that mediate immunological memory to *Mycobacterium tuberculosis* infection in mice. Infect Immun **68:**621-9.

2. **Arens, R., K. Schepers, M. A. Nolte, M. F. van Oosterwijk, R. A. van Lier, T. N. Schumacher, and M. H. van Oers.** 2004. Tumor rejection induced by CD70-mediated quantitative and qualitative effects on effector $CD8^+$ T cell formation. J Exp Med **199:**1595-605.

3. **Badovinac, V. P., A. R. Tvinnereim, and J. T. Harty.** 2000. Regulation of antigen-specific $CD8^+$ T cell homeostasis by perforin and interferon-γ. Science **290:**1354-8.

4. **Baily, G. V.** 1980. Tuberculosis prevention trial, Madras. Indian J Med Res **72 Suppl:**1-74.

5. **Barber, D. L., E. J. Wherry, D. Masopust, B. Zhu, J. P. Allison, A. H. Sharpe, G. J. Freeman, and R. Ahmed.** 2006. Restoring function in exhausted CD8 T cells during chronic viral infection. Nature **439:**682-7.

6. **Becker, T. C., E. J. Wherry, D. Boone, K. Murali-Krishna, R. Antia, A. Ma, and R. Ahmed.** 2002. Interleukin 15 is required for proliferative renewal of virus-specific memory CD8 T cells. J Exp Med **195:**1541-8.

7. **Behar, S. M., C. C. Dascher, M. J. Grusby, C. R. Wang, and M. B. Brenner.** 1999. Susceptibility of mice deficient in CD1D or TAP1 to infection with *Mycobacterium tuberculosis*. J Exp Med **189:**1973-80.

8. **Bertram, E. M., P. Lau, and T. H. Watts.** 2002. Temporal segregation of 4-1BB versus CD28-mediated costimulation: 4-1BB ligand influences T cell numbers late in the primary response and regulates the size of the T cell memory response following influenza infection. J Immunol **168:**3777-85.

9. **Burkett, P. R., R. Koka, M. Chien, S. Chai, D. L. Boone, and A. Ma.** 2004. Coordinate expression and trans presentation of interleukin (IL)-15Rα and IL-15 supports natural killer cell and memory $CD8^+$ T cell homeostasis. J Exp Med **200:**825-34.

10. **Burkett, P. R., R. Koka, M. Chien, S. Chai, F. Chan, A. Ma, and D. L. Boone.** 2003. IL-15Rα expression on $CD8^+$ T cells is dispensable for T cell memory. Proc Natl Acad Sci U S A **100:**4724-9.

11. **Chu, N. R., M. A. DeBenedette, B. J. Stiernholm, B. H. Barber, and T. H. Watts.** 1997. Role of IL-12 and 4-1BB ligand in cytokine production by $CD28^+$ and $CD28^-$ T cells. J Immunol **158:**3081-9.

12. **Colditz, G. A., T. F. Brewer, C. S. Berkey, M. E. Wilson, E. Burdick, H. V. Fineberg, and F. Mosteller.** 1994. Efficacy of BCG vaccine in the prevention of tuberculosis. Meta-analysis of the published literature. Jama **271:**698-702.

13. **Dagarag, M., H. Ng, R. Lubong, R. B. Effros, and O. O. Yang.** 2003. Differential impairment of lytic and cytokine functions in senescent human immunodeficiency virus type 1-specific cytotoxic T lymphocytes. J Virol **77:**3077-83.

14. **Dalton, D. K., L. Haynes, C. Q. Chu, S. L. Swain, and S. Wittmer.** 2000. Interferon-γ eliminates responding CD4 T cells during mycobacterial infection by inducing apoptosis of activated CD4 T cells. J Exp Med **192:**117-22.

15. **D'Souza, C. D., A. M. Cooper, A. A. Frank, S. Ehlers, J. Turner, A. Bendelac, and I. M. Orme.** 2000. A novel nonclassic β_2-microglobulin-restricted mechanism influencing early lymphocyte accumulation and subsequent resistance to tuberculosis in the lung. Am J Respir Cell Mol Biol **23:**188-93.

16. **Feng, C. G., A. G. Bean, H. Hooi, H. Briscoe, and W. J. Britton.** 1999. Increase in gamma interferon-secreting $CD8^+$, as well as $CD4^+$, T cells in lungs following aerosol infection with *Mycobacterium tuberculosis*. Infect Immun **67:**3242-7.

17. **Florido, M., J. E. Pearl, A. Solache, M. Borges, L. Haynes, A. M. Cooper, and R. Appelberg.** 2005. Gamma interferon-induced T-cell loss in virulent *Mycobacterium avium* infection. Infect Immun **73:**3577-86.

18. **Flynn, J. L., J. Chan, K. J. Triebold, D. K. Dalton, T. A. Stewart, and B. R. Bloom.** 1993. An essential role for interferon-γ in resistance to *Mycobacterium tuberculosis* infection. J Exp Med **178:**2249-54.

19. **Flynn, J. L., M. M. Goldstein, J. Chan, K. J. Triebold, K. Pfeffer, C. J. Lowenstein, R. Schreiber, T. W. Mak, and B. R. Bloom.** 1995. Tumor necrosis factor-α is required in the protective immune response against *Mycobacterium tuberculosis* in mice. Immunity **2:**561-72.

20. **Flynn, J. L., M. M. Goldstein, K. J. Triebold, B. Koller, and B. R. Bloom.** 1992. Major histocompatibility complex class I-restricted T cells are required for resistance to *Mycobacterium tuberculosis* infection. Proc Natl Acad Sci U S A **89:**12013-7.

21. **Goldrath, A. W., P. V. Sivakumar, M. Glaccum, M. K. Kennedy, M. J. Bevan, C. Benoist, D. Mathis, and E. A. Butz.** 2002. Cytokine requirements for acute and basal homeostatic proliferation of naive and memory $CD8^+$ T cells. J Exp Med **195:**1515-22.

22. **Gonzalez-Juarrero, M., O. C. Turner, J. Turner, P. Marietta, J. V. Brooks, and I. M. Orme.** 2001. Temporal and spatial arrangement of lymphocytes within

lung granulomas induced by aerosol infection with *Mycobacterium tuberculosis*. Infect Immun **69:**1722-8.

23. **Gravestein, L. A., J. D. Nieland, A. M. Kruisbeek, and J. Borst.** 1995. Novel mAbs reveal potent co-stimulatory activity of murine CD27. Int Immunol **7:**551-7.

24. **Halstead, E. S., Y. M. Mueller, J. D. Altman, and P. D. Katsikis.** 2002. *In vivo* stimulation of CD137 broadens primary antiviral $CD8^+$ T cell responses. Nat Immunol **3:**536-41.

25. **Hamann, D., S. Kostense, K. C. Wolthers, S. A. Otto, P. A. Baars, F. Miedema, and R. A. van Lier.** 1999. Evidence that human $CD8^+CD45RA^+CD27^-$ cells are induced by antigen and evolve through extensive rounds of division. Int Immunol **11:**1027-33.

26. **He, Y. W., and M. J. Bevan.** 1999. High level expression of CD43 inhibits T cell receptor/CD3-mediated apoptosis. J Exp Med **190:**1903-8.

27. **Hendriks, J., L. A. Gravestein, K. Tesselaar, R. A. van Lier, T. N. Schumacher, and J. Borst.** 2000. CD27 is required for generation and long-term maintenance of T cell immunity. Nat Immunol **1:**433-40.

28. **Hendriks, J., Y. Xiao, and J. Borst.** 2003. CD27 promotes survival of activated T cells and complements CD28 in generation and establishment of the effector T cell pool. J Exp Med **198:**1369-80.

29. **Hendriks, J., Y. Xiao, J. W. Rossen, K. F. van der Sluijs, K. Sugamura, N. Ishii, and J. Borst.** 2005. During viral infection of the respiratory tract, CD27, 4-1BB, and OX40 collectively determine formation of $CD8^+$ memory T cells and their capacity for secondary expansion. J Immunol **175:**1665-76.

30. **Hintzen, R. Q., S. M. Lens, K. Lammers, H. Kuiper, M. P. Beckmann, and R. A. van Lier.** 1995. Engagement of CD27 with its ligand CD70 provides a second signal for T cell activation. J Immunol **154:**2612-23.

31. **Hubbard, R. D., C. M. Flory, and F. M. Collins.** 1991. Memory T cell-mediated resistance to *Mycobacterium tuberculosis* infection in innately susceptible and resistant mice. Infect Immun **59:**2012-6.

32. **Hurtado, J. C., Y. J. Kim, and B. S. Kwon.** 1997. Signals through 4-1BB are costimulatory to previously activated splenic T cells and inhibit activation-induced cell death. J Immunol **158:**2600-9.

33. **Kaech, S. M., S. Hemby, E. Kersh, and R. Ahmed.** 2002. Molecular and functional profiling of memory CD8 T cell differentiation. Cell **111:**837-51.

34. **Kaech, S. M., J. T. Tan, E. J. Wherry, B. T. Konieczny, C. D. Surh, and R. Ahmed.** 2003. Selective expression of the interleukin 7 receptor identifies effector CD8 T cells that give rise to long-lived memory cells. Nat Immunol **4:**1191-8.

35. **Lee, H. W., S. J. Park, B. K. Choi, H. H. Kim, K. O. Nam, and B. S. Kwon.** 2002. 4-1BB promotes the survival of $CD8^+$ T lymphocytes by increasing expression of Bcl-x_L and Bfl-1. J Immunol **169:**4882-8.

36. **Lyadova, I. V., S. Oberdorf, M. A. Kapina, A. S. Apt, S. L. Swain, and P. C. Sayles.** 2004. CD4 T cells producing IFN-γ in the lungs of mice challenged with mycobacteria express a CD27-negative phenotype. Clin Exp Immunol **138:**21-9.

37. **Mogues, T., M. E. Goodrich, L. Ryan, R. LaCourse, and R. J. North.** 2001. The relative importance of T cell subsets in immunity and immunopathology of airborne *Mycobacterium tuberculosis* infection in mice. J Exp Med **193:**271-80.

38. **Monney, L., C. A. Sabatos, J. L. Gaglia, A. Ryu, H. Waldner, T. Chernova, S. Manning, E. A. Greenfield, A. J. Coyle, R. A. Sobel, G. J. Freeman, and V. K. Kuchroo.** 2002. Th1-specific cell surface protein Tim-3 regulates macrophage activation and severity of an autoimmune disease. Nature **415:**536-41.

39. **Muller, I., S. P. Cobbold, H. Waldmann, and S. H. Kaufmann.** 1987. Impaired resistance to *Mycobacterium tuberculosis* infection after selective *in vivo* depletion of $L3T4^+$ and $Lyt\text{-}2^+$ T cells. Infect Immun **55:**2037-41.

40. **Olsen, A. W., L. Brandt, E. M. Agger, L. A. van Pinxteren, and P. Andersen.** 2004. The influence of remaining live BCG organisms in vaccinated mice on the maintenance of immunity to tuberculosis. Scand J Immunol **60:**273-7.

41. **Onami, T. M., L. E. Harrington, M. A. Williams, M. Galvan, C. P. Larsen, T. C. Pearson, N. Manjunath, L. G. Baum, B. D. Pearce, and R. Ahmed.** 2002. Dynamic regulation of T cell immunity by CD43. J Immunol **168:**6022-31.

42. **Orme, I. M.** 1987. The kinetics of emergence and loss of mediator T lymphocytes acquired in response to infection with *Mycobacterium tuberculosis*. J Immunol **138:**293-8.

43. **Orme, I. M., E. S. Miller, A. D. Roberts, S. K. Furney, J. P. Griffin, K. M. Dobos, D. Chi, B. Rivoire, and P. J. Brennan.** 1992. T lymphocytes mediating protection and cellular cytolysis during the course of *Mycobacterium tuberculosis* infection. Evidence for different kinetics and recognition of a wide spectrum of protein antigens. J Immunol **148:**189-96.

44. **Pulle, G., M. Vidric, and T. H. Watts.** 2006. IL-15-dependent induction of 4-1BB promotes antigen-independent CD8 memory T cell survival. J Immunol **176:**2739-48.

45. **Reignat, S., G. J. Webster, D. Brown, G. S. Ogg, A. King, S. L. Seneviratne, G. Dusheiko, R. Williams, M. K. Maini, and A. Bertoletti.** 2002. Escaping high viral load exhaustion: CD8 cells with altered tetramer binding in chronic hepatitis B virus infection. J Exp Med **195:**1089-101.

46. **Rolph, M. S., B. Raupach, H. H. Kobernick, H. L. Collins, B. Perarnau, F. A. Lemonnier, and S. H. Kaufmann.** 2001. MHC class Ia-restricted T cells partially account for β_2-microglobulin-dependent resistance to *Mycobacterium tuberculosis*. Eur J Immunol **31:**1944-9.

47. **Rook, G. A., R. Hernandez-Pando, K. Dheda, and G. Teng Seah.** 2004. IL-4 in tuberculosis: implications for vaccine design. Trends Immunol **25:**483-8.

48. **Rowley, T. F., and A. Al-Shamkhani.** 2004. Stimulation by soluble CD70 promotes strong primary and secondary $CD8^+$ cytotoxic T cell responses *in vivo*. J Immunol **172:**6039-46.

49. **Sabatos, C. A., S. Chakravarti, E. Cha, A. Schubart, A. Sanchez-Fueyo, X. X. Zheng, A. J. Coyle, T. B. Strom, G. J. Freeman, and V. K. Kuchroo.** 2003. Interaction of Tim-3 and Tim-3 ligand regulates T helper type 1 responses and induction of peripheral tolerance. Nat Immunol **4:**1102-10.

50. **Sallusto, F., D. Lenig, R. Forster, M. Lipp, and A. Lanzavecchia.** 1999. Two subsets of memory T lymphocytes with distinct homing potentials and effector functions. Nature **401:**708-12.

51. **Sanchez-Fueyo, A., J. Tian, D. Picarella, C. Domenig, X. X. Zheng, C. A. Sabatos, N. Manlongat, O. Bender, T. Kamradt, V. K. Kuchroo, J. C. Gutierrez-Ramos, A. J. Coyle, and T. B. Strom.** 2003. Tim-3 inhibits T helper type 1-mediated auto- and alloimmune responses and promotes immunological tolerance. Nat Immunol **4:**1093-101.

52. **Sandau, M. M., K. S. Schluns, L. Lefrancois, and S. C. Jameson.** 2004. Cutting edge: transpresentation of IL-15 by bone marrow-derived cells necessitates expression of IL-15 and IL-15Rα by the same cells. J Immunol **173:**6537-41.

53. **Saoulli, K., S. Y. Lee, J. L. Cannons, W. C. Yeh, A. Santana, M. D. Goldstein, N. Bangia, M. A. DeBenedette, T. W. Mak, Y. Choi, and T. H. Watts.** 1998. CD28-independent, TRAF2-dependent costimulation of resting T cells by 4-1BB ligand. J Exp Med **187:**1849-62.

54. **Serbina, N. V., and J. L. Flynn.** 1999. Early emergence of $CD8^+$ T cells primed for production of type 1 cytokines in the lungs of *Mycobacterium tuberculosis*-infected mice. Infect Immun **67:**3980-8.

55. **Skeiky, Y. A., M. R. Alderson, P. J. Ovendale, J. A. Guderian, L. Brandt, D. C. Dillon, A. Campos-Neto, Y. Lobet, W. Dalemans, I. M. Orme, and S. G.**

Reed. 2004. Differential immune responses and protective efficacy induced by components of a tuberculosis polyprotein vaccine, Mtb72F, delivered as naked DNA or recombinant protein. J Immunol **172:**7618-28.

56. **Sousa, A. O., R. J. Mazzaccaro, R. G. Russell, F. K. Lee, O. C. Turner, S. Hong, L. Van Kaer, and B. R. Bloom.** 2000. Relative contributions of distinct MHC class I-dependent cell populations in protection to tuberculosis infection in mice. Proc Natl Acad Sci U S A **97:**4204-8.

57. **Tan, J. T., B. Ernst, W. C. Kieper, E. LeRoy, J. Sprent, and C. D. Surh.** 2002. Interleukin (IL)-15 and IL-7 jointly regulate homeostatic proliferation of memory phenotype $CD8^+$ cells but are not required for memory phenotype $CD4^+$ cells. J Exp Med **195:**1523-32.

58. **Tan, J. T., J. K. Whitmire, K. Murali-Krishna, R. Ahmed, J. D. Altman, R. S. Mittler, A. Sette, T. C. Pearson, and C. P. Larsen.** 2000. 4-1BB costimulation is required for protective anti-viral immunity after peptide vaccination. J Immunol **164:**2320-5.

59. **Tascon, R. E., E. Stavropoulos, K. V. Lukacs, and M. J. Colston.** 1998. Protection against *Mycobacterium tuberculosis* infection by $CD8^+$ T cells requires the production of gamma interferon. Infect Immun **66:**830-4.

60. **Tuberculosis Research Centre (ICMR) Chennai.** 1999. Fifteen year follow up of trial of BCG vaccines in south India for tuberculosis prevention. Indian J Med Res **110:**56-69.

61. **Urdahl, K. B., D. Liggitt, and M. J. Bevan.** 2003. $CD8^+$ T cells accumulate in the lungs of *Mycobacterium tuberculosis*-infected $K^{b-/-}D^{b-/-}$ mice, but provide minimal protection. J Immunol **170:**1987-94.

62. **Wherry, E. J., D. L. Barber, S. M. Kaech, J. N. Blattman, and R. Ahmed.** 2004. Antigen-independent memory CD8 T cells do not develop during chronic viral infection. Proc Natl Acad Sci U S A **101:**16004-9.

63. **Wherry, E. J., J. N. Blattman, K. Murali-Krishna, R. van der Most, and R. Ahmed.** 2003. Viral persistence alters CD8 T-cell immunodominance and tissue distribution and results in distinct stages of functional impairment. J Virol **77:**4911-27.

64. **Wherry, E. J., V. Teichgraber, T. C. Becker, D. Masopust, S. M. Kaech, R. Antia, U. H. von Andrian, and R. Ahmed.** 2003. Lineage relationship and protective immunity of memory CD8 T cell subsets. Nat Immunol **4:**225-34.

65. **Yajima, T., K. Yoshihara, K. Nakazato, S. Kumabe, S. Koyasu, S. Sad, H. Shen, H. Kuwano, and Y. Yoshikai.** 2006. IL-15 regulates $CD8^+$ T cell contraction during primary infection. J Immunol **176:**507-15.

66. **Zhu, C., A. C. Anderson, A. Schubart, H. Xiong, J. Imitola, S. J. Khoury, X. X. Zheng, T. B. Strom, and V. K. Kuchroo.** 2005. The Tim-3 ligand galectin-9 negatively regulates T helper type 1 immunity. Nat Immunol **6:**1245-52.

Chapter 3

Tracking Antigen-Specific CD8 T Lymphocytes in the Lungs of Mice Vaccinated with the Mtb72F Polyprotein

Introduction

The facultative intracellular pathogen *Mycobacterium tuberculosis* currently infects one-third of the world's population, and the 2-3 million deaths per year make it the leading cause of death by a single bacterial agent [13, 50]. Bacille Calmette-Guérin (BCG), an attenuated strain of *Mycobacterium bovis*, is currently the only available prophylactic vaccine [7, 9]. Although vaccination with BCG is widespread throughout the world, it has been shown in clinical studies to possess variable protective efficacy that can also decline with age [9, 15, 16, 19]. While BCG has been shown to protect children from disseminated tuberculosis (TB), it often fails to prevent adult pulmonary TB [4, 46]. Due to the global prevalence of tuberculosis and the limitations of the current vaccine, a major research effort is currently underway to identify new vaccine candidates [2, 33, 36, 37].

Although the nature of protective immunity to TB is not completely understood [5, 30, 35], CD4 T cells have been shown to be essential mediators of protection [8, 38, 40]. Production of gamma interferon (IFN-γ) is essential as shown by increased susceptibility in IFN-γ or IFN-γ receptor gene disrupted animal models, as well as in humans possessing a rare mutation in the IFN-γ receptor [10, 17, 25]. In addition to this, however, there has been a growing realization over the past decade or more that CD8 T cells also contribute significantly to protective immunity. Adoptive transfer of immune CD8 T cells can confer protection in mice [32, 34], and such cells accumulate in the lungs of aerosol infected mice, where they secrete IFN-γ [14, 41]. Antibody depletion of CD8 T cells during infection, as well as the use of mouse models possessing gene

disruptions that result in significantly reduced numbers of CD8 T cells also support a role for CD8 T cells in protective immunity [3, 18, 22, 31, 45, 48].

Culture filtrate proteins (CFP) from *M. tuberculosis* have been previously identified as a rich source of immunogenic antigens, some of which can confer protection in animal models of tuberculosis [1, 23, 24]. In order to screen the large number of protein components of CFP for potential subunit vaccine candidates, the Corixa Corporation created a genomic expression library of *M. tuberculosis* H37Ra [44]. Rabbit antiserum generated by immunization with CFP was used to screen the expression library to identify potential antigenic vaccine candidates. Further screening of selected antigenic targets against peripheral blood monocytes from healthy PPD^+ individuals identified Mtb32 and Mtb39 as two lead candidate antigens that stimulated strong T cell proliferative responses and IFN-γ production. Following *in silico* analysis, the Mtb32 protein was identified as a trypsin-like serine protease that was found to possess autocatalytic activity and significant toxicity upon expression in *E. coli*. To facilitate high-level recombinant expression, Mtb32 was expressed as a 20 kDa N-terminal fragment and an overlapping 14 kDa C-terminal fragment [44]. It was later discovered that the 14 kDa C-terminal portion of the Mtb32 protein was able to efficiently drive high-level expression of heterologous proteins in *E. coli* when linked to their N-terminus [49].

The other primary lead candidate that was discovered through serological expression cloning was the Mtb39 protein [12]. Mtb39 is a 39 kDa putative cell wall spanning protein of unknown function that belongs to the PPE family of mycobacterial proteins. This protein was also shown to elicit significant T cell reactivity from PPD^+

individuals. Based upon the premise that a successful tuberculosis vaccine should include multiple T cell epitopes, a fusion protein construct was generated by combining the 132 amino acid Mtb32 C-terminal fragment followed by the full-length Mtb39 protein linked to the 195 amino acid Mtb32 N-terminal fragment [43]. When expressed in *E. coli*, this novel fusion protein has a molecular weight of 72 kDa.

Previous studies have shown that mice immunized with Mtb72F, either as a protein and adjuvant formulation or in the form of a DNA vaccine, were protected against aerosol challenge with *M. tuberculosis* H37Rv at a level comparable to that of BCG [43]. Furthermore, when used as a boost in guinea pigs primed with BCG, survival of these animals to aerosol challenge was doubled from one to two years compared to animals given BCG only [6]. These animals had substantial evidence of lesion resolution and very low bacterial numbers in the lungs.

Further experiments by the Corixa Corporation using IFN-γ ELISPOT assays revealed that the C-terminal fragment of the Mtb32 protein possessed significant CD8 T cell reactivity in C57BL/6 mice [43]. Utilizing overlapping 15-mer peptide fragments, the immunodominant CD8 T cell epitope; GAPINSATAM, was identified. This Mtb32-derived CD8 T cell epitope was previously shown to be strongly recognized by cytolytic and IFN-γ secreting CD8 T cells [43]. Since the precise role that CD8 T cells play during infection with *M. tuberculosis* has not been completely defined, we decided to examine the Mtb32 antigen-specific CD8 T cell response to this peptide epitope in the lungs of mice. Using a MHC class I H-2D^{b} tetramer reagent containing the GAPINSATAM peptide, we were able to track CD8 T cells recognizing this epitope in the lungs of mice vaccinated with a DNA vaccine encoding Mtb72F and/or challenged by aerosol exposure

to *M. tuberculosis*. The results of this study show that significant numbers of tetramer-positive CD8 T cells accumulate in the lungs of vaccinated mice, and expand further in response to challenge infection. These cells expressed markers of cellular activation, and a subpopulation up-regulated expression of a recently identified early memory cell marker [27], the interleukin 7 receptor alpha chain (IL-7Rα). Approximately one-third of the CD8 T cells in the lungs expressed IL-7Rα when Mtb72F protein was delivered in a novel liposomal formulation aimed at inducing CD8 T cell responses. These data show that antigen-specific CD8 T cells traffic to the lungs after vaccination and respond to subsequent infection with *M. tuberculosis*.

While CD4 T cells are known to be essential for protective immunity to *M. tuberculosis* infection, the exact role that these cells play in initiating and/or sustaining the CD8 T cell response during pulmonary tuberculosis is unclear. Utilizing the Mtb32 MHC class I tetramer reagent, we were able to examine the CD8 T cell response in mice lacking CD4 T cells (CD4KO). In addition, immunization of CD4KO mice allowed us to examine the impact of CD4 T cells upon the CD8 memory recall response. These results demonstrated that CD4 T cells play a significant role in the generation of primary CD8 T cell immunity and in the effectiveness of the CD8 T cell memory response following immunization and secondary challenge with *M. tuberculosis*.

Materials and Methods

Mice. Studies were performed using 8-10 week old specific pathogen-free female C56BL/6 mice purchased from Charles River Laboratories (Wilmington, MA). For the CD4KO experiments, 8-10 week old B6.129S2-Cd4^{tm1Mak} mice and age matched controls were purchased from The Jackson Laboratory (Bar Harbor, ME). All mice were maintained within a biosafety level III facility at Colorado State University for the duration of the experiments, and had free access to sterile water and standard mouse chow. The specific pathogen-free nature of the mouse colonies was demonstrated by testing sentinel animals, which were shown to be negative for 13 known mouse pathogens. All experimental procedures were approved by the Colorado State University Animal Care and Use Committee.

Bacterial Strains. *M. tuberculosis* strain H37Rv, originally obtained from the Trudeau Mycobacteria Collection (TMCC #102), and *M. bovis* BCG Pasteur were grown from low passage seed lots in Proskauer-Beck liquid media containing 0.05% Tween 80 to mid-log phase, and 1.5 ml aliquots were frozen at -70°C until use.

Amplification of Mtb72F Plasmid DNA. The original Mtb72F plasmid DNA (pDNA) construct (kindly supplied by the Corixa Corporation) was electroporated into *E. coli* DH5α and incubated at 37°C overnight in 5 ml of Luria-Bertani (LB) broth (Becton, Dickinson and Company, Sparks, CA) containing 100 μg/ml ampicillin (Sigma-Aldrich, St. Louis, MO). Single colonies were isolated on LB agar plates containing 100 μg/ml

ampicillin and pDNA was purified using a Plasmid Mini Prep kit (Qiagen, Valencia, CA) per the manufacturer's instructions. Presence of the pDNA construct was verified by restriction digest. Single colonies were used to inoculate 5 L of LB broth containing 100 μg/ml ampicillin. After overnight incubation at 37°C, the amplified pDNA was purified using an EndoFree Plasmid Giga kit (Qiagen) per the manufacturer's instructions. Following isopropanol precipitation and ethanol washing, purified pDNA was resuspended in PBS and the pDNA concentration was determined by spectrophotometric analysis. Sequence verification (Macromolecular Resources, Colorado State University, CO) was performed on the Mtb72F fusion protein sequence and found to be identical to the supplied construct. Aliquots of pDNA at 1 mg/ml were frozen at -70°C until use.

Immunizations and Aerosol Infection. Mice were immunized 3 times at 3 week intervals with either 100 μg of Mtb72F DNA or phosphate buffered saline (PBS) via the intramuscular (tibialis) route. For each immunization, mice were injected with a total volume of 100 μl/mouse using 50 μl/leg. For BCG immunizations, mice were immunized with 10^6 CFU of *M. bovis* BCG Pasteur in 100 μl of PBS via the subcutaneous (s.c.) route. Three weeks following the last immunization, mice were infected via the aerosol route using a Glas-Col aerosol generator (Glas-Col, Terre Haute, IN), such that ~100 viable bacteria were deposited in the lungs of each animal. The number of viable bacteria in the lungs was determined at specific timepoints by plating 10-fold serial dilutions of individual partial organ homogenates on nutrient Middlebrook 7H11 agar, and counting bacterial colonies after 21 days of incubation at 37°C.

Preparation of Cationic Liposome-DNA Complexes. Liposomes were prepared by dissolving the cationic lipid DOTIM (octadecenolyoxy{ethyl-2-heptadecenyl-3 hydroxyethyl} imidazolinium chloride; Sigma-Aldrich) and cholesterol (Avanti Polar Lipids, Alabaster, AL) in chloroform and adding equimolar concentrations to round bottom 15 ml glass tubes. The solution was then dried overnight in a vacuum desiccator to a thin film. The lipids were rehydrated in 5% dextrose in water to form liposomes at a final concentration of 20 mM. Liposomes were incubated at 50°C for 50 minutes, followed by incubation for 2 hours at room temperature. The liposomes were then extruded through a series of 1 μm, 0.45 μm and 0.20 μm filters to form the final liposomes, as described previously [47]. Non-coding plasmid DNA was prepared under very low endotoxin conditions (< 0.25 EU/mg; Althea Technologies). Complexes of liposomes and non-coding plasmid DNA were prepared by first dissolving liposomes in 5% dextrose in water at a concentration of 100 μl liposomes per 1 ml dextrose solution. Next, plasmid DNA was added to the liposome solution at a final concentration of 100 μg DNA per ml of liposome solution and complexes were formed spontaneously by gentle pipetting. To prepare vaccines, recombinant Mtb72F protein (kindly provided by the Corixa Corporation and GlaxoSmithKline) was added to pre-formed liposome-DNA complexes and mixed by gentle pipetting. After preparation, vaccines were kept at room temperature and administered within 30 minutes. For immunizations using cationic liposome-DNA complexes, mice were immunized two times, 14 days apart via the intraperitoneal route using 10 μg/mouse of either Mtb72F protein or ova albumin (Sigma-Aldrich) in a total volume of 200 μl of liposome formulation.

Single-Cell Suspension Preparation. Animals were sacrificed by carbon dioxide asphyxiation and were perfused through the heart with 10 ml cold PBS containing 3 U/ml heparin (Sigma-Aldrich). The lungs were removed from the pulmonary cavity and placed in cold Dulbecco's minimal essential medium (DMEM; Cellgro, Herndon, VA). The lung tissue was disrupted using sterile razor blades and incubated for 30 minutes at 37°C in a final volume of 2 ml DMEM containing 0.7 mg/ml collagenase D (Roche Applied Science, Indianapolis, IN) and 30 μg/ml deoxyribonuclease (Sigma-Aldrich). Following incubation, the digested lung tissue was gently passed through a sterile 70 μm nylon screen, rinsed using 8 ml cold DMEM supplemented with 10% heat-inactivated endotoxin low fetal bovine serum (Atlas Biologicals, Fort Collins, CO), 10 mM HEPES buffer (Sigma-Aldrich), 2 mM L-glutamine (Sigma-Aldrich), 2% MEM-nonessential amino acids (100x; Sigma-Aldrich), 50 μM 2-mercaptoethanol (Sigma-Aldrich) and centrifuged at 200 × *g*. Red blood cells were lysed using Gey's solution (0.15 M NH_4Cl, 10 mM $KHCO_3$) and the samples were centrifuged and resuspended in DMEM plus supplements. Cells were counted using a hemacytometer and aliquots were taken for flow cytometric analysis.

Flow Cytometry. Single-cell suspensions from individual mice were resuspended in PBS containing 0.1% sodium azide (Fisher Chemicals, Fairlawn, NJ). Cells were incubated in the dark for 20 minutes at 4°C with specific antibody (directly conjugated to fluorescein isothiocyanate [FITC], phycoerythrin [PE], peridinin chlorophyll *a* protein [PerCP], or allophycocyanin [APC] at 3 μg/ml), followed by 2 washes using PBS with sodium azide. Cells were analyzed immediately using a FACSCalibur dual laser flow cytometer (BD

Biosciences, Mountain View, CA) and the data were analyzed using CellQwest software (BD Biosciences, San Jose, CA) and Summit software (DakoCytomation, Fort Collins, CO). Viable lymphocytes were gated based upon their forward- and side-scatter characteristics and cell populations were analyzed by expression of fluorochrome-labeled markers. All analyses were performed with a minimum acquisition of 200,000 events.

Cell surface markers were analyzed with the following specific antibodies: FITC anti-CD44 (clone IM7), anti-CD3ε (clone 145-2C11), anti-CD62L (clone MEL-14), anti-CD45RB (clone 16A), anti-γδ TCR (clone GL3); PerCP anti-CD8α (clone 53-6.7); APC anti-CD3ε (clone 145-2C11), anti-NK1.1 (clone PK136), and anti-CD127 (clone A7R34; eBioscience, San Diego, CA). Cell suspensions were also stained with a PE-Mtb32 H-$2D^b$ MHC class I tetramer (Beckman Coulter Immunomics, San Diego, CA) containing the peptide GAPINSATAM. Background staining with this tetramer reagent was less than 0.15% when staining cells from naïve mice or from MHC mismatched (Balb/c, H-2^d) mice.

For intracellular antibody staining, single-cell suspensions were resuspended in DMEM with supplements and stimulated with 0.1 μg/ml anti-CD3ε (clone 145-2C11) and 1 μg/ml anti-CD28 (clone 37.51), in the presence of 3 μM monensin for 4 hours at 37°C, 5% CO_2. Cells were stained with antibodies for cell-surface molecules as described above, before fixation and permeabilization with BD Cytoperm/Cytofix (BD PharMingen, San Diego, CA) according to the manufacturer's instructions. Cells were incubated with FITC anti-IFN-γ (clone XMG1.2) or APC anti-granzyme B (clone GB12; Caltag Laboratories, Burlingame, CA) for 20 minutes at 4°C, washed twice, and resuspended in PBS with sodium azide before analysis. Appropriate isotype controls were

prepared simultaneously and were included in each analysis. Unless otherwise noted, all antibodies were purchased from BD PharMingen.

Histology. Individual lung lobes were removed from euthanized animals and first perfused and then immersed in 10% phosphate-buffered formalin solution and embedded in paraffin wax. Sections of 5 μm thickness were prepared and stained using hematoxylin and eosin, and examined by a trained pathologist in a double-blinded fashion.

Results

The Mtb72F fusion protein construct. Following amplification in *E. coli*, the Mtb72F DNA vaccine was sequenced to verify that the amplified construct was identical to the DNA construct provided by the Corixa Corporation (Figure 3.1). While no mutations occurred during our amplification process, a G→A single base pair substitution was present in the original DNA vaccine construct when compared to the *M. tuberculosis* H37Rv genomic sequence. This mutation, highlighted in black in Figure 3.1, is a silent mutation and does not affect the resulting protein sequence.

A pictorial representation illustrating construction of the Mtb72F vaccine is shown in Figure 3.2A. The full-length protein sequence of the Mtb72F DNA vaccine is shown in Figure 3.2B. The CD8 T cell epitope used to make the MHC class I tetramer reagent is highlighted in black.

The Mtb72F DNA vaccine confers protection to aerosol challenge in the lungs of mice. Immunization of C57BL/6 mice with a DNA vaccine encoding the Mtb72F fusion protein conferred approximately 1-$\log_{10}$ of protection in the lungs of mice at 21 days post challenge (Figure 3.3). This increased ability of immunized mice to more rapidly control bacterial replication in the lung was a transient effect, as bacterial numbers were similar between immunized and nonimmunized mice at all timepoints beyond 21 days post challenge. In addition, vaccination with Mtb72F failed to prevent bacterial dissemination to the spleen, and failed to control bacterial replication within this organ better than control saline treated mice (Figure 3.4).

Kinetics of accumulation of tetramer-specific CD8 T cells in the lungs. To determine if antigen-specific CD8 T cells were generated either by vaccination or challenge infection resulting in their accumulation in the lungs, lung cells were analyzed at various times by flow cytometry. Cells were gated on the CD3/CD8 positive population and further analyzed for CD44 expression and tetramer staining. As shown in Figure 3.5, at all timepoints, background tetramer staining in naïve mice was < 0.15%. In infected mice, a small but detectable number of antigen-specific CD8 T cells could be found by day 16. These cells increased by day 30 and then slowly declined. In contrast, in mice vaccinated with Mtb72F prior to challenge, by day 16 of infection ~11% of CD8 T cells in the lungs recognized the Mtb72F epitope GAPINSATAM. The number of these cells also slowly declined over time.

Relative cell numbers are shown in Figure 3.6. These data indicated that vaccinated mice generated much higher numbers of antigen-specific CD8 T cells in the

lungs earlier during infection, but that by day 30 the numbers of such cells are much the same. This coincides with immunological control of *M. tuberculosis* replication in the lungs of mice, and occurs when we consistently observe a 1-$\log_{10}$ reduction in bacterial numbers between vaccinated and nonvaccinated animals [43].

Functional characteristics of antigen-specific CD8 T cells. To further determine the functional nature of the lung CD8 T cells, lung cells were stained using the tetramer and also by intracellular staining with antibodies for IFN-γ or granzyme B. As shown in Figure 3.7 a large percentage of tetramer-positive cells were also positive for IFN-γ, whereas only a very low percentage were positive for the cytocidal molecule granzyme B.

Kinetics of emergence of CD8 T cells expressing the IL-7 receptor. There is increasing evidence to show that CD8 T cells in a state of memory immunity express high levels of the IL-7Rα [27]. To determine if expression of this receptor could be detected on CD8 T cells entering the lungs, cells were further analyzed for tetramer staining and staining for IL-7Rα. As shown in Figure 3.8, cells expressing this memory marker could be detected in nonimmunized infected mice by day 30, and numbers increased steadily through day 100. In mice vaccinated with Mtb72F prior to challenge, more than half of the antigen-specific CD8 T cells expressed IL-7Rα by day 16, and this declined slowly through day 100. Relative total cell numbers are shown in Figure 3.9 and illustrate the large numbers of such cells present in the lungs over the initial stage of the

infection where vaccinated mice showed approximately a 1-$\log_{10}$ reduction in the lung bacterial load (data not shown).

Cationic liposomal immunization induces antigen-specific CD8 T cells. In a final study, we wished to determine if Mtb72F delivered as protein could generate a detectable antigen-specific CD8 response in the lung, even prior to infection. For these studies, we used a novel cationic liposome adjuvant formulated with non-coding plasmid DNA and Mtb72F protein. Figure 3.10 shows that five days after the second boosting vaccine 17% of all CD8 T cells in the lungs were tetramer-positive, which decreased to 10% on day 28 post-immunization. As shown in Figure 3.11 virtually all of these cells had an activated phenotype [$CD44^{hi}$ $CD62L^{lo}$]. By day 28 the majority had a $CD45RB^{mid}$ phenotype, indicating a transition from an activated to an early memory state. Very few tetramer-positive cells expressed the IL-7Rα initially, but by day 28 nearly a third possessed this phenotype.

Immunization with *M. bovis* BCG Pasteur elicits Mtb32-specific CD8 T cells. The *M. bovis* BCG vaccine has been given to approximately three billion people worldwide and has proven to be a remarkably safe vaccine [20]. Due to its widespread use and excellent safety profile, many tuberculosis vaccination strategies currently being tested seek to augment the protective efficacy of BCG through utilization of a BCG prime followed by a subunit vaccine boost. As such, we wished to examine the Mtb32-specific CD8 T cell response to immunization with BCG in order to determine the suitability of the Mtb72F vaccine for use in a BCG prime Mtb72F boost regimen. C57BL/6 mice were immunized

with 10^6 CFU of *M. bovis* BCG Pasteur via the subcutaneous route. At three weeks and six weeks following immunization, lungs were harvested and analyzed by flow cytometry. Although Mtb32-specific CD8 T cells were detected in the lungs of immunized mice by 21 days post immunization as shown in Figure 3.12, the magnitude of the antigen-specific response was relatively small when compared to that elicited by infection with virulent *M. tuberculosis* H37Rv. In addition, this response declined over time to a level barely detectable at 6 weeks post immunization.

We next wanted to determine if the Mtb32-specific CD8 T cells induced by vaccination with BCG would proliferate in response to aerosol challenge with *M. tuberculosis*. C57BL/6 mice were immunized with either 10^6 CFU BCG s.c. or saline treated and challenged with *M. tuberculosis* H37Rv. At 30 days following infection, lungs were harvested and examined for Mtb32-specific CD8 T cells. As shown in Figure 3.13, tetramer-positive CD8 T cells generated by immunization with BCG did expand in response to challenge with *M. tuberculosis*, but the magnitude of this proliferative response was muted when compared to the response seen following aerosol infection alone.

Immunization with the Mtb72F DNA vaccine fails to protect CD4KO mice better than control mice. Previously, it was reported that CD4 T cells are required for the acquisition of CD8 T cell cytotoxic function but not for efficient priming and expansion of the CD8 T cell response following pulmonary infection with tuberculosis [42]. The ability to examine the CD8 T cell response at the antigen-specific cellular level gave us a powerful tool with which to examine the initiation of a CD8 T cell response during the

infectious process. We therefore wanted to characterize the kinetics and magnitude of the Mtb32 antigen-specific CD8 T cell response in the absence of CD4 T cell-mediated help using this more sensitive antigen-specific assay. CD4KO mice and background matched control mice were immunized with either the Mtb72F DNA vaccine or saline treated three times at three week intervals. Three weeks following the final immunization, mice were infected with approximately 100 viable *M. tuberculosis* H37Rv CFU via the aerosol route. While no statistically significant differences in recoverable bacterial numbers were observed at 20 days following infection, by 37 days a 1-$\log_{10}$ reduction in bacterial numbers was evident in the lungs of Mtb72F immunized wild-type mice when compared to saline treated wild-type mice (Figure 3.14). In contrast, CD4KO mice immunized with the Mtb72F DNA vaccine possessed only 0.5-$\log_{10}$ fewer bacteria in the lungs when compared to saline treated CD4KO mice, although this difference was not statistically significant ($P < 0.10$). Additionally, in wild-type C57BL/6 mice as well as CD4KO mice, immunization with the Mtb72F DNA vaccine failed to prevent bacterial dissemination to the spleen and failed to control bacterial replication within the spleen better than control mice (Figure 3.15).

In the absence of CD4 T cells, CD4KO mice do not recruit more CD8 T cells into the lungs following infection. We next wanted to examine if wild-type or CD4KO mice immunized with the Mtb72F DNA vaccine were able to recruit greater numbers of CD8 T cells into the lungs during pulmonary infection. At 20 days following infection, no differences existed between any of the groups (Figure 3.16). By 37 days, a significant reduction in the number of CD8 T cells was evident in Mtb72F immunized wild-type

mice, which occurred at a time when these mice possessed approximately 1-$\log_{10}$ fewer bacteria in the lungs. Although larger numbers of CD8 T cells were present in Mtb72F immunized CD4KO mice when compared to saline treated CD4KO mice, these cells failed to reduce bacterial numbers in the lungs comparable to wild-type mice.

CD4 T cell help is required for the efficient generation and expansion of Mtb32-specific CD8 T cells. Utilizing a MHC class I H-2D^b tetramer reagent, we wanted to determine if the absence of CD4 T cells impacted the CD8 T cell response at the antigen-specific level. As previously described, immunization with the Mtb72F DNA vaccine resulted in increased numbers of antigen-specific CD8 T cells in the lungs of wild-type mice at 20 days following infection (Figure 3.17). By 37 days, the percentages as well as the numbers (Figure 3.18) of these cells in the lungs were similar. In contrast, in the absence of CD4 T cell help, CD4KO mice primed a Mtb32 antigen-specific CD8 T cell response of similar magnitude to wild-type mice at 20 days, but this response failed to expand to a similar magnitude as wild-type mice by 37 days following infection. Immunization with the Mtb72F vaccine partially overcame this proliferative deficit, although the expansion of Mtb32-specific cells was delayed and the overall magnitude was reduced in Mtb72F immunized CD4KO mice.

IFN-γ production by CD8 T cells is delayed in CD4KO mice. Since IFN-γ is known to be protective during pulmonary infection with *M. tuberculosis*, we wanted to examine the kinetics of CD8 T cell-mediated IFN-γ production in the lungs. Using flow cytometry and intracellular cytokine staining, we quantified the number of IFN-γ^+CD3$^+$CD8$^+$ T cells in

the lungs of Mtb72F immunized and nonimmunized mice as illustrated in Figure 3.19. Twenty days after infection, the number of CD8 T cells producing IFN-γ was reduced in CD4KO mice, as compared to wild-type mice. Immunization with Mtb72F could not overcome this deficit. Surprisingly, by 37 days following infection the number of CD8 T cells producing IFN-γ was reduced in Mtb72F immunized wild-type mice. This may correlate with decreased pulmonary inflammation due to a reduction in bacterial numbers in the lung. In the absence of CD4 T cells, both immunized and nonimmunized mice had similar numbers of IFN-γ^+ CD8 T cells when compared to wild-type mice, although these mice had significantly more bacteria in the lungs.

We next examined the total number of IFN-γ producing cells in the lungs of CD4KO and wild-type mice to determine if IFN-γ production was being augmented by other cell types. Figure 3.20 shows that the number of IFN-γ^+ cells in the lungs of CD4KO mice was reduced compared to control mice, even though the CD4KO mice had more extensive inflammation and larger numbers of bacilli in the lungs. When the total number of IFN-γ^+ CD8 T cells was compared to the total number of IFN-γ^+ cells (Figure 3.21), it became apparent that CD8 T cells producing IFN-γ constituted 30-40% of the total number of IFN-γ^+ cells in wild-type mice. However in CD4KO mice, CD8 T cells represented the majority of IFN-γ^+ cells in the lung, indicating that CD4KO mice were unable to compensate for the lack of CD4 T cell-derived IFN-γ production.

In the absence of CD4 T cells, CD4KO mice do not recruit greater numbers of NK cells or γδ cells into the lung. Since other cell types are known to secrete IFN-γ and may play an anti-mycobacterial role in host pulmonary defense, we wanted to examine the

recruitment of other cell subsets by CD4KO mice. Flow cytometric analysis of the number of $NK1.1^+$ cells in the lungs of infected mice revealed that CD4KO mice actually possessed fewer $NK1.1^+$ cells in the lungs when compared to wild-type control mice (Figure 3.22). Additionally, CD4KO mice also had lesser numbers of γδ cells in the lungs early during infection, and similar numbers by day 37 (Figure 3.23).

The generation of memory precursor cells proceeds normally in the absence of CD4 T cells. Utilizing an Mtb32 MHC class I tetramer reagent in conjunction with antibodies for the IL-7Rα chain, we previously documented the differentiation of antigen-specific CD8 T cells from an $IL\text{-}7R^{lo}$ effector phenotype to an $IL\text{-}7R^{hi}$ memory precursor phenotype following Mtb72F immunization. In these experiments, we wanted to determine if the absence of CD4 T cells abrogated memory cell formation. Phenotypic analysis revealed that CD4KO mice were still able to generate normal percentages of memory precursor cells as indicated by expression of the IL-7Rα (Figure 3.24). In addition, the total number of CD8 T cells re-expressing the IL-7Rα was similar between wild-type and CD4KO mice (Figure 3.25). Therefore the absence of CD4 T cell help did not impact the initial stages of memory cell differentiation. It should be noted that the functionality of these memory precursor cells was not assayed in these experiments.

Histological analysis of lung sections. At 20 days following aerosol infection, wild-type mice possessed cellular aggregates surrounding infectious foci that were distinctly smaller than Mtb72F immunized mice. More importantly, lymphocytes recruited into the lungs of nonimmunized mice were primarily localized to perivascular and peribronchiolar

regions, and did not migrate extensively into the pulmonary interstitial tissue. In contrast, lymphocytes recruited into the lungs of wild-type mice immunized with Mtb72F appeared to exhibit increased directional migration and infiltrated more extensively into the interstitium, resulting in larger cellular aggregates located within the proximity of infectious foci. Mice lacking CD4 T cells possessed cellular aggregates of similar size to wild-type mice, but these aggregates contained fewer lymphocytes and tended to be more macrophage-dominated. It was also observed that lymphocytes from CD4KO mice immunized with the Mtb72F vaccine also tended to display an increased directional migration and possessed the ability to migrate beyond perivascular regions, although this trend was less pronounced when compared to Mtb72F immunized wild-type mice.

By 37 days following infection, saline treated wild-type mice possessed large coalescing granulomatous structures, while the pulmonary granulomas of Mtb72F immunized wild-type mice were generally smaller in size and more delineated than their saline treated counterparts. The granulomas present in wild-type mice contained large numbers of lymphocytes, and were generally more organized structures possessing distinct regions of lymphocytic foci. The granulomas of saline treated and Mtb72F immunized CD4KO mice did not differ significantly upon histological examination at this timepoint. Both groups had large coalescing granulomas accompanied by excessive pulmonary infiltrate that occupied significant amounts of the total lung volume. In addition, these granulomas were distinctly macrophage-dominated, and lacked higher-level organization typically seen in the granulomas of wild-type mice.

Discussion

The results of this study showed that infection of mice by aerosol exposure resulted in the accumulation in the lung tissues of large numbers of CD8 T cells that were specific for a 10-mer peptide of the *M. tuberculosis* protein Mtb32. This peptide, which is highly immunogenic for CD8 T cells capable of cytolysis and cytokine secretion *in vitro*, is a major component of the effective tuberculosis vaccine candidate Mtb72F [6, 43]. In this regard, when mice were vaccinated with Mtb72F DNA prior to challenge, a much larger and more rapid accumulation of antigen-specific CD8 T cells was observed. While it is not known if the antigen-specific cells identified in this study actually contribute to protective immunity to the challenge infection, that was not the purpose of the current study. The purpose instead was to determine if T cells recognizing a dominant MHC class-I restricted epitope could traffic to the lungs after intramuscular inoculation of the Mtb72F candidate tuberculosis vaccine, and this indeed proved to be the case. Studies are currently underway to see if cell sorted tetramer-positive CD8 T cells can adoptively protect recipient mice following aerosol infection.

The data further showed that the antigen-specific CD8 T cells in the lungs of infected mice were capable of producing IFN-γ, which is known to be essential for protection following aerosol challenge with *M. tuberculosis*. In contrast, the majority of these cells did not produce granzyme B early during infection, suggesting that CD8 T cells entering the sites of infection in the lungs at early timepoints are more likely to control *M. tuberculosis* infection indirectly through activation of local macrophages via IFN-γ secretion, rather than to directly lyse infected target cells by secretion of perforin

and granzyme B. This is in keeping with the observation that perforin gene knock-out mice are not less resistant to aerosol challenge [11, 29]. These results, however do not preclude cytolytic activity at timepoints later during the infectious process, as observed by others [28, 39]. Further experiments utilizing an *in vivo* cytotoxic assay will delineate the lytic function of these antigen-specific CD8 T cells late in infection. That antigen-specific CD8 T cells capable of producing IFN-γ preferentially accumulate in the lungs of mice following aerosol infection confirms the findings of a recent paper by Kamath *et al.*, which examined the response to two vaccine candidates, CFP10 and Mtb10.4 [28].

Using IL-7Rα as a marker, we found that a subset of *M. tuberculosis*-specific CD8 T cells that accumulated in the lungs of infected mice gradually assumed a memory precursor phenotype over the course of the infection. In contrast to the nonimmunized mice, if the mice were first vaccinated with Mtb72F, then memory precursor CD8 T cells comprised a major component of the early cellular response in the lungs after challenge. The actual numbers [and percentages] of these cells then declined for unknown reasons, but might indicate transition of these cells to an effector phenotype.

Whether the antigen-specific cells entered the lungs following infection or were already there prior to challenge was not addressed in the Mtb72F DNA vaccination experiments. However, pilot studies using a BCG infection model indicated a substantial establishment of activated protective T cells [A. Kipnis, I. Orme, unpublished data] similar to those demonstrated in chronic infection [26]. Furthermore, recruitment of activated T cells to the lungs following immunization was demonstrated here by studies in which we examined the lungs of mice vaccinated with Mtb72F protein delivered in a CD8-directed liposomal formulation. This study showed that a strong antigen-specific

CD8 T cell response could be elicited in the lungs of mice in the absence of infection, and that one month after two immunizations, about one-third of the antigen-specific CD8 T cells in the lungs expressed the IL-7Rα. Moreover, by this time most of these cells had begun to reduce the expression of CD45RB from high to moderate, which is a further suggestion of transition to a memory state [21].

The data presented here demonstrate preferential recruitment and accumulation of activated, antigen-specific CD8 T cells into the lungs of mice following aerosol challenge with *M. tuberculosis*. Furthermore, that these cells were capable of producing IFN-γ upon restimulation suggests that they could be actively participating in the control of bacterial replication. It was also shown that vaccination with the Mtb72F DNA vaccine significantly increased the number of these cells in the lungs following infection, and indicates that the CD8 T cell component of adaptive immunity can be specifically targeted by vaccination. Further studies currently in progress will quantify the amount of protection conferred by this population of Mtb32-specific CD8 T cells, to further define the relevance of the CD8 T cell response to *M. tuberculosis* infection. These experiments, as well as others in progress, will ultimately determine whether CD8 T cell epitopes should be included in future *M. tuberculosis* candidate vaccines.

Utilizing a mouse model that lacks helper T lymphocytes, we examined the contribution of CD4 T cells to the initiation and the memory recall response of CD8 T cells. The results of these experiments indicate that while immunization of CD4KO mice with Mtb72F does result in some increased protective effect as measured by recoverable bacilli from the lungs, the amount of protection is reduced when compared to wild-type Mtb72F immunized mice.

While the total numbers of CD8 T cells in the lungs of infected mice were similar early during infection, examination of CD8 T cell priming at the antigen-specific level revealed that immunization with Mtb72F failed to result in an increased precursor frequency of antigen-specific CD8 T cells in CD4KO mice when compared to the increase observed in their Mtb72F immunized wild-type counterparts. Not only was the effectiveness of Mtb72F DNA immunization compromised in CD4KO mice, but the Mtb32-specific CD8 T cells from these mice also failed to proliferate to a similar level as wild-type mice by 37 days following infectious challenge. Therefore in the absence of CD4 T cell help, the antigen-specific CD8 T cell response exhibited defects in the kinetics and overall magnitude of clonal proliferation in response to antigen. These results contradict the findings of Serbina *et al.* as they observed no proliferative defect in the absence of CD4 T cell help [42]. The reasons for these differences could be explained by the increased sensitivity of our antigen-specific assay conditions as opposed to examination of the CD8 T cell response in total, as was performed in those studies. Another possible explanation is that the antigen-specific CD8 T cell response to the Mtb32 antigen may not be representative of the CD8 T cell response to other *M. tuberculosis*-derived antigens present during infection. Examination of the host response to other CD8 T cell epitopes is currently in progress to address this question.

Examination of the number of IFN-γ producing CD8 T cells in the lungs demonstrated that CD4KO mice have much fewer of these cells early following infection, and that while the number of these cells increases to wild-type levels by day 37, these mice still fail to control bacterial replication at a level similar to control mice. When the number of IFN-γ producing cells is overlaid upon the total number of IFN-γ producing

cells in the lung, it becomes apparent that in CD4KO mice, the majority of IFN-γ production is CD8 T cell-derived. Therefore these mice are unable to adequately compensate for the lack of CD4 T cell-derived IFN-γ. These experiments confirm and extend the observation that IFN-γ producing CD8 T cells accumulate in the lungs of infected CD4KO mice, but fail to control infection [8]. Examination of the cellular influx into the infected lung determined that CD4KO mice do not recruit more NK cells or γδ cells to compensate for the lack of CD4 T lymphocytes.

Interestingly, while the magnitude of the antigen-specific CD8 T cell response was significantly affected by the lack of CD4 T cell help, the critical attribute of memory CD8 T cell generation appeared to be unimpaired in CD4 KO mice. Similar numbers and percentages of Mtb32-specific CD8 T cells were able to upregulate expression of the IL-7R, indicating that the early stages of transition into memory cells was not impaired in the absence of CD4 T cell help. It remains to be determined if the antigen-specific cells generated in the absence of CD4 T cell help possess functional defects or are able to persist at levels similar to memory cells generated in the presence of CD4 T cell costimulation.

Taken together, these data indicate defective CD8 T cell priming in the absence of adequate CD4 T cell costimulation that immunization with Mtb72F cannot overcome, and that CD4 T cells are required for optimum CD8 T cell-mediated protection in the lungs. Further elucidation of the precise contribution of CD8 T cells during pulmonary tuberculosis will aid in rational vaccine design and contribute to the overall success of tuberculosis vaccine development.

ATGACGGCCGCGTCCGATAACTTCCAGCTGTCCCAGGGTGGGCAGGGATTCGCCATTCC
GATCGGGCAGGCGATGGCGATCGCGGGCCAGATCCGATCGGGTGGGGGGTCACCCACCG
TTCATATCGGGCCTACCGCCTTCCTCGGCTTGGGTGTTGTCGACAACAACGGCAACGGC
GCACGAGTCCAACGCGTGGTCGGGAGCGCTCCGGCGGCAAGTCTCGGCATCTCCACCGG
CGACGTGATCACCGCGGTCGACGGCGCTCCGATCAACTCGGCCACCGCGATGGCGGACG
CGCTTAACGGGCATCATCCCGGTGACGTCATCTCGGTGACCTGGCAAACCAAGTCGGGC
GGCACGCGTACAGGGAACGTGACATTGGCCGAGGGACCCCCGGCCGAATTCATGGTGGA
TTTCGGGGCGTTACCACCGGAGATCAACTCCGCGAGGATGTACGCCGGCCCGGGTTCGG
CCTCGCTGGTGGCCGCGGCTCAGATGTGGGACAGCGTGGCGAGTGACCTGTTTTCGGCC
GCGTCGGCGTTTCAGTCGGTGGTCTGGGGTCTGACGGTGGGGTCGTGGATAGGTTCGTC
GGCGGGTCTGATGGTGGCGGCGGCCTCGCCGTATGTGGCGTGGATGAGCGTCACCGCGG
GGCAGGCCGAGCTGACCGCCGCCCAGGTCCGGGTTGCTGCGGCGGCCTACGAGACGGCG
TATGGGCTGACGGTGCCCCCGCCGGTGATCGCCGAGAACCGTGCTGAACTGATGATTCT
GATAGCGACCAACCTCTTGGGGCAAAACACCCCGGCGATCGCGGTCAACGAGGCCGAAT
ACGGCGAGATGTGGGCCCAAGACGCCGCCGCGATGTTTGGCTACGCCGCGGCGACGGCG
ACGGCGACGGCGACGTTGCTGCCGTTCGAGGAGGCGCCGGAGATGACCAGCGCGGGTGG
GCTCCTCGAGCAGGCCGCCGCGGTCGAGGAGGCCTCCGACACCGCCGCGGCGAACCAGT
TGATGAACAATGTGCCCCAGGCGCTGCAACAGCTGGCCCAGCCCACGCAGGGCACCACG
CCTTCTTCCAAGCTGGGTGGCCTGTGGAAGACGGTCTCGCCGCATCGGTCGCCGATCAG
CAACATGGTGTCGATGGCCAACAACCACATGTCGATGACCAACTCGGGTGTGTCGATGA
CCAACACCTTGAGCTCGATGTTGAAGGGCTTTGCTCCGGCGGCGGCCGCCCAGGCCGTG
CAAACCGCGGCGCAAAACGGGGTCCGGGCGATGAGCTCGCTGGGCAGCTCGCTGGGTTC
TTCGGGTCTGGGCGGTGGGGTGGCCGCCAACTTGGGTCGGGCGGCCTCGGTCGGTTCGT
TGTCGGTGCCGCAGGCCTGGGCCGCGGCCAACCAGGCAGTCACCCCGGCGGCGCGGGCG
CTGCCGCTGACCAGCCTGACCAGCGCCGCGGAAAGAGGGCCCGGGCAGATGCTGGGCGG
GCTGCCGGTGGGGCAGATGGGCGCCAGGGCCGGTGGTGGGCTCAGTGGTGTGCTGCGTG
TTCCGCCGCGACCCTATGTGATGCCGCATTCTCCGGCAGCCGGCGATATCGCCCCGCCG
GCCTTGTCGCAGGACCGGTTCGCCGACTTCCCCGCGCTGCCCCTCGACCCGTCCGCGAT
GGTCGCCCAAGTGGGGCCACAGGTGGTCAACATCAACACCAAACTGGGCTACAACAACG
CCGTGGGCGCCGGGACCGGCATCGTCATCGATCCCAACGGTGTCGTGCTGACCAACAAC
CACGTGATCGCGGGCGCCACCGACATCAATGCGTTCAGCGTCGGCTCCGGCCAAACCTA
CGGCGTCGATGTGGTCGGGTATGACCGCACCCAGGATGTCGCGGTGCTGCAGCTGCGCG
GTGCCGGTGGCCTGCCGTCGGCGGCGATCGGTGGCGGCGTCGCGGTTGGTGAGCCCGTC
GTCGCGATGGGCAACAGCGGTGGGCAGGGCGGAACGCCCCGTGCGGTGCCTGGCAGGGT
GGTCGCGCTCGGCCAAACCGTGCAGGCGTCGGATTCGCTGACCGGTGCCGAAGAGACAT
TGAACGGGTTGATCCAGTTCGATGCCGCGATCCAGCCCGGTGATTCGGGCGGGCCCGTC
GTCAACGGCCTAGGACAGGTGGTCGGTATGAACACGGCCGCGTCC

Figure 3.1. The Mtb72F DNA vaccine sequence. The DNA information was obtained upon sequence analysis of the Mtb72F DNA vaccine following amplification in *E. coli*. The nucleotides in blue are derived from the Mtb32 protein, while those in red are from the Mtb39 protein. The nucleotides highlighted in green are residual bases left over from construction of the vaccine construct. The adenine highlighted in black is a silent single base pair substitution (G→A) present in the original DNA vaccine construct provided by the Corixa Corporation.

A.

B.

MTAASDNFQLSQGGQGFAIPIGQAMAIAGQIRSGGGSPTVHIGPTAFLGLGVVDNNGNG
ARVQRVVGSAPAASLGISTGDVITAVDGAPINSATAMADALNGHHPGDVISVTWQTKSG
GTRTGNVTLAEGPPAEFMVDFGALPPEINSARMYAGPGSASLVAAAQMWDSVASDLFSA
ASAFQSVVWGLTVGSWIGSSAGLMVAAASPYVAWMSVTAGQAELTAAQVRVAAAAYETA
YGLTVPPPVIAENRAELMILIATNLLGQNTPAIAVNEAEYGEMWAQDAAAMFGYAAATA
TATATLLPFEEAPEMTSAGGLLEQAAAVEEASDTAAANQLMNNVPQALQQLAQPTQGTT
PSSKLGGLWKTVSPHRSPISNMVSMANNHMSMTNSGVSMTNTLSSMLKGFAPAAAAQAV
QTAAQNGVRAMSSLGSSLGSSGLGGGVAANLGRAASVGSLSVPQAWAAANQAVTPAARA
LPLTSLTSAAERGPGQMLGGLPVGQMGARAGGGLSGVLRVPPRPYVMPHSPAAGDIAPP
ALSQDRFADFPALPLDPSAMVAQVGPQVVNINTKLGYNNAVGAGTGIVIDPNGVVLTNN
HVIAGATDINAFSVGSGQTYGVDVVGYDRTQDVAVLQLRGAGGLPSAAIGGGVAVGEPV
VAMGNSGGQGGTPRAVPGRVVALGQTVQASDSLTGAEETLNGLIQFDAAIQPGDSGGPV
VNGLGQVVGMNTAAS

Figure 3.2. The protein sequence of the Mtb72F fusion protein vaccine construct. The amino acids in blue are derived from the Mtb32 protein, while those in red are from the Mtb39 protein. The amino acids highlighted in green are residues left over from construction of the fusion protein construct. The 10-mer peptide sequence highlighted in black is the CD8 T cell epitope utilized in subsequent Mtb32 antigen-specific experiments.

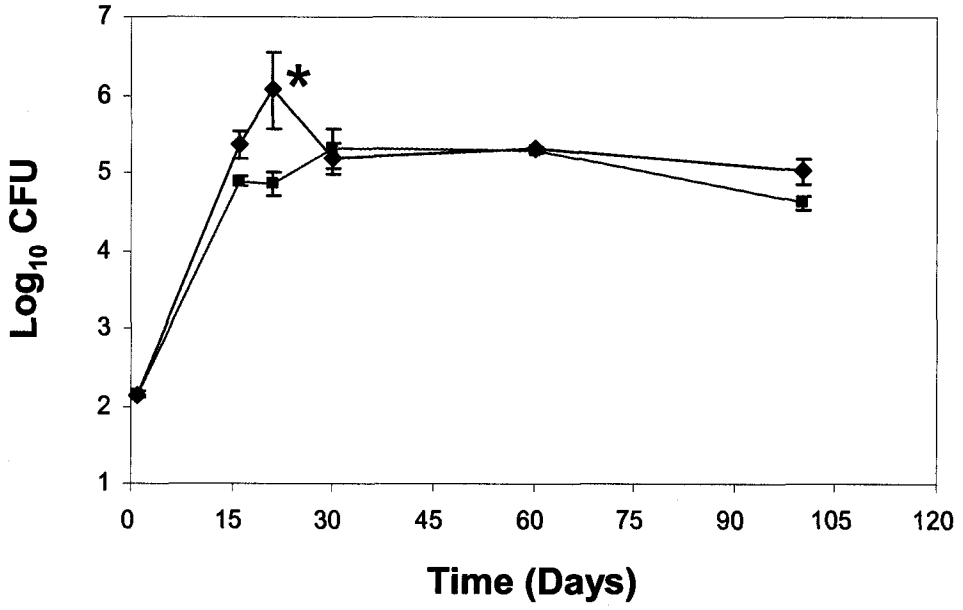

Figure 3.3. Immunization with the Mtb72F DNA vaccine confers approximately 1-$\log_{10}$ of protection in the lungs of mice at 21 days, although this protective effect is transient in nature. C57BL/6 mice (n=4) were immunized with the Mtb72F DNA vaccine or saline treated three times at three week intervals, followed by three weeks of rest. Following low dose aerosol infection (LDA) with *M. tuberculosis* H37Rv, partial lung homogenates were plated onto Middlebrook 7H11 agar and colonies were enumerated after 2-3 weeks. Data are expressed as the means ± the standard deviation. Statistical significance based upon a comparison of Mtb72F immunized and nonimmunized groups was determined using Student's t test and is indicated by an asterisk ($P < 0.05$). ♦ - Saline treated, ■ - Mtb72F immunized.

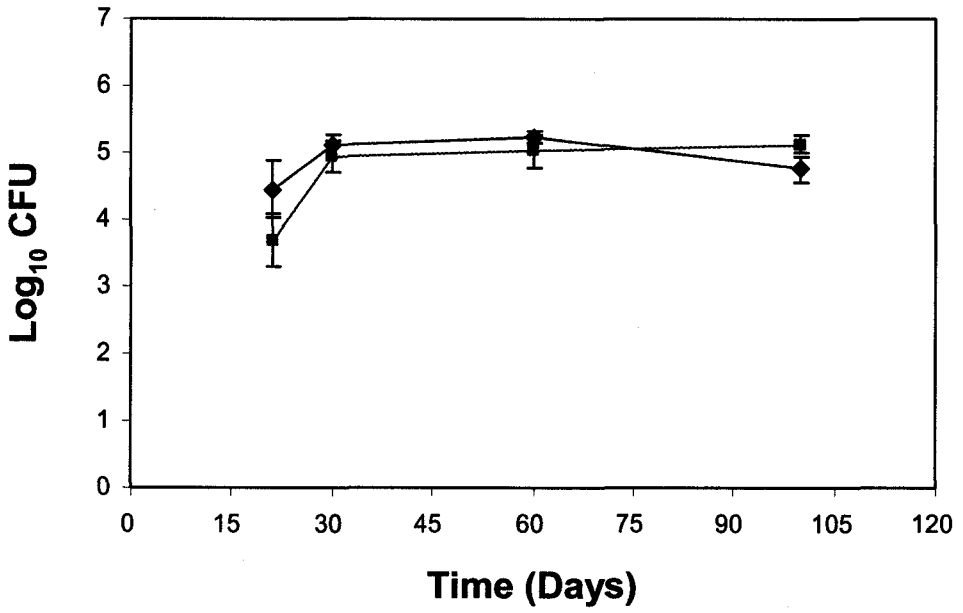

Figure 3.4. Immunization with the Mtb72F DNA vaccine does not confer increased resistance in the spleens of recipient mice. At all timepoints observed, there were no statistical differences in bacterial numbers between immunized and nonimmunized mice. Data are expressed as the means ± the standard deviation. ♦ - Saline treated, ■ - Mtb72F immunized.

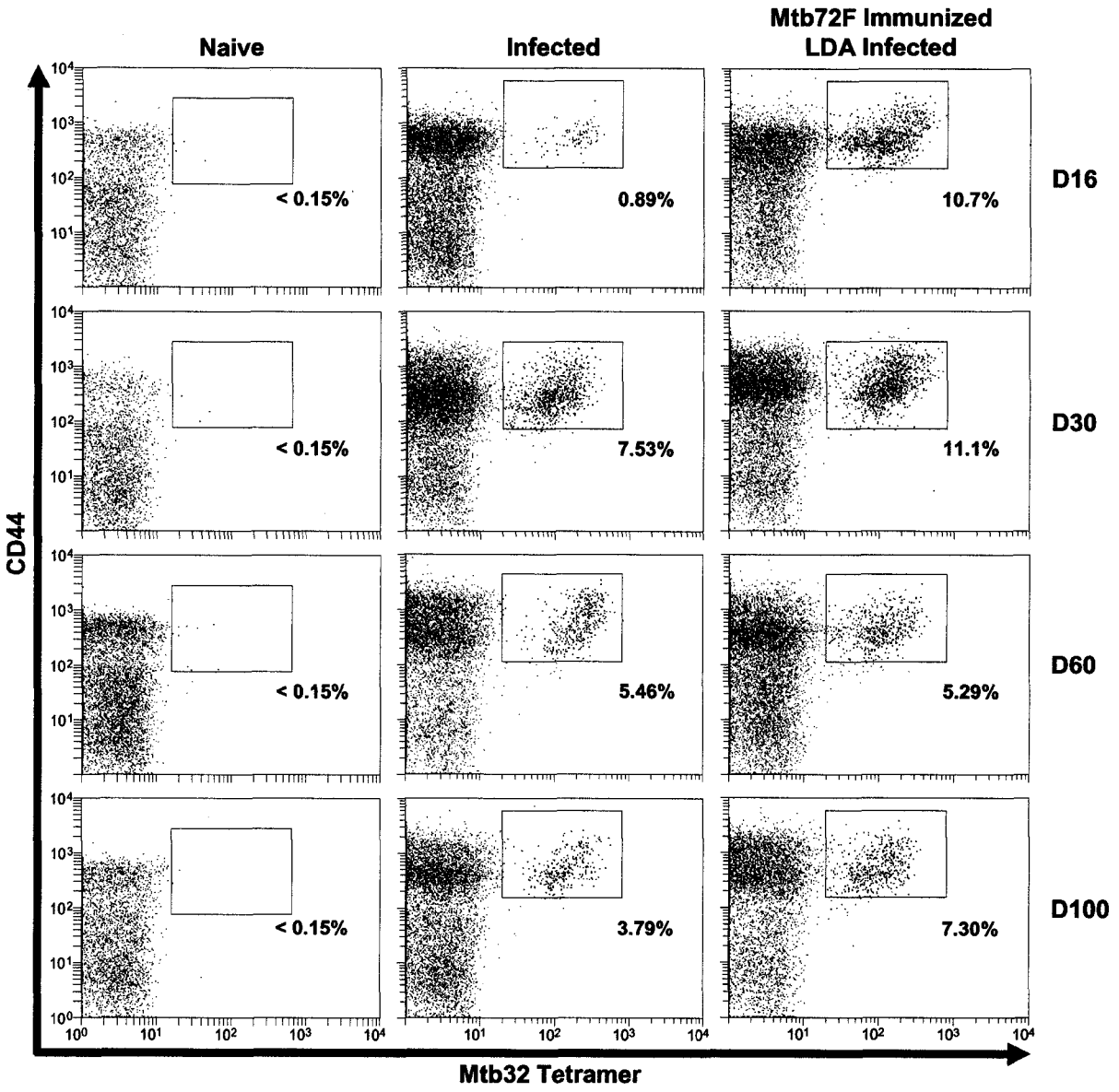

Figure 3.5. Kinetic analysis of the Mtb32 antigen-specific CD8 T cell response in nonimmunized mice and in mice immunized with Mtb72F followed by low dose aerosol infection with *M. tuberculosis*. C57BL/6 mice were immunized three times at three week intervals via the intramuscular route. Mice were challenged three weeks following the last immunization. Timepoints represent the number of days after infection. Lung cells were stained with the Mtb32 H-2D^b tetramer and antibodies specific for CD3, CD8, and CD44. Lymphocytes were gated based upon characteristic size and granularity, and further gated based upon concurrent CD3 and CD8 expression. The data are from one mouse and are representative of n=4 mice. Percentages represent the number of CD44^{hi} tetramer$^+$ cells as compared to the total number of CD3$^+$/CD8$^+$ cells. In all cases, background tetramer staining in naïve mice was < 0.15%.

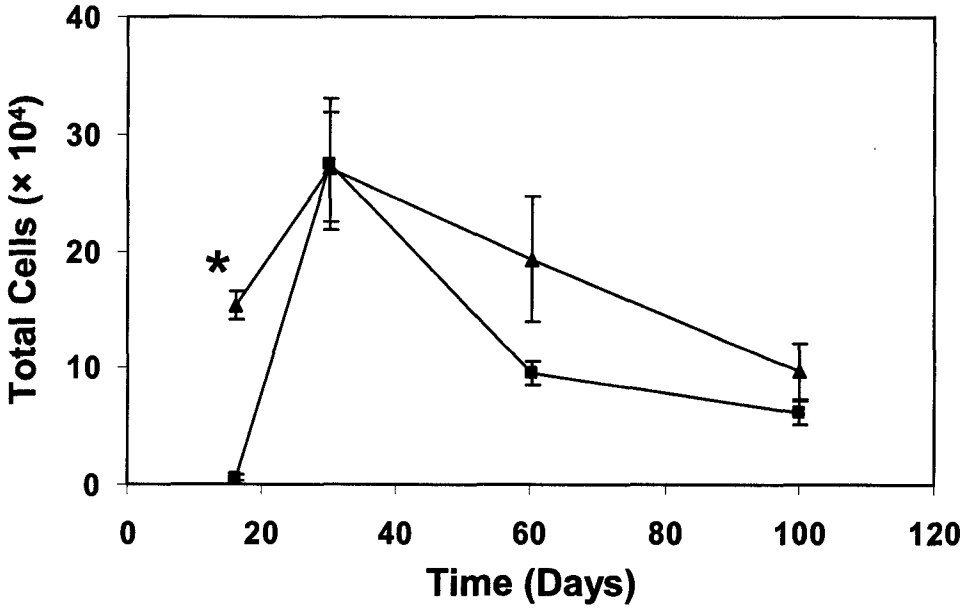

Figure 3.6. Immunization with Mtb72F resulted in greater numbers of antigen-specific CD8 T cells in the lungs of mice following infection. Data are expressed as the means ± the standard errors of the means and are from four mice per group per timepoint. Triangles, Mtb72F immunized mice; Squares, nonimmunized mice. Statistical significance based upon a comparison of Mtb72F immunized and nonimmunized groups was determined using Student's *t* test and is indicated by an asterisk ($P < 0.005$).

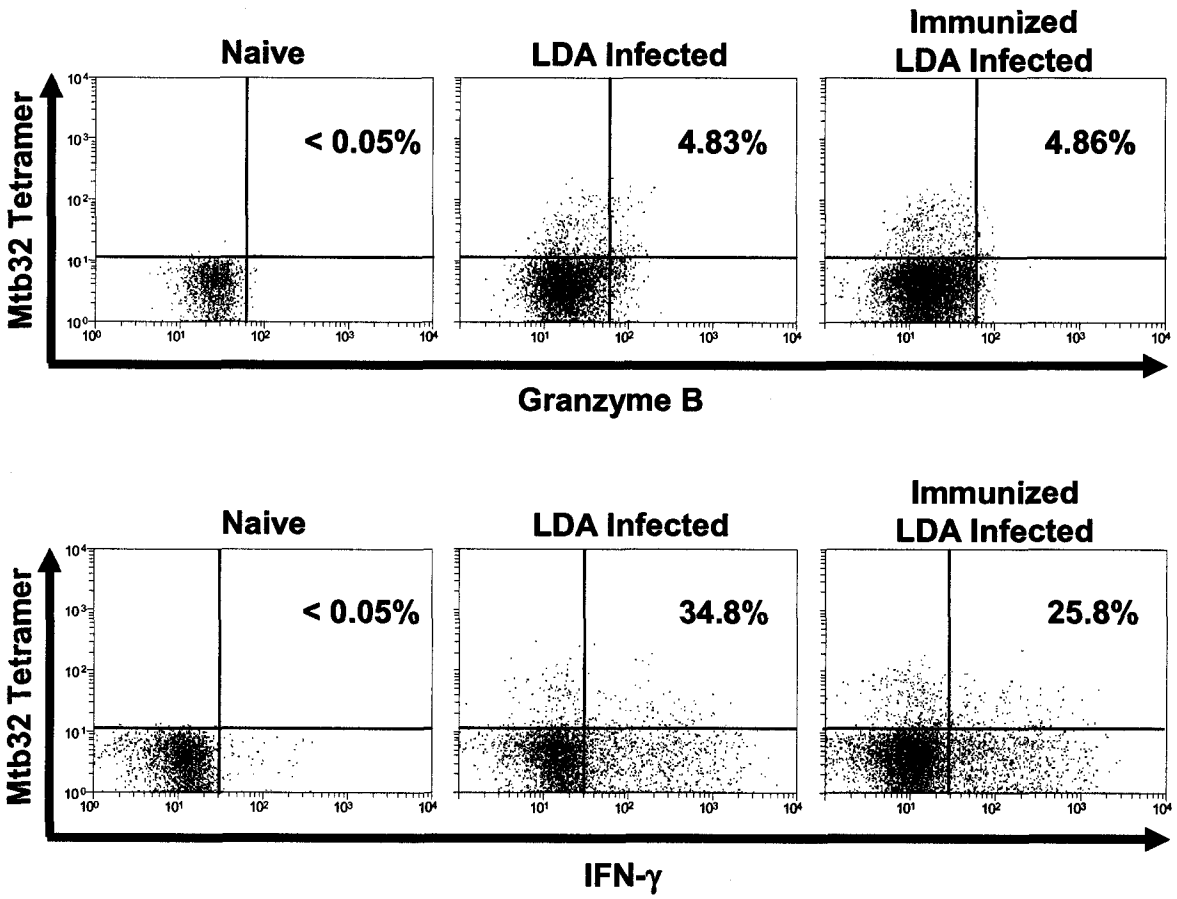

Figure 3.7. Intracellular cytokine staining of lung-derived cells for granzyme B and IFN-γ at 30 days following aerogenic infection suggests that the tetramer$^+$ cells are primarily IFN-γ producing rather than cytolytic. The data are from one mouse and are representative of n=4. Percentages represent the number of antigen-specific IFN-γ$^+$ or granzyme B$^+$ cells as compared to the total number of tetramer$^+$ cells.

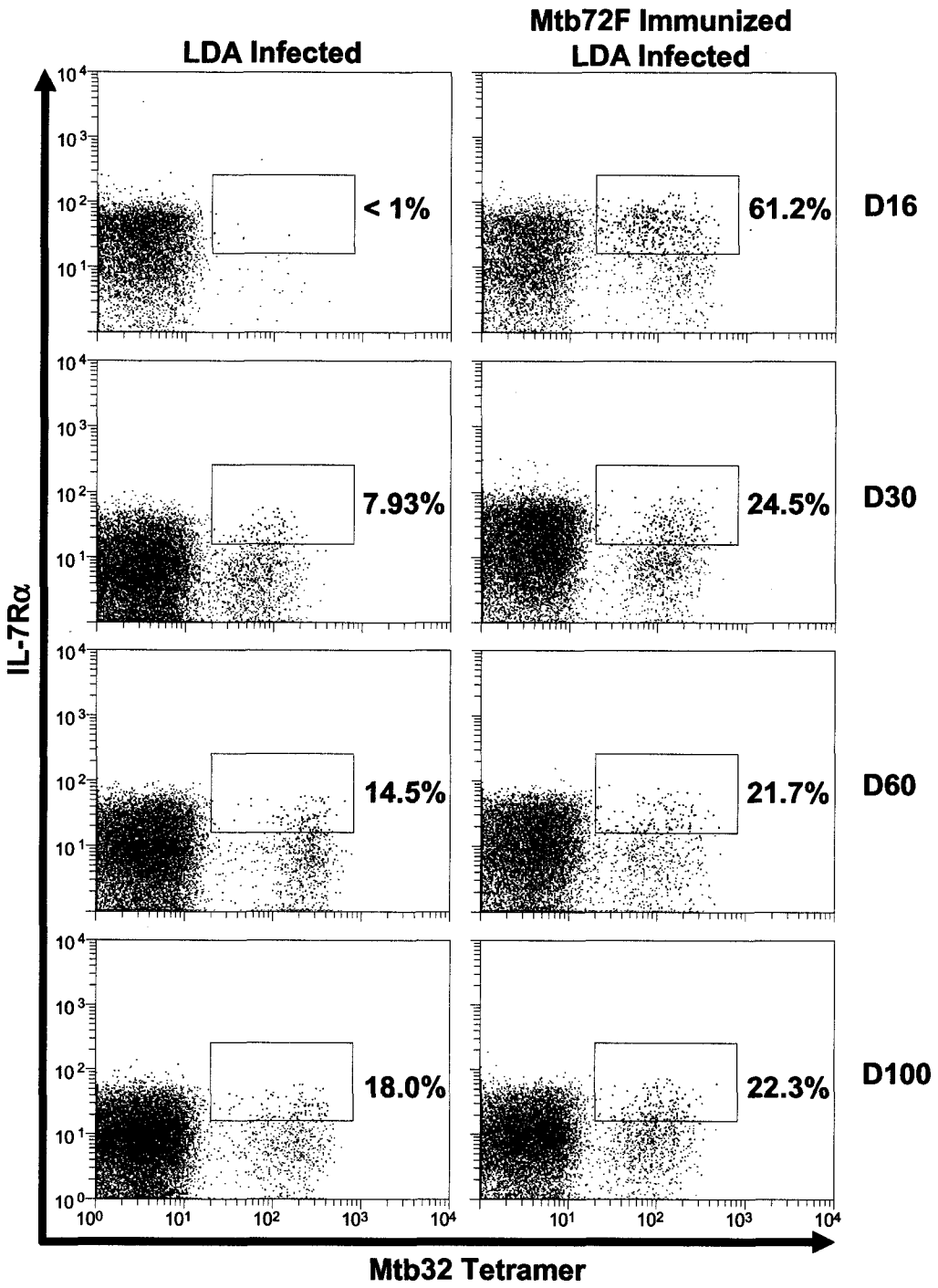

Figure 3.8. Mtb32 tetramer$^+$ CD8 T cells in the lung express high levels of IL-7Rα following immunization with Mtb72F and subsequent aerogenic challenge. At multiple timepoints, lung cells were stained with the H-2D^b tetramer and antibodies specific for CD3, CD8, and IL-7Rα. Lymphocytes were gated based upon characteristic size and granularity, and further gated based upon concurrent CD3 and CD8 expression. The data are from one mouse and are representative of n=4. Percentages represent the number of IL-7Rα^{hi} tetramer$^+$ cells as compared to the total number of tetramer$^+$ cells. In all cases, background tetramer staining in naïve mice was < 0.15%.

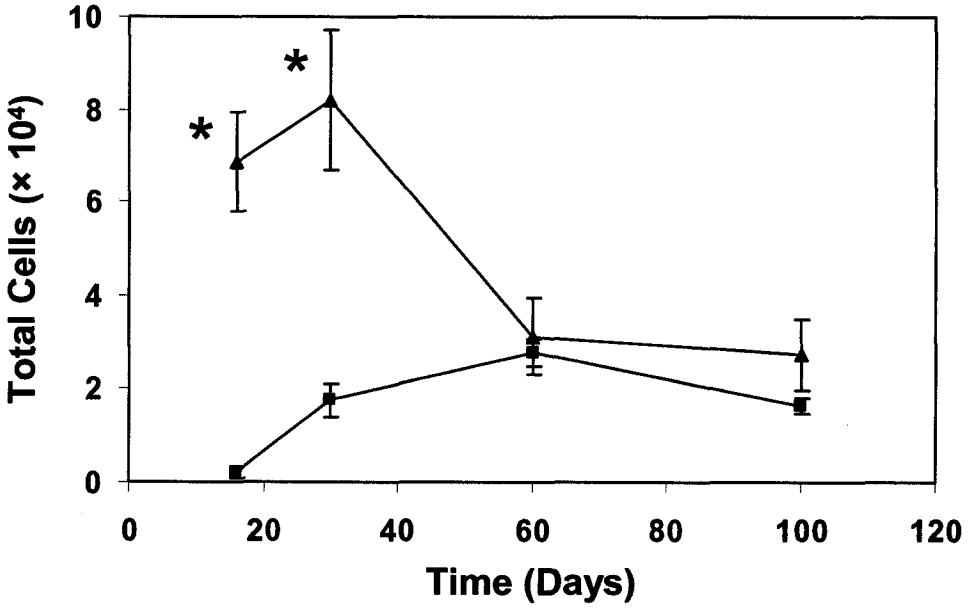

Figure 3.9. Greater numbers of Mtb32-specific IL-7Rα^{hi} CD8 memory precursor T cells were present in the lungs of Mtb72F immunized mice prior to day 60 as compared to nonimmunized mice following *M. tuberculosis* infection. Data are expressed as the means ± the standard errors of the means (n=4 mice/group/timepoint). Triangles, Mtb72F immunized mice; Squares, nonimmunized mice. Statistical significance based upon a comparison of Mtb72F immunized and nonimmunized groups was determined using Student's t test and is indicated by an asterisk ($P < 0.05$).

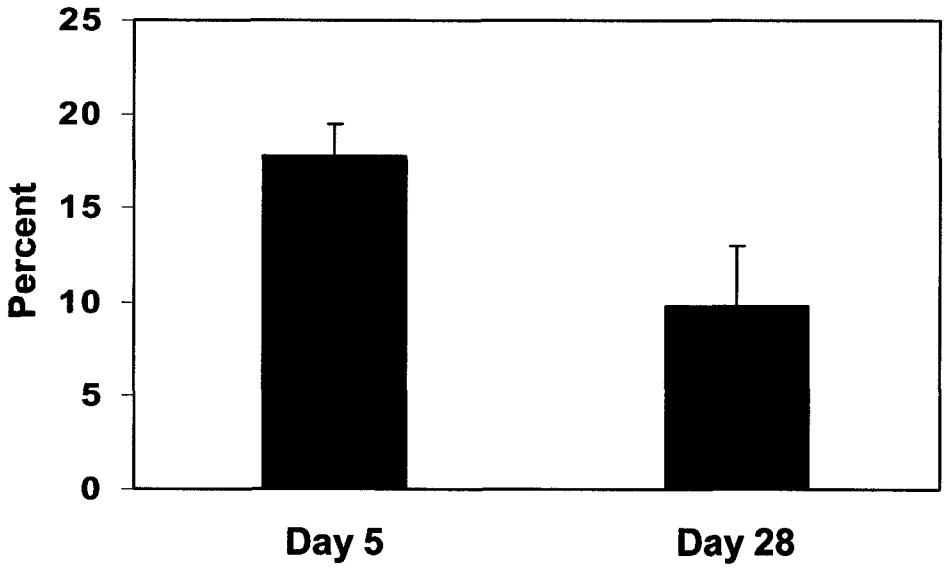

Figure 3.10. Immunization with Mtb72F protein in conjunction with cationic liposome complexes and non-coding DNA results in a strong pulmonary antigen-specific CD8 T cell response in the absence of infection. Percentages represent the number of $CD3^+/CD8^+/tetramer^+$ cells as compared to the total number of $CD3^+/CD8^+$ T cells in the lung. C57BL/6 mice (n=4 mice/group/timepoint) were immunized two times, 14 days apart via the intraperitoneal route. Five days and 28 days following the second immunization, lung cells were isolated and stained with the H-$2D^b$ tetramer and antibodies specific for CD3, CD8, and CD44. Lymphocytes were gated based upon characteristic size and granularity, and further gated based upon concurrent CD3 and CD8 expression. Data are expressed as the means ± the standard errors of the means.

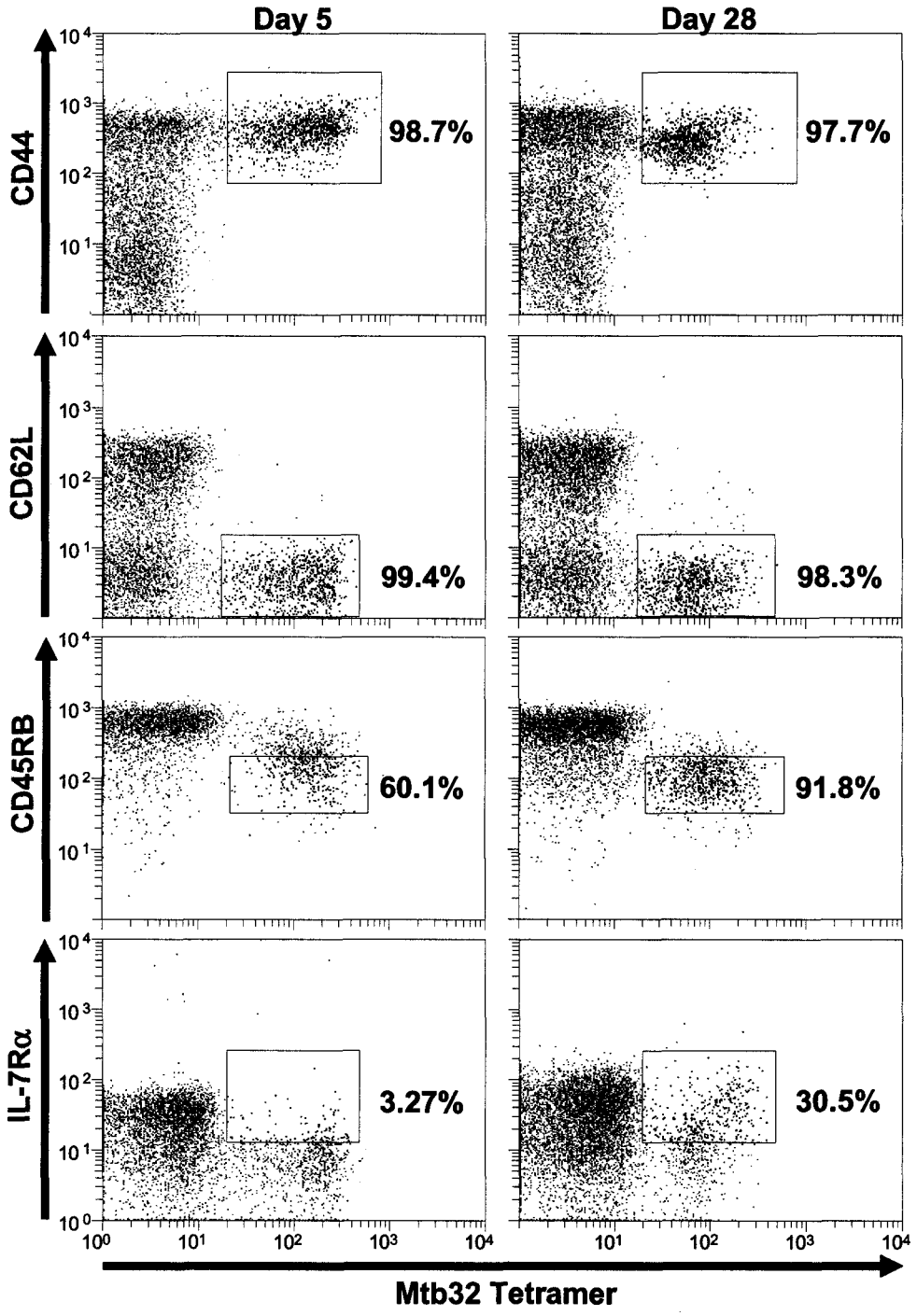

Figure 3.11. Mtb32-specific CD8 T cells isolated from lungs of mice following immunization possess an activated phenotype. Mice (n=4 mice/group/timepoint) were immunized two times, 14 days apart via the intraperitoneal route with cationic liposomes plus Mtb72F protein. Five days and 28 days following the second immunization, lung cells were isolated and stained with the H-2D^b tetramer and antibodies specific for CD3, CD8, and surface activation markers. Representative dot plots are shown where the percentages represent the number of tetramer$^+$ cells falling within the indicated region as compared to the total number of tetramer$^+$ cells.

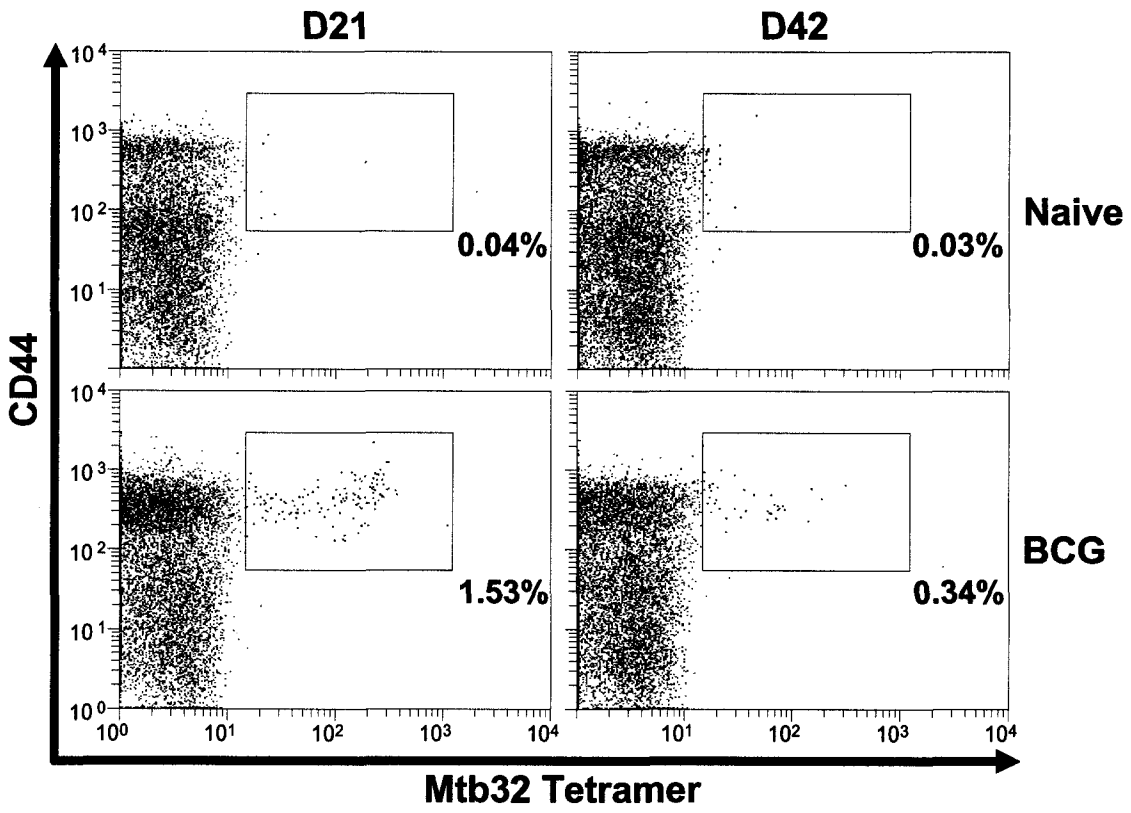

Figure 3.12. Mtb32 antigen-specific CD8 T cells are recruited to the lungs following immunization with BCG Pasteur. C57BL/6 mice (n=5) were immunized with either 10^6 CFU of BCG or saline via the subcutaneous route. Twenty-one days and 42 days following immunization, lungs were harvested and analyzed by flow cytometry. Cells were gated based upon characteristic forward- vs. side-scatter profiles and expression of CD3 and CD8. Percentages represent the number of Mtb32 tetramer$^+$ cells as compared to the total number of CD3$^+$/CD8$^+$ T cells.

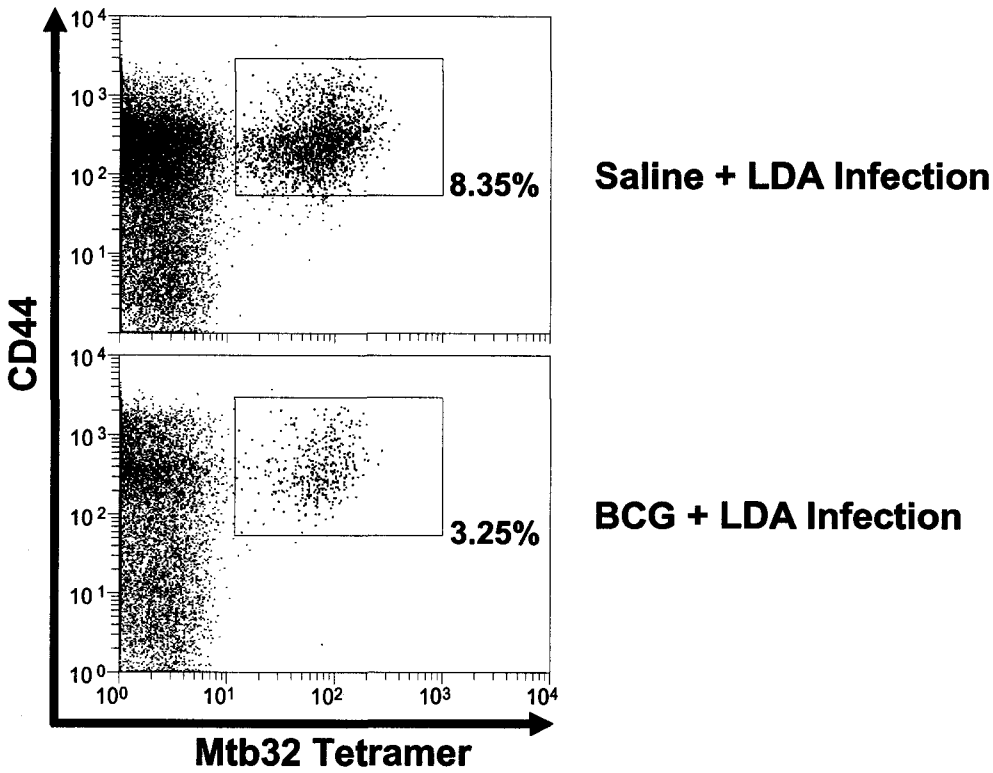

Figure 3.13. Mtb32 antigen-specific CD8 T cells elicited by immunization with BCG Pasteur proliferate following subsequent aerosol challenge with *M. tuberculosis* H37Rv, although to a lesser degree than in nonimmunized mice. C57BL/6 mice (n=5) were immunized with either BCG Pasteur or saline three weeks prior to low dose aerosol infection. Flow cytometric analysis was performed 30 days following aerosol infection. Cells were gated based upon characteristic forward- vs. side-scatter profiles and expression of CD3 and CD8. Percentages represent the number of Mtb32 tetramer$^+$ cells as compared to the total number of CD3$^+$/CD8$^+$ T cells.

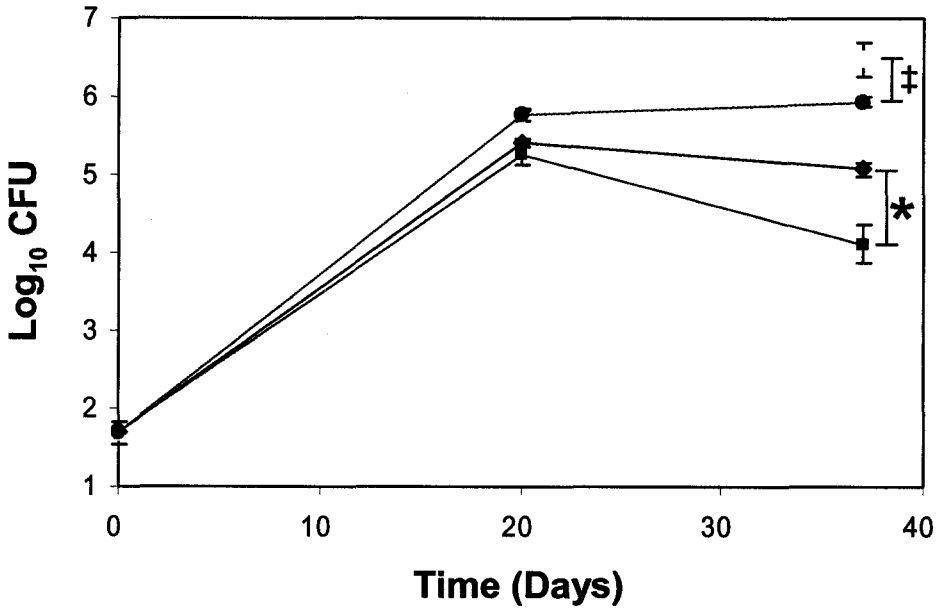

Figure 3.14. In the absence of CD4 T cells, immunization with the Mtb72F vaccine failed to protect recipient mice to the same level as wild-type control mice. C57BL/6 and CD4KO mice (n=4) were immunized with Mtb72F DNA three times at three week intervals, followed by 3 weeks of rest. Following low dose aerosol infection, partial lung homogenates were plated onto Middlebrook 7H11 agar and colonies were enumerated after 2-3 weeks. Data are expressed as the means ± the standard deviation. Statistical significance based upon a comparison of Mtb72F immunized and nonimmunized wild-type and CD4KO groups was determined using Student's t test (* = $P < 0.01$, ‡ = $P < 0.10$). ♦ - C57BL/6 saline treated, ■ - C57BL/6 Mtb72F immunized, - CD4KO saline treated, ● - CD4KO Mtb72F immunized.

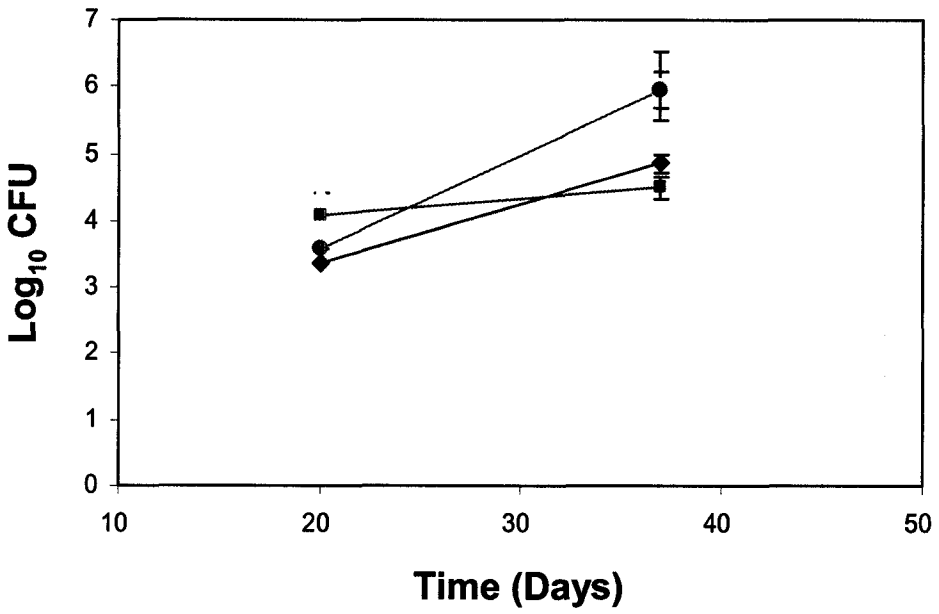

Figure 3.15. Immunization with the Mtb72F DNA vaccine does not control bacterial replication in the spleen mice better than control mice. Mice were immunized as previously described. Data are expressed as the means ± the standard deviation. ♦ - C57BL/6 saline treated, ■ - C57BL/6 Mtb72F immunized, - CD4KO saline treated, ● - CD4KO Mtb72F immunized.

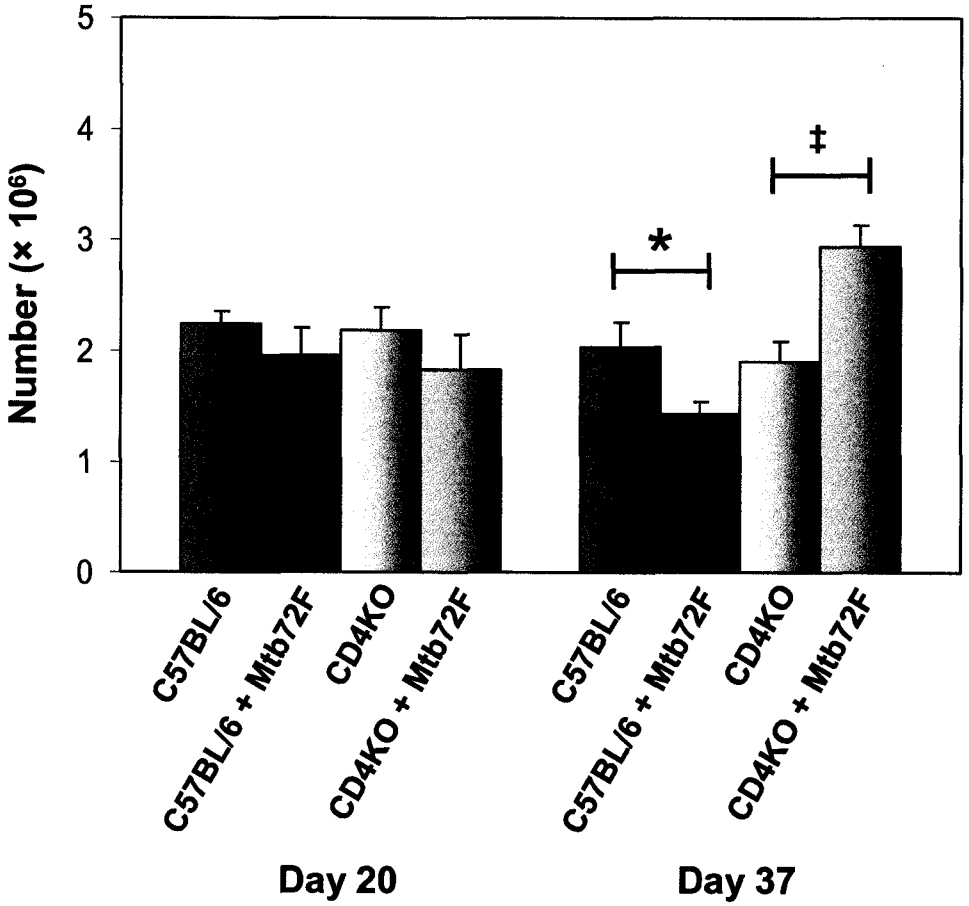

Figure 3.16. In the absence of CD4 T cells, comparable numbers of CD8 T cells are recruited into the lungs of mice infected with *M. tuberculosis*. Data are expressed as the means ± the standard errors of the means and are from four mice per group per timepoint. Statistical significance based upon a comparison of Mtb72F immunized and nonimmunized groups was determined using Student's *t* test (* = $P < 0.05$, ‡ = $P < 0.01$).

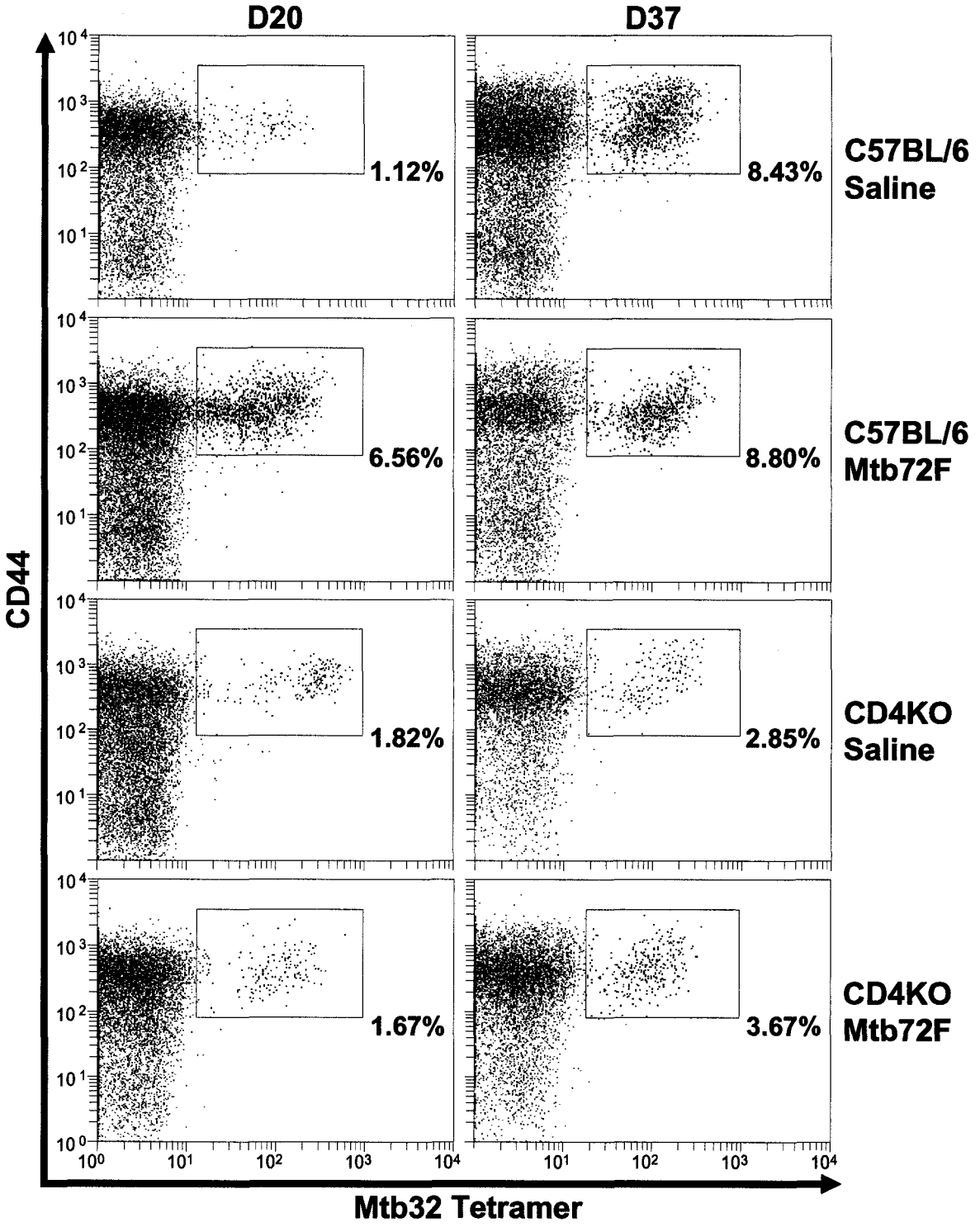

Figure 3.17. CD4 T cells are required for the efficient generation and expansion of Mtb32-specific CD8 T cells following immunization with Mtb72F and LDA infection with *M. tuberculosis* H37Rv. C57BL/6 or CD4KO mice (n=4) were immunized three times, at three week intervals via the intramuscular route. Lymphocytes were gated based upon characteristic size and granularity, and further gated based upon concurrent CD3 and CD8 expression. Percentages represent the number of $CD44^{hi}$ $tetramer^{+}$ cells as compared to the total number of $CD3^{+}/CD8^{+}$ cells. In all cases, background tetramer staining in naïve mice was < 0.15%.

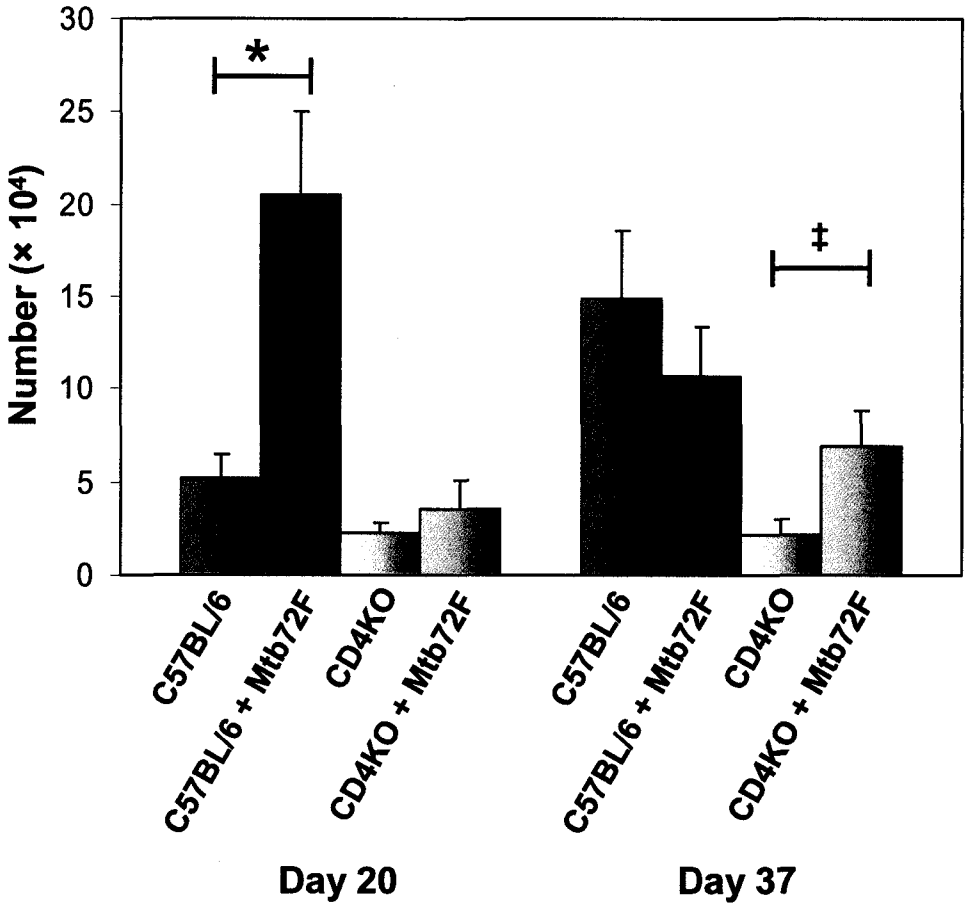

Figure 3.18. Total number of Mtb32-specific CD8 T cells in the lungs of C57BL/6 or CD4KO mice following immunization with Mtb72F and subsequent aerosol infection with *M. tuberculosis* H37Rv. At 20 days and 37 days following aerosol infection, lungs were harvested and stained using the Mtb32 H-2D^b tetramer reagent and antibodies specific for CD3, CD8, and CD44. Data are expressed as the means ± the standard errors of the means and are from four mice per group per timepoint. Statistical significance based upon a comparison of Mtb72F immunized and nonimmunized groups was determined using Student's *t* test (* = $P < 0.05$, ‡ = $P < 0.1$).

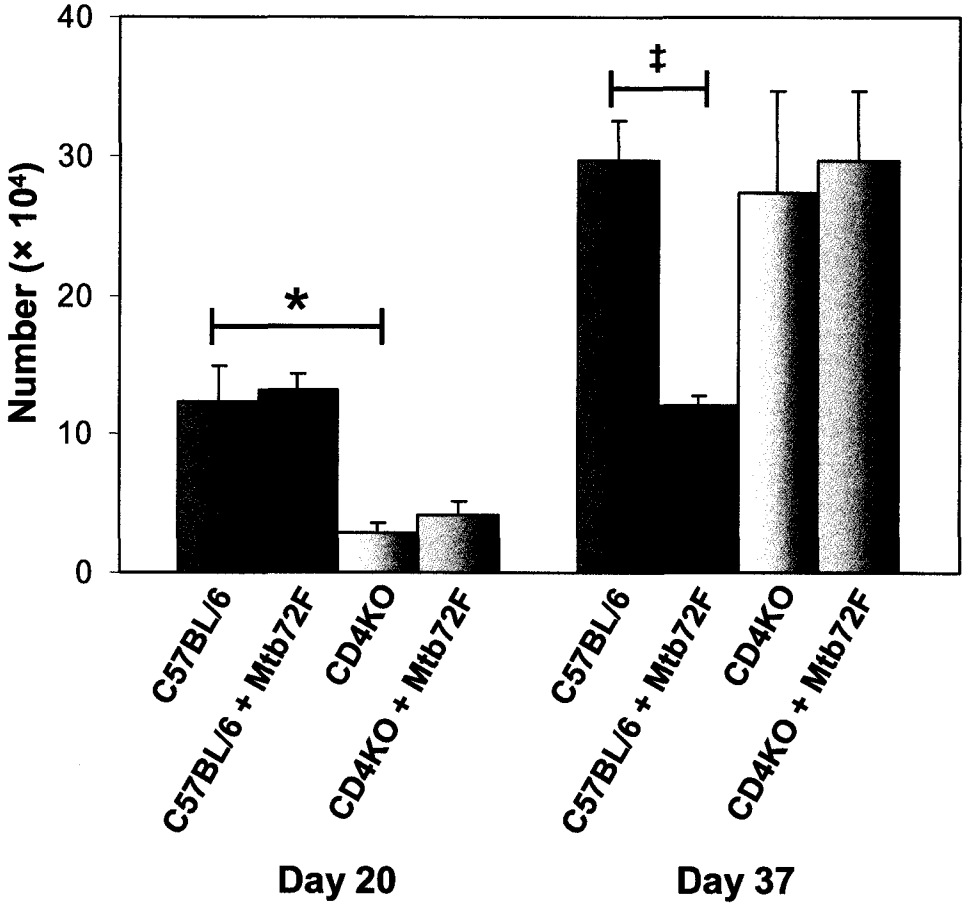

Figure 3.19. Total number of CD8 T cells producing IFN-γ in the lungs of immunized and nonimmunized mice. Data are expressed as the means ± the standard errors of the means and are from four mice per group per timepoint. Statistical significance based upon a comparison of Mtb72F immunized and nonimmunized or wild-type and CD4KO groups was determined using Student's *t* test (* = $P < 0.005$, ‡ = $P < 0.001$).

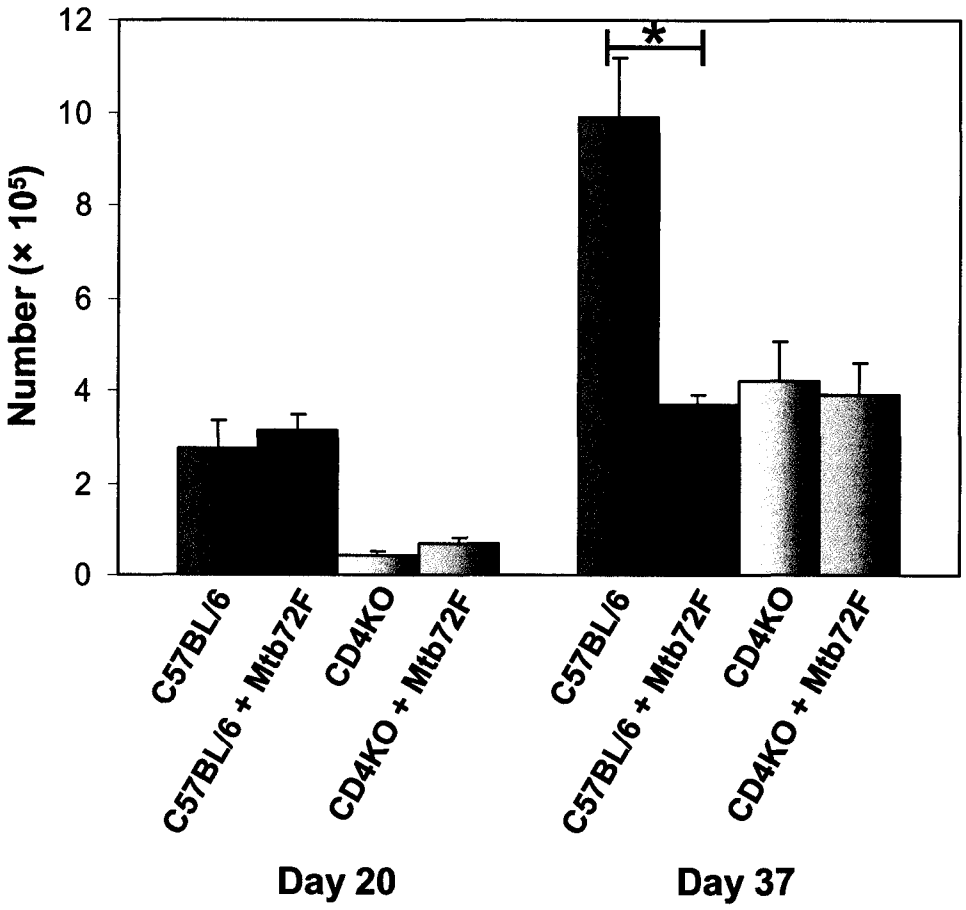

Figure 3.20. Total number of IFN-γ^+ cells in the lungs of mice. IFN-γ production is delayed in CD4KO mice, and the total number of IFN-γ^+ cells is reduced when compared to wild-type mice. Data are expressed as the means ± the standard errors of the means and are from four mice per group per timepoint. Statistical significance based upon a comparison of Mtb72F immunized and nonimmunized groups was determined using Student's *t* test and is indicated by an asterisk ($P < 0.005$).

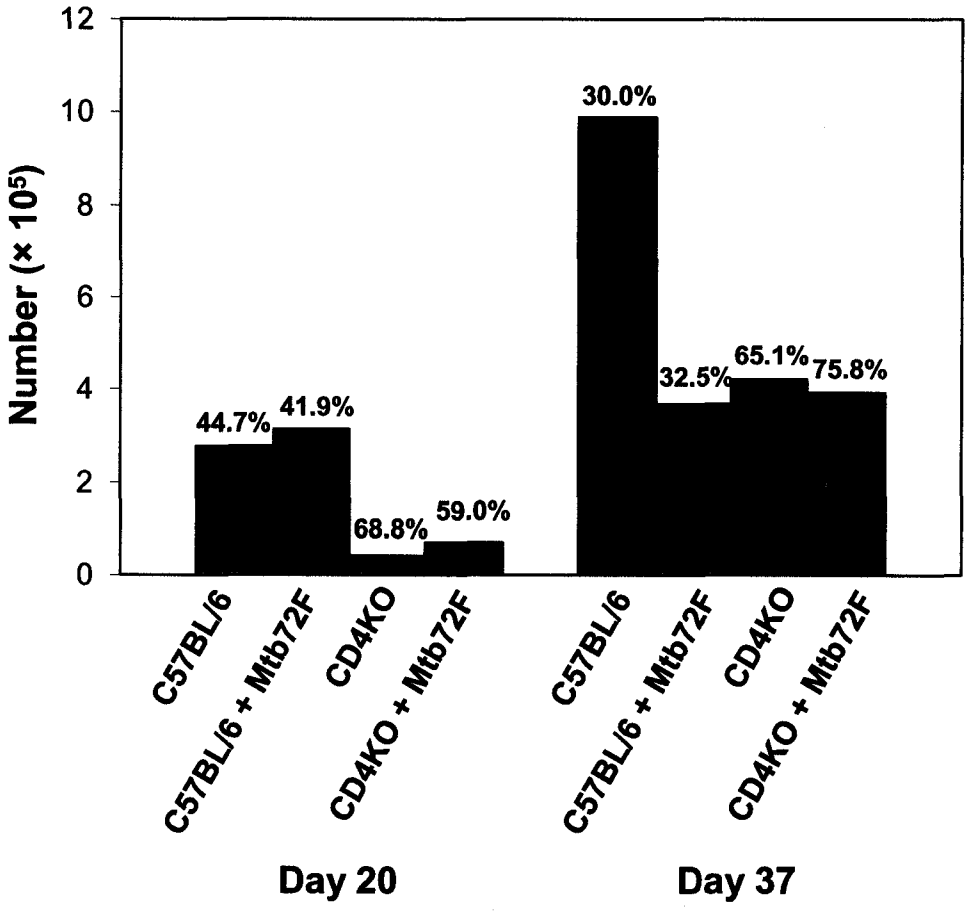

Figure 3.21. CD8 T cells account for the majority of IFN-γ producing cells in the lungs of CD4KO mice. The total number of CD8 T cells producing IFN-γ (green bars) is compared to the total number of IFN-γ producing cells in the lung (orange bars). Percentages represent the mean number of IFN-γ^+ CD8 T cells as compared to the mean total number of IFN-γ^+ cells.

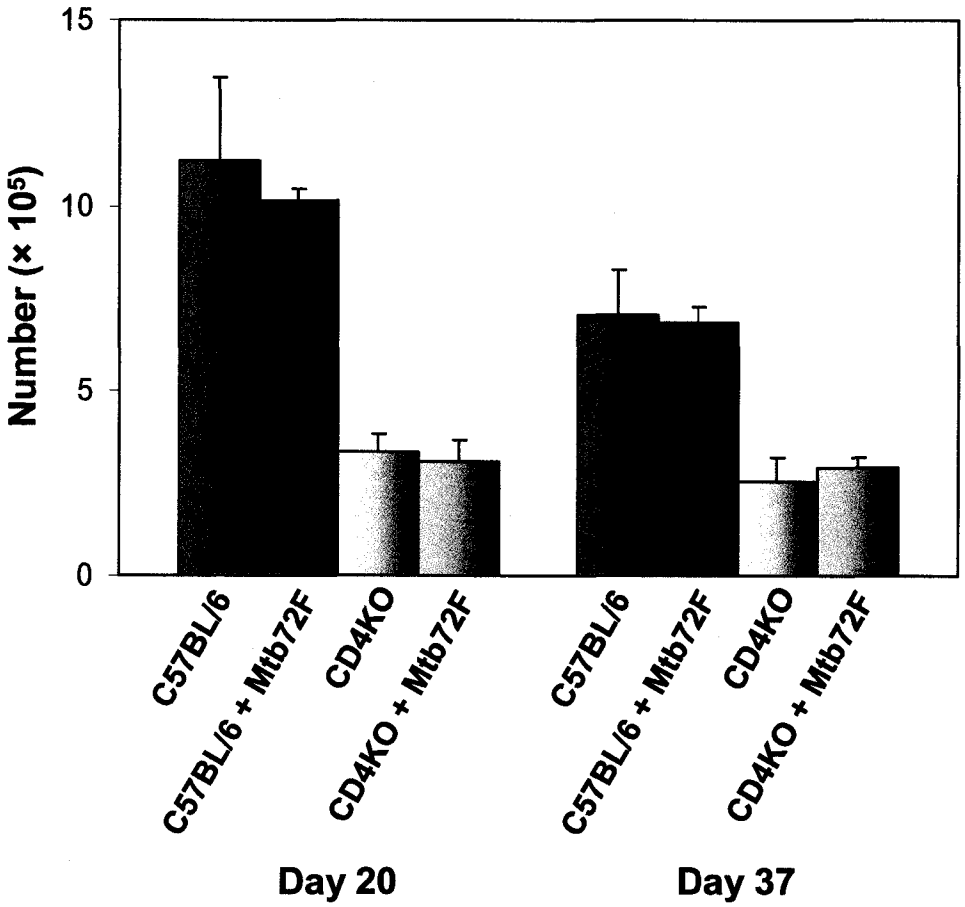

Figure 3.22. In the absence of CD4 T cells, CD4KO mice do not recruit more NK1.1$^+$ cells into the lung. Histogram represents the total number of NK1.1$^+$ cells in the lung. Data are expressed as the means ± the standard errors of the means and are from four mice per group per timepoint. Statistical significance based upon a comparison of Mtb72F immunized and nonimmunized groups was determined using Student's *t* test and no significant differences were present.

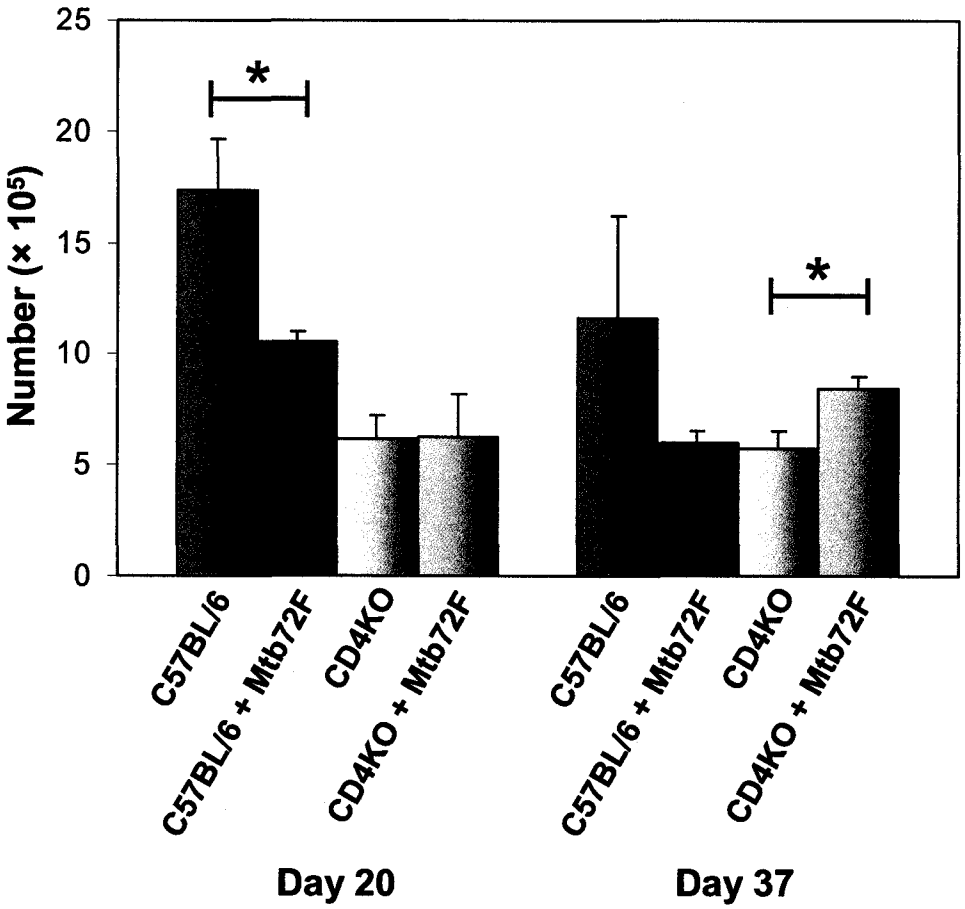

Figure 3.23. CD4KO mice do not recruit more γδ cells into the lung. Histogram represents the total number of γδ cells in the lung. Data are expressed as the means ± the standard errors of the means and are from four mice per group per timepoint. Statistical significance based upon a comparison of Mtb72F immunized and nonimmunized groups was determined using Student's *t* test and is indicated by an asterisk ($P < 0.05$).

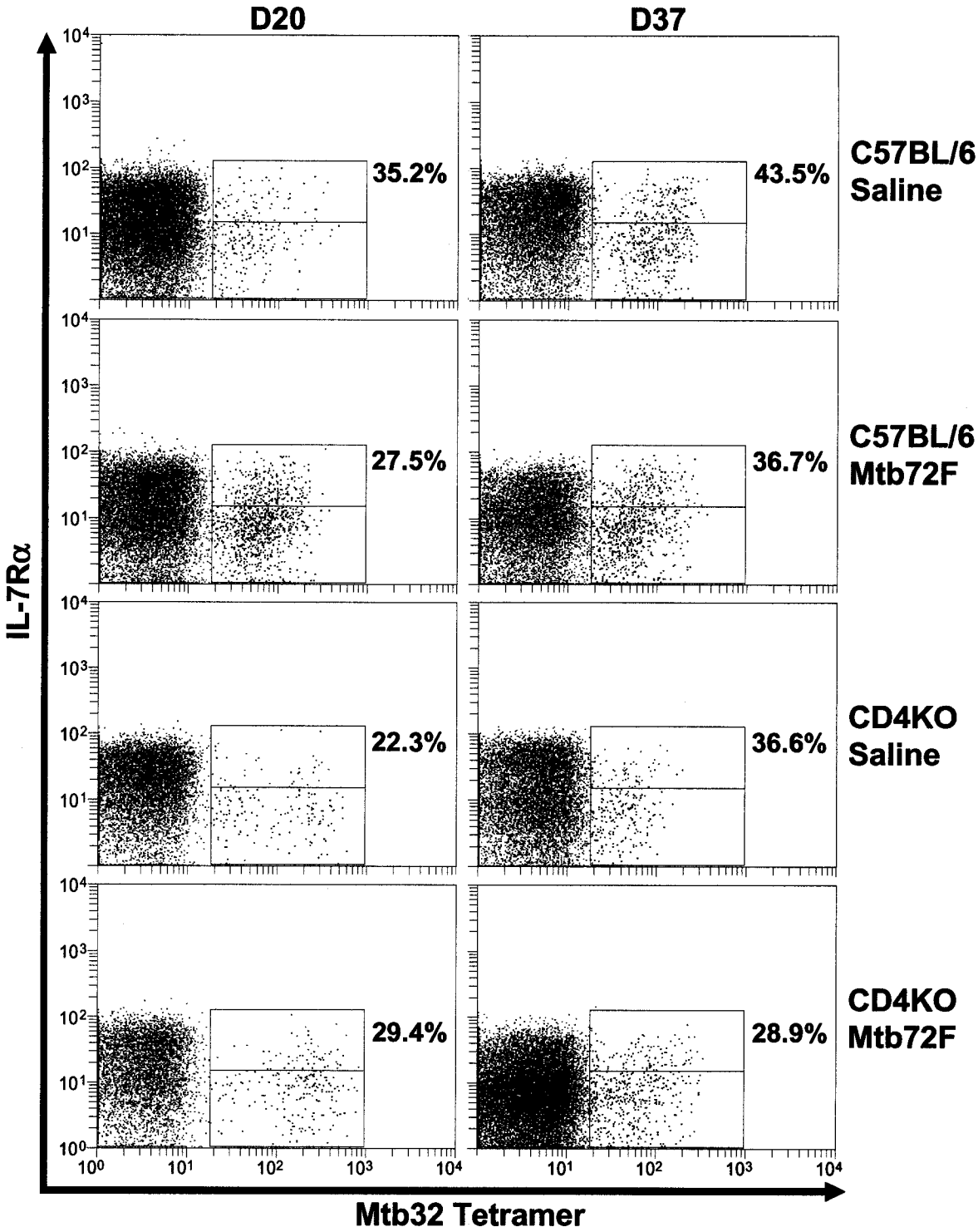

Figure 3.24. The absence of CD4 T cells does not prevent the generation of CD8 T cells with a memory precursor phenotype. Lung cells were stained with the H-2D^b tetramer and antibodies specific for CD3, CD8, and IL-7Rα. Lymphocytes were gated based upon characteristic size and granularity, and further gated based upon concurrent CD3 and CD8 expression. The data are from one mouse, and are representative of n=4. Percentages represent the number of IL-7Rα^{hi} tetramer$^+$ cells as compared to the total number of tetramer$^+$ cells. In all cases, background tetramer staining in naïve mice was < 0.15%.

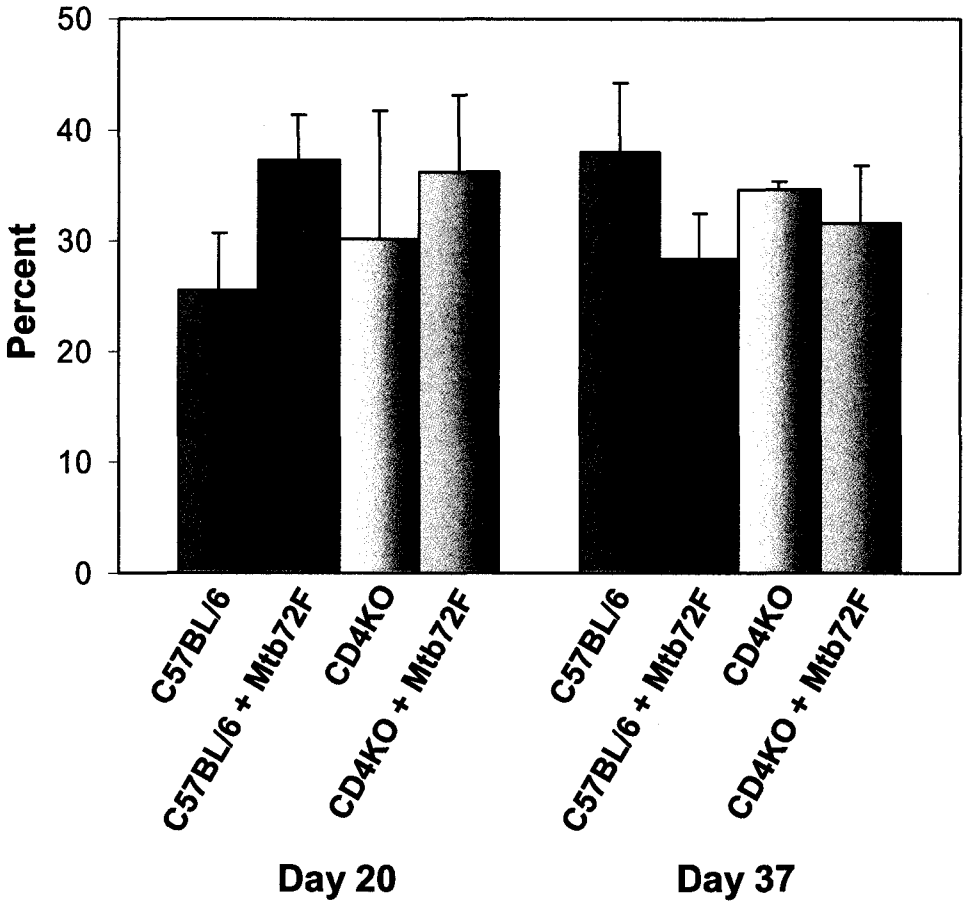

Figure 3.25. Percent of Mtb32 tetramer$^+$ CD8 T cells expressing IL-7Rα. Percentages represent the mean number of IL-7Rα$^+$ Mtb32 tetramer$^+$ CD8 T cells as compared to the total number of Mtb32 tetramer$^+$ CD8 T cells in the lung. Data are expressed as the means ± the standard errors of the means and are from four mice per group per timepoint. Statistical significance based upon a comparison of Mtb72F immunized and nonimmunized groups was determined using Student's *t* test and no significant differences were present.

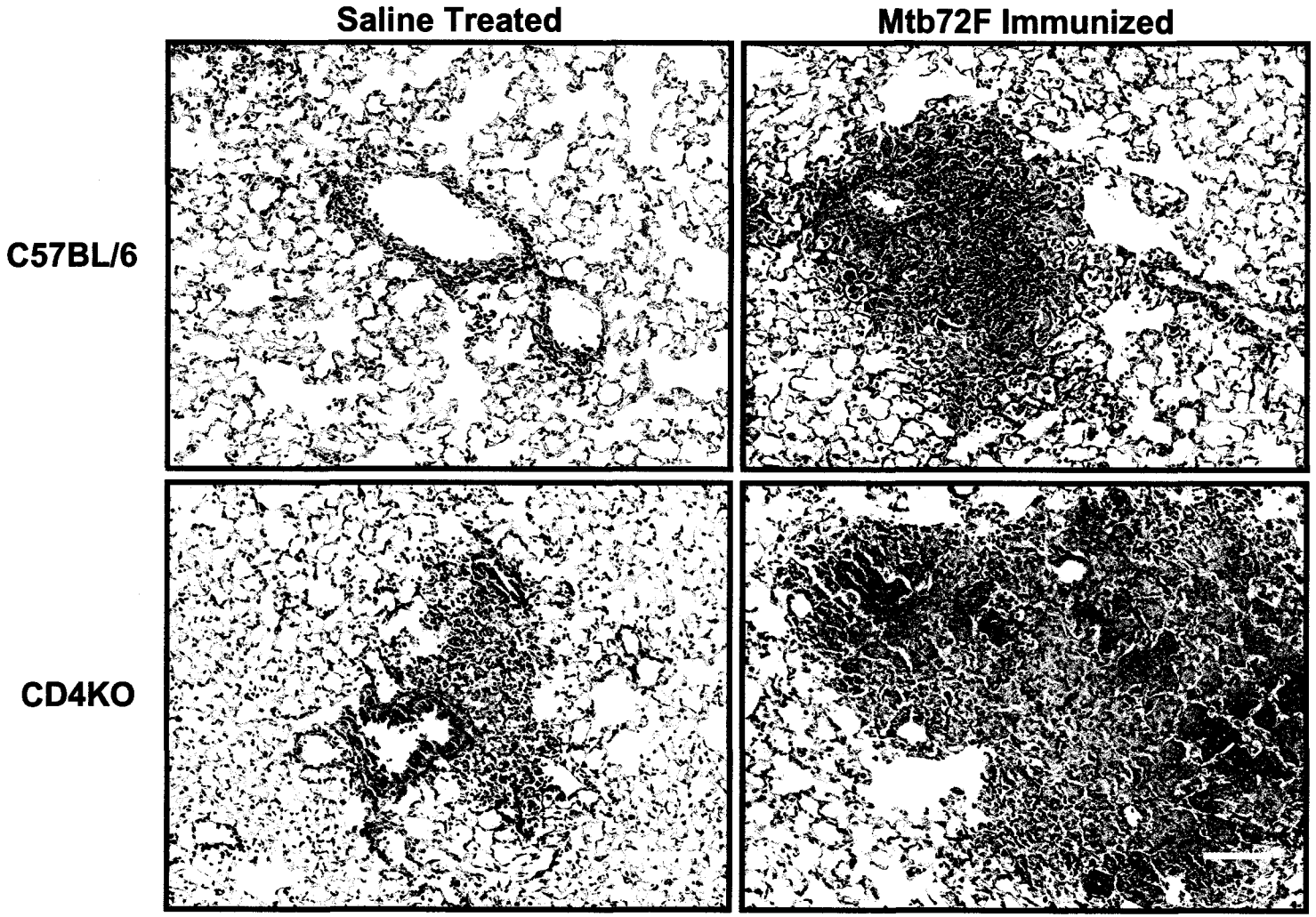

Figure 3.26. Histological comparison of lung tissue obtained from either wild-type C57BL/6 or CD4KO mice 20 days following LDA infection. Mice were immunized as previously described. Yellow size bar represents 200 μm.

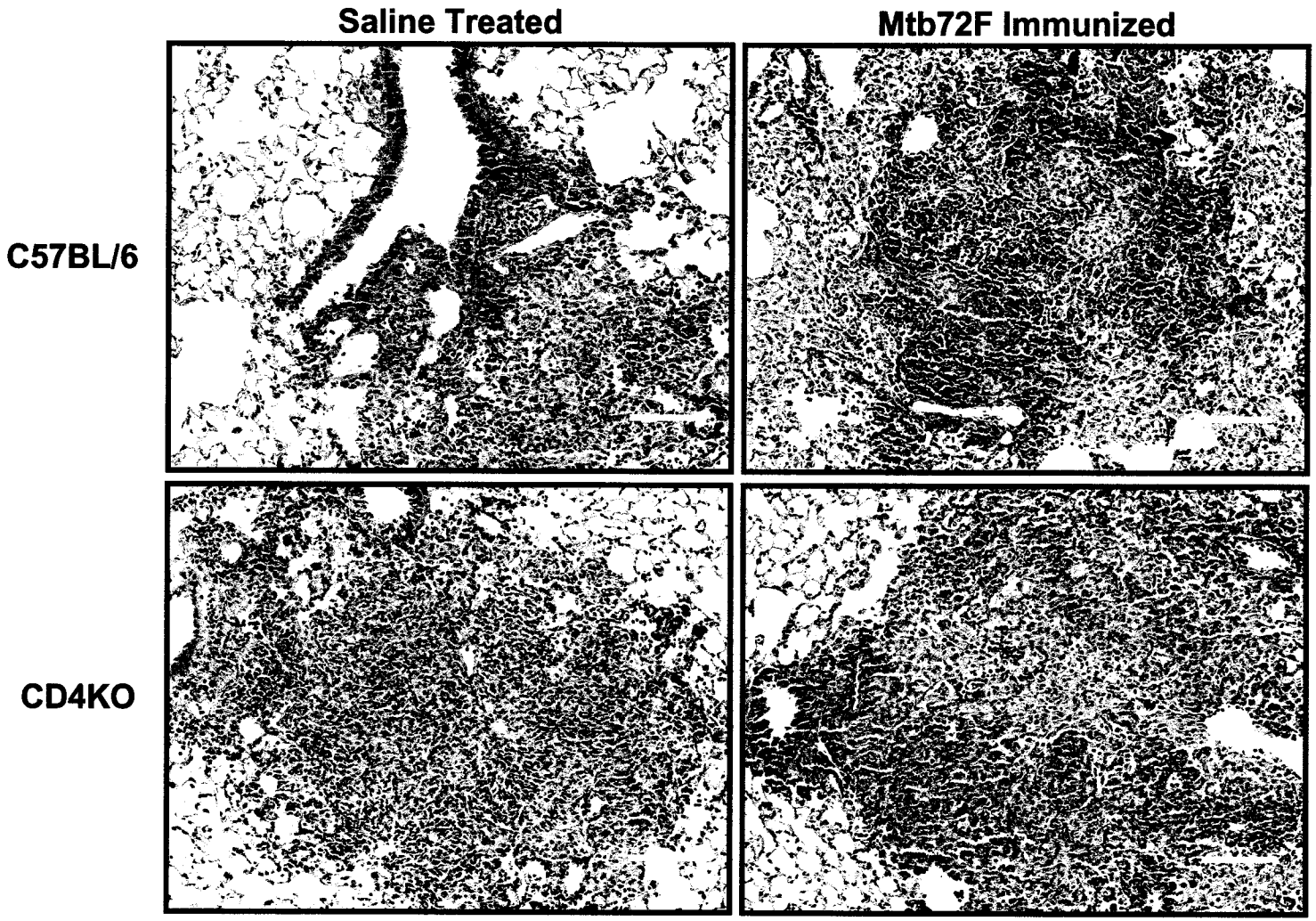

Figure 3.27. Histological comparison of lung tissue obtained from either wild-type C57BL/6 or CD4KO mice 37 days following LDA infection. Mice were immunized as previously described. Yellow size bar represents 200 μm.

References

1. **Andersen, P.** 1994. Effective vaccination of mice against *Mycobacterium tuberculosis* infection with a soluble mixture of secreted mycobacterial proteins. Infect Immun **62:**2536-44.

2. **Andersen, P.** 2001. TB vaccines: progress and problems. Trends Immunol **22:**160-8.

3. **Behar, S. M., C. C. Dascher, M. J. Grusby, C. R. Wang, and M. B. Brenner.** 1999. Susceptibility of mice deficient in CD1D or TAP1 to infection with *Mycobacterium tuberculosis*. J Exp Med **189:**1973-80.

4. **Bloom, B. R., and C. J. Murray.** 1992. Tuberculosis: commentary on a reemergent killer. Science **257:**1055-64.

5. **Boom, W. H.** 1996. The role of T-cell subsets in *Mycobacterium tuberculosis* infection. Infect Agents Dis **5:**73-81.

6. **Brandt, L., Y. A. Skeiky, M. R. Alderson, Y. Lobet, W. Dalemans, O. C. Turner, R. J. Basaraba, A. A. Izzo, T. M. Lasco, P. L. Chapman, S. G. Reed, and I. M. Orme.** 2004. The protective effect of the *Mycobacterium bovis* BCG vaccine is increased by coadministration with the *Mycobacterium tuberculosis* 72-kilodalton fusion polyprotein Mtb72F in *M. tuberculosis*-infected guinea pigs. Infect Immun **72:**6622-32.

7. **Brewer, T. F., and G. A. Colditz.** 1995. Relationship between bacille Calmette-Guérin (BCG) strains and the efficacy of BCG vaccine in the prevention of tuberculosis. Clin Infect Dis **20:**126-35.

8. **Caruso, A. M., N. Serbina, E. Klein, K. Triebold, B. R. Bloom, and J. L. Flynn.** 1999. Mice deficient in CD4 T cells have only transiently diminished levels of IFN-γ, yet succumb to tuberculosis. J Immunol **162:**5407-16.

9. **Colditz, G. A., T. F. Brewer, C. S. Berkey, M. E. Wilson, E. Burdick, H. V. Fineberg, and F. Mosteller.** 1994. Efficacy of BCG vaccine in the prevention of tuberculosis. Meta-analysis of the published literature. Jama **271:**698-702.

10. **Cooper, A. M., D. K. Dalton, T. A. Stewart, J. P. Griffin, D. G. Russell, and I. M. Orme.** 1993. Disseminated tuberculosis in interferon gamma gene-disrupted mice. J Exp Med **178:**2243-7.

11. **Cooper, A. M., C. D'Souza, A. A. Frank, and I. M. Orme.** 1997. The course of *Mycobacterium tuberculosis* infection in the lungs of mice lacking expression of either perforin- or granzyme-mediated cytolytic mechanisms. Infect Immun **65:**1317-20.

12. **Dillon, D. C., M. R. Alderson, C. H. Day, D. M. Lewinsohn, R. Coler, T. Bement, A. Campos-Neto, Y. A. Skeiky, I. M. Orme, A. Roberts, S. Steen, W. Dalemans, R. Badaro, and S. G. Reed.** 1999. Molecular characterization and human T-cell responses to a member of a novel *Mycobacterium tuberculosis* mtb39 gene family. Infect Immun **67:**2941-50.

13. **Dye, C., S. Scheele, P. Dolin, V. Pathania, and M. C. Raviglione.** 1999. Consensus statement. Global burden of tuberculosis: estimated incidence, prevalence, and mortality by country. WHO Global Surveillance and Monitoring Project. Jama **282:**677-86.

14. **Feng, C. G., A. G. Bean, H. Hooi, H. Briscoe, and W. J. Britton.** 1999. Increase in gamma interferon-secreting $CD8^+$, as well as $CD4^+$, T cells in lungs following aerosol infection with *Mycobacterium tuberculosis*. Infect Immun **67:**3242-7.

15. **Fine, P. E.** 1989. The BCG story: lessons from the past and implications for the future. Rev Infect Dis **11 Suppl 2:**S353-9.

16. **Fine, P. E.** 1995. Variation in protection by BCG: implications of and for heterologous immunity. Lancet **346:**1339-45.

17. **Flynn, J. L., J. Chan, K. J. Triebold, D. K. Dalton, T. A. Stewart, and B. R. Bloom.** 1993. An essential role for interferon-γ in resistance to *Mycobacterium tuberculosis* infection. J Exp Med **178:**2249-54.

18. **Flynn, J. L., M. M. Goldstein, K. J. Triebold, B. Koller, and B. R. Bloom.** 1992. Major histocompatibility complex class I-restricted T cells are required for resistance to *Mycobacterium tuberculosis* infection. Proc Natl Acad Sci U S A **89:**12013-7.

19. **Ginsberg, A. M.** 1998. The tuberculosis epidemic. Scientific challenges and opportunities. Public Health Rep **113:**128-36.

20. **Girard, M. P., U. Fruth, and M. P. Kieny.** 2005. A review of vaccine research and development: Tuberculosis. Vaccine.

21. **Griffin, J. P., and I. M. Orme.** 1994. Evolution of CD4 T-cell subsets following infection of naive and memory immune mice with *Mycobacterium tuberculosis*. Infect Immun **62:**1683-90.

22. **Guleria, I., R. Mukherjee, and S. H. Kaufmann.** 1993. *In vivo* depletion of CD4 and CD8 T lymphocytes impairs *Mycobacterium w* vaccine-induced protection against *M. tuberculosis* in mice. Med Microbiol Immunol (Berl) **182:**129-35.

23. **Horwitz, M. A., B. W. Lee, B. J. Dillon, and G. Harth.** 1995. Protective immunity against tuberculosis induced by vaccination with major extracellular proteins of *Mycobacterium tuberculosis*. Proc Natl Acad Sci U S A **92:**1530-4.

24. **Hubbard, R. D., C. M. Flory, and F. M. Collins.** 1992. Immunization of mice with mycobacterial culture filtrate proteins. Clin Exp Immunol **87:**94-8.

25. **Jouanguy, E., S. Lamhamedi-Cherradi, F. Altare, M. C. Fondaneche, D. Tuerlinckx, S. Blanche, J. F. Emile, J. L. Gaillard, R. Schreiber, M. Levin, A. Fischer, C. Hivroz, and J. L. Casanova.** 1997. Partial interferon-γ receptor 1 deficiency in a child with tuberculoid bacillus Calmette-Guérin infection and a sibling with clinical tuberculosis. J Clin Invest **100:**2658-64.

26. **Junqueira-Kipnis, A. P., J. Turner, M. Gonzalez-Juarrero, O. C. Turner, and I. M. Orme.** 2004. Stable T-cell population expressing an effector cell surface phenotype in the lungs of mice chronically infected with *Mycobacterium tuberculosis*. Infect Immun **72:**570-5.

27. **Kaech, S. M., J. T. Tan, E. J. Wherry, B. T. Konieczny, C. D. Surh, and R. Ahmed.** 2003. Selective expression of the interleukin 7 receptor identifies effector CD8 T cells that give rise to long-lived memory cells. Nat Immunol **4:**1191-8.

28. **Kamath, A. B., J. Woodworth, X. Xiong, C. Taylor, Y. Weng, and S. M. Behar.** 2004. Cytolytic $CD8^+$ T cells recognizing CFP10 are recruited to the lung after *Mycobacterium tuberculosis* infection. J Exp Med **200:**1479-89.

29. **Laochumroonvorapong, P., J. Wang, C. C. Liu, W. Ye, A. L. Moreira, K. B. Elkon, V. H. Freedman, and G. Kaplan.** 1997. Perforin, a cytotoxic molecule which mediates cell necrosis, is not required for the early control of mycobacterial infection in mice. Infect Immun **65:**127-32.

30. **Mogues, T., M. E. Goodrich, L. Ryan, R. LaCourse, and R. J. North.** 2001. The relative importance of T cell subsets in immunity and immunopathology of airborne *Mycobacterium tuberculosis* infection in mice. J Exp Med **193:**271-80.

31. **Muller, I., S. P. Cobbold, H. Waldmann, and S. H. Kaufmann.** 1987. Impaired resistance to *Mycobacterium tuberculosis* infection after selective *in vivo* depletion of $L3T4^+$ and $Lyt\text{-}2^+$ T cells. Infect Immun **55:**2037-41.

32. **Orme, I. M.** 1987. The kinetics of emergence and loss of mediator T lymphocytes acquired in response to infection with *Mycobacterium tuberculosis*. J Immunol **138:**293-8.

33. **Orme, I. M.** 2001. The search for new vaccines against tuberculosis. J Leukoc Biol **70:**1-10.

34. **Orme, I. M., and F. M. Collins.** 1984. Adoptive protection of the *Mycobacterium tuberculosis*-infected lung. Dissociation between cells that passively transfer protective immunity and those that transfer delayed-type hypersensitivity to tuberculin. Cell Immunol **84:**113-20.

35. **Orme, I. M., and F. M. Collins.** 1983. Protection against *Mycobacterium tuberculosis* infection by adoptive immunotherapy. Requirement for T cell-deficient recipients. J Exp Med **158:**74-83.

36. **Orme, I. M., and A. A. Izzo.** 2005. TB Vaccine Preclinical Screening and Development, p. 561-571. *In* S. T. Cole (ed.), *Tuberculosis and the Tubercle Bacillus*. ASM Press, Washington, DC.

37. **Orme, I. M., D. N. McMurray, and J. T. Belisle.** 2001. Tuberculosis vaccine development: recent progress. Trends Microbiol **9:**115-8.

38. **Orme, I. M., A. D. Roberts, J. P. Griffin, and J. S. Abrams.** 1993. Cytokine secretion by CD4 T lymphocytes acquired in response to *Mycobacterium tuberculosis* infection. J Immunol **151:**518-25.

39. **Romano, M., O. Denis, S. D'Souza, X. M. Wang, T. H. Ottenhoff, J. M. Brulet, and K. Huygen.** 2004. Induction of *in vivo* functional D^b-restricted cytolytic T cell activity against a putative phosphate transport receptor of *Mycobacterium tuberculosis*. J Immunol **172:**6913-21.

40. **Scanga, C. A., V. P. Mohan, K. Yu, H. Joseph, K. Tanaka, J. Chan, and J. L. Flynn.** 2000. Depletion of $CD4^+$ T cells causes reactivation of murine persistent tuberculosis despite continued expression of interferon gamma and nitric oxide synthase 2. J Exp Med **192:**347-58.

41. **Serbina, N. V., and J. L. Flynn.** 1999. Early emergence of $CD8^+$ T cells primed for production of type 1 cytokines in the lungs of *Mycobacterium tuberculosis*-infected mice. Infect Immun **67:**3980-8.

42. **Serbina, N. V., V. Lazarevic, and J. L. Flynn.** 2001. $CD4^+$ T cells are required for the development of cytotoxic $CD8^+$ T cells during *Mycobacterium tuberculosis* infection. J Immunol **167:**6991-7000.

43. **Skeiky, Y. A., M. R. Alderson, P. J. Ovendale, J. A. Guderian, L. Brandt, D. C. Dillon, A. Campos-Neto, Y. Lobet, W. Dalemans, I. M. Orme, and S. G. Reed.** 2004. Differential immune responses and protective efficacy induced by components of a tuberculosis polyprotein vaccine, Mtb72F, delivered as naked DNA or recombinant protein. J Immunol **172:**7618-28.

44. **Skeiky, Y. A., M. J. Lodes, J. A. Guderian, R. Mohamath, T. Bement, M. R. Alderson, and S. G. Reed.** 1999. Cloning, expression, and immunological evaluation of two putative secreted serine protease antigens of *Mycobacterium tuberculosis*. Infect Immun **67:**3998-4007.

45. **Sousa, A. O., R. J. Mazzaccaro, R. G. Russell, F. K. Lee, O. C. Turner, S. Hong, L. Van Kaer, and B. R. Bloom.** 2000. Relative contributions of distinct MHC class I-dependent cell populations in protection to tuberculosis infection in mice. Proc Natl Acad Sci U S A **97:**4204-8.

46. **Sterne, J. A., L. C. Rodrigues, and I. N. Guedes.** 1998. Does the efficacy of BCG decline with time since vaccination? Int J Tuberc Lung Dis **2:**200-7.

47. **Templeton, N. S., D. D. Lasic, P. M. Frederik, H. H. Strey, D. D. Roberts, and G. N. Pavlakis.** 1997. Improved DNA: liposome complexes for increased systemic delivery and gene expression. Nat Biotechnol **15:**647-52.

48. **Turner, J., C. D. D'Souza, J. E. Pearl, P. Marietta, M. Noel, A. A. Frank, R. Appelberg, I. M. Orme, and A. M. Cooper.** 2001. CD8- and CD95/95L-dependent mechanisms of resistance in mice with chronic pulmonary tuberculosis. Am J Respir Cell Mol Biol **24:**203-9.

49. **Wang, A., J. Clapper, J. A. Guderian, T. M. Foy, G. R. Fanger, M. W. Retter, and Y. A. Skeiky.** 2003. A novel method for increasing the expression level of recombinant proteins. Protein Expr Purif **30:**124-33.

50. **World Health Organization.** 2004. The World Health Report 2004. World Health Organization.

Chapter 4

The Antigen-Specific CD8 T Cell Response to Mtb10.3/4

Introduction

Mycobacterium tuberculosis is a highly successful facultative intracellular pathogen that infects approximately one-third of the world's population [3]. Due to the variable protective efficacy of the bacille Calmette-Guérin (BCG) vaccine, development of a safe and more effective vaccine has become a global priority. In order to facilitate rational vaccine design, small animal models of tuberculosis infection have been utilized to characterize the correlates of protection, and to screen potential vaccine candidates. It has been established that a protective immune response to tuberculosis relies on the induction of cell-mediated immunity, primarily involving CD4 T cells. However, there is also increasing experimental evidence in support of a protective role for CD8 T cells. It has been shown that CD8 T cells rapidly accumulate at the sites of infection, and that these cells can produce IFN-γ, which is known to be essential for protection during *M. tuberculosis* infection [4, 12]. Experiments using CD8 knock-out (KO), MHC class I KO, and H-2K^b/D^b KO mouse models all support a protective role for CD8 T cells [9, 11, 13-15]. In addition, antibody depletion of CD8 T cells increases susceptibility to aerosol infection with *M. tuberculosis*, with the greatest CD8 T cell-mediated effect being evident during the chronic stage of infection [10, 16].

In a recent publication, a murine CD8 T cell epitope was defined that was present in Mtb10.3 and Mtb10.4; two related *M. tuberculosis*-derived proteins of unknown function in the ESAT-6 family of low molecular weight, secreted proteins [8]. Unfortunately, this paper did not examine the *in vivo* immunological reactivity of this epitope during infection with *M. tuberculosis*, nor did it examine whether this antigenic

epitope was protective in a low dose aerosol mouse model of tuberculosis infection. As such, we sought to determine if this epitope conferred protection and therefore should be considered for inclusion in candidate tuberculosis vaccines. We also wished to define the extent of immunological reactivity to this single antigenic epitope to further define the role that CD8 T cells play during pulmonary infection with tuberculosis. By utilizing a MHC class I H-2K^d tetramer reagent, we were able to examine the magnitude and kinetics of the Mtb10.3/4 antigen-specific CD8 T cell response in Balb/c mice during the course of infection.

Materials & Methods

Mice. Studies were performed using 8-10 week old specific pathogen-free female Balb/c mice purchased from Charles River Laboratories (Wilmington, MA). All mice were maintained within a biosafety level III facility at Colorado State University for the duration of the experiments, and had free access to sterile water and standard mouse chow. The specific pathogen-free nature of the mouse colonies was demonstrated by testing sentinel animals, which were shown to be negative for 13 known mouse pathogens. All experimental procedures were approved by the Colorado State University Animal Care and Use Committee.

Bacterial Strains. *M. tuberculosis* strain H37Rv, originally obtained from the Trudeau Mycobacteria Collection (TMCC #102), was grown from low passage seed lots in

Proskauer-Beck liquid media containing 0.05% Tween 80 to mid-log phase, and 1.5 ml aliquots were frozen at -70°C until use.

Immunizations and Aerosol Infection. Mice were immunized 3 times at 3 week intervals with either 25 μg of GYAGTLQSL peptide in monophosphoryl lipid A-squalene emulsion (MPL-SE; Corixa Corporation, 25 μg/dose) and dimethyl dioctadecylammonium bromide (DDA; Eastman Kodak, Inc., Rochester, N.Y., 250 μg/dose), MPL-SE/DDA adjuvant, phosphate buffered saline (PBS), or 50 μg low molecular weight culture filtrate protein (LMW CFP; Colorado State University, Fort Collins, CO) in MPL-SE/DDA. All immunizations were performed via the intramuscular (tibialis) route. For each immunization, mice were injected with a total volume of 100 μl/mouse using 50 μl/leg. Three weeks following the last immunization, mice were infected via the aerosol route using a Glas-Col aerosol generator (Glas-Col, Terre Haute, IN), such that ~100 viable bacteria were deposited in the lungs of each animal. The number of viable bacteria in the lungs was determined at specific timepoints by plating 10-fold serial dilutions of individual partial organ homogenates on nutrient Middlebrook 7H11 agar, and counting bacterial colonies after 21 days of incubation at 37°C.

Single-Cell Suspension Preparation. Animals were sacrificed by carbon dioxide asphyxiation and were perfused through the heart with 10 ml cold PBS containing 3 U/ml heparin (Sigma-Aldrich, St. Louis, MO). The lungs were removed from the pulmonary cavity and placed in cold Dulbecco's minimal essential medium (DMEM; Cellgro, Herndon, VA). The lung tissue was disrupted using sterile razor blades and incubated for

30 minutes at 37°C in a final volume of 2 ml DMEM containing 0.7 mg/ml collagenase D (Roche Applied Science, Indianapolis, IN) and 30 μg/ml deoxyribonuclease (Sigma-Aldrich). Following incubation, the digested lung tissue was gently passed through a sterile 70 μm nylon screen, rinsed using 8 ml cold DMEM supplemented with 10% heat-inactivated endotoxin low fetal bovine serum (Atlas Biologicals, Fort Collins, CO), 10 mM HEPES buffer (Sigma-Aldrich), 2 mM L-glutamine (Sigma-Aldrich), 2% MEM-nonessential amino acids (100x; Sigma-Aldrich), 50 μM 2-mercaptoethanol (Sigma-Aldrich) and centrifuged at 200 × *g*. Red blood cells were lysed using Gey's solution (0.15 M NH_4Cl, 10 mM $KHCO_3$) and the samples were centrifuged and resuspended in DMEM plus supplements. Cells were counted using a hemacytometer and aliquots were taken for flow cytometric analysis.

Flow Cytometry. Single-cell suspensions from individual mice were resuspended in PBS containing 0.1% sodium azide (Fisher Chemicals, Fairlawn, NJ). Cells were incubated in the dark for 20 minutes at 4°C with specific antibody (directly conjugated to fluorescein isothiocyanate [FITC], phycoerythrin [PE], peridinin chlorophyll *a* protein [PerCP], or allophycocyanin [APC] at 3 μg/ml), followed by 2 washes using PBS with sodium azide. Cells were analyzed immediately using a FACSCalibur dual laser flow cytometer (BD Biosciences, Mountain View, CA) and the data were analyzed using CellQwest software (BD Biosciences, San Jose, CA) and Summit software (DakoCytomation, Fort Collins, CO). Viable lymphocytes were gated based upon their forward- and side-scatter characteristics and cell populations were analyzed by expression of fluorochrome-labeled markers. All analyses were performed with a minimum acquisition of 200,000 events.

Cell surface markers were analyzed with the following specific antibodies: FITC anti-CD44 (clone IM7); PE anti-CD62L (clone MEL-14), anti-NK1.1 (clone PK136); PerCP anti-CD8α (clone 53-6.7); and APC anti-CD3ε (clone 145-2C11). Cell suspensions were also stained with a PE-Mtb10.3/4 H-2K^d MHC class I tetramer (NIH Tetramer Facility, Bethesda, MD) containing the peptide GYAGTLQSL. Background staining with this tetramer reagent was less than 0.5% when staining cells from naïve mice or from MHC mismatched (C57BL/6, H-2^b) mice.

***In vivo* Cytolytic Assay.** Whole splenocytes were harvested from naïve Balb/c donor mice and red blood cells were lysed using Gey's solution. Half of the splenocytes were stained with 0.5 μM carboxyfluorescein diacetate, succinimidyl ester (CFSE^{lo}; Invitrogen, Carlsbad, CA) and the other half were stained with 5 μM CFSE (CFSE^{hi}) in PBS for 10 minutes at room temperature in the dark. Cells were washed two times with DMEM plus supplements and the CFSE^{hi} cells were pulsed with 10 μM GYAGTLQSL peptide for 1 hour at 37°C. Cells were washed two times in PBS, and resuspended in PBS at a concentration of 5×10^7 cells/ml. CFSE^{hi} and CFSE^{lo} cells were mixed in a 1:1 ratio, and 10^7 total cells in a volume of 200 μl were transferred i.v. into naïve mice and mice that had been infected with *M. tuberculosis* H37Rv for 30 days by low dose aerosol infection. Lungs and spleens were harvested 18 hours later and examined by flow cytometry.

Histology. Individual lung lobes were first perfused and then immersed in 10% phosphate-buffered formalin solution and embedded in paraffin wax. Sections of 5 μm

thickness were prepared and stained using hematoxylin and eosin, and examined by a trained pathologist in a double-blinded fashion.

Data & Results

A large, persistent Mtb10.3/4 antigen-specific CD8 T cell response is induced in the lungs of Balb/c mice following aerosol challenge with virulent *M. tuberculosis*. Utilizing a H-2K^d MHC class I tetramer reagent, the antigen-specific CD8 T cell response to the Mtb10.3/4-derived GYAGTLQSL epitope was examined at various timepoints following aerosol challenge (Figure 4.1). As a positive control to obtain higher frequency tetramer staining, mice were immunized with specially prepared low molecular weight *M. tuberculosis* culture filtrate protein (LMW CFP), which contained low molecular weight secreted proteins including Mtb10.3/4 (data not shown). Large numbers of Mtb10.3/4-specific CD8 T cells were present in the lungs of mice by 30 days following infection (Figure 4.2). The response to this peptide epitope was both prolonged and continuous, with large numbers of antigen-specific cells still present in the lungs at 180 days following infection. Incredibly, greater than 50% of the total CD3/CD8-positive cells in the lungs of some mice were specific for the GYAGTLQSL epitope, indicating the immunodominant nature of this epitope.

Immunization with the Mtb10.3/4 peptide epitope does not elicit an increase in CD4 T cells expressing an activated phenotype. To ensure that the peptide immunization

regimen employed in these experiments did not induce an aberrant CD4 T cell response, the number of CD4 T cells in the lungs expressing an activated surface phenotype was analyzed by flow cytometry at multiple timepoints (Figure 4.3). Activated CD4 T cells were identified by concurrent expression of CD3, CD4, and CD44 as well as the absence of CD62L ($CD3^{+}CD4^{+}CD44^{hi}CD62L^{lo}$). No differences in the number of activated CD4 T cells were observed between peptide immunized and nonimmunized mice at the timepoints examined.

The total number of CD8 T cells expressing an activated phenotype does not increase with immunization. Using flow cytometry, the total number of CD8 T cells possessing an activated surface phenotype was examined at multiple timepoints following infection (Figure 4.4). Activated CD8 T cells were identified by concurrent expression of CD3, CD8, and CD44 as well as the absence of CD62L ($CD3^{+}CD8^{+}CD44^{hi}CD62L^{lo}$). Immunization with the Mtb10.3/4 peptide failed to result in increased numbers of activated CD8 T cells within the lungs. No differences in the number of activated CD8 T cells were observed between peptide immunized and nonimmunized mice at the timepoints examined.

The GYAGTLQSL peptide epitope induces significant CD8 T cell cytolytic activity in previously infected mice. Using a novel *in vivo* antigen-specific cytolytic assay, we examined whether CD8 T cells specific for the Mtb10.3/4-derived GYAGTLQSL peptide epitope were able to efficiently lyse adoptively-transferred peptide pulsed target cells [2]. The results of this assay demonstrated that *M. tuberculosis* infected Balb/c mice were

able to mount a significant cytolytic response both in the lungs and in the spleen directed against this epitope (Figure 4.5).

Histological examination of the lungs of infected mice. Hematoxylin and eosin stained lung sections were examined by a trained pathologist in a double-blinded evaluation. At 30 days following infection, control Balb/c mice exhibited pronounced lymphocytic infiltration within the lungs, primarily confined to perivascular and peribronchiolar regions, some of which extended into neighboring regions containing large numbers of epithelioid macrophages (Figure 4.6). Although small numbers of isolated polymorphonuclear cells (PMNs) were present, PMN influx into infectious foci was rare at this stage of infection. Isolated plasma cells were evident, primarily localized to the periphery of the developing granulomatous lesions.

By 60 days following infection, large highly vacuolated foamy macrophages were present in significant numbers (Figure 4.7). Lymphocytes were primarily confined to perivascular and peribronchiolar cuffs, with densely-packed clusters extending into the lung parenchyma, often surrounded by large numbers of epithelioid and foamy macrophages in various stages of early degeneration. In addition, small clusters of PMNs were evident, and appeared to preferentially localize within granulomas adjacent to dense concentrations of foamy macrophages. Small foci of localized necrosis were present as foamy macrophages began to break down and disintegrate. Small aggregates of plasma cells were observed, primarily in association with blood vessels adjacent to granulocytic foci.

By day 120, many foamy macrophages possessed prominent intracellular cholesterol clefts (Figure 4.8). Many of these foamy macrophages coalesced into large areas of prominent necrosis, some of which contained cellular debris. Fibrotic encapsulation of necrotic areas was also apparent in many instances. There was also a prominent PMN influx resulting in large numbers of neutrophilic clusters primarily localized to regions adjacent to cellular necrosis. Polymorphonuclear cells were conspicuously present within blood vessels, indicating continuous recruitment of large numbers of these cells into the lung. The prominent, densely-packed lymphocytic clusters became increasingly separated and were surrounded by epithelioid and foamy macrophage-dominated regions as the granulomatous organization began to break down. As the cellularity within the granulomas continued to progressively increase, individual granulomas coalesced into large regions of pulmonary consolidation. Small numbers of multinucleated giant cells were present.

At 180 days following infection, consolidation of large regions of the lung and prominent multifocal necrosis were indicative of the progressively worsening pathology within the lung (Figure 4.9). Cellular debris was present within necrotic foci, as well as within alveolar spaces. It was evident that pulmonary capacity was significantly reduced by cellular accumulation at existing lesions as well as by compaction of alveoli in areas adjacent to continuously expanding granulomatous lesions. Cellular composition within granulomas continued to progress towards a more macrophage-dominated lesion, characterized by increasingly isolated, smaller lymphocytic clusters surrounded by large areas of epithelioid and foamy macrophages in various stages of degeneration.

Although no significant histopathological differences existed between the saline treated, adjuvant treated, and the peptide immunized groups, a significantly improved immunopathological response was observed in Balb/c mice immunized with low molecular weight secreted proteins derived from *M. tuberculosis* cultures. At 30 days following infection, increased early lymphocytic influx was observed, characterized by larger perivascular and peribronchiolar sheaths. By 60 days, the pulmonary lesions from these mice continued to exhibit a pronounced lymphocytic bias in granuloma composition, with large numbers of these cells readily migrating into the vasculature and localizing around infectious foci. Fewer foamy macrophages were present, and a reduction in PMN influx was evident. By 120 days, the amount of multifocal necrosis was reduced in LMW CFP immunized mice when compared to nonimmunized mice. These mice continued to have predominantly lymphocyte-dominated granulomas. In addition, more epithelioid-like and fewer foamy macrophages were present, which correlated with a reduction in cellular degeneration, necrosis, and the associated neutrophilic influx commonly observed in control mice. By 180 days following infection, the histological differences between saline treated mice and LMW CFP immunized mice were striking. Immunized mice continued to possess much larger numbers of lymphocytes than control mice, and these lymphocytes tended to exhibit an increased migrational ability, often penetrating deep within clusters of epithelioid-like macrophages. In addition, average lesion size and the total amount of pulmonary tissue involvement were reduced in immunized mice. Interestingly, larger numbers of multinucleated giant cells were evident in LMW CFP immunized mice.

Immunization with the Mtb10.3/4 peptide epitope fails to protect recipient mice. Although large numbers of Mtb10.3/4 antigen-specific CD8 T cells were elicited following aerosol infection with *M. tuberculosis* H37Rv, these cells failed to control bacterial replication within the lung better than control mice. Examination of the number of recovered bacilli from the lungs of infected mice revealed no significant difference between Mtb10.3/4 peptide immunized and control mice (Figure 4.10). In addition, immunization with the Mtb10.3/4 peptide failed to prevent or reduce bacterial dissemination to the spleen, and did not control bacterial replication within the spleen better than control mice (Figure 4.11). In contrast, mice immunized with LMW CFP had greater than 1-$\log_{10}$ reduction in pulmonary bacterial numbers, which persisted for 180 days following aerosol infection. The protective effect of LMW CFP was also apparent in the spleen, as evidenced by a reduction in bacterial dissemination at 30 days following infection as well as lower numbers of recoverable bacteria through 120 days.

Discussion

Previously, work by Majlessi *et al.* defined a murine CD8 T cell epitope shared between the related Mtb10.3 and Mtb10.4 secreted proteins [8]. Although this paper identified a strong H-2K^d CD8 T cell epitope using *in vitro* methodology, it failed to examine the immune response to this epitope *in vivo*, and it did not address whether the CD8 T cells elicited in response to this antigen were protective. We therefore sought to examine these immunological parameters to further elucidate the protective efficacy of

the CD8 T cell response during pulmonary tuberculosis infection, and to determine the suitability of the Mtb10.3/4 proteins for inclusion in novel candidate tuberculosis vaccines. In these studies, we demonstrated that following low dose aerosol infection with *M. tuberculosis* H37Rv, an extremely robust antigen-specific CD8 T cell response was directed against this single epitope, which was not increased by prior immunization with the peptide epitope at the timepoints examined. This response occurred early in the lungs, and persisted at very high levels throughout infection for at least 180 days. Somewhat surprisingly, at later timepoints greater than 50% of the total CD8 T cells in the lungs of infected mice were specific for this single epitope, indicating that the Mtb10.3/4 proteins represent highly immunodominant CD8 T cell antigens. This high level of reactivity was recently observed by Kamath *et al.* [6]. While the percentages of tetramer-positive cells observed in that report were somewhat lower, subtle differences in methodology most likely account for these discrepancies.

As expected, immunization with the peptide epitope failed to result in increased numbers of CD4 T cells with an activated phenotype in the lungs of mice, affirming the CD8-specific immunization methodology utilized in these experiments. However, peptide immunization also failed to induce a detectable increase in activated CD8 T cells. In addition, immunization with the Mtb10.3/4 peptide epitope failed to induce an observable increase in tetramer-positive CD8 T cells at the timepoints examined in these studies. Previously, our laboratory examined the antigen-specific CD8 T cell response to the Mtb32 protein in C57BL/6 mice [5]. Immunization with Mtb72F; a DNA vaccine encoding a fusion protein construct containing the Mtb32 protein, also failed to elicit Mtb32-specific CD8 T cell responses that were different from nonimmunized control

mice at 30 days following infectious challenge. However, significantly greater numbers of tetramer-positive cells were observed at 16 days following infection. Had timepoints prior to infection or earlier following infection been examined in these studies, we believe that differences between immunized and nonimmunized groups would have been evident. Studies are currently underway to examine this question.

Irrespective of the failure to observe detectable increases in tetramer-positive cells following immunization, the primary question we wanted to address was whether the Mtb10.3/4 CD8 T cell epitope protected mice following challenge with virulent *M. tuberculosis*. Despite the induction of a robust Mtb10.3/4 antigen-specific CD8 T cell response within the lungs of infected mice, this response failed to reduce bacterial numbers in the lungs better than control groups, and failed to have a beneficial impact upon histological examination of pulmonary tissue. Therefore, the GYAGTLQSL epitope does not appear to be suitable for inclusion in novel tuberculosis vaccines, since the cells elicited by this epitope apparently fail to mediate a long-term protective effect. Although not directly examined within these studies, it is interesting that a response of this magnitude failed to have an observable effect upon the course of *M. tuberculosis* infection. While further studies will be required to determine the exact defect in the CD8 T cell response to the Mtb10.3/4 antigens, a failure to induce large numbers of Mtb10.3/4-specific IFN-γ producing cells, induction of a pathological cytolytic response, and/or induction of tolerized or anergic antigen-specific CD8 T cells are possible explanations that need to be experimentally investigated. The results of the *in vivo* cytolytic assay demonstrated that significant CD8 T cell-mediated cytolytic activity was

directed against the Mtb10.3/4 peptide epitope. Whether this cytolytic response is beneficial or pathological in nature remains to be investigated.

In previous studies examining the CD8 T cell response to the Mtb72F DNA vaccine, we observed an initially strong antigen-specific CD8 T cell response that progressively declined over time [5]. Interestingly, the antigen-specific CD8 T cell response characterized here differed not only in the significantly greater number of tetramer-positive CD8 T cells in the Balb/c mice used for these experiments, but also in the persistent duration of this response. Further studies should be performed to determine why induction of a CD8 T cell response of this magnitude failed to result in a decrease in bacterial numbers in the lung.

Although Mtb10.3/4 peptide immunization failed to protect mice following pulmonary challenge with *M. tuberculosis*, examination of the LMW CFP immunized control group proved interesting. The large reduction in bacterial numbers (> 1-$\log_{10}$) in the lungs of immunized mice confirms earlier reports regarding the antigenicity and protective efficacy of culture filtrate proteins [1, 7]. In addition, histological examination revealed distinct differences within this group, extending the results of the previously published studies. Immunization with LMW CFP markedly increased the number of lymphocytes that accumulated at the sites of infection and also appeared to have a positive effect upon the migrational abilities of these cells, allowing them to more rapidly and effectively surround, infiltrate, and contain infectious foci. It was also observed that LMW CFP immunization appeared to decrease or at least delay the destructive, progressive cellular degeneration of foamy macrophages evident in saline treated control mice. The observed reduction in intracellular cholesterol deposits and cellular necrosis

also correlated with a concomitant reduction in the number of neutrophilic clusters commonly observed in association with destructive necrotic foci in nonimmunized mice. The exact mechanisms responsible for this protective effect were not examined, as the primary purpose of this study was to determine if a single CD8 T cell epitope could protect mice from subsequent aerosol challenge. However, since immunization with LMW CFP reduced pulmonary bacterial burden to levels equal to or exceeding those commonly observed following BCG immunization (data not shown), further investigation of the cellular composition and spatial positioning of immune cells within granulomas from LMW CFP immunized mice may reveal histological correlates of protection that could be targeted by novel tuberculosis vaccines.

Although the highly immunodominant GYAGTLQSL CD8 T cell epitope ultimately failed to protect mice upon aerosol challenge, elicitation of such a large antigen-specific CD8 T cell response following aerosol infection was an unexpected and immunologically significant observation that deserves further study. Further elucidation of the precise role that CD8 T cells play during infection with *M. tuberculosis* will allow for better definition of the correlates of protection in the lung, and ultimately aid in rational tuberculosis vaccine design.

Acknowledgements

Low molecular weight CFP was prepared and distributed by NIH, NIAID Contract No. HHSN266200400091C, entitled "Tuberculosis Vaccine Testing and Research Materials", awarded to Colorado State University.

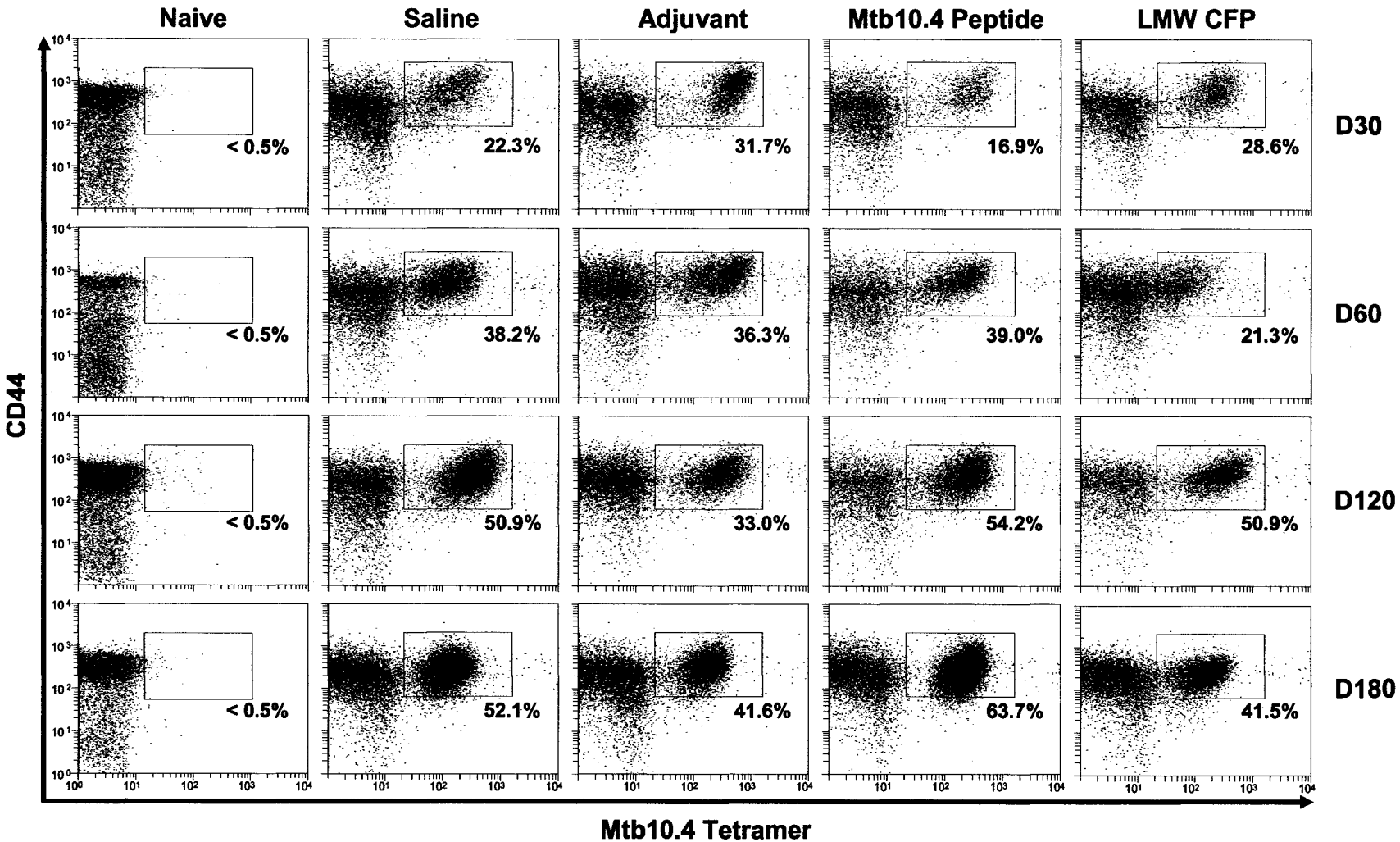

Figure 4.1. Kinetic assessment of the Mtb10.3/4 antigen-specific CD8 T cell response over time following aerosol infection. Balb/c mice (n=4) were immunized with either MPLSE-DDA, the Mtb10.3/4 GYAGTLQSL peptide in MPLSE-DDA, LMW CFP, or saline treated. Cells were gated by characteristic forward- and side-scatter patterns and concurrent CD3/CD8 expression. Percentages represent the number of tetramer$^+$ cells compared to the total number of CD3$^+$/CD8$^+$ T cells.

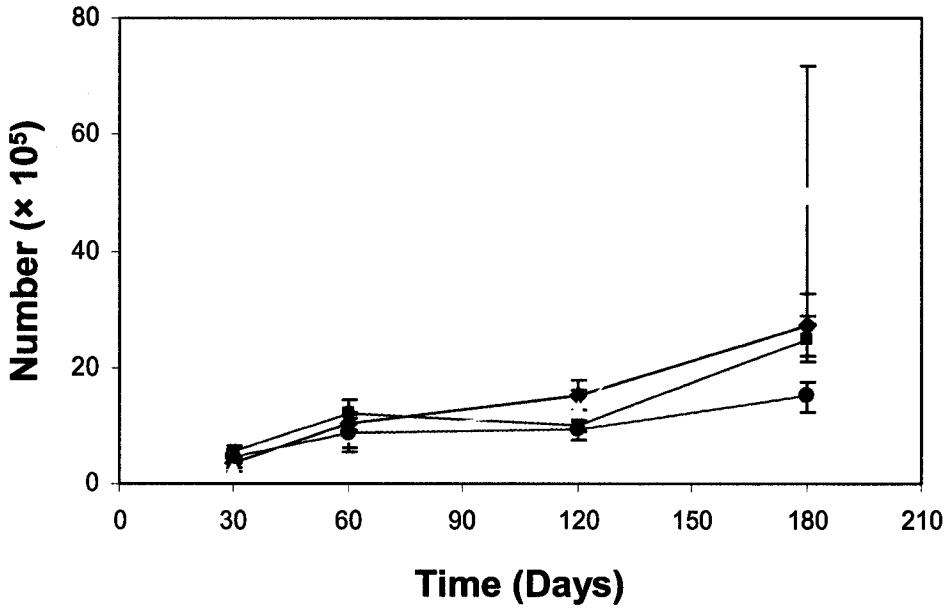

Figure 4.2. The total number of Mtb10.3/4 antigen-specific CD8 T cells in the lungs following LDA infection. At the timepoints observed, immunization with the Mtb10.3/4 peptide epitope failed to result in increased numbers of Mtb10.3/4-specific CD8 T cells present in the lungs. Single cell suspensions from the lungs of Balb/c mice were stained with the H-2K^d tetramer reagent in conjunction with antibodies specific for CD3, CD8, and CD44. Lymphocytes were gated based upon characteristic forward- vs. side-scatter profiles. Data are expressed as the means ± the standard errors of the means and are from 4 mice per group per timepoint. ♦ - Saline treated, ■ - Adjuvant treated, - Mtb10.4 peptide immunized, ● - LMW CFP immunized.

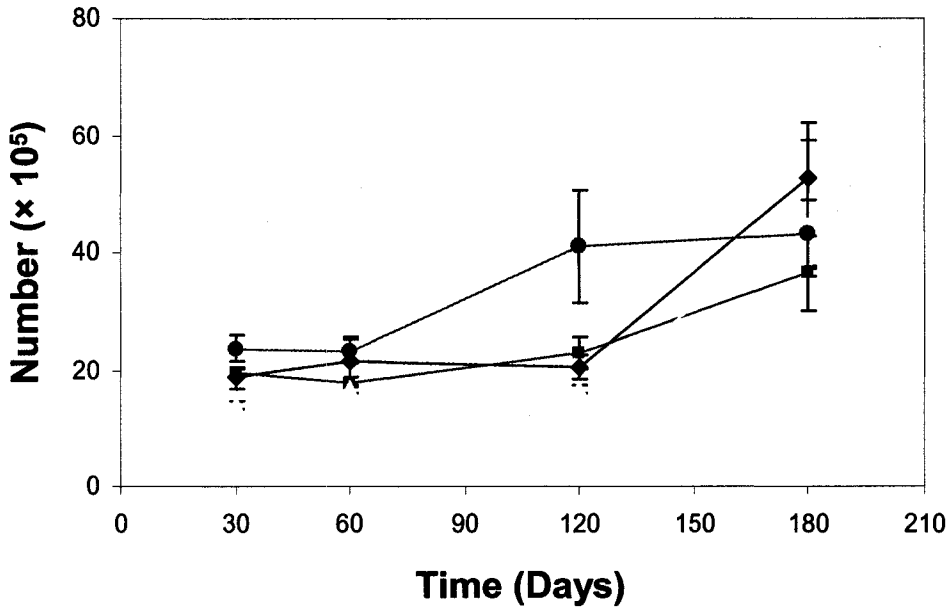

Figure 4.3. The total number of activated CD4 T cells in the lungs of infected mice is not affected by immunization with the Mtb10.3/4 peptide epitope. Single cell suspensions from the lungs of Balb/c mice were stained with anti-CD3, -CD4, -CD44, and -CD62L antibodies. Lymphocytes were gated based upon characteristic forward- vs. side-scatter profiles. Activated CD4 T cells were phenotypically identified by $CD3^+/CD4^+/CD44^{hi}/CD62L^{lo}$ expression. Data are expressed as the means ± the standard errors of the means and are from 4 mice per group per timepoint. ♦ - Saline treated, ■ - Adjuvant treated, - Mtb10.4 peptide immunized, ● - LMW CFP immunized.

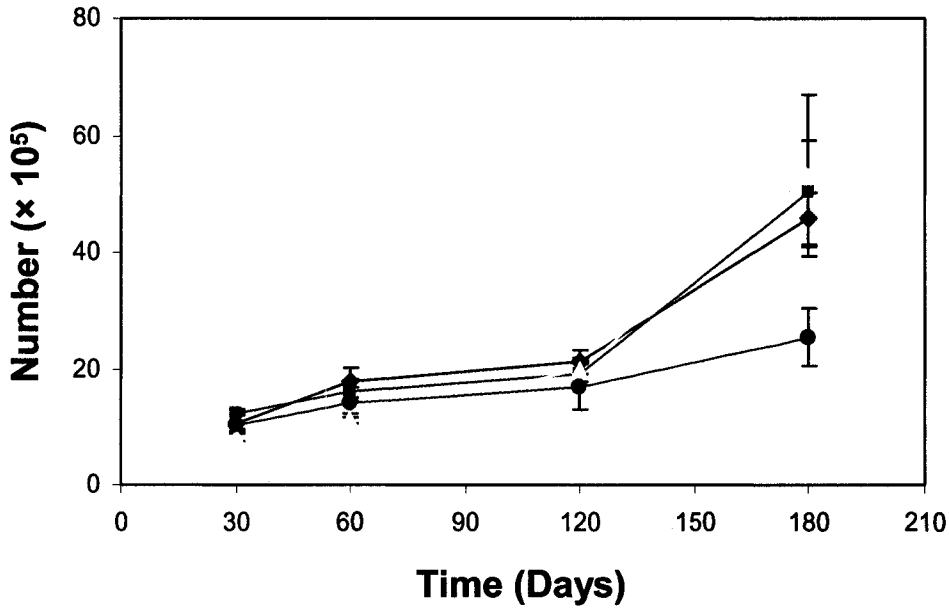

Figure 4.4. The total number of activated CD8 T cells in the lungs of infected mice is not affected by immunization with the Mtb10.3/4 peptide epitope. Single cell suspensions from the lungs of Balb/c mice were stained with anti-CD3, -CD8, -CD44, and -CD62L antibodies. Lymphocytes were gated based upon characteristic forward- vs. side-scatter profiles. Activated CD8 T cells were phenotypically identified by $CD3^{+}/CD8^{+}/CD44^{hi}/CD62L^{lo}$ expression. Data are expressed as the means ± the standard errors of the means and are from 4 mice per group per timepoint. ♦ - Saline treated, ■ - Adjuvant treated, - Mtb10.4 peptide immunized, ● - LMW CFP immunized.

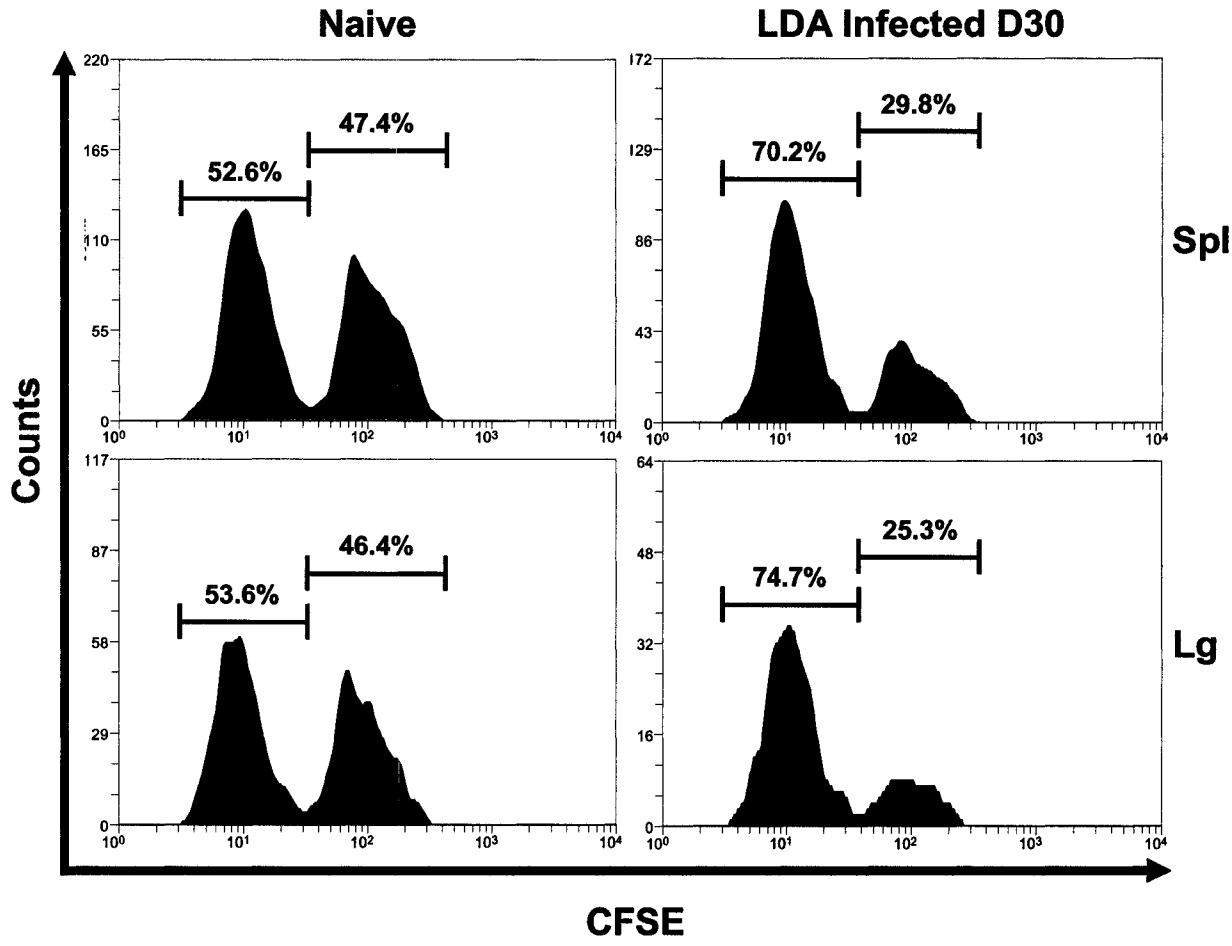

Figure 4.5. An *in vivo* cytolytic assay detected significant Mtb10.3/4-specific lytic activity in *M. tuberculosis* infected mice. Half of the splenocytes harvested from naïve donor mice were labeled with 0.5 μM CFSE ($CFSE^{lo}$) and half were labeled with 5.0 μM CFSE ($CFSE^{hi}$). The $CFSE^{hi}$ cells were then pulsed with the GYAGTLQSL peptide epitope. Following extensive washing, the $CFSE^{hi}$ and $CFSE^{lo}$ cells were mixed in a 1:1 ratio and adoptively transferred into naïve or infected syngeneic recipient mice. Cells were harvested 18 hours later from lungs (Lg) and spleens (Spl) and analyzed by flow cytometry. A reduction in the number of $CFSE^{hi}$ cells in infected mice is indicative of CD8 T cell-mediated antigen-specific cytolytic activity, which was present in both the lungs and spleen.

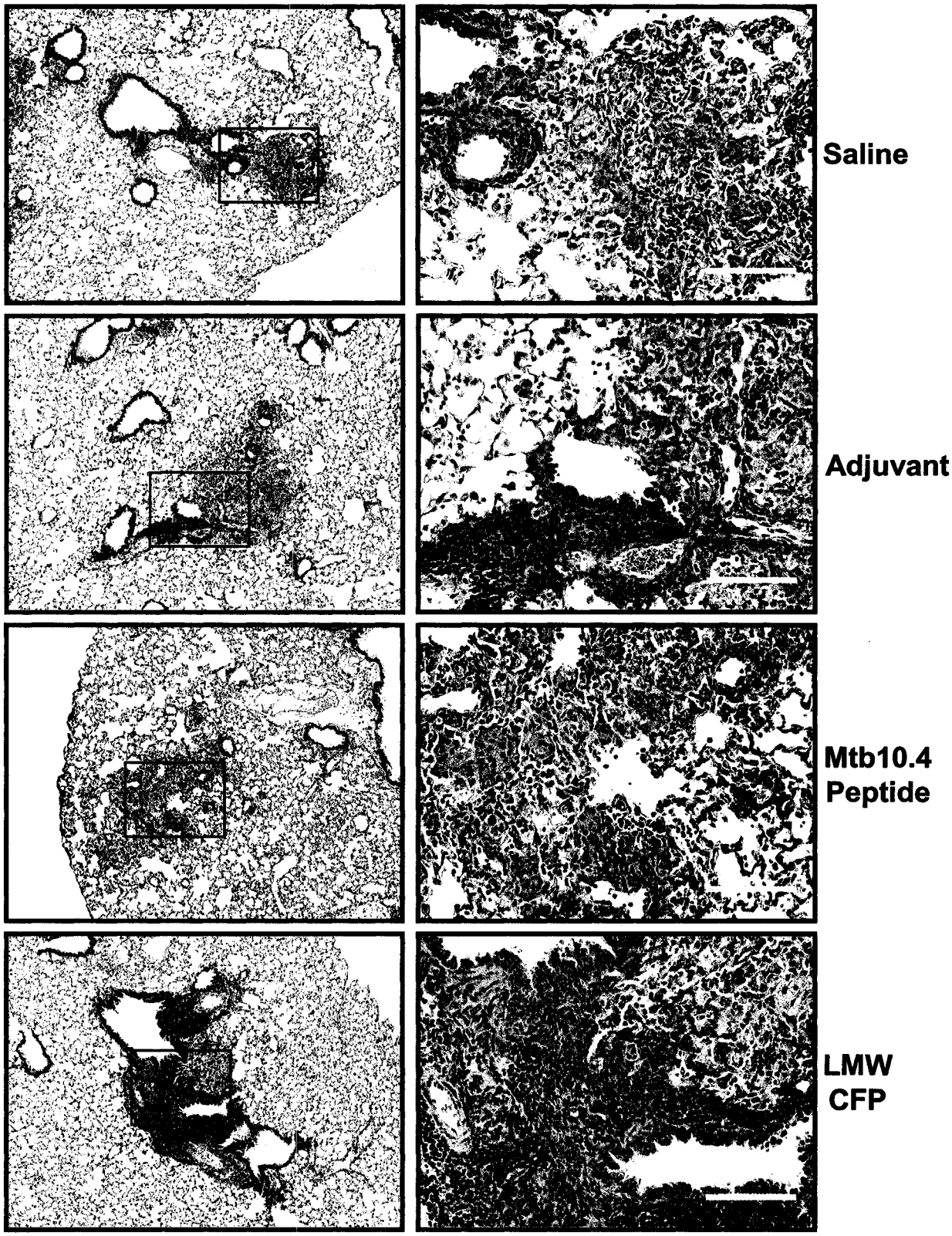

Figure 4.6. Histological comparison of hematoxylin and eosin stained lung tissue 30 days following aerosol infection. Balb/c mice were immunized as previously described, and micrographs are representative of n=4 mice/group. Size bar represents 100 μm.

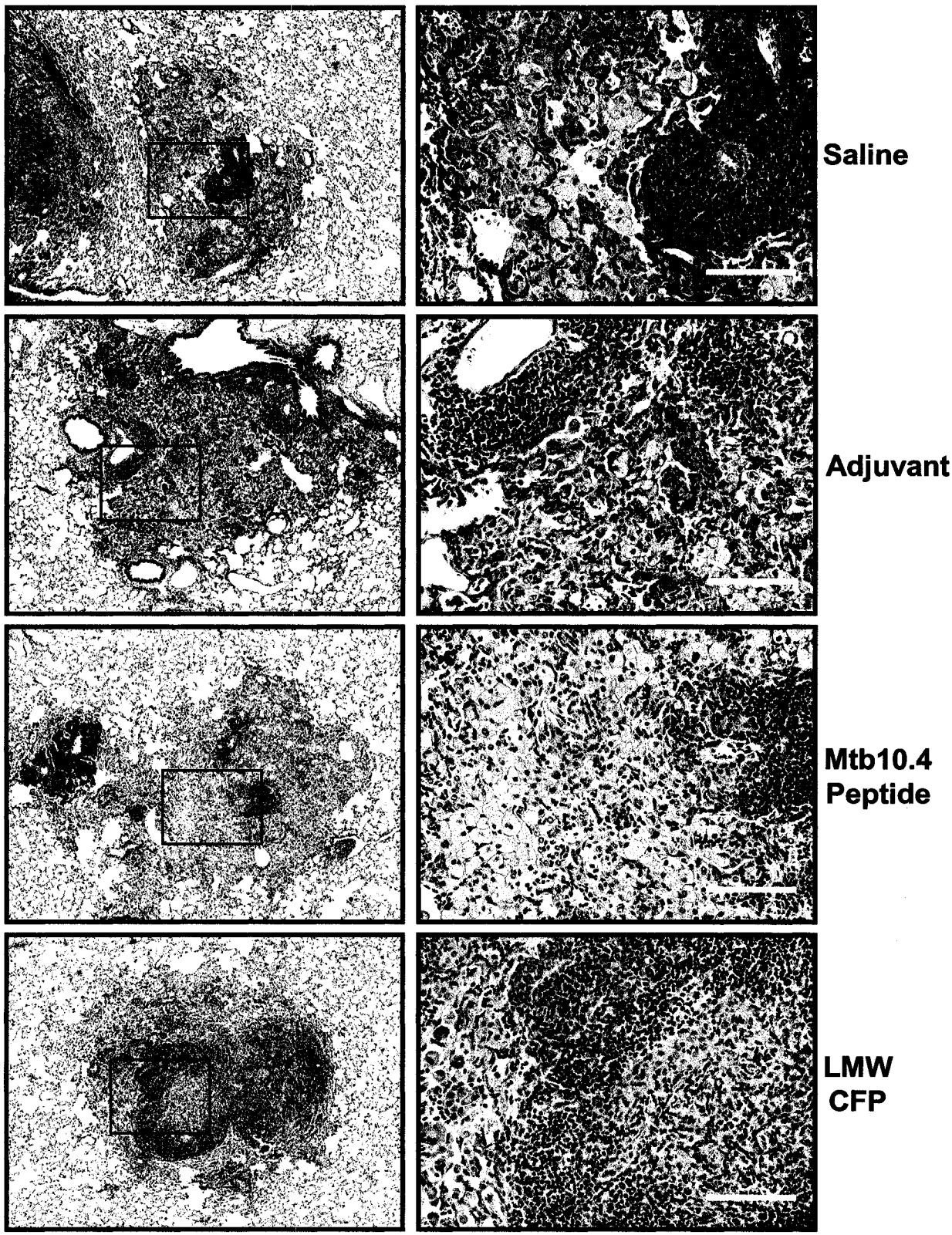

Figure 4.7. Histological comparison of hematoxylin and eosin stained lung tissue 60 days following aerosol infection. Balb/c mice were immunized as previously described, and micrographs are representative of n=4 mice/group. Size bar represents 100 μm.

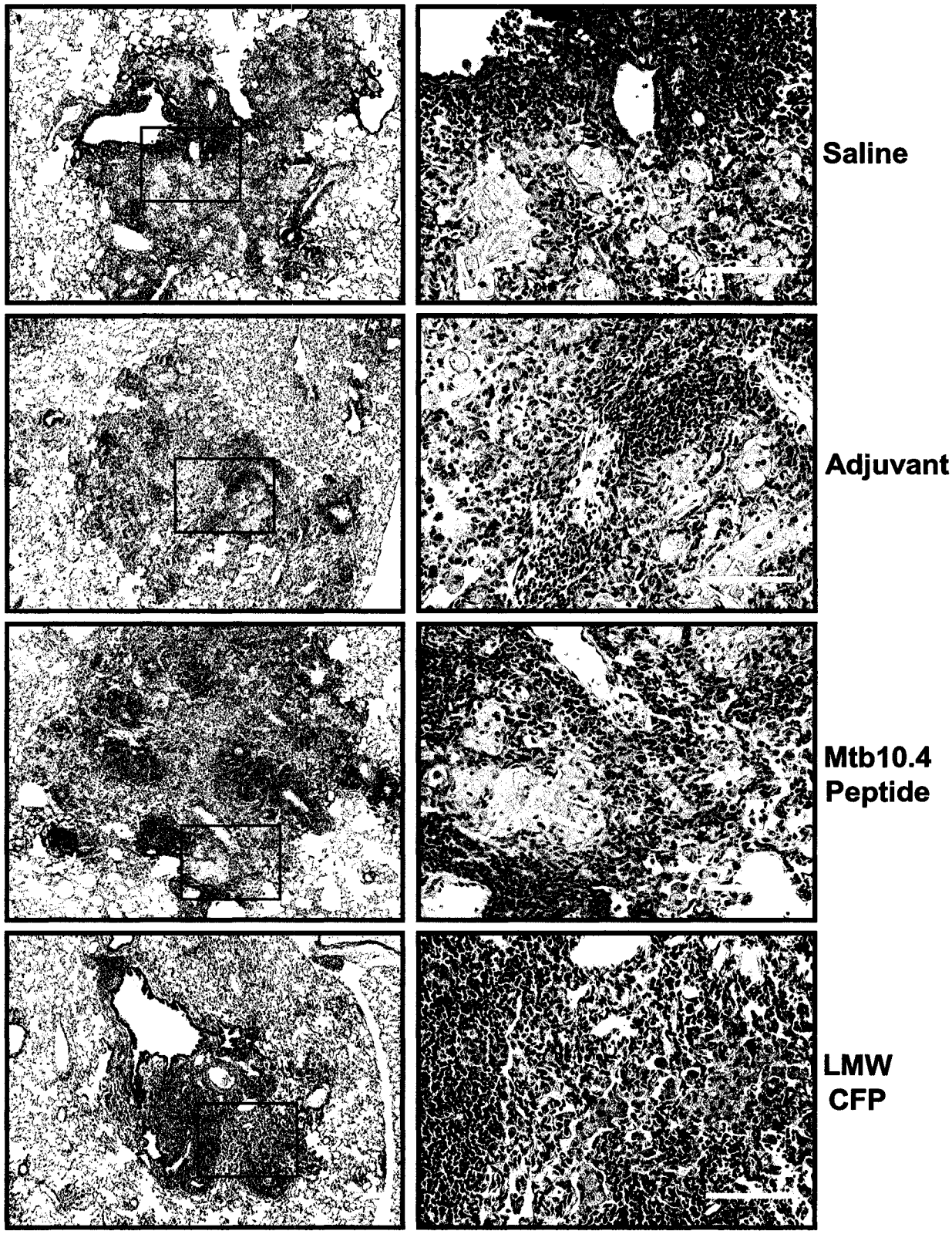

Figure 4.8. Histological comparison of hematoxylin and eosin stained lung tissue 120 days following aerosol infection. Balb/c mice were immunized as previously described, and micrographs are representative of n=4 mice/group. Size bar represents 100 μm.

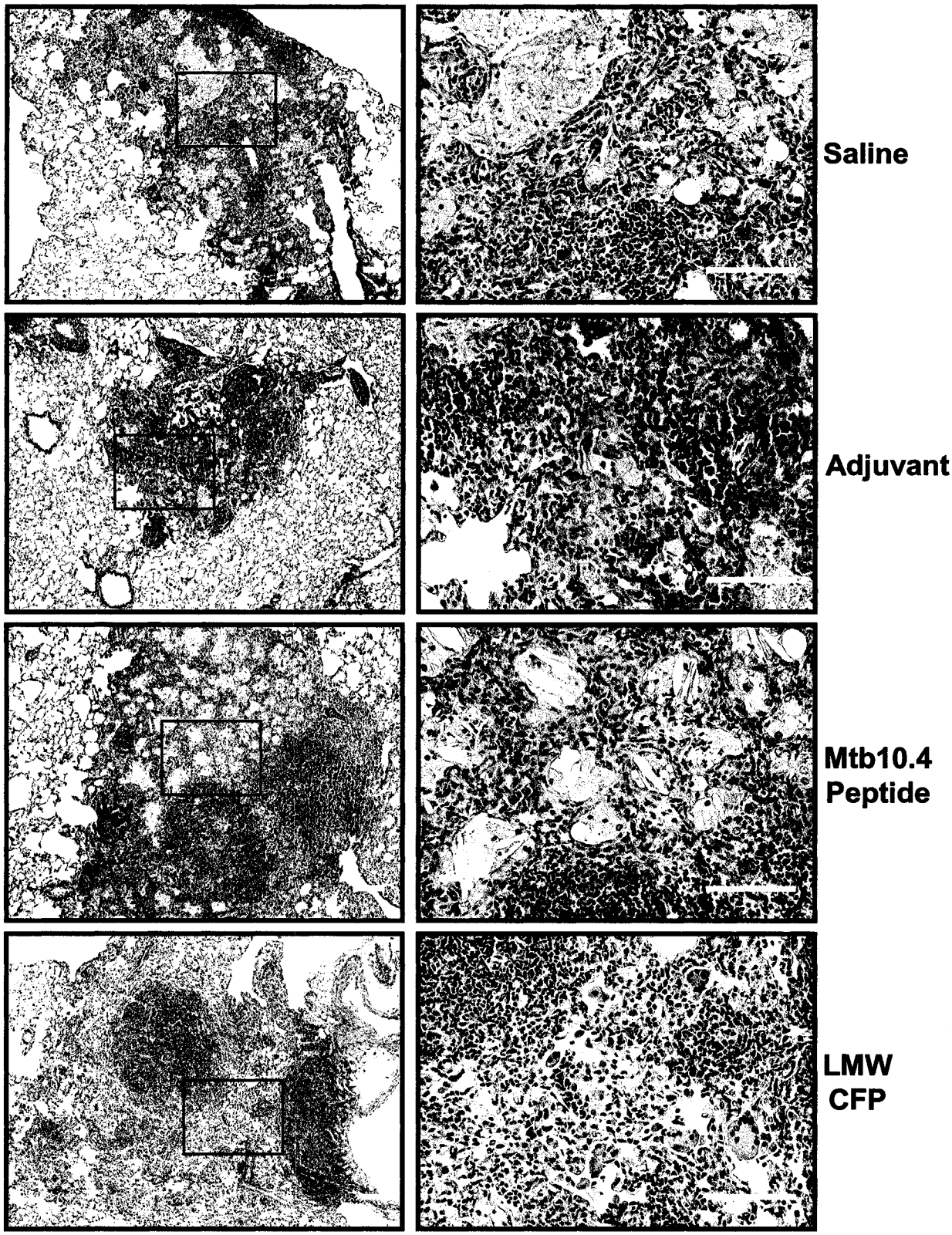

Figure 4.9. Histological comparison of hematoxylin and eosin stained lung tissue 180 days following aerosol infection. Balb/c mice were immunized as previously described, and micrographs are representative of n=4 mice/group. Size bar represents 100 μm.

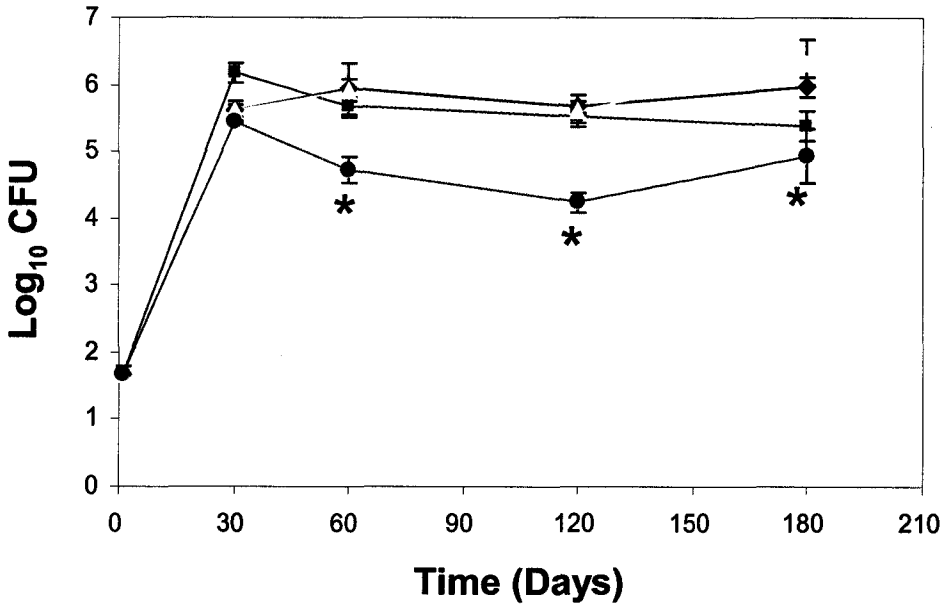

Figure 4.10. Immunization with the Mtb10.3/4 CD8 T cell peptide epitope fails to protect recipient mice following LDA infection with *M. tuberculosis* H37Rv, as indicated by the number of viable organisms recovered from the lungs. Balb/c mice (n=4) were immunized with either adjuvant, Mtb10.3/4 peptide in adjuvant, LMW CFP in adjuvant, or saline treated three times at three week intervals, followed by 3 weeks of rest. Partial lung homogenates were plated onto Middlebrook 7H11 agar and colonies were enumerated after 2-3 weeks. Data are expressed as the means ± the standard deviation. Statistical significance based upon a comparison of saline treated and LMW CFP immunized groups was determined using Student's t test (* = $P < 0.05$).
♦ - Saline treated, ■ - Adjuvant treated, - Mtb10.4 peptide immunized, ● - LMW CFP immunized.

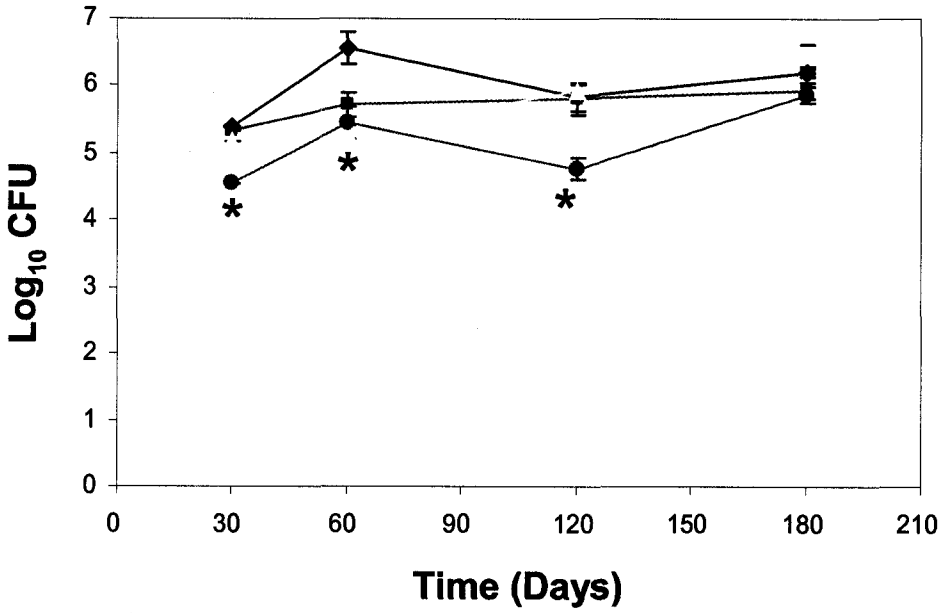

Figure 4.11. Mice immunized with the Mtb10.3/4 peptide fail to control bacterial growth in the spleen better than nonimmunized mice following LDA challenge. Data are expressed as the means ± the standard deviation. Statistical significance based upon a comparison of saline treated and LMW CFP immunized groups was determined using Student's *t* test (* = $P < 0.05$). ♦ - Saline treated, ■ - Adjuvant treated, - Mtb10.4 peptide immunized, ● - LMW CFP immunized.

References

1. **Andersen, P.** 1994. Effective vaccination of mice against *Mycobacterium tuberculosis* infection with a soluble mixture of secreted mycobacterial proteins. Infect Immun **62:**2536-44.

2. **Barber, D. L., E. J. Wherry, and R. Ahmed.** 2003. Cutting edge: rapid *in vivo* killing by memory CD8 T cells. J Immunol **171:**27-31.

3. **Corbett, E. L., C. J. Watt, N. Walker, D. Maher, B. G. Williams, M. C. Raviglione, and C. Dye.** 2003. The growing burden of tuberculosis: global trends and interactions with the HIV epidemic. Arch Intern Med **163:**1009-21.

4. **Feng, C. G., A. G. Bean, H. Hooi, H. Briscoe, and W. J. Britton.** 1999. Increase in gamma interferon-secreting $CD8^+$, as well as $CD4^+$, T cells in lungs following aerosol infection with *Mycobacterium tuberculosis*. Infect Immun **67:**3242-7.

5. **Irwin, S. M., A. A. Izzo, S. W. Dow, Y. A. Skeiky, S. G. Reed, M. R. Alderson, and I. M. Orme.** 2005. Tracking antigen-specific CD8 T lymphocytes in the lungs of mice vaccinated with the Mtb72F polyprotein. Infect Immun **73:**5809-16.

6. **Kamath, A. B., J. Woodworth, X. Xiong, C. Taylor, Y. Weng, and S. M. Behar.** 2004. Cytolytic $CD8^+$ T cells recognizing CFP10 are recruited to the lung after *Mycobacterium tuberculosis* infection. J Exp Med **200:**1479-89.

7. **Lindblad, E. B., M. J. Elhay, R. Silva, R. Appelberg, and P. Andersen.** 1997. Adjuvant modulation of immune responses to tuberculosis subunit vaccines. Infect Immun **65:**623-9.

8. **Majlessi, L., M. J. Rojas, P. Brodin, and C. Leclerc.** 2003. $CD8^+$ T-cell responses of mycobacterium-infected mice to a newly identified major histocompatibility complex class I-restricted epitope shared by proteins of the ESAT-6 family. Infect Immun **71:**7173-7.

9. **Mogues, T., M. E. Goodrich, L. Ryan, R. LaCourse, and R. J. North.** 2001. The relative importance of T cell subsets in immunity and immunopathology of airborne *Mycobacterium tuberculosis* infection in mice. J Exp Med **193:**271-80.

10. **Orme, I. M.** 1987. The kinetics of emergence and loss of mediator T lymphocytes acquired in response to infection with *Mycobacterium tuberculosis*. J Immunol **138:**293-8.

11. **Rolph, M. S., B. Raupach, H. H. Kobernick, H. L. Collins, B. Perarnau, F. A. Lemonnier, and S. H. Kaufmann.** 2001. MHC class Ia-restricted T cells

partially account for β_2-microglobulin-dependent resistance to *Mycobacterium tuberculosis*. Eur J Immunol **31:**1944-9.

12. **Serbina, N. V., and J. L. Flynn.** 1999. Early emergence of $CD8^+$ T cells primed for production of type 1 cytokines in the lungs of *Mycobacterium tuberculosis*-infected mice. Infect Immun **67:**3980-8.

13. **Sousa, A. O., R. J. Mazzaccaro, R. G. Russell, F. K. Lee, O. C. Turner, S. Hong, L. Van Kaer, and B. R. Bloom.** 2000. Relative contributions of distinct MHC class I-dependent cell populations in protection to tuberculosis infection in mice. Proc Natl Acad Sci U S A **97:**4204-8.

14. **Turner, J., C. D. D'Souza, J. E. Pearl, P. Marietta, M. Noel, A. A. Frank, R. Appelberg, I. M. Orme, and A. M. Cooper.** 2001. CD8- and CD95/95L-dependent mechanisms of resistance in mice with chronic pulmonary tuberculosis. Am J Respir Cell Mol Biol **24:**203-9.

15. **Urdahl, K. B., D. Liggitt, and M. J. Bevan.** 2003. $CD8^+$ T cells accumulate in the lungs of *Mycobacterium tuberculosis*-infected $K^{b-/-}D^{b-/-}$ mice, but provide minimal protection. J Immunol **170:**1987-94.

16. **van Pinxteren, L. A., J. P. Cassidy, B. H. Smedegaard, E. M. Agger, and P. Andersen.** 2000. Control of latent *Mycobacterium tuberculosis* infection is dependent on CD8 T cells. Eur J Immunol **30:**3689-98.

Chapter 5

Concluding Remarks

Discussion

Tuberculosis is a disease that is currently estimated to infect one-third of the world's population [3]. Historically, it has been responsible for more suffering and death than any other human pathogen. Although modern sanitation practices and chemotherapeutic treatments have contributed to a steady decline in the incidence of tuberculosis in industrialized nations, with the emergence of the human immunodeficiency virus (HIV) and its subsequent pandemic spread, there has been a concomitant increase in the world-wide incidence of tuberculosis. The exquisite synergism between HIV infection and the increased susceptibility to *Mycobacterium tuberculosis* infection and recrudescence of latent disease have fueled this resurgence in tuberculosis cases, reversing the downward trend observed in many countries. In addition, the necessity for long chemotherapeutic treatment regimens fosters patient noncompliance and the generation and spread of multidrug-resistant strains of tuberculosis. Unless this problem is contained, the combination of HIV-tuberculosis coinfection and multidrug-resistant tuberculosis threatens to overwhelm the limited resources of underdeveloped nations and once again reemerge as a leading killer within developed nations.

Many countries with the highest tuberculosis prevalence lack the sound health care infrastructure required to support tuberculosis surveillance and treatment programs. Even in countries with adequate health care support, transient socioeconomic factors often lead to critical breakdowns in tuberculosis control policies. As the tuberculosis outbreaks in Miami and New York in the 1990s illustrate, a failure to control tuberculosis

on a world-wide scale threatens to undermine successful tuberculosis eradication programs, even within industrialized countries.

Although a live attenuated vaccine for tuberculosis is currently used throughout the world, *M. bovis* BCG has been shown to have variable protective efficacy which declines over time and also fails to protect adults from pulmonary tuberculosis; the most common form of tuberculosis. In addition, BCG can cause disease in immunocompromised individuals, or individuals with certain immunological deficits. Given the fact that underdeveloped nations harbor the vast majority of tuberculosis cases, a safer, low-cost, short-duration treatment option is desperately needed. Development of a more effective tuberculosis vaccine is an increasingly attractive, cost-effective alternative to the significantly higher expenses and antibiotic resistance associated with the long-term chemotherapy regimen required for successful anti-tuberculosis treatment.

Currently we have the immunological and microbiological tools to combat this organism. The question is only whether we possess the social conscience and economic resolve required to eliminate this pathogen.

CD8 T cells are specialized for the detection and destruction of intracellular pathogens such as viruses and intracellular bacteria. Therefore, from a purely immunological perspective, it would seem that CD8 T cells would represent a critical line of defense against *M. tuberculosis*; a facultative intracellular pathogen. In the case of this organism; however, this does not appear to be the case. Although the majority of reports in the literature support a protective role for CD8 T cells, the exact role that these cells play during pulmonary infection is controversial. The fact that mice lacking CD8 T cells have a moderately reduced ability to control mycobacterial growth in the lungs indicates

a positive role for these cells during infection [10]. In addition, in mice lacking CD4 T cells, CD8 T cells provide some level of protection to infectious challenge [7, 9, 10]. However; perforin, granzyme, and Fas/FasL knock-out (KO) mice all control bacterial proliferation similar to wild-type mice during the first 80 days following infection [1, 2, 14]. These results argue against a protective cytolytic component, at least early during the infectious process. A reasonable case can be made that CD8 T cells exert their protective effect primarily through interferon-gamma (IFN-γ) production [13]. This minor protective role can only be readily appreciated in the absence of CD4 T cells, as CD8 T cells are less efficient producers of IFN-γ than responding CD4 T cells, and their contribution would be masked in the presence of an intact CD4 T cell response. Only in this non-physiological setting can the CD8 T cell IFN-γ contribution be easily observed.

While the exact reason that CD8 T cells fail to play a predominant role during mycobacterial infection is unclear, two hypotheses can be advanced. Perhaps the protective efficacy of the CD8 T cell response is either subverted by the pathogen itself to avoid detection and to prolong its survival, or perhaps the cytolytic potential that CD8 T cells possess preferentially induces a destructive pathological response rather than a protective bacteriocidal function.

The current paradigm regarding the role of CD8 T cells during mycobacterial infection involves CD8 T cells exerting a minor or negligible protective effect early during the course of infection, primarily through the production of IFN-γ [11]. However, during chronic infection CD8 T cells are believed to provide an immunosurveillance function by preventing the escape of infected macrophage cells from the protective confines of the granuloma. As the organization of the granuloma begins to break down,

CD8 T cells can access and lyse infected macrophages, releasing viable bacilli which are then taken up by activated macrophages capable of more efficient intracellular killing of internalized bacilli [6, 15].

Although this is the generally accepted view regarding the contribution of CD8 T cells, one piece of evidence argues against the latter portion of this model. The mouse model of tuberculosis exhibits a prolonged period following the peak of infection where bacterial numbers remain relatively constant. If infected macrophages were being lysed, and if activated macrophages possessed the capability to kill the released bacilli, then we would expect bacterial numbers in the lung to steadily decrease in the face of a persistent cytolytic response. Since this clearly is not the case, either bacterial replication within the lung exactly equals bacterial destruction, or activated macrophages are able to control bacterial replication, but fail to efficiently kill internalized bacilli and themselves become persistently infected. Recent experimental evidence supports the latter hypothesis [8].

One other possible explanation bears examination. While possessing many advantages for the study of tuberculosis, the mouse model of infection may ultimately not be the best model in which to examine the potential protective merits of the CD8 T cell response. Mice lack granulysin, a molecule found in humans that is known to possess anti-mycobacterial properties [12]. One could argue that in the absence of granulysin the murine cytolytic CD8 T cell response to mycobacterial infection is crippled. In fact, lysing infected host cells in the absence of bacterial killing may actually exacerbate the infectious process within the lung by fostering a perpetual cycle of lytic destruction of infected macrophages, release of live bacilli, bacterial uptake by noninfected macrophages, followed by lysis of these newly-infected host cells. This may contribute to

the excessive pathology and persistent, progressive inflammation observed in the murine lung.

With many questions still surrounding the CD8 T cell response to mycobacterial infection, we sought to characterize the CD8 T cell response during pulmonary infection using a murine infection model. In order to better understand the CD8 T cell response, we wanted to characterize the response in terms of cellular recruitment into the lung, expression of surface markers, and cytokine secretion patterns. We then wanted to track antigen-specific CD8 T cells during the course of normal infection as well as following immunization with multiple vaccine delivery systems.

Efficient recruitment of effector lymphocytes is essential to rapid control of bacterial proliferation within the lung. The upregulation of adhesion molecules on activated lymphocytes is a crucial step enabling these cells to extravasate from the blood into the pulmonary tissue and direct their migration to the sites of infection. Based upon initial observations by Gonzalez-Juarrero *et al.* of the predominantly peripheral location of CD8 T cells within murine granulomas, we wanted to investigate whether this defective migration was the result of poor adhesion molecule expression [4]. Because of their importance in cellular trafficking, we examined the expression patterns of four integrin molecules (VLA-4, LFA-1, LPAM-1, and HML-1) expressed on the surface of CD4 and CD8 T cells.

Although we succeeded in characterizing the expression patterns of these integrin molecules by CD8 T cells during experimental infection with virulent *M. tuberculosis*, these experiments ultimately failed to identify a defect in integrin molecule upregulation by CD8 T cells responding to pulmonary tuberculosis infection. Future studies could

examine the expression patterns of chemokine receptor molecules to attempt to answer this question. The recent commercial availability of monoclonal antibodies specific for these receptors now makes this examination feasible.

In order to develop a more complete picture of the CD8 T cell response to *M. tuberculosis* infection, we wanted to characterize the surface phenotype of both effector CD8 T cells actively responding to infection as well as memory CD8 T cells generated following combination drug treatment to reduce bacterial numbers to undetectable levels. For these experiments, we generated MHC class I tetramer reagents to precisely examine the dynamics of a clonal CD8 T cell response at the cellular level as well as at the population level within the lungs and the spleens of mice following infection. We examined a series of activation markers, costimulatory and inhibitory receptors, and memory-associated markers over time to define the phenotype of both effector and memory CD8 T cells following infection with *M. tuberculosis*. These experiments revealed a large, early influx of CD8 T cells possessing an activated phenotype into the lungs following infection, with continued maintenance of significant numbers of these cells throughout the course of infection. Although large numbers of CD8 (and CD4) T cells were continuously present, the majority of these cells failed to secrete IFN-γ or TNF-α upon restimulation, and did not produce detectable levels of cytolytic effector molecules upon *ex vivo* restimulation, leaving the effector function of most of the T cells in the lungs unknown. Examination of two inhibitory receptors with critical functions in the downmodulation of inflammatory T cell responses may provide an explanation for this paradox. We observed rapid and persistent high-level expression of both PD-1 and Tim-3, two receptors associated with immunosuppression, tolerance induction, and

effector cell apoptosis. It is interesting to speculate that tolerization and/or functional exhaustion in the continued presence of high antigenic burden may be responsible for the lack of observable CD8 T cell reactivity in these experiments.

Alternately, one could argue that many of these cells are functioning in a contact-dependent manner, utilizing effector molecules not examined in these studies. While the exact explanation for the lack of observable CD8 T cell reactivity is unknown, further experiments may elucidate the mechanisms involved and provide useful therapeutic targets to treat chronic infection.

Utilizing MHC class I tetramer technology, we were able to identify Mtb32 antigen-specific CD8 T cells in the lungs of mice previously infected with *M. tuberculosis* [5]. We observed that detectable numbers of these cells were recruited into the lungs early following infection, and that these cells preferentially produced IFN-γ as opposed to exhibiting cytolytic activity. Importantly, prior immunization with the Mtb72F DNA vaccine encoding the Mtb32 protein resulted in increased numbers of these antigen-specific cells, many of which possessed markers indicative of a state of memory. Interestingly, peak numbers of Mtb32-specific CD8 T cells occurred at 30 days following infection, which coincided with immunological control of bacterial replication within the lung. In addition, we were able to use a novel cationic liposomal reagent in combination with recombinant Mtb72F protein to induce an antigen-specific CD8 T cell response of greater magnitude than DNA immunization, and were able to phenotypically track the acquisition of memory markers on the population of cells elicited by vaccination.

Since the *M. bovis* BCG vaccine is currently used throughout the world, we wanted to examine whether mice immunized with BCG mounted an Mtb32 antigen-

specific CD8 T cell response. Following BCG immunization, we were able to observe and track this response, demonstrating the potential feasibility of a BCG prime, Mtb72F boost regimen.

One of the important questions involving the CD8 T cell response is whether CD4 T cell help is required for optimal CD8 T cell expansion and/or memory cell generation. Utilizing CD4 KO mice in conjunction with Mtb32-tetramer staining, we demonstrated that although CD4 KO mice were able to initially prime an antigen-specific response, the magnitude of this response was significantly reduced when compared to wild-type mice at 37 days following aerosol challenge. While prior immunization of CD4 KO mice with the Mtb72F DNA vaccine could partially overcome the proliferative defect, the ultimate size of the Mtb32-specific response was still significantly smaller than that found in mice possessing functional CD4 T cell help. In addition, we were able to show that the reacquisition of the IL-7R alpha chain; a recently discovered identifier of CD8 memory precursor T cells, proceeded normally in CD4 KO mice, although the number of such cells was smaller than in wild-type mice. Together, these results suggest that there is a reduced requirement for CD4 help during the generation of CD8 memory T cells; however CD4 T cell help is required for the optimal expansion of antigen-specific CD8 effector and memory T cell responses.

In the final studies presented here, we again used tetramer technology to track antigen-specific CD8 T cells to a shared epitope within the related Mtb10.3/4 proteins, and we were able to examine the induction and persistent expansion of a significant population of CD8 T cells specific for this single epitope. We were further able to document significant CD8 T cell-mediated cytolytic activity present in both the lungs and

spleens of mice previously infected with *M. tuberculosis*. In addition, we demonstrated that prior immunization with the peptide epitope in MPL-SE/DDA adjuvant failed to provide any detectable protection in the lungs or spleen, as evidenced by bacterial CFU counts and histological examination. It is interesting to contrast these results with the previous experiments examining the Mtb32-specific response. Although it is tempting to speculate that antigen-specific CD8 T cell IFN-γ-producing responses are protective while strongly cytolytic responses are not, further experiments will need to be performed to conclusively determine the exact nature of the CD8 T cell cytolytic response during pulmonary tuberculosis infection.

In these experiments, we have shown that we can elicit a strong antigen-specific CD8 T cell response with a DNA vaccine, a protein/liposomal formulation, and protein in adjuvant combination. Furthermore, we were able to identify and track the generation of antigen-specific effector CD8 T cells during the course of infection and in response to prior immunization. In addition, we were able to observe the transition of these cells to a state of memory following vaccination. As the goal of vaccination is to generate protective, long-lasting memory cells, this technology will prove invaluable for screening multiple antigen/adjuvant vaccine combinations and different vaccine delivery systems for their ability to stimulate specific memory cell subsets.

Whether the memory cells generated by immunization represent central memory or effector memory subpopulations remains to be determined. Indeed, a pertinent question that remains to be answered is whether central memory or effector memory subpopulations provide the most durable and protective population, and as such, should

be targeted by novel tuberculosis vaccines. This represents the next major challenge for the creation of an effective tuberculosis vaccine.

For the most part, the results presented in this dissertation support the previously outlined model of CD8 T cell function during pulmonary infection with tuberculosis. We demonstrated that antigen-specific CD8 T cells arrive in the lungs early following infection, and are primarily cytokine-secreting rather than cytolytic [5]. These studies support the idea that during acute infection, the primary role of CD8 T cells is IFN-γ secretion to aid in macrophage activation and control of bacterial replication. Further studies; however, do not support a protective role for cytolytic CD8 T cells during chronic infection. Antigen-specific tracking of CD8 T cells responding to the Mtb10.3/4 proteins revealed significant cytolytic activity and failed to protect mice, especially at timepoints late during chronic infection. In addition, infected mice exhibited histological indications of a destructive, necrotic response within the lungs, further suggesting that a strong cytolytic response is detrimental rather than beneficial. However, care should be taken to avoid inferring too much from this study. While the correlation between cytolytic activity and a lack of protection is intriguing, it is by no means conclusive proof that this cytolytic response in particular or that all cytolytic responses in general are detrimental. Further experiments utilizing adoptive transfer of CD8 T cells derived from perforin KO donor mice or from IFN-γ KO donor mice should resolve this question in a more definitive manner.

These studies have added to our understanding of how CD8 T cells respond to pulmonary infection with *M. tuberculosis*, in the hope that a more complete

understanding of this process will aid in rational vaccine design, and ultimately contribute to the realization of a more effective tuberculosis vaccine.

References

1. **Canaday, D. H., R. J. Wilkinson, Q. Li, C. V. Harding, R. F. Silver, and W. H. Boom.** 2001. $CD4^+$ and $CD8^+$ T cells kill intracellular *Mycobacterium tuberculosis* by a perforin and Fas/Fas ligand-independent mechanism. J Immunol **167:**2734-42.

2. **Cooper, A. M., C. D'Souza, A. A. Frank, and I. M. Orme.** 1997. The course of *Mycobacterium tuberculosis* infection in the lungs of mice lacking expression of either perforin- or granzyme-mediated cytolytic mechanisms. Infect Immun **65:**1317-20.

3. **Corbett, E. L., C. J. Watt, N. Walker, D. Maher, B. G. Williams, M. C. Raviglione, and C. Dye.** 2003. The growing burden of tuberculosis: global trends and interactions with the HIV epidemic. Arch Intern Med **163:**1009-21.

4. **Gonzalez-Juarrero, M., O. C. Turner, J. Turner, P. Marietta, J. V. Brooks, and I. M. Orme.** 2001. Temporal and spatial arrangement of lymphocytes within lung granulomas induced by aerosol infection with *Mycobacterium tuberculosis*. Infect Immun **69:**1722-8.

5. **Irwin, S. M., A. A. Izzo, S. W. Dow, Y. A. Skeiky, S. G. Reed, M. R. Alderson, and I. M. Orme.** 2005. Tracking antigen-specific CD8 T lymphocytes in the lungs of mice vaccinated with the Mtb72F polyprotein. Infect Immun **73:**5809-16.

6. **Kaufmann, S. H.** 1988. $CD8^+$ T lymphocytes in intracellular microbial infections. Immunol Today **9:**168-74.

7. **Mogues, T., M. E. Goodrich, L. Ryan, R. LaCourse, and R. J. North.** 2001. The relative importance of T cell subsets in immunity and immunopathology of airborne *Mycobacterium tuberculosis* infection in mice. J Exp Med **193:**271-80.

8. **Munoz-Elias, E. J., J. Timm, T. Botha, W. T. Chan, J. E. Gomez, and J. D. McKinney.** 2005. Replication dynamics of *Mycobacterium tuberculosis* in chronically infected mice. Infect Immun **73:**546-51.

9. **Orme, I. M.** 1987. The kinetics of emergence and loss of mediator T lymphocytes acquired in response to infection with *Mycobacterium tuberculosis*. J Immunol **138:**293-8.

10. **Rolph, M. S., B. Raupach, H. H. Kobernick, H. L. Collins, B. Perarnau, F. A. Lemonnier, and S. H. Kaufmann.** 2001. MHC class Ia-restricted T cells partially account for β_2-microglobulin-dependent resistance to *Mycobacterium tuberculosis*. Eur J Immunol **31:**1944-9.

11. **Serbina, N. V., and J. L. Flynn.** 1999. Early emergence of $CD8^+$ T cells primed for production of type 1 cytokines in the lungs of *Mycobacterium tuberculosis*-infected mice. Infect Immun **67:**3980-8.

12. **Stenger, S., D. A. Hanson, R. Teitelbaum, P. Dewan, K. R. Niazi, C. J. Froelich, T. Ganz, S. Thoma-Uszynski, A. Melian, C. Bogdan, S. A. Porcelli, B. R. Bloom, A. M. Krensky, and R. L. Modlin.** 1998. An antimicrobial activity of cytolytic T cells mediated by granulysin. Science **282:**121-5.

13. **Tascon, R. E., E. Stavropoulos, K. V. Lukacs, and M. J. Colston.** 1998. Protection against *Mycobacterium tuberculosis* infection by $CD8^+$ T cells requires the production of gamma interferon. Infect Immun **66:**830-4.

14. **Turner, J., C. D. D'Souza, J. E. Pearl, P. Marietta, M. Noel, A. A. Frank, R. Appelberg, I. M. Orme, and A. M. Cooper.** 2001. CD8- and CD95/95L-dependent mechanisms of resistance in mice with chronic pulmonary tuberculosis. Am J Respir Cell Mol Biol **24:**203-9.

15. **van Pinxteren, L. A., J. P. Cassidy, B. H. Smedegaard, E. M. Agger, and P. Andersen.** 2000. Control of latent *Mycobacterium tuberculosis* infection is dependent on CD8 T cells. Eur J Immunol **30:**3689-98.